The Development of a Model to Stimulate Channel Deformation in Alluvial Rivers

BKS Consulting Engineers

WRC Report No.236/1/93

Water Research Commission

The development of a model to simulate channel deformation in alluvial rivers

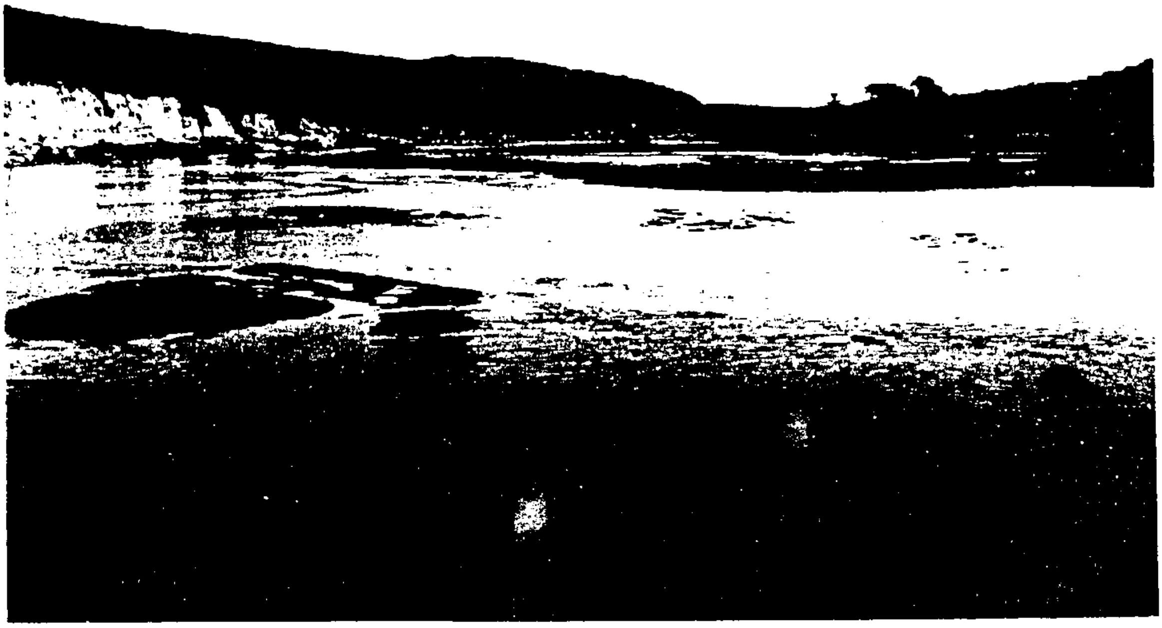

JUNE 1993

BKS INCORPORATED
CONSULTING ENGINEERS
PO BOX 3173, PRETORIA 0001

WRC REPORT NO. 236/1/93
ISBN 1 86845 024 4

PREFACE

Rivers have fascinated generations of hydraulic engineers with their variety of form and behaviour. The large potential benefits of successful river engineering works, as well as the dire consequences of failures, have provided some of the greatest challenges to the profession.

Rivers are some of the most active agents in shaping the surface of the earth and the landforms asssociated with a particular river therefore provide a record, which may be detailled, of the rivers' past and present activity.

Many river engineering problems unfortunately lie outside areas where research or routine observations have been concentrated and thus have to be solved by a combination of intuition, past experience and interpretation of fluvial features as seen on aerial photographs and in the field.

THE DEVELOPMENT OF A MODEL TO SIMULATE CHANNEL DEFORMATION IN ALLUVIAL RIVERS

by

A du P LE GRANGE

and

A ROOSEBOOM

BKS Incorporated
Consulting Engineers
373 Pretorius Street, Pretoria,
0001
South Africa

Specialist Advisor
Department of Civil Engineering
University of Stellenbosch, Stellenbosch,
7600
South Africa

BKS Report No I04/29/01/01(P)

THE DEVELOPMENT OF A MODEL TO SIMULATE CHANNEL DEFORMATION IN ALLUVIAL RIVERS

EXECUTIVE SUMMARY

A river is continually changing its position and shape as a consequence of hydraulic forces acting on its bed and banks. The geometry of an alluvial river channel is determined by the interaction between the flowing water, the magnitude and characteristics of the sediment load as well as the composition of the bed and bank materials. The general problem of alluvial channel stability revolves around the question as to how a river channel with deformable boundaries react to changing water and sediment discharges.

A model which can be used to predict equilibrium alluvial river behaviour which will facilitate investigations into alluvial river behaviour and will be of assistance in river engineering work is discussed in this report.

The problem of determining a stable or equilibrium cross-sectional geometry for an alluvial channel has been the subject of considerable research and continues to be of great practical interest. As many of the numerous attempts are dissimilar in their approach to the problem, it is not surprising that the equations that have been developed give significantly different results when used for design purposes.

Although several computational models exist in literature, none of these has been developed from a well founded theory. The only models of an acceptable nature are those based on extremal hypotheses or variational principles. Although these models apparently provide an attractive solution to river regime problems, they will have to be redefined to meet certain objections before they can be used in computational hydraulic models. Thus, existing models of flow in mobile boundary channels have only limited applicability, leaving room for further improvements in the area of model development for mobile boundary flows.

Consensus does not exist regarding the relationship which should be used to determine channel geometry or stability. A general model for describing the hydraulic geometry of a river is therefore being sought. The aim of this research project was to develop a general mathematical hydraulic model which could be used to solve problems in the field of river engineering related to the deformation of river channels under varying flow conditions.

Although any self-adjustable channel possesses five degrees-of-freedom within which change can take place through the processes of aggradation and degradation, i.e. width, depth, velocity, slope and sinuosity, these variables are insufficient to depict the hydraulic geometry of an alluvial river channel uniquely. Thus, the research emphasis was on the river regime stability problem, i.e. the determination of the equilibrium geometry of a river's cross-section, which can be formulated as follows:

> *Given a discharge and an accompanying known sediment size, what width, depth and bed slope will the river channel adopt in order to convey both the water and sediment from one point to another if the discharge is to flow between banks and over a bed, all consisting of the river's own sediment?*

Severe floods caused extensive damage to rivers in southeastern Africa during 1984 and 1987. The floods which occured in the Komati, Mkuze, Black Mfolozi and White Mfolozi rivers during 1984 together with the 1987 flood in the Mhlatuze River were the largest on record in these rivers and caused extensive bed and bank erosion.

The Department of Water Affairs and Forestry (DWA&F) performed surveys of specific river reaches (see ***Figure 1****). From the recorded maximum flood levels it was possible to determine peak discharges that had occurred and to compare these values with the depths and widths to which the alluvial rivers had been eroded. This information was used in an attempt to verify the empirical and fundamental approaches regarding alluvial river behaviour as discussed in this report.*

Results of an empirical analysis of the field data based on the theory of Blench [1957] show a fair degree of general agreement between calculated values of mean channel width and average measured values of the top width. However, the level of scatter between calculated and measured values of mean flow depth proves to be high.

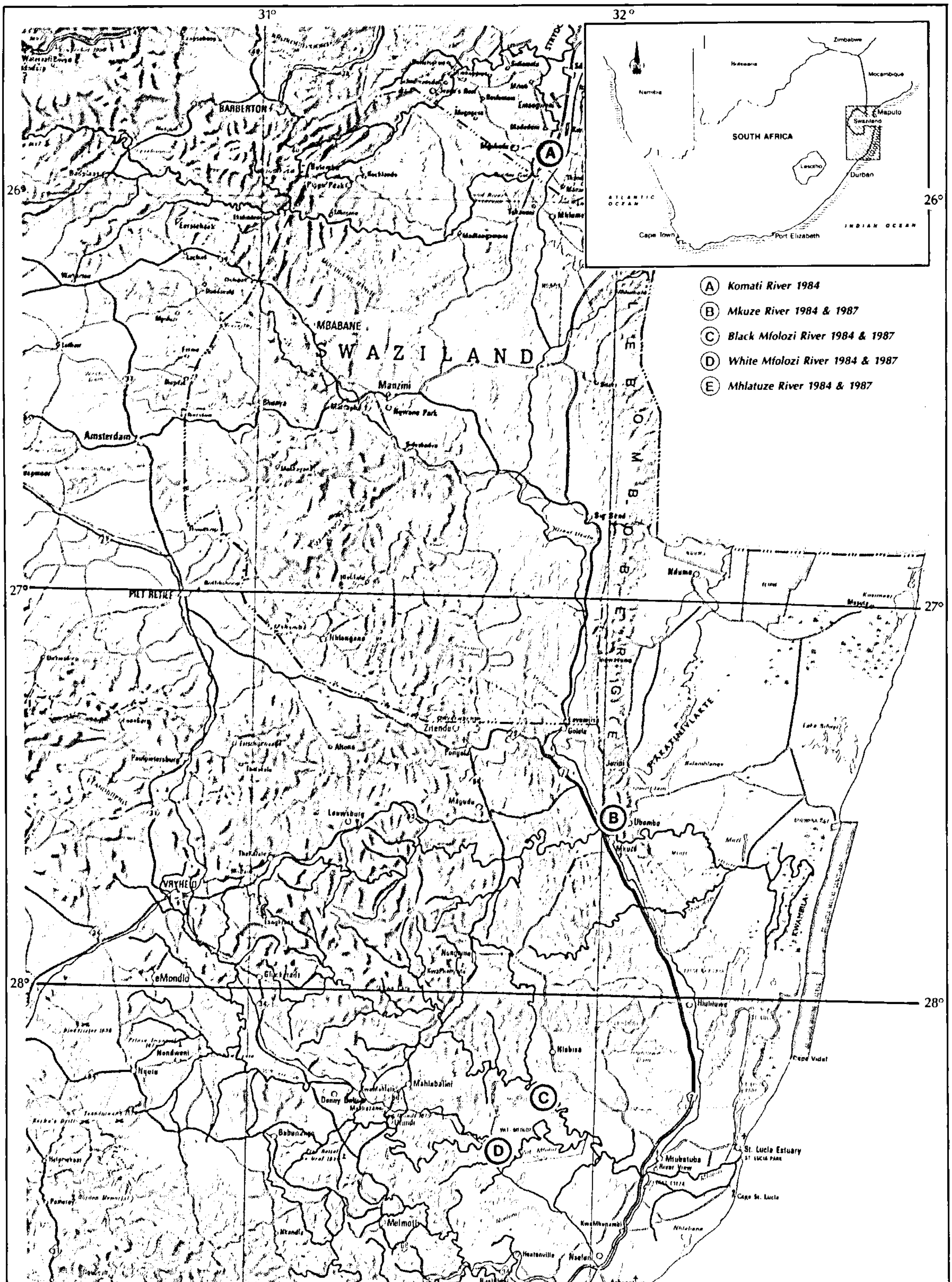
SOUTH AFRICA
ATLANTIC OCEAN
INDIAN OCEAN
Cape Town
Port Elizabeth
Durban
Maputo
Swaziland
Lesotho
Namibia
Botswana
Zimbabwe
Mocambique
(A) Komati River 1984
(B) Mkuze River 1984 & 1987
(C) Black Mfolozi River 1984 & 1987
(D) White Mfolozi River 1984 & 1987
(E) Mhlatuze River 1984 & 1987
SWAZILAND
NATAL
LEBOMBO BERGE
BARBERTON
MBABANE
Manzini
Amsterdam
PIET RETIEF
VRYHEID
eMondlo
Ulundi
Melmoth
Hluhluwe
Mtubatuba
St. Lucia Estuary
Richards Bay
Arboretum
Empangeni
Ubombo
Mkuze
Golela
26°
27°
28°
31°
32°

The analysis based on the theory of Parker [1979] shows good correlation between dimensionless parameters of top width, flow depth and discharge respectively. It has been concluded that the Parker-type empirical equations are more accurate than the Blench approach with regard to the rivers under consideration. The empirical relationships based on Parker's theory can be used as a simple but reliable method determining width and depth of a river cross-section for a given discharge and sediment size. However, it must be kept in mind that such empirical relationships provide answers for specific conditions and give no explanation of how and why a channel adjusts its hydraulic geometry according to a set of external constraints. Great care should be taken not to apply any empirical relationships out of context.

Because alluvial channel deformation primarily involves the interaction of water with the bed and banks of a channel, a logical approach to develop a method for describing alluvial channel stability needs to be based on this interaction.

It might be expected that when extremely large floods with high sediment carrying capacities occur in rivers with erodible bed and bank materials, scour will continue to take place until the erosive capacity of the stream approaches the minimum value required to transport the available material.

A stream will transport sediment only if the critical condition is exceeded. The critical stage is reached when the transporting capacity of a stream equals that which is required to dislodge material from the channel. A number of criteria have been developed which depict the critical stage where a stream's transporting capacity becomes sufficient to transport the available material. Classical examples of such criteria are presented by the Hjulström [1935], Shields [1936] and Liu [1957] diagrams.

Whilst these diagrams were developed primarily on an intuitive basis, rigorous theoretical analysis of flow transporting capacity and sediment transportability leads to the type of relationships represented in the Liu-diagram [Rooseboom, 1974; 1991]. The success of this applied power approach is attributed to the fact that both flow transporting capacity and sediment transportability can be expressed in directly comparable scalar terms.

A cross-section will just be stable when critical conditions, i.e. a state of incipient motion, exists along the stream channel. Therefore critical applied stream power $(\tau \frac{dv}{dy})$ *will be constant along the wetted perimeter [Rooseboom, 1991], i.e.*

$$\frac{(\tau \frac{dv}{dy})_{side}}{(\tau \frac{dv}{dy})_{bed}} = 1$$

If the geometry of a typical river cross-section is considered, the maximum flow depth is likely to occur near the centre. A hyperbolic cosine function has been developed to represent the cross-sectional profile. The relevant geometrical parameters for a stable hydraulic section with impending sediment motion (critical condition) all over on the wetted perimeter can all be written as functions of the flow depth at the channel centre. A problem remains in defining this maximum depth and the accompanying absolute roughness along the flow boundary.

It is a general characteristic of flowing media that whatever alternative modes of flow exist, that mode which requires the least amount of unit power will be followed. Accordingly fluid flowing over movable material will not transport such material unless this will result in a decrease in the amount of unit power which is required to maintain motion. Alternatively if two modes of yielding exists, yielding will take place according to that mode which offers the least resistance [Rooseboom, 1974].

Where flow takes place over movable material and the relatively large amount of unit power required to maintain motion along the bed becomes greater than that which would be required in the process of deformation of the bed, the stream will begin to transport the bed material rather than persist in its existing mode of flow [Rooseboom, 1974].

In terms of the concept of minimum applied power, the stream will begin to entrain particles when the power required to suspend the particles become less than the power required to maintain the status quo, i.e. incipient motion. Two distinct relationships are identified in terms of this concept [Rooseboom, 1974], i.e. the condition of incipient sediment motion under rough turbulent flow conditions which is depicted by $\frac{\sqrt{gDS}}{v_{ss}}$ = *constant with the value of the constant* $= 0{,}12$ *for values of* $\frac{\sqrt{gDS}}{\upsilon} d > 13$. *Accordingly, the relationship for values of* $\frac{\sqrt{gDS}}{\upsilon} d < 13$, *i.e. the condition of incipient motion for smooth turbulent and completely* *laminar flow (see **Figure 2**), is found to be*

$$\frac{\sqrt{gDS}}{v_{ss}} = \frac{1{,}6}{\frac{\sqrt{gDS}}{\upsilon}\, d}$$

with g representing acceleration due to gravity, D the depth of flow, S the energy slope, υ the kinematic viscosity (of water), d the sediment particle size and v_{ss} the settling velocity of the sediment particles.

***Table 1** contains measured data and derived values of $\frac{\sqrt{gDS}}{v_{ss}}$ and $\frac{\sqrt{gDS}}{\upsilon} d_{85}$ for the different river reaches under consideration.*

Table 1: Sediment characteristics and flow parameters

Site	River	Year	Representative particle diameter d_{85} (mm)	Absolute roughness k_s (m)	Settling velocity v_{ss} (m/s)	Liu-diagram parameters		
						$\frac{\sqrt{gDS}}{v_{ss}}$	$\frac{\sqrt{gDS}}{\upsilon} d_{85}$	$\frac{\sqrt{gDS}}{v_{ss}}\left(\frac{d_{85}}{k_s}\right)^{1/3}$
A84	Komati	1984	2,33	1,13	0,217	1,33	672	0,167
B84	Mkuze	1984	0,429	1,5	0,063	6,52	176,21	0,423
B87	Mkuze	1987	0,88	1,28	0,113	2,53	251,6	0,222
C84	Black Mfolozi	1984	0,205	1,48	0,028	16,3	93,56	0,803
C87	Black Mfolozi	1987	0,530	0,89	0,076	3,84	154,68	0,32
D84	White Mfolozi	1984	0,605	1,16	0,085	4,14	212,9	0,331
D87	White Mfolozi	1987	1,7	0,8	0,178	1,81	547,7	0,228
E84	Mhlatuze	1984	0,368	1,11	0,055	8,63	174,67	0,592
E87	Mhlatuze	1987	0,471	0,87	0,069	6,31	214,82	0,528

*By plotting the functions $\frac{\sqrt{gDS}}{v_{ss}}$ and $\frac{\sqrt{gDS}}{\upsilon} d_{85}$ on the Liu-diagram (**Figure 2**) the variation in $\frac{\sqrt{gDS}}{v_{ss}}$ follows the same pattern as for laminar boundary conditions and the question arises as to whether viscosity does come into the picture. Whereas one expects in terms of the Liu-diagram that the value of $\frac{\sqrt{gDS}}{v_{ss}}$ should be constant for cases where turbulent boundary layer flow conditions ought to prevail, the recorded values presented in **Table 1** vary significantly. All the evidence seems to indicate that somehow, even under extreme flood conditions, laminar boundary conditions develop below the highly turbulent*

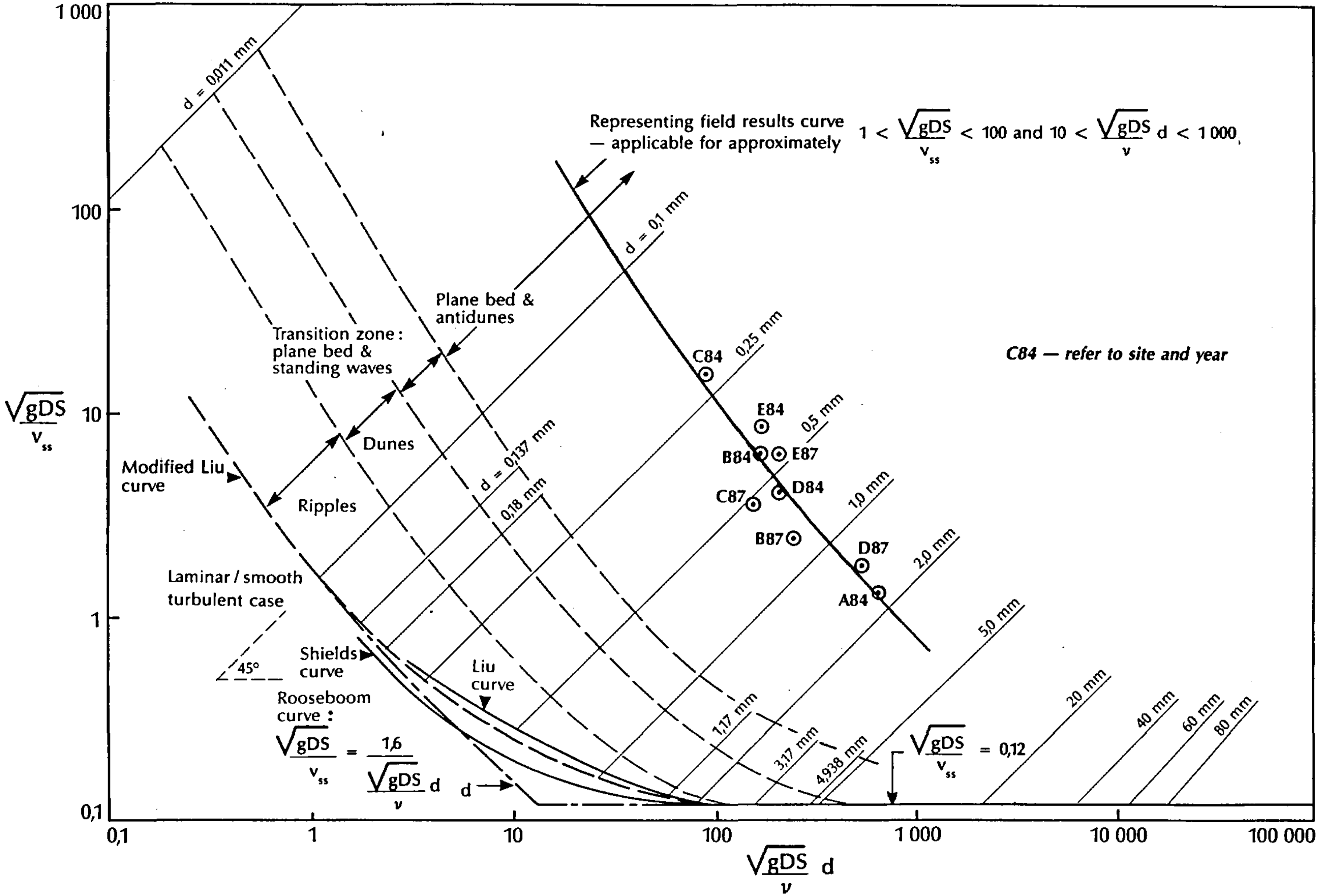

Representing field results curve
— applicable for approximately $1 < \frac{\sqrt{gDS}}{v_{ss}} < 100$ and $10 < \frac{\sqrt{gDS}}{\nu} d < 1000$
d = 0,011 mm
d = 0,1 mm
0,25 mm
0,5 mm
1,0 mm
2,0 mm
5,0 mm
20 mm
40 mm
60 mm
80 mm
d = 0,137 mm
0,18 mm
1,17 mm
3,17 mm
4,938 mm
Plane bed & antidunes
Transition zone: plane bed & standing waves
Dunes
Ripples
Modified Liu curve
Laminar / smooth turbulent case
45°
Shields curve
Liu curve
Rooseboom curve: $\frac{\sqrt{gDS}}{v_{ss}} = \frac{1,6}{\frac{\sqrt{gDS}}{\nu} d}$
d
$\frac{\sqrt{gDS}}{v_{ss}} = 0,12$
C84 — refer to site and year
C84
E84
B84
E87
C87
D84
B87
D87
A84
$\frac{\sqrt{gDS}}{v_{ss}}$
$\frac{\sqrt{gDS}}{\nu} d$
1 000
100
10
1
0,1
0,1
1
10
100
1 000
10 000
100 000

flows that prevail above. However, the influence of the absolute roughness k_s *should be taken into account in the determination of the Liu-diagram parameters.*

In the original mathematical derivation of the parameter $\frac{\sqrt{gDS}}{v_{ss}}$ *used in the Liu-diagram, Rooseboom [1974] proved to represent the ratio*

$$\frac{\textit{unit applied power along bed}}{\textit{unit power required to suspend sediment particles}}$$

Because of the fact that the power being applied along the bed by the flowing fluid is a function of the size of the eddies along the bed, allowance has to be made for varying eddy size. The original derivation assumed a flat bed with the diameter of turbulent boundary layer eddies $\approx$ *particle diameter.*

Thus, when the bed is not flat, the particle diameter d *is no longer representative of the absolute roughness* k_s *and the power being applied along the bed becomes proportional to* $\frac{\rho g DS\sqrt{gDS}}{k_s}$ *instead of* $\frac{\rho g DS\sqrt{gDS}}{d}$.

The amount of unit stream power applied along the bed can be reduced through the formation of ripples, dunes, etc. whereby eddies with larger radii are formed along the beds. The absolute roughness k_s *is determined by the size of these eddies. As the even bed of a river is deformed through the deformation of bedforms, the absolute roughness value* k_s *increases proportionally with the size of the eddies being formed inbetween the bedforms.*

As the value of the absolute roughness k_s *increases, the transporting capacity, represented by the applied power function, decreases, whilst the unit power required to suspend particles with a given settling velocity remains the same, namely* $(\rho_s-\rho)gv_{ss}$. *Critical conditions are now represented by* $\frac{\sqrt{gDS}}{v_{ss}} = \textit{constant}\left(\frac{k_s}{d}\right)^{\frac{1}{3}}$ *which indicates that* $\frac{\sqrt{gDS}}{v_{ss}} \neq \textit{constant}$ *for alluvial river flows with bed irregularities leading to increased eddy sizes and representative absolute roughness* (k_s) *values. Recorded values of the function* $\frac{\sqrt{gDS}}{v_{ss}}\left(\frac{d_{85}}{k_s}\right)^{1/3}$ *presented in* ***Table 1****, however, vary considerably and differ greatly from the expected constant value of 0,12.*

Mere adjustment of the $\frac{\sqrt{gDS}}{v_{ss}}$ *parameter to allow for variations in absolute roughness and consequential variation in applied power therefore does not clarify matters.*

With the river behaviour being described by using the absolute roughness k_s *instead of the particle diameter* ***d*** *in describing the relationship between the applied unit stream power maintaining motion along the bed and unit power required to suspend a particle it is evident that in the case of flow over a flat alluvial bed, there may exist a laminar boundary layer or laminar sub-layer against the boundary even if the main flow is turbulent. Viscosity is dominant in such a laminar zone. If the laminar zone, which is usually very thin, is considered as an interface between the superposed fluid and the alluvial bed, the problem of alluvial river behaviour at equilibrium or critical conditions will become a problem of interface instability.*

With reference to ***Figure 3*** *the turbulent boundary eddies depicted in size by* k_s *represent the turbulent boundary conditions. As their size is increased through deformation of the bed, the applied (turbulent) power along the bed given by*

$$\text{applied power} \propto \frac{\rho g D S \sqrt{gDS}}{k_s}$$

decreases.

It must be expected that the value of this function will drop to the point where it approaches the critical value when equilibrium scour is approached. If it is assumed that a laminar boundary layer develops below the eddy, the applied (turbulent) power will be $\propto$ *(laminar) power required to pick up the particles. There is good reason for believing that laminar boundary conditions will develop. It is evident from* ***Figure 2*** *that for sand particles less than say 2 mm in diameter incipient motion is always associated with laminar boundary conditions. Accordingly*

$$\rho g D S \frac{\sqrt{gDS}}{k_s} \propto (\rho_s - \rho) g v_{ss}$$

with v_{ss} *the settling velocity under viscous conditions. Substitution of* v_{ss} *for laminar suspension leads to*

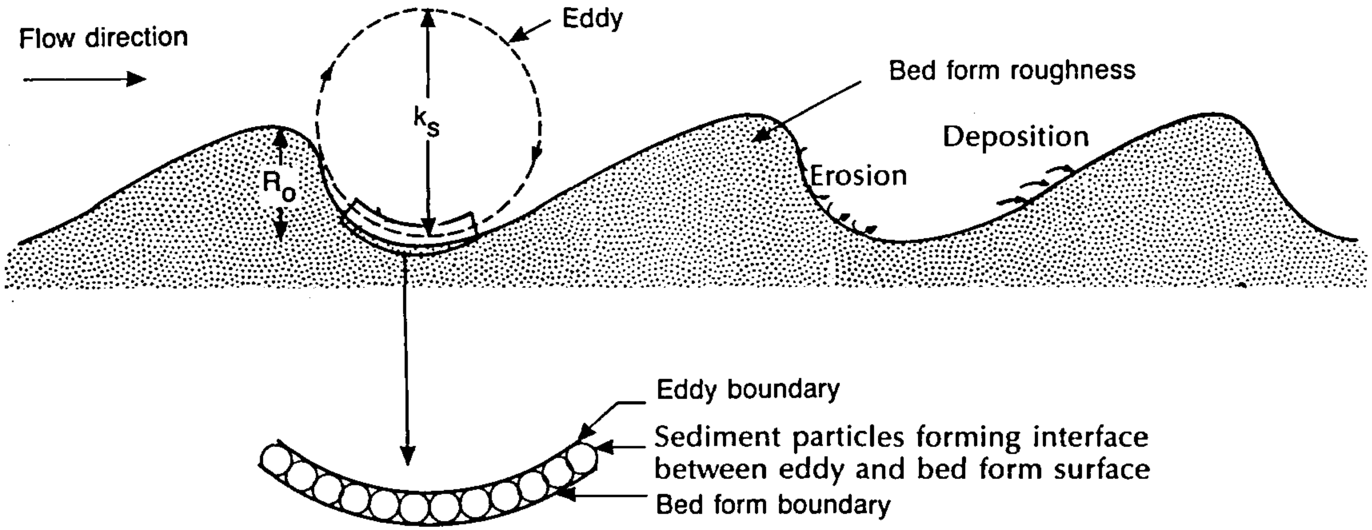
Flow direction
Eddy
k_s
R_o
Bed form roughness
Deposition
Erosion
Eddy boundary
Sediment particles forming interface between eddy and bed form surface
Bed form boundary

$$\frac{\sqrt{gDS}}{v_{ss}} \propto \sqrt{\frac{k_s}{d}\,\frac{1}{\frac{\sqrt{gDS}}{\upsilon}\,d}}$$

Using the data in ***Table 1,*** *the validity of this relationship appears to be fully indicated in* ***Figure 4*** *which can be approximated by*

$$\frac{\sqrt{gDS}}{v_{ss}} = 1{,}63\sqrt{\frac{k_s}{d}\,\frac{1}{\frac{\sqrt{gDS}}{\upsilon}\,d}}$$

By equating the applied unit turbulent power along the bed with the unit power required to suspend the particles, it is thus possible to determinate at what stage a sand bed river will reach equilibrium in terms of scouring its bed. The relationship between applied stream power and power required to entrain sediment as depicted on the Liu-diagram ***(Figure 2)*** *can thus be applied to predict maximum scour depths.*

It was the aim to test the fundamental approach involving critical applied stream power along the flow boundary and equilibrium flow conditions against the field data.

Although the fundamental approach is based on the energy slope, cross-sectional geometry was predicted using both the energy slope S_f *which was determined by means of the* ***CFP*** *program and the bed slope* S_o *which was either known before a flood or obtained form 1:50 000 maps.*

Results of the verification of the fundamental approach are presented in ***Table 2.***

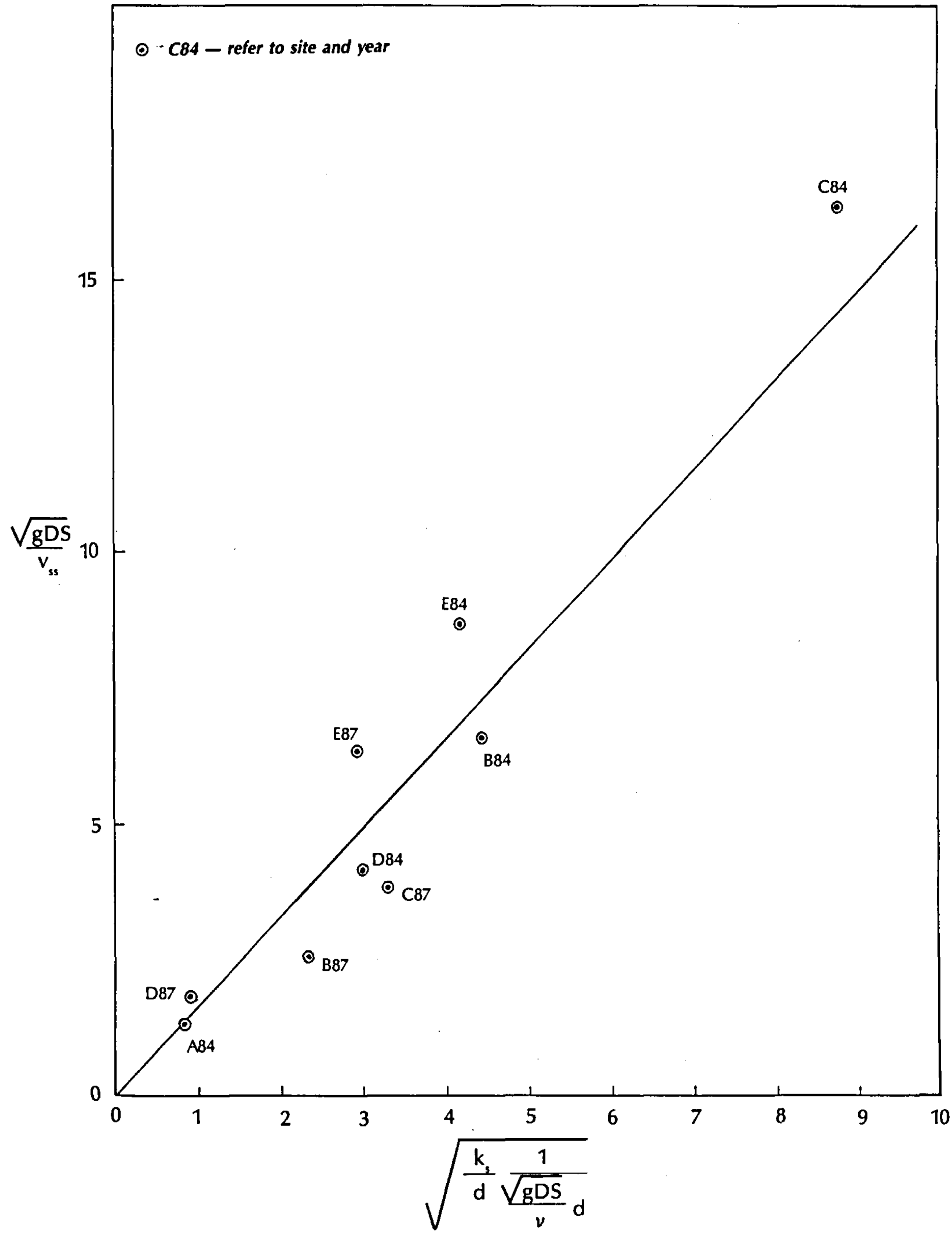
⊙ C84 — refer to site and year
C84
E84
E87
B84
D84
C87
B87
D87
A84
0
5
10
15
0
1
2
3
4
5
6
7
8
9
10
$\frac{\sqrt{gDS}}{v_{ss}}$
$\sqrt{\frac{k_s}{d}\frac{1}{\frac{\sqrt{gDS}}{\nu}d}}$

Table 2: Comparison between observed and predicted reach averaged values of flow depth and width

Site	River	Year	Observed river behaviour			Predicted river behaviour						Comments
			Flow depth	Bottom width	Top width[1]	Bed slope[2]			Energy slope[3]			
			D_f (m)	B_m (m)	B_T (m)	Flow depth D_f (m)	Bottom width B_m (m)	Top width B_T (m)	Flow depth D_f (m)	Bottom width B_m (m)	Top width B_T (m)	
A84	Komati	1984	11,0	57,8	168,6	13,2	41,2	76	10,75	60	88,3	satisfactory prediction except for under-estimation of top width
B84	Mkuze	1984	11,5	103,2	275,2	12,3	79,2	111,6	11	94,4	123,4	satisfactory prediction except for under-estimation of top width
B87	Mkuze	1987	4	95,9	132,2	4,8	58,4	71	5,9	42,6	58,1	unsatisfactory prediction
C84	Black Mfolozi	1984	15,2	105,3	566,1	15	116,9	156,4	13,85	131,8	168,5	satisfactory prediction except for under-estimation of top width
C87	Black Mfolozi	1987	5,2	107,8	153,7	11,7	19,1	49,9	8,6	37,35	60,05	unsatisfactory prediction
D84	White Mfolozi	1984	12,4	119,8	304,9	13,2	92,3	127,1	13,3	90,8	125,8	satisfactory prediction except for under-estimation of top width
D87	White Mfolozi	1987	5	112,8	177,7	6,88	85	103,1	5,2	125,9	139,6	prediction satisfactory
E84	Mhlatuze	1984	6,7	57,3	131,5	13,3	21,2	56,2	5,3	106,5	120,5	unsatisfactory prediction
E87	Mhlatuze	1987	7,4	85,7	154,8	13,0	42,0	76,2	6,2	133,7	150	unsatisfactory prediction

[1] *according to CFP (included overbank flow)*
[2] *according to bed slope* S_e
[3] *according to energy slope* S_f

The application of the fundamental approach to measured river cross-sections indicated that some of the field data do not exactly represent the assumed critical or equilibrium condition. This can be attributed to:

- *i) time lag between time of flood and time of survey, i.e. influence of other inbetween flows*
- *ii) non-representative sample of sediment due to variation in sediment characteristics with depth*
- *iii) assuming bank material to be alluvial*
- *iv) approximation of bank roughness by using an overall roughness parameter for a cross section*
- *v) ignoring vegetation, especially bank vegetation*
- *vi) approximate discharge calculation of flow by means of the slope-area method*
- *vii) influence of sinuosity*
- *viii) the fact that southern African rivers do not flow at bankfull stage for long periods, but only for short times.*

The most important of these factors might be the simplified way in which the banks were represented in the analysis. This is reflected in the differences between predicted and actual observed channel widths, especially with top widths generally being under-estimated. However, it can be concluded that the scoured sections of the alluvial rivers as surveyed point to equilibrium being approached during the floods of 1984 and 1987. The surveyed depths can thus be regarded as being critical or very near to critical.

The fundamental approach regarding alluvial river behaviour shows much promise. The fact that it can be proved, that, whilst rivers experience bed form changes, limiting scour conditions can still be expressed in terms of the basic relationship which depict critical conditions, is a valuable contribution to river hydraulics. Although cross-sectional geometry is not predicted accurately in all cases, the fundamental approach provides insight into the deformation of river channels during extreme floods.

This analysis is also the first calibration of the ***Rooseboom theory*** *regarding critical conditions by means of field data representing extreme flood conditions. A most important result is the ability to predict absolute roughness values.*

The results of this study can be used to predict aggradation (deposition) and degradation (erosion) of sand bed stream channels in a simplified way. This can be done by means of the empirical approach based on Parker's theory or the fundamental approach as developed in this report.

The empirical approach can only predict an average top width and a flow depth without any indication of channel shape. Care should also be taken to apply empirical relationships for circumstances comparable to those originally analysed and not out of context. The fundamental approach, on the other hand, can be used for predictions of top width, bottom width, average flow depth and channel shape. Although top width may be under-estimated, the methodology could be improved in future research by allowing for bank retreat, bank material characteristics and bank vegetation. Such a geomorphological model could easily be linked to the more sophisticated open channel hydraulic flow models to predict loose boundary channel flow behaviour.

It is suggested that the accuracy of predictions of hydraulic geometry can be markedly improved by future research through empirical modification of the calculated widths and depths to account for bank material and vegetation effects. Adequate field research and additional information on the geomorphological characteristics, i.e. strength properties of bank material, are needed and should be recorded with particular attention to the type of bank material and the type and density of bank vegetation. This, together with information regarding the bed level variation at the banks could help in the explanation of channel width variations.

6615G/sw
1993-06-01

ACKNOWLEDGEMENTS

The research in this report emanated from a project funded by the Water Research Commission and entitled:

The development of a model to simulate flow in alluvial rivers.

The Steering Committee responsible for this project, consisted of the following persons:

Mr H C Chapman	Water Research Commission (Chairman)
Mr P W Weideman	Water Research Commission (Secretary)
Mr H Maaren	Water Research Commission
Dr G W Annandale	Steffen Robertson and Kirsten Incorporated (till April 1991)
Prof A Rooseboom	University of Stellenbosch (from April 1991)
Dr M S Basson	BKS Incorporated
Mr A du P le Grange	BKS Incorporated (Researcher)
Dr S C J Joubert	National Parks Board
Mr R N Porter	Natal Parks Board
Mr Z P Kovács	Department of Water Affairs and Forestry
Mr D van Bladeren	Department of Water Affairs and Forestry
Mr J v R Stander	Department of Environment Affairs
Mr P J Strumpher	Department of Agricultural Development

The financing of the project by the Water Research Commission and the contribution of the members of the Steering Committee is acknowledged gratefully.

This project was only possible with the co-operation of many individuals and institutions. The authors therefore wish to record their sincere thanks to the following:

Water Research Commission for financing and extension of the project, and particularly **Mr H C Chapman** and **Mr P W Weideman** for their receptiveness of circumstances;

Dr G W Annandale (Steffen Robertson and Kirsten Inc) who initiated the project;

BKS Incorporated for the research opportunity, in particularly **Dr M S Basson** and **Dr S J van Vuuren** for their continuous interest and support. **Dr Basson's** continuous inspiration is highly appreciated;

Department of Water Affairs and Forestry, in particularly **Mr Z Kovács, Mr D van Bladeren** and **Mr P Boshoff** for field data and personal experience of floods. **Mr Van Bladeren's** knowledge of field circumstances, supplying of data and continuous willing to help was of great benefit to this project and is greatly appreciated;

Natal Parks Board for the permission to use the two survey sites in the Mfolozi Game Reserve, and in particularly **Mr R N Porter**, as initial contact with the Natal Parks Board, and **Mr T Sandwith** of the Mfolozi Game Reserve for his assistance and help during field surveys;

Engineering Computing Company, a venture of **Ninham Shand Inc**, for the contribution of the Channel Flow Profile (CFP) program to the research project;

Mrs M Mertz, librarian of BKS Inc, for going out of her way in getting applicable literature for this study;

Mr C de Ruyter, Merss J Erasmus, E Pienaar, L Gallagher, W Gous, H van Loggerenberg, K van Rensburg, S Whiteman and **Misses S Vermaak** and **R Coetzee**, all of BKS Inc, and **Miss E Feldman** of Repro for the technical grooming of the project report.

A special word of thanks is recorded to **Prof A Rooseboom (University of Stellenbosch)** who was involved as specialist advisor since April 1991 for his valuable contribution to the project. His guidance was of great benefit to this project. It was a great opportunity to be guided by an expert like him.

TABLE OF CONTENTS

LIST OF FIGURES

LIST OF TABLES

LIST OF SYMBOLS

A	:	flow area
A_s	:	flow area of side channel
a	:	coefficient
B	:	width, bottom width
$\bar{B}$	:	mean channel width
B_m	:	width of centre channel section
B_s	:	top width of side channel section
B_T	:	top width of total channel
B_T^*	:	dimensionless top width
b	:	exponent
C_d	:	drag coefficient
CA	:	catchment area
c	:	coefficient, cohesion parameter, subscript referring to critical conditions
D, $\bar{D}$	:	cross-sectionally averaged (hydraulic) depth
D_s	:	surveyed flow depth
D_f	:	calculated flow depth according to energy slope
D_o	:	calculated flow depth according to bottom slope
D^*	:	dimensionless flow depth
d	:	representative sediment diameter, differential
d_{50}	:	mean sediment particle size (diameter)
d_{85}	:	size of sediment material for which 85 percent is finer
$\frac{dv}{dy}$	:	velocity gradient
dSV	:	calculation interval
F_s	:	Blench side factor
f	:	friction factor, silt factor, function, exponent
g	:	gravity acceleration
k	:	coefficient, constant
k_s	:	absolute roughness height
M	:	momentum
MAP	:	mean annual precipitation
MAR	:	mean annual rainfall
m	:	mass, exponent
n	:	constant, Manning roughness coefficient
o	:	subscript referring to bed

P	:	wetted perimeter
P_s	:	wetted perimeter of side channel
p	:	pressure, storm rain
Q	:	water discharge, flood peak
Q_m	:	water discharge through centre channel section
Q_s	:	sediment discharge, water discharge through side channel section
Q_t	:	total water discharge
$\tilde{Q}$	:	dimensionless water discharge
Q_*	:	dimensionless sediment discharge
q	:	unit water discharge
R	:	hydraulic radius, radius of eddy
R_s	:	hydraulic radius of side channel
R_o	:	radius of eddy on bottom/bed
R_{eff}	:	effective eddy radius
R_e	:	Reynolds number
R_*	:	particle/sedimentation Reynolds number
r	:	inner radius of eddy element, correlation coefficient
S	:	slope
S_f	:	energy slope
S_o	:	bottom slope
S_w	:	water level slope
SA	:	slope area
SV	:	stake value
s	:	subscript referring to side/bank or sediment, sinuosity
T	:	return period
TR	:	Technical Report
TW	:	top width (used in Appendix A)
V	:	volume
W	:	weight
δt	:	time interval
u	:	eddy element velocity perpendicular to stream direction
v	:	flow velocity, eddy element velocity in stream direction
$\bar{v}$	:	mean flow velocity
v_*	:	shear velocity
v^*	:	dimensionless velocity
v_{ss}	:	fall or settling velocity

x	:	x-direction
y	:	y-direction, flow depth
y_o	:	flow depth where flow velocity equals zero
α	:	velocity coefficient, angle
γ	:	specific weight
Δ	:	incremental
δ	:	differential
κ	:	von Karman constant
ℓ	:	Prandtl mixing length
μ	:	dynamic viscosity
υ	:	kinematic viscosity
ρ	:	density of water sediment mixture
ρ_s	:	density of sediment
τ	:	shear stress
τ_o	:	shear stress on bed
τ_s	:	fluid shear stress on bank (side slope)
θ	:	angle of side slope
ϕ	:	angle of repose of bank material
$\phi_{1,2,3}$	:	function
$\propto$	:	proportional to

"Nature is a labyrinth in which
the very haste you move with
will make you lose your way."

Francis Bacon

"Although this may seem a
paradox, all exact science
is dominated by the idea of
approximation."

Bertrand Russell

"Man was not born to solve the
problems of the Universe, but to
put his finger on the problem
and then to keep within the
limits of the comprehensible."

J W von Goethe

1. INTRODUCTION

1.1 GENERAL

Since earliest times rivers have played keyroles in most civilizations. Various human projects have, therefore, been undertaken for the utilization of river run-off and to reduce the destructive power of floods.

A river course is often considered as to be static, i.e. unchanging in shape, dimensions and pattern. However, the flow in a river generally varies with time, and as a result the river is continually changing its position and shape as a result of hydraulic forces acting on its bed and banks. These changes may take place slowly or rapidly and may be caused by natural environmental changes or by man's activities.

The geometry of an alluvial river channel is determined by the interaction between flowing water, the magnitude and characteristics of the sediment load as well as the composition of the bed and bank materials. Physical characteristics of channels include their cross-sectional geometry, the configuration of the bed including components of bed roughness, the longitudinal profile of the river channel, and the channel pattern, i.e. the configuration of the river in plan - straight, meandering, or braided.

1.2 JUSTIFICATION

South Africa's scarce water resources have reached a very high level of utilization and appropriated technology is required to manage them and to assess the influence of current and future developments on the environment. It has been estimated that the direct and indirect costs due to the impacts of sediment loads of rivers in southern Africa amount to millions of Rand annually *[Braune, 1984]*.

It was also concluded at the 1987 - *International Conference on River Regime* (Wallingford, England) that the complexities of river regime changes have been underestimated for a long time and that very little is actually known of the behaviour of river channels.

Reservoir sedimentation, scour damage to bridge structures, flooding of developed areas, damage to the natural environment, etc. are some typical examples of the impacts of the water-sediment mixture in rivers.

A model which can be used to predict alluvial river behaviour will facilitate investigation into these problems and will be of assistance in river engineering work.

Several computational models like MOBED *[Krishnappan, 1981]*, IALLUVIAL *[Karim et al., 1982]*, FLUVIAL *[Chang and Hill, 1977; etc.]*, GSTARS *[Yang et al., 1988]*, etc. exist in the literature. However, none of these has been developed from founded theory. The only models of an acceptable nature are those based on as extremal hypotheses or variational principles *[Davies and Sutherland, 1983; Griffiths, 1984]*.

Although the variational approach or extremal hypothesis apparently provides the appearance of an attractive solution to river regime, the hypotheses will have to be redefined to meet certain objections before they can be used in computational hydraulic models. Results which are incompatible with observations have been obtained thus far *[Griffiths, 1984]*.

Consensus does not exist regarding the relationship which should be used to determine channel geometry or stability. Thus, existing models of flow in mobile boundary channels have only limited applicability *[Krishnappan, 1985]*, leaving room for further improvements in the area of model development for mobile boundary flows. A general model for describing the hydraulic geometry of a river is therefore being sought.

1.3 AIM OF RESEARCH PROPOSAL

The aim of the research project was to develop a model to simulate flow in alluvial rivers. Possible fields of application are the:

i) calculation of aggradation and degradation in river channels due to changes in flow regime resulting from water resource development

ii) modelling of the time-dependent behaviour of water levels, flow velocities and discharges in deformable alluvial river channels

iii) development of management policies for the simulation of natural floods in developed river basins to preserve ecologies

iv) modelling of the effect of changes in flow on the scour and deposition of sediment in river meanders

v) modelling of the effect of interbasin transfer of water on the channel geometry of receiving streams due to continuous increased discharge, especially along the upper reaches of rivers

vi) modelling of sediment aggradation and degradation in river mouths and estuaries

vii) modelling of sediment deposition in reservoirs.

It needs to be emphasised that it was not the intend to solve all these problems during the course of the proposed research project. The aim of the proposed research project was to develop a general mathematical hydraulic model which can be used to study various problems in the field of river engineering.

The intention was to validate the model by using existing data which had been collected by the Department of Water Affairs and Forestry (DWA&F) on alluvial rivers and also to make use of data to be collected during the course of the proposed research project.

Whilst the original aim was to develop a comprehensive model, there was a change of emphasis during the project.

1.4 RESEARCH EMPHASIS CHANGE

1.4.1 <u>General</u>

During the course of the research it was concluded that the most fundamental challenge in modelling river regime still is to be able to predict changes in cross-section accurately.

The general problem of alluvial channel stability revolves around the question as to how a river channel with deformable boundaries react to changing water and sediment discharges. It is the interplay of the fluid and the material along the wetted perimeter that determine the hydraulic geometry. With an equilibrium hydraulic geometry the water and sediment (if any) supplied to the channel are transported without any significant net erosion or deposition on the bed and banks.

The problem of the determination of the geometry of a river's cross-section can be formulated as:

> *Given a discharge and an accompanying known sediment size, what width, depth and bed slope will the river channel adopt in order to convey both the water and sediment from one point to another if the discharge is to flow between banks and over a bed, all consisting of the river's own sediment?*

The solution should be based on fundamental principles. In terms of the changed emphasis an additional tool was sought which would be easier to use and to understand than a complex computational model. Such a tool could then be linked to an existing computer flow model.

This report contains a discussion on the regime behaviour of rivers and factors influencing it, as well as tools for solving the river stability problem based on two approaches:

i) an empirical approach based on measured field data
ii) a fundamental approach based on theoretical principles and verified with field data.

1.4.2 Empirical approach

Empirical regime theory has little firm theoretical basis but, from experience over almost a century, has proven to present an approximate representation of the dominant aspects of channel geometry *[Bettess et al., 1988]*.

The results of

i) the verification of Blench's regime theory as well as
ii) Parker's dimensional analysis

for southern African alluvial river conditions are presented in this report.

1.4.3 Fundamental approach

A fundamental approach based on hydraulic principles, applied stream power theory and critical conditions is presented for the solution to the problem of river regime or cross-sectional variability.

This approach has been based on:

i) the basic hydraulic principles of flow in alluvial river channels
ii) constant applied stream power along the wetted perimeter of the stream
iii) the use of critical entrainment functions.

6607G/KvR/sv/sw
1993-03-25

2. HISTORY OF HYDRAULICS AND RIVER MECHANICS

2.1 INTRODUCTION

Hydraulics was part of ancient science. A relationship has existed between man and rivers since the beginning of civilization because water has always been an integral part in man's development. Even the oldest discovered hydraulic achievements give evidence that man had knowledge and appreciation of what water can do to man and what man can do to water. There is sufficient historic and even prehistoric evidence that man did study natural streams - and at times even changed or realigned them - e.g. the Egyptians and Babylonians who constructed canals, both for irrigation and for defensive purposes. River channels, canals, and aqueducts are also found as part of extensive irrigation systems in China, as part of a dense net of waterways in Mesopotamia, and as part of domestic water supply systems throughout the Roman Empire *[Graf, 1971; Shen, 1971a]*.

Apparently no attempts were made at that time to discover or, if they did, to record those laws of nature that governed the water and sediment movement in these watercourses. It would be surprising if the engineers of the remote past who handed down knowledge from generation to generation did not have insight into the movement of water. Although they did not have the aid of formulas, which are based on rational deductions, it did not hamper them in their pursuit of greatness *[Graf, 1971]*.

The first notable attempts to analyse pressure and flow patterns were undertaken by the Greeks. Development continued slowly until the time of the Renaissance, when men such as *Leonardo Da Vinci* began to publish the result of their observations. Ideas which emerged then, respecting conservation of mass, frictional resistance, etc. are still in use, although sometimes in a more refined form *[Graf, 1971]*.

2.2 HYDRAULICS AS A SCIENCE

The genius of the Italian Renaissance, *Leonardo da Vinci*, showed a keen interest in the problem of water flow not only as a practising engineer but also as an experimenter. The following statements by *Da Vinci* are quoted directly from *Rouse and Ince [1957]*:

"A straight river with equal width, depth, and slope requires a degree of velocity for each degree of motion. This is evident from the proportion of motion according to which an object, the more it moves in its own natural course, the more it gathers speed as in any other matter.

Water has higher speed on the surface than at the bottom. This happens because water on the surface borders on air which is of little resistance ... and water at the bottom is touching the earth which is of high resistance......."

Domenico Guglielmini stated *[Rouse and Ince, 1957]*:

"A stream with sufficient velocity scours its bed, and with the increase in depth the slope is lessened, and late in its motion, if it turns turbid, the stream will deposit sediment on the bed........

It is certain that a stream widens and deepens in proportion to the violence of the motion which erodes and carries away the earth that forms its sides and bottom; it is therefore necessary that the scouring force be greater than the resistance of the earth or other materials that forms the bed ... It is always necessary to say that in the scouring process of a stream either the force of the water gradually decreases or the resistance of the soil increases ... until some sort of equilibrium is reached".

Other contributions to the history of river mechanics were given by *Du Buat* who published the second edition of "*Principles D'Hydraulique*" in 1786 in which the formation and migration of sand dunes, stability of channel cross-sections, bottom velocity, bed-armoring, fluvial morphology, etc. were discussed *[Graf, 1971]*. On the other hand, a man like *De Saint Venant* devoted his efforts to gradually varied open channel flow problems. Various other contributions and efforts were made to the study of river mechanics and hydraulics.

The foundations, when and where hydraulics, and in particular channel and river hydraulics, began is hidden in antiquity and probably will remain so.

3. THE ALLUVIAL RIVER CHANNEL STABILITY PROBLEM

3.1 INTRODUCTION

Alluvial channels are very dynamic and experience significant changes in depth, width, alignment and stability with time, particularly during floods of long duration. These changes are closely interrelated to each other and may be defined as *scour, degradation, aggradation* and *lateral migration* which can occur naturally or as a result of a change in the environment.

In contrast to *scour*, which refers to local and often temporary lowering of bed levels over a short distance, the terms *degradation* and *aggradation* implies an extensive and often progressive lowering or raising, respectively of the river-bed over a fairly long distance. *Lateral migration* results from bank line shifting and bank sloughing.

The general and enigmatic problem of river regime or alluvial channel stability is the prediction of how a river reach adjusts to transmit imposed water and sediment discharges. Rivers with boundaries composed of non-cohesive materials possess self-formed active beds and banks. Thus, the stability problem is dualistic because a description is required of both the container and the flow *[Parker, 1978]*.

The problem of determining a stable, cross-sectional geometry and slope for an alluvial channel has been the subject of considerable research and continues to be of great practical interest. As many of the numerous attempts are dissimilar in their approach to the problem it is not surprising that the equations that have been developed give significantly different results when used for design purposes. This has led to the suggestion that the problem is indeterminate despite the observed regularity of channel shapes and patterns.

A common formulation *[Henderson, 1966]* is to ignore plan geometry and to attempt to resolve relationships between six pertinent variables: water discharge, sediment discharge, sediment size and channel width, depth and slope.

In order to visualize the interdependence of all the variables involved it is convenient to adopt a design viewpoint of some channel carrying specified flows of water and sediment. In most cases the first three variables are known and form the original specification of the problem. The remaining three are unknown and would be determined absolutely if three governing relationships were absolutely determinate. The governing relationships must be a resistance equation, a sediment transport equation, and a limitation imposed by bank stability. However, this is not so: the bank competence criterion does not completely determine the width-to-depth ratio, but merely sets a lower limit to it *[Henderson, 1966]*.

Ignoring plan geometry, an alluvial channel can adjust its width, depth, slope and velocity to achieve a stable condition in which it can transport a certain amount of water and sediment. Thus, it has four degrees-of-freedom and the problem is to establish relationships which determine these four quantities of width, depth, slope and velocity. According to *Blench [1961]* a fifth degree of freedom develops if the canal - and especially a river - is left all by itself. Artificially straight sections are found to be unstable, erosive attacks at the sides will increase and ultimately develop into meanders. This fifth degree of freedom can be described as a channel's sinuosity.

However, any system with more than one degree of freedom will take considerable time - depending on the number of degrees - until equilibrium is reached. Researchers in this field have chosen to replace the word *equilibrium* with *regime*. Some controversies have existed and, at times, still exist about the proper definition of regime. *Inglis [1949]* gives this definition:

> *"Channels which do not alter appreciably from year to year - though they may vary during the year - are said to be in regime ...."*

Blench [1961] says:

> *"Regime suggests considerable freedom of individual behaviour within a framework of laws and has no short-period connotation ..... the term regime channel will be used, meaning that it is capable of acquiring regime, or equilibrium eventually by self-adjustment of its non-fluid boundaries, if the imposed conditions do not change on a long-term average ....."*

Blench [1969] defines *regime* as:

> *"…. the behaviour of a channel, over a period, based on conditions of water and sediment discharge, breadth, depth, slope, meander form and progress, bar movement, etc. …."*

Unconventionally, but descriptively, *Blench [1969]* stated that *regime* can be called *"the climate of a channel"* since it implies a behaviour that is appreciated in terms of many fluctuating factors whose average values, over a sufficient period, are either steady or change relatively slowly.

The relationship between the discharge (of water and sediment) to be conveyed and the channel geometry to be established in the soil material must be subject to investigation. The general problem of channel stability can thus be expressed as:

> *How will a river or canal adjust its channel so as to accommodate itself to the water and sediment flow which are fed into it?*

3.2 DEGREES-OF-FREEDOM

Although natural channels are free to adjust their overall width, depth, slope, velocity and sinuosity, these five variables are insufficient to uniquely define the hydraulic geometry of alluvial channels.

Firstly, the cross-sectional geometry of a channel is not accurately defined by width and average depth. There are a multiplicity of shapes for a given width and average depth. With the exception of minor images a unique definition of cross-sectional shape is provided by the wetted perimeter, hydraulic radius and maximum flow depth and significantly, they have greater hydraulic relevance (see **Figure 3.1**) than (top) width B_T and depth D *[Hey, 1978]*.

Secondly, bed forms often develop in sand bed streams and, as they are also a response of the system to external constraints, it is necessary to predict their size and shape if a determinate solution is to be obtained *[Yalin, 1965]*.

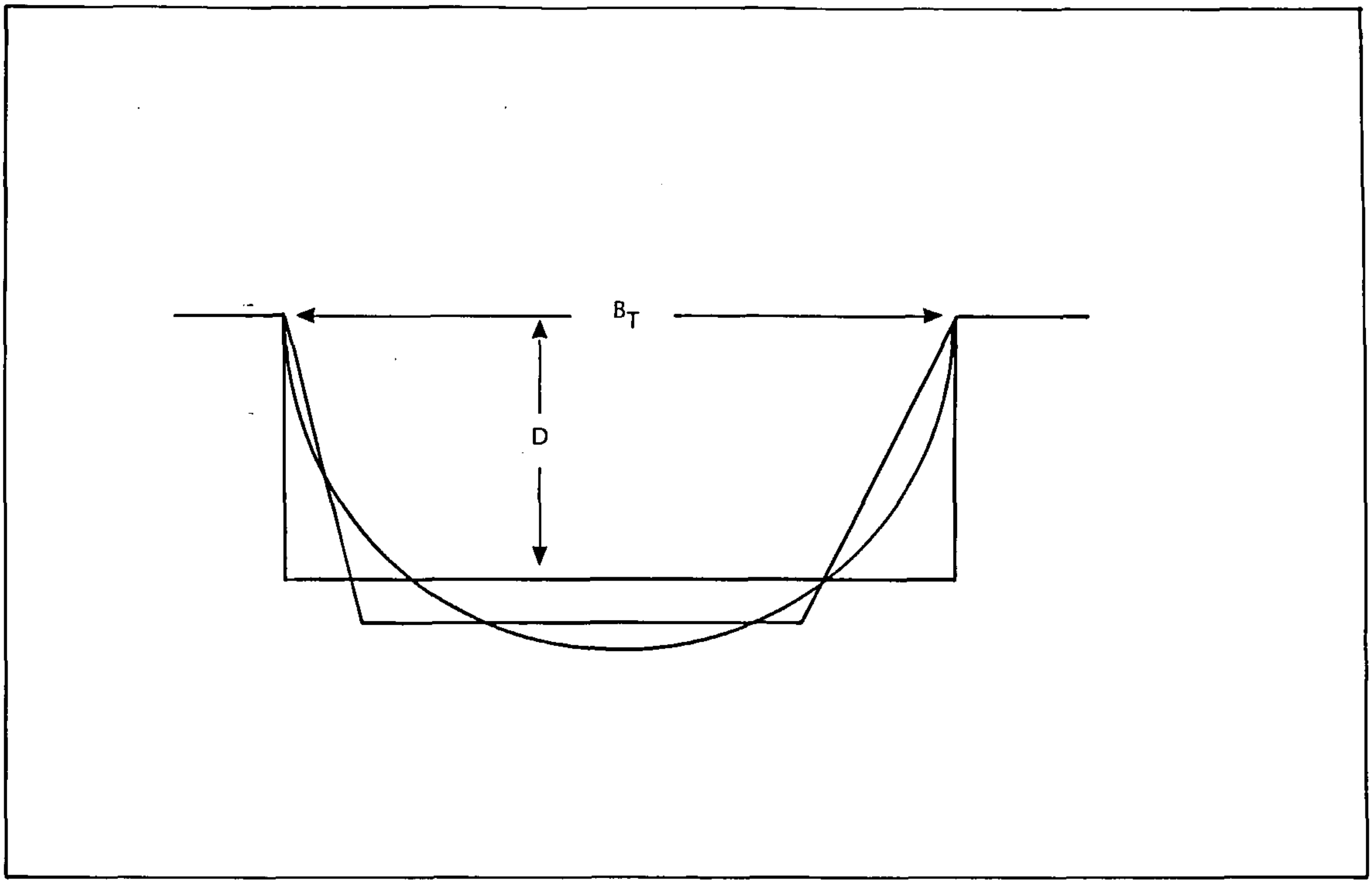

ALLUVIAL RIVER STUDY

Multivalued cross-sectional shape for given bankfull width and average flow depth (Hey, 1978) **3.1**

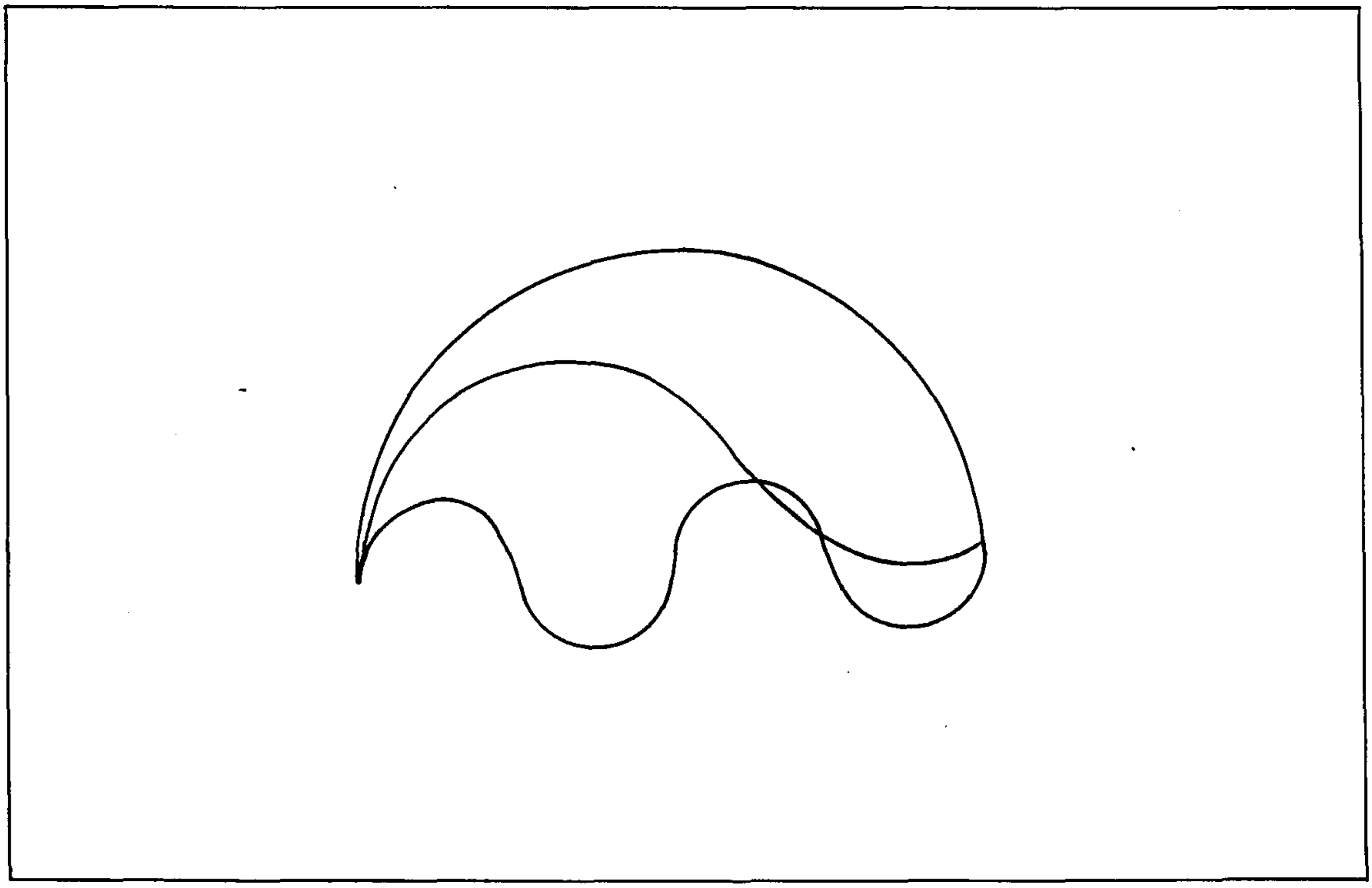

ALLUVIAL RIVER STUDY

Multivalued plan geometry for given value of channel sinuosity (Hey, 1978) **3.2**

Finally, sinuosity s, defined as the ratio of channel length to valley length, does not uniquely define the plan geometry. For a given value of sinuosity almost an infinite number of patterns are possible (see **Figure 3.2**). Provided arc length, i.e. the channel distance between successive inflection points, is also specified, then plan geometry can be uniquely defined.

3.3 EQUILIBRIUM STABILITY

The natural long-term evolution of alluvial streams produce slopes, widths, depths and velocities such that their flows transport the imposed sediment discharges with the corresponding hydrological run-offs from the contributing watersheds, i.e. channel shape (width - depth ratio) is directly related to sediment load and run-off.

Although many rivers can achieve a state of approximate equilibrium throughout long reaches which can be considered stable for engineering purposes, many of them contain long reaches that are actively aggrading or degrading. Degradation or aggradation occurs in a reach of an alluvial river when the rate at which sediment is transported into the reach differs from that at which it is carried out of the reach. When the sediment discharge into the upstream end of the reach exceeds that from the downstream end, aggradation occurs, and when the sediment-outflow rate exceeds the discharge, degradation results. Over a long period of time a river will adjust itself such that the feed into the reach of the river under consideration equals the outflow of sediment at the end of this reach, i.e. equilibrium is reached.

When viewed over shorter time periods, rivers are found to continuously finetune these water - and sediment-transport balances to accommodate deviations from the long-term balances. For this, they have at their disposal the considerable flexibility common to all open-channel flow systems that stems from their freedom to adjust their depth and hence also their velocity. Alluvial streams have an added important degree-of-freedom, i.e. the variable roughness attendant to bed - configuration changes which in turn are produced by variations in depth, velocity, or sediment concentration. This enables streams to maintain a nearly continuous balance between the sediment and water discharge they receive and must convey. On an intermediate time scale rivers can also modify their large-scale channel geometry, including width, depth, slope and plan form, in seeking to accommodate imposed changes of their geometrical characteristics of their hydrologic and sedimentary regimes. These changes often require movement of relatively large quantities of sediment by the stream, and hence their rates are strongly influenced by the sediment-transport capability of the river.

3.4 FACTORS INFLUENCING CHANNEL STABILITY

3.4.1 River bank stability

In the broader context of the hydraulic and sedimentary process-response systems with which a river controls the size and shape of its channel, bank erosion is of primary importance. The width of a channel should be related to the characteristics of the bank material as well as to the discharge (of both water and sediment).

The stability of a river bank is dependent on the erosional resistance of the bank material and the stresses acting on it, i.e. the stability depends on the balance of forces, motive and resistive, associated with the most critical mechanism of failure.

3.4.2 Fluvial entrainment

Flow in a channel generates entrainment forces acting on the bed and banks with the resultant influence in the direction of flow. One of these forces is a tractive force exerted on the sediment particles at the channel boundary by the flow. When this force exceeds a certain critical value, i.e. *critical tractive force*, erosion of sediment particles occurs if there is no sediment introduced upstream. In order to remain in equilibrium the boundary material must supply an internally derived, equal and opposite shear stress. A point is eventually reached where the resistance to motion of the boundary material is balanced by the fluid shear stress. Any further increase in fluid shear stress will result in entrainment of boundary material *[Henderson, 1963]*.

3.4.3 Discharge magnitude

In most rivers bank full conditions are only approached by floods well in excess of the median annual flood. The floods between bed full and bank full conditions can be regarded as those that can change a river channel dominantly. Over-bank flows cause radical changes in the conditions of flow, and while the damage they cause may be severe, they do not appear to play a major part in the location or properties of the river channel itself. Small flows have very little effect on large scale river morphology.

3.4.4 Sediment

The sediment in alluvial channels consists of mineral and organic matter. Since the appearance of organic sediment, is irregular, being limited to certain occasions, and their movement is of a random character, this study was only focussed on mineral matter.

The interaction between the flow of the water-sediment mixture and the alluvial sediment moulds the bed into different bed configurations which changes resistance to flow and sediment transport, and thus changes the depth of flow, stage of the river, elevation of the bed, velocity of flow, etc.

Fine sediments are easily transported and are generally to be found across the whole river cross-section. If a large amount of fine sediment is present in the flow, it may deposit on the bank and the bed to decrease the erodibility of the material there. On the other hand, fine sediment may increase the viscosity of the flow, increase the tractive force, decrease the bed irregularities and the bed form roughness. Another possibility is the building up of berms to narrow a channel. These berms, under the active influence of flow, are being built up alternately in the longitudinal direction, and as a result, greatly augment the channel to meander *[Shen, 1971b]*.

The sudden injection of the large sized sediments into the channel may cause local aggradation, thereby steepening the channel, increasing the flow velocities and possibly causing instability in the river at that site. Over a long period of time after the injection has ceased, the river will return to its former geometry.

3.4.5 Secondary circulation or transverse flow

Secondary circulation, concentrated near the corner of the boundary, has a significant effect on the stability of a channel. It was found that the strong circulation developing at a junction between smooth bed and rough wall can actually enhance meandering tendencies in straight alluvial channels.

3.4.6 Seepage force

In general, seepage from the channel to the ground tends to stabilize the channel, and a deep and narrow channel cross-section is formed. Seepage from the groundwater to the channel tends to increase the erodibility of the banks, and a shallow and wide cross-section is formed *[Shen, 1971b]*. However, seepage into the ground might enhance the erosion process under certain conditions by bringing high velocity flows closer to the ground and thus increasing the local tractive force acting on the sediment particles under certain conditions *[Martin, 1964]*.

3.4.7 Longitudinal slope

It is known that the longitudinal slope of a stream has a major effect on stream channel form *[Lane, 1957]*. *Leopold and Wolman [1957]* presented evidence that seems to indicate that meandering occurs more at lower channel slopes than at braided or straight channels for the same bank full discharge.

3.4.8 Vegetation on channel banks

Vegetative growth greatly influences the stability of channel banks. Vegetation plays an important role in limiting the effectiveness of bank erosion by detachment and entrainment of individual grains or aggregates of bank material. Vegetation not only protects the soil surface directly, but also the roots and rhizomes of plants reinforce the soil and introduce extra cohesion. Also, vegetation reduces the near boundary velocity gradient, thereby reducing the shear stress and the erosion *[Thorne and Osman, 1988]*.

4. <u>REVIEW OF EXISTING THEORIES REGARDING THE CHANNEL STABILITY PROBLEM</u>

4.1 INTRODUCTION

The various approaches to the channel stability problem fall into two broad categories: the *regime* and *rational* or *analytical* approaches. The regime approach is an empirical method which relies on available data and attempts to determine appropriate relationships from the data. An early approach was that of *Kennedy [1895]*, who collected data from canals which appeared to be stable or in regime and used this data to derive a relationship between the mean velocity and depth of flow. In other similar approaches empirical equations were derived which related the variables specifying the channel dimensions, such as the width, to the discharge. More recently attempts have been made to derive regime relationships by using descriptions of the fundamental processes involved. This has been termed *rational regime theory [Bettess et al., 1988]*.

The analytical approach relies on specifying equations which describe the dominant individual processes such as sediment transport, flow resistance, and bank stability. This approach can only be successful if the dominant processes are correctly identified and appropriate equations exist to describe them adequately.

In the analytical approach, two sets of equations are readily available defining the sediment transport and the frictional characteristics, but it is unclear what constitutes an appropriate third relationship *[White et al., 1982]*. Some attempts at resolving this conjecture are concerned with bank stability *[Thorne, 1978; Parker, 1978; Osman and Thorne, 1988]*, constancy of total sediment concentration *[Griffiths, 1983]* or tractive force theory *[Lane, 1955]*. Others invoke an external hypothesis or variational principle which includes proposals like minimum stream power *[Chang, 1980]*, minimum unit stream power *[Yang and Song, 1979]*, minimum energy dissipation rate *[Yang et al., 1981]*, maximum friction factor *[Davies and Sutherland, 1980]* and maximum sediment transport rate *[White et al., 1982]*.

A brief overview of existing theories regarding the channel stability problem is presented below:

4.2 METHODS OF HYDRAULIC GEOMETRY DETERMINATION

4.2.1 Empirical regime theory

Empirical regime theory has little firm theoretical basis but, by the nature of its derivation and from its history of almost a century, it is known that it presents an approximate representation of the dominant aspects of channel form and shape *[Bettess et al., 1988]*.

Among the subsequent contribution that is the best known is that by *Lacey [1929, 1933, 1958]* who wrote the Kennedy type formula in terms of the hydraulic mean radius $\boldsymbol{R}$ as

$$v = kR^n \tag{4.1}$$

where v represents mean velocity of flow and k, n are constants.

Whatever other empirical methods are suggested for determining regime conditions must be broadly comparable with this form *[Bettess et al., 1988]*. The success of this type of equation in the channels for which data sets it is derived for and its lack of applicability in many other areas implies that there are other variables beside discharge and bed sediment size controlling the bankfull hydraulic geometry of alluvial channels. The inadequacy of the regime canal formulas for rivers in general has been pointed out by *Lane [1957]* who has observed that the width-depth ratio of streams is at least partly a function of the slope and not of the discharge alone.

The exclusion of a number of important independent variables indicates that the coefficient in **Equation 4.1** is partly dependent on the numerical values of these discarded variables. Theoretically they should only reflect physical constants and not variables that are fortuitously constant. For this reason this equation can only be applied when these critical conditions are satisfied.

The usefulness of this method depends on the quality of the data and the validity of the assumed form of the relationships. It has always been acknowledged that the various coefficients derived may not be truly constant and that the equations should only be applied in situations similar to those for which the data was collected *[White et al., 1982]*. All empirical equations have similar disadvantages and great care should always be taken not to apply them out of context. They only describe quantitatively what and where and give no explanation of how and why a channel adjusts its hydraulic geometry to a set of external constraints.

4.2.2 Tractive force theory

The ideal stable hydraulic cross-sectional shape is that for which a stage of impending motion is reached at all points around the cross-section at the same time. For a given soil and discharge this ideal section has the least excavation and least width, and maximum mean velocity.

Based on this, the U.S. Bureau of Reclamation developed the tractive force theory for stability of banks of non-cohesive material along lines laid down by *Lane [1955]*. This theory is generally referred to as *Lane's theory*. The theory relates the shearing force of the fluid on the banks to the geometry of the cross-section and the weight of the individual particles.

According to *Lane [1952, 1955]* no sloughing or sliding analysis is included in the stability criteria because these *" ..... have been to a large extent developed." Henderson [1963]* employed Lane's tractive force theory to relate fluid shear stress on non-cohesive bank and bed particles to the discharge and width and hence to some of the Lacey regime equations.

Tractive force theory is recognised by two relationships, i.e.

i) a relationship between the applied fluid stress on the bed and the applied fluid stress on the banks, both in the direction of flow and

ii) a relationship between flow depth and maximum flow depth.

4.2.3 Bank stability analysis

With the postulation that channel shape is controlled by the stability of the banks, soil mechanical parameters of the bank material are used to determine a critical bank height which cannot be exceeded. If the actual bank height is greater, then bank failure will take place. There are a number of possible failure mechanisms depending upon the nature of the situation. A particular property of mathematical equations for this type of analysis is that they are independent of the discharge.

4.2.4 <u>Parker's diffusion theory</u>

Parker [1978a] introduced a theory for self-formed sand-silt rivers in equilibrium that explicitly includes mechanisms for bank erosion and for deposition. Bank erosion is ascribed to lateral bed load from the banks to the bed of the river generated by gravity and related to the longitudinal bed load. Deposition is provided by the lateral diffusion of suspended sediment generated by the non-uniform distribution of suspended sediment across the river section.

Parker's theory gives a complete regime approach and comparison with other regime theories show that it provides larger depths for smaller channels and smaller depths for larger channels. As the predicted depth and width are linked, it is probable that a similar sort of discrepancy would arise in the prediction of channel width. Though this discrepancy is disappointing it need not suggest that the basic approach to the problem is at fault.

4.2.5 <u>Extremal hypotheses</u>

Much interest has been generated by demonstrations that the equilibrium geometry of self-formed alluvial streams can be predicted successfully under a variety of circumstances. The method of prediction in each case is to combine a semi-empirical sediment transport relationship with a semi-empirical flow resistance rule and to assume that equilibrium will occur when the stream power or rate of energy dissipation of the stream is a minimum, the value of which is dictated by local conditions of bed or bank material.

This assumption was initially *[Yang, 1971a]* based on questionable thermodynamic analogy as stated by *Prigogine [1955]*

> *"...... in the evolution of the stationary state of an open system, the rate of entropy production per unit volume corresponds to a minimum compatible with the constraints imposed on the system ....."*

and *Lewis and Randall [1961]*

> *"...... the most probable distribution of energy in a system is such that the entropy of the whole system is a maximum ......".*

The above principles were considered to be analogous to a stream system in which the most probable distribution of energy dissipation is therefore that which will maximize the entropy of the system. It is concluded that this implies uniformity of energy dissipation per unit of stream length and hence maximization of the variance of hydraulic properties along a stream system.

Definitions for extremal hypotheses of river regime are given below, together with brief descriptions of their usage:

Minimum stream power

This hypothesis is stated as *[Chang, 1980b]*

> *"For an alluvial channel the necessary and sufficient condition of equilibrium occurs when the stream power per unit channel length, γQS , is a minimum subject to given constraints. Hence, an alluvial channel with water discharge Q , and sediment (discharge) Q_s, as independent variables, tends to establish its width B, depth D and slope S such that γQS is a minimum. Since S is a given parameter, minimum γQS also means minimum channel slope S."*

Note that γ is the specific weight of water. *Chang [1979a, b; 1980 a, b]* employed this hypothesis to explain channel patterns of natural rivers, width-depth ratios of rivers in regime, width-depth ratios of alluvial canals, and the width, depth, and sediment discharge of gravel bed streams. The form of delta streams was also explained by *Chang and Hill [1977]* using the hypothesis. *Song and Yang [1979]* predicted velocity profiles in turbulent open channel flows on the basis of minimization of stream power, but where sand waves were of significant size and sediment motion occurred, their predictions were less successful.

Song and Yang [1980] make the point that stream power and total energy dissipation are not equivalent when the stream boundary is moving with appreciable velocity. Under normal flow and sediment conditions (in the lower flow regime, for example) the two hypotheses are effectively equivalent.

Minimum unit stream power

Yang and Song [1979] stated

> *"....... for subcritical flow in an alluvial channel, the channel will adjust its velocity, slope, roughness and geometry in such a manner that a minimum amount of unit stream power is used to transport a given sediment and water discharge. The value of minimum unit stream power depends on the constraints .... applied to the channel. If the flow deviates from its equilibrium condition, it will adjust its velocity, slope, roughness and channel geometry in such a manner that the unit stream power is minimized until the equilibrium condition can be regained".*

The hypothesis of minimum unit stream power was used by *Yang [1976]* to explain the equilibrium flow conditions of alluvial streams in laboratory and field conditions. *Song and Yang [1980]* stated that the hypothesis of minimum unit stream power is *"somewhat different from"* but *"of a similar nature to"* that of minimum stream power, and that both *"can be regarded as special cases of a more general"* hypothesis, that of minimum energy dissipation rate. *Chang and Hill [1977]* showed that the channel width predicted by minimum unit stream power differs from that predicted by minimum stream power. *Song and Yang [1980]* stated that where flow conditions are strongly non-uniform, such that the local velocity and slope can no longer be represented by their average values, the hypothesis of minimum unit stream power is preferable to that of minimum stream power.

Minimum energy dissipation rate

In its most recent form the minimum energy description rate hypothesis is stated *[Yang et al., 1981]* as follows:

"A system is in an equilibrium condition when its rate of energy dissipation is at a minimum value. This minimum value depends on the constraints applied to the system. When a system is not in an equilibrium condition, its rate of energy dissipation is not at its minimum value. However, the system will adjust in such a manner that the rate of energy dissipation can be reduced until it reaches the minimum and regains equilibrium".

Previously *[Song and Yang, 1980]* a slightly different statement was used:

"A river may adjust its flow as well as its boundary such that the total energy loss (or, for a fixed bed the total stream power) is minimised. The principal means of adjusting the boundary is sediment transport. If there is no sediment transport, then the river can only adjust its velocity distribution. In achieving the condition of minimum stream power, the river is constrained by the law of conservation of mass and the sediment transport relations".

A similar hypothesis was advanced by *Yang [1971a]*, on the basis of an analogy between stream behaviour and linear thermodynamics, and used to explain the occurrence of meanders *[Yang, 1971b]* and of riffle-pool systems *[Yang, 1971c]*. *Yang and Song [1979]* used the hypothesis of minimum energy dissipation rate to explain measured hydraulic parameters.

Maximum friction factor

Davies and Sutherland [1980] gave the definition:

"If the flow of a fluid past an originally plane boundary is able to deform the boundary to a non-planar shape, it will do so in such a way that the friction factor increases. The deformation will cease when the shape of the boundary is that which gives rise to a local maximum of friction factor. Thus the equilibrium shape of a non-planar self-formed flow boundary or channel corresponds to a local maximum of the friction factor".

Maximum sediment transport rate

White et al. [1982] stated the maximum sediment transport rate hypothesis as "*.... for a particular water discharge and slope the width of the channel adjusts to maximise the sediment transport rate.*" They used the hypothesis to predict the hydraulic and geometrical characteristics of both sand and gravel bed alluvial channels. A similar hypothesis was proposed by *Ramette [1979].*

Shortcomings of extremal hypotheses

Although the variational approach provides the appearance of an attractively simple solution to the problem of river regime, the hypotheses will have to be redefined to meet certain objections *[Davey and Davies, 1979; Griffiths, 1984].*

Under certain conditions some hypotheses are equivalent, or one may be a special case of another or of a very similar nature. The extremal hypotheses of minimum stream power, minimum unit stream power, minimum energy dissipation rate, and maximum sediment transport rate, when combined with conventional sediment transport and flow resistance equations, lead to conclusions incompatible with observations *[Griffiths, 1984].* For wide, straight, unconstrained alluvial reaches in equilibrium, these conclusions include that the Einstein sediment discharge and Shields entrainment functions are nearly constant, the magnitude of the particular constants depending only on the hypothesis and equations used, whereas data from flumes and natural rivers show that both expressions are highly variable in stable channels. Constancy of the Einstein and Shields expressions provides, in fact, a sufficient but unnecessary condition for channel stability. In the maximum friction factor hypothesis there is no maximum for friction factor when channel width, depth, and slope are dependent variables. Variational principles may one day supply a solution to the problem of alluvial channel stability, but current formulations of the mentioned hypotheses require redefinition.

4.3 CONCLUSIONS

At the moment there is no consensus about what relationship should be used to determine channel geometry or stability, in fact, opinions differs markedly.

The general assumption is that if the discharge down an alluvial channel increases then there is a tendency for bank erosion to take place and the channel dimensions to increase. This is incorporated either explicitly or implicitly in most of the theories regarding channel geometry. It should not, however, be forgotten that if the discharge is reduced then there is a tendency for deposition to take place and for the channel dimensions to decrease. It can thus be seen that the regime geometry is achieved only as a balance between the opposing mechanisms tending to cause erosion and hence increase channel geometry and tending to cause deposition and so decrease channel geometry. The fact that there are two opposing mechanisms that must be considered that is missing in some of the channel geometry theories and the diversity of opinion has given rise to the demand for a general model to describe the hydraulic geometry of a river.

However, such a solution should be well based on theoretical principles and different from the existing theories as discussed above. The ideal general model should be simple in its application to predict river regime behaviour and should be easier to use and understand than a complicated computational model.

5. CHARACTERISTICS OF SITES AND FIELD DATA

5.1 INTRODUCTION

After the February 1977 floods along the north-eastern coast of South Africa slope-area surveys were carried out by the Sub-directorate Flood Studies of the Directorate Hydrology of the South African Department of Water Affairs and Forestry (DWA&F). These surveys covered three sites in the alluvial valleys of the Mfolozi catchment area and one site downstream of the gauging station W1H009 on the Mhlatuze River. The Mfolozi sites were on the Black Mfolozi and White Mfolozi rivers within the Mfolozi Game Reserve and on the Mfolozi River 6 km upstream of the N2 road bridge across the Mfolozi River near Mtubatuba. The same sites were resurveyed after the passing of cyclone Domoina in January 1984 with the double aim of flood peak determination and checking of cross-sectional changes. Other alluvial sites on the Komati and Mkuze rivers, that were also affected by Domoina, were also surveyed. A programme of monitoring sites along alluvial rivers commenced in this way.

The floods of 1984 and 1987 were the only floods which had occurred since the beginning of the monitored period that caused significant changes to river geometry. Only field data of 1984 and 1987 applicable to some of the monitored sites is thus used in the analysis presented in this report. It was noted in 1984 that the Black Mfolozi River had peaked about 6 to 7 hours before the White Mfolozi River, with the time-lag corresponding to the north-south movement of cyclone Domoina. Consequently the Mfolozi River downstream of the confluence of the White and Black Mfolozi rivers experienced a multiple peak type flood *[Kovács et al., 1985]*. Given the uncertainty as to how different flood peaks had contributed to the cross-sectional changes, it was decided not to use the Mfolozi River site data in the analysis.

5.2 SITE LOCATION AND DESCRIPTION

Sedimentation and erosion surveys of straight reaches of the Komati (1984), Mkuze (1984; 1987), Black Mfolozi (1984; 1987), White Mfolozi (1984; 1987) and Mhlatuze (1984; 1987) rivers were used in the analysis presented in this report. The location of the sites used are shown in **Figure 5.1.** A brief general description of each of the sites, is given below:

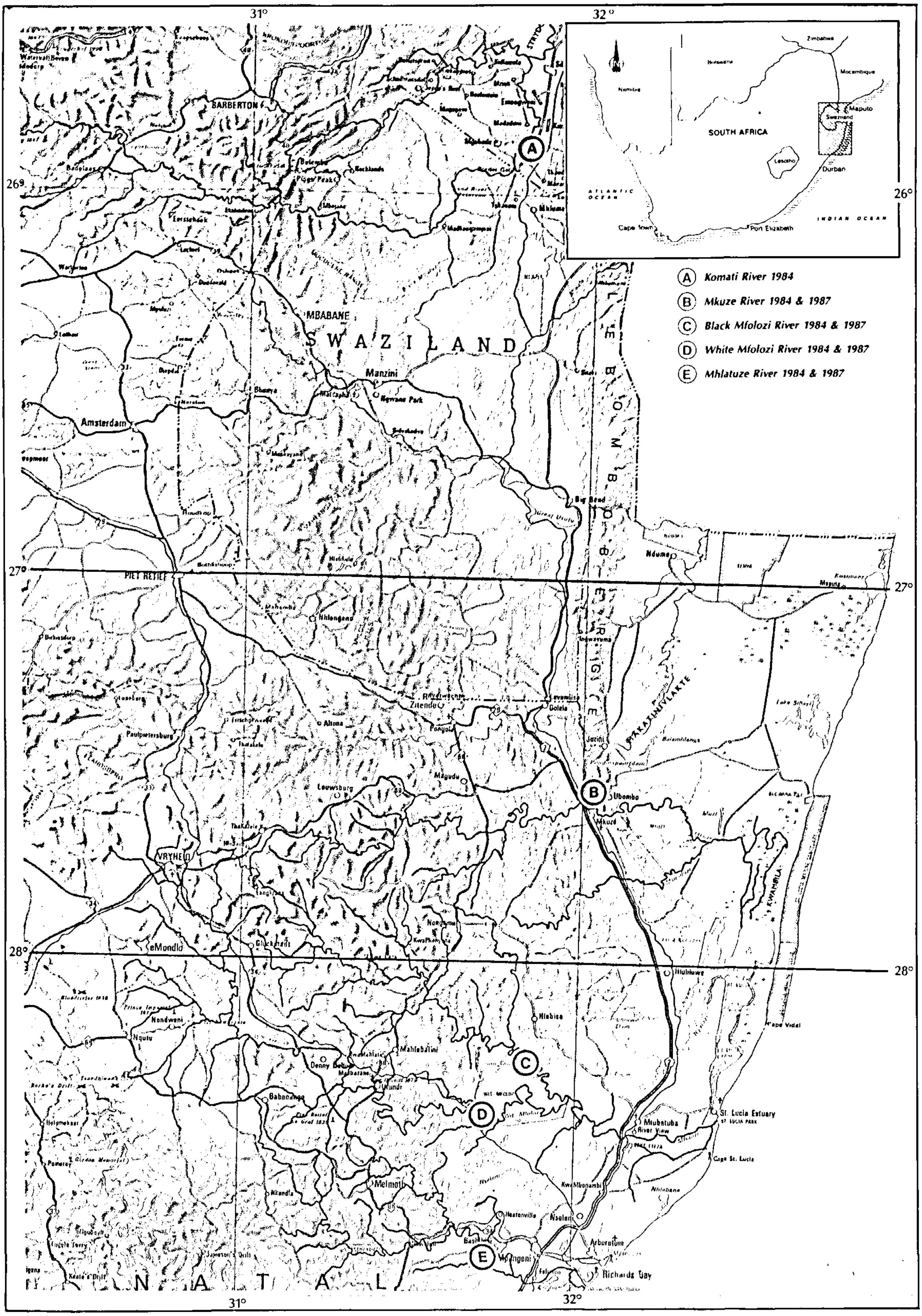

ALLUVIAL RIVER STUDY

Field site locations

5.1

SITE A: KOMATI RIVER - TRADING SITE 507

Site A is described as site 56 in the DWA&F Technical Report TR 122 *[Kovács et al., 1985]*. This site on the Komati River is located at Trading Site 507 at latitude 25 ° 52′ and longitude 31 °49′ and has a catchment area of 8 040 km^2. The nearest working gauging station is X1H003 downstream at Tonga Rapids with a catchment area of 8 614 km^2.

The site contains a reach of 920 m in length with a clear, straight and uniform main channel and a mild upstream bend. Both banks consist of a clayey, sandy material. The bed consists of alluvial sand with a gravel layer of pebblestone at some places. Vegetation along the banks consists of a narrow band of trees and grass.

SITE B: MKUZE RIVER - MORGENSTOND, MKUZE

Site B is described by the DWA&F as sites 23 and 97 in their Technical Reports TR 122 *[Kovács et al., 1985]* and TR 139 *[Van Bladeren and Burger, 1989]* respectively. This site on the Mkuze River is located at Morgenstond nearby Mkuze at latitude 27 ° 36′ and longitude 32 ° 01′ just downstream of the old Mkuze - Pongola road bridge and has a catchment area of 2 647 km^2. The nearest gauging station is W3H006 at Doornhoek with a catchment area of 2 571 km^2 and is located about 5 km upstream.

The site contains a straight reach, 640-930 m in length with a mild bend upstream and a sharp bend downstream of the site. Both banks consist of in situ weathered soil overlain by sandy silt. Due to the influence of the bridge and the rock outcrop at section 1 this section was not used in the analysis. The river bed is sandy with rock 2,5 m below the main bed level. Pre-flood vegetation was dense on the left bank consisting of grass, bushes and trees. Right bank vegetation was slightly sparser. In the main channel, riverine vegetation consisted mostly of grass and reeds. During the 1984 flood, all the riverine and bank vegetation was removed by the flood.

SITE C: BLACK MFOLOZI RIVER - MFOLOZI GAME RESERVE

Site C is described by the DWA&F as sites 17 and 90 in their Technical Reports TR 122 and TR 139 respectively. This site on the Black Mfolozi River is located within the Mfolozi Game Reserve at latitude 28 ° 16′ and longitude 31 ° 51′ and has a catchment area of 3 396 km^2. The nearest gauging station that is still operating is W2H006 with a catchment area of 1 648 km^2 and is located 84 km upstream. Between the site in the game reserve and the weir at W2H006 two major tributaries join the Black Mfolozi River. They are the Vuma River just below W2H006 and the Mona River just outside the game reserve.

The site contains a straight reach, 700 - 900 m in length, with a mild bend upstream and a sharp bend downstream. The left bank is bounded by sandstone, whereas the right bank consists of silty sand. The river bed consists of alluvial sand with evidence of rock located at a depth of more than 4 m below the main bed level. Pre-flood vegetation on both banks was dense consisting of trees, bushes and grass. Riverine vegetation in the main channel was mostly grass and reeds. The floods of 1984 removed all the vegetation and only a slight recovery was evident during later surveys.

SITE: D: WHITE MFOLOZI RIVER - MFOLOZI GAME RESERVE

Site D is described by the DWA&F as sites 13 and 86 in their Technical Reports TR 122 and TR 139 respectively. This site on the White Mfolozi River is located on the boundary of the Mfolozi Game Reserve at latitude 28 ° 24′ and longitude 31 ° 43′ and has a catchment area of 4 776 km^2. The nearest gauging station that is still operating is W2H005 at Overvloed close to Ulundi, some 45 km upstream and with a catchment area of 3 939 km^2.

The site contains a straight reach of 1 200 m in length with a sharp upstream bend. The banks on both sides consist of in situ weathered mudstone overlain by silty sand of alluvial origin. The bed is sandy with rock occurring only at depths of more than 5 m. Pre-flood vegetation on both banks was dense consisting of trees, bushes and grass. Riverine vegetation in the main channel consisted mostly of grass and reeds. The 1984 flood removed all vegetation and later observations showed that more recovery took place along the White Mfolozi River than along the Black Mfolozi River.

SITE E: MHLATUZE RIVER - W1H009 - RIVERVIEW

Site E is described by the DWA&F as sites 8 and 80 in their Technical Reports TR 122 and TR 139 respectively. This site on the Mhlatuze River is located just upstream of the R34 road bridge crossing the Mhlatuze River at Riverview and the gauging station W1H009 at latitude 28 °45′ and longitude 31 ° 45′ and has a catchment area of 2 409 km^2 (excluding that of the Goedertrouw Dam (1980) = 1 136 km^2). However, the gauging station W1H009 was destroyed during the 1987 flood.

The site contains a 500 m long straight reach which serves as a transition zone between an upstream and downstream bend. The right bank consists of clayey sand overlain by alluvial silt. The left bank is bounded by rock. There is evidence of rock occurring at shallow depths of approximately 1 m below the sandy river bed. Dense bush and trees occur on the left bank and on the right bank the vegetation is more scattered with grass. Reeds form the most common riverine vegetation occurring within the main river channel. The flood of 1987 only removed vegetation and soil along right bank.

5.3 FIELD SURVEYS

Field surveys comprised the survey of a longitudinal flood profile defined by flood marks and four cross-sections. The selection of river reaches and the slope-area (SA) surveys were done in accordance with standard rules derived from hydraulic considerations and years of practice *[Du Plessis and Dunn, 1984]*.

Main difficulties encountered during field surveys during the monitoring period since 1984 were as follows:

i) impossibility of surveying during times of flood
ii) on steep rocky banks or in thick bush it was hard to find good flood marks
iii) the use of light boats in strong currents was hazardous
iv) frequent rains caused delays
v) presence of crocodile, hippotami and snakes as dangerous hazards in the water.

Longitudinal sections of the various sites are represented in **Figures 5.2 - 5.6**. Cross-sections, as well as comparative pre-flood and post-flood cross-sectional data, where available, of the various sites are given in **Appendix A**.

5.4 FLOOD EVENTS STUDIED

The applicable flood sizes at the various sites were determined by the DWA&F by means of the Slope Area Method (SA) as described in Technical Reports TR 122 *[Kovács et al., 1985]* and TR 139 *[Van Bladeren and Burger, 1989]*. The 1984-floods for the Komati, Mkuze, Black Mfolozi and White Mfolozi rivers and the 1987-flood for the Mhlatuze River were the highest on record at all sites *[Van Bladeren, 1989]*. **Table 5.1** shows the floods studied and the catchment characteristics of each site.

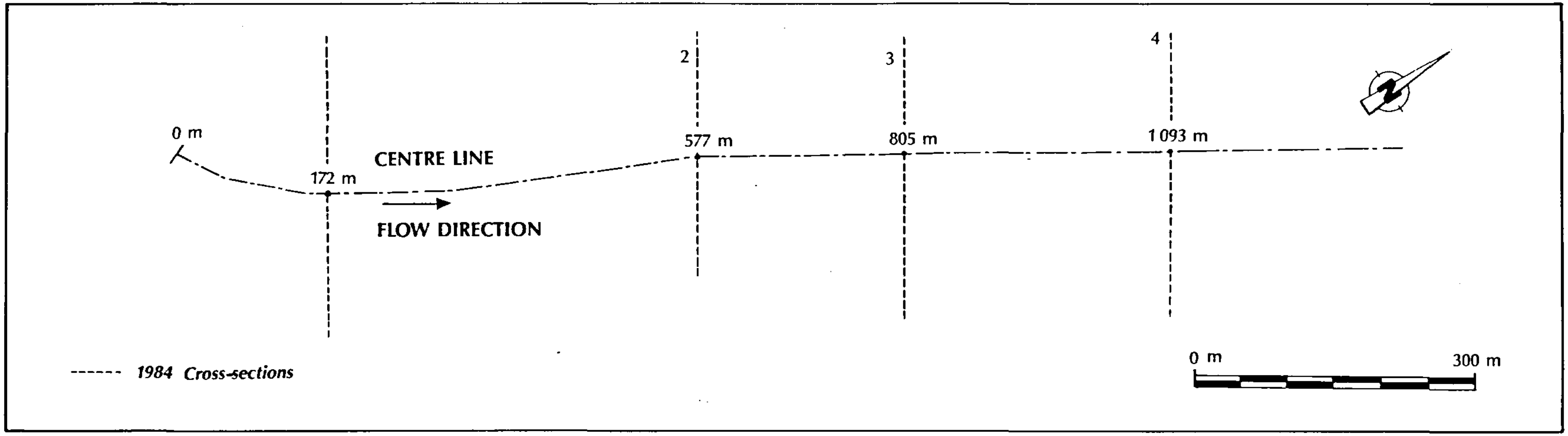

ALLUVIAL RIVER STUDY | **Cross-section positions: Site A - Komati River** | **5.2**

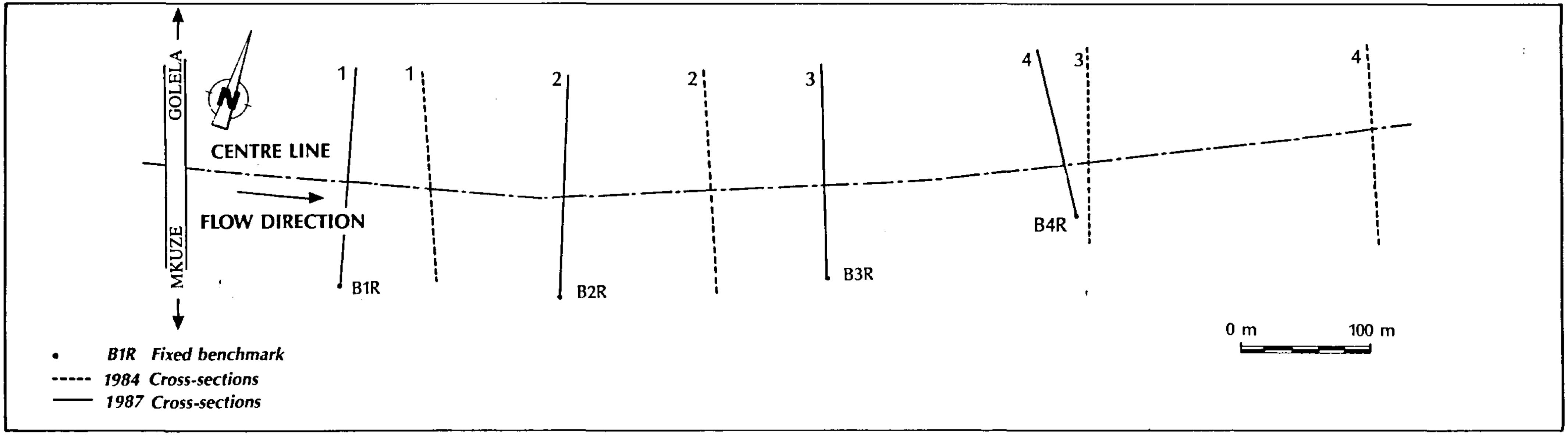

ALLUVIAL RIVER STUDY | **Relative cross-section positions: Site B - Mkuze River** | **5.3**

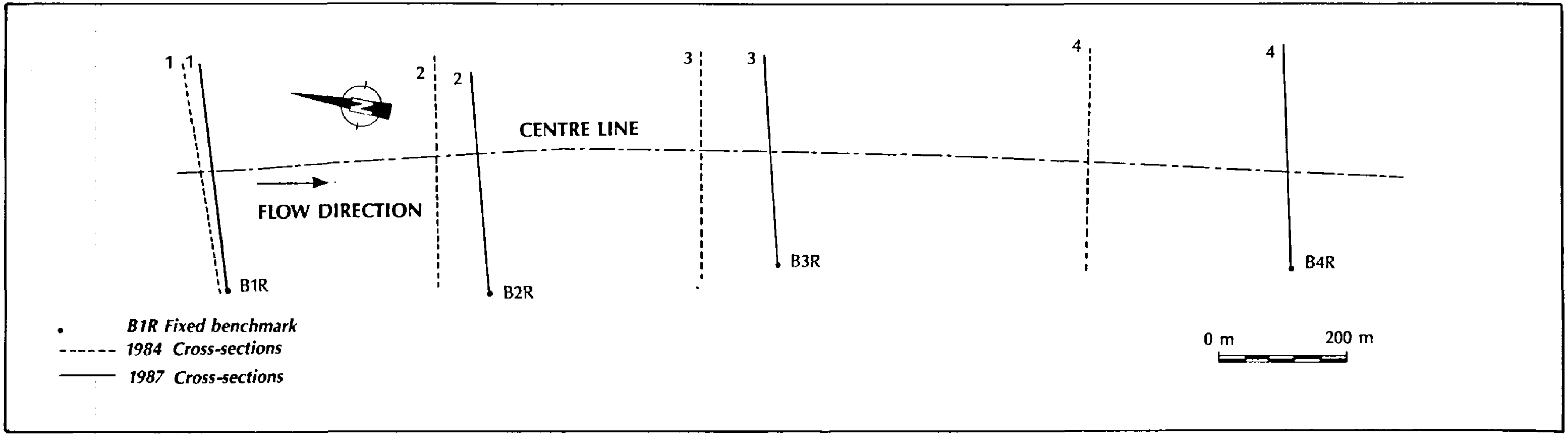

ALLUVIAL RIVER STUDY

Relative cross-section positions : Site C — Black Mfolozi River **5.4**

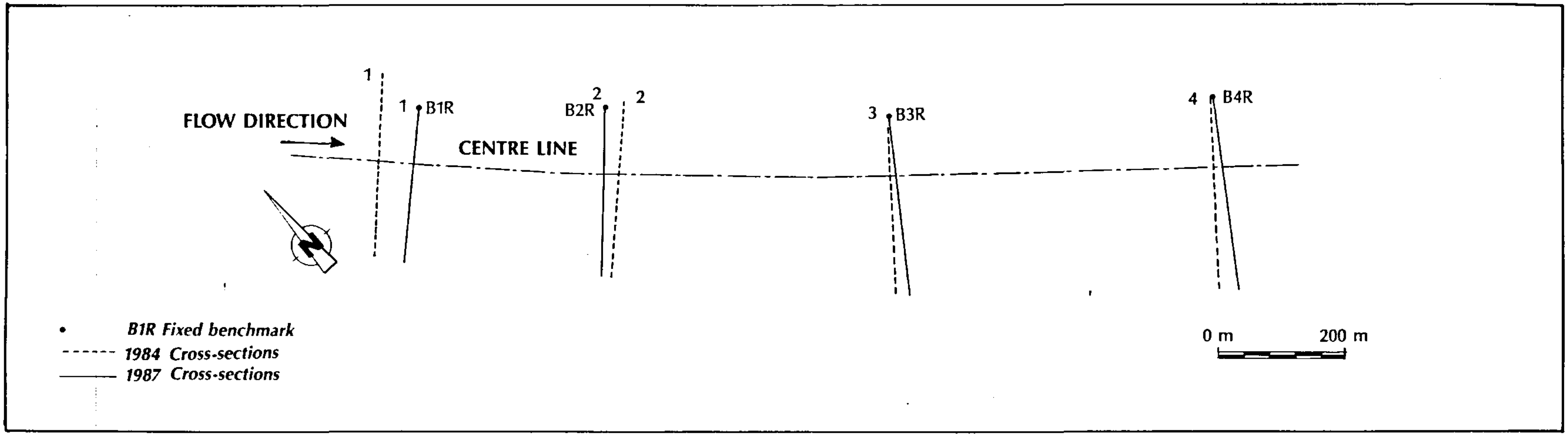

ALLUVIAL RIVER STUDY

Relative cross-section positions : Site D — White Mfolozi River **5.5**

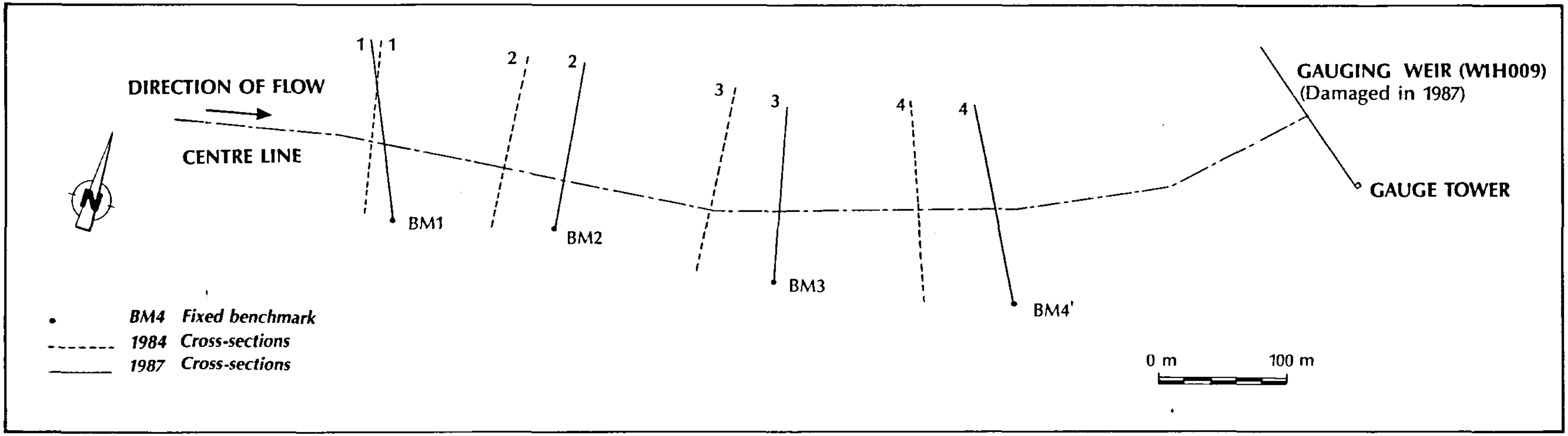

ALLUVIAL RIVER STUDY

Relative cross-section positions : Site E — Mhlatuze River

5.6

Table 5.1: Site and flood characteristics *[Kovács et al., 1985; Van Bladeren and Burger, 1989]*

	Unit	Komati River	Mkuze River	Black Mfolozi River	White Mfolozi River	Mhlatuze River
Site Characteristics Location		Trading site	Morgenstond	Game Reserve	Game Reserve	Riverview (W1H009)
Catchment Area (CA)	km^2	8 040	2 647	3 396	4 776	2 409[1)]
Mean Annual Runoff (MAR)	$10^6 m^3$		95	343	255	178
Mean Annual Precipitation (MAP)	mm		898	965	791	996
Flood Data						
Date (1984)		31-01-1984	31-10-1984	31-01-1984	31-01-1984	31-01-1984
Method of flood peak calculation		SA	SA	SA	SA	SA
Bed slope (from 1:50 000 maps)	m/m	0,00062	0,0013	0,0012	0,0015	0,0013
Flood peak (Q)	m^3/s	2 640	5 500	10 000	6 500	2 400[2)]
Flood line slope (S)	m/m	0,00061	0,00163	0,0012	0,001	0,003
Storm rain (p)	mm	285	480	580	445	370[2)]
Return period (T)	yr	20-50	50-200	0,93 RMF	50-200	20-50[2)]
Date (1987)		-	29-09-1987	29-09-1987	29-09-1987	29-09-1987
Method of flood peak calculation			SA	SA	SA	SA
Bed slope (from 1:50 000)	m/m		0,00125	0,0012	0,00152	0,00128
Flood peak (Q)	m^3/s	-	1 060	1 740	2 150	3 600
Flood line slope (S)	m/m	-	0,00188	0,00183	0,0022	0,00223
Storm rain (p)	mm	-	165	262	247	436
Return period (T)	yr	-	<10	10	15	50 to 100

[1)] Catchment excluding Goedertrouw Dam (1980) = 1 136 km^2
[2)] Refer to CA at Goedertrouw Dam
SA = slope area
CA = catchment area

5.5 SEDIMENT CHARACTERISTICS

5.5.1 Grading of sediment samples

The basic bed sediment properties at the monitored sites are given in **Table 5.2**. Sediment grading curves are shown in **Figures 5.7** and **5.8**. Although pre-flood and post-flood sediment samples were taken during 1987 it was decided to use only the post-flood data in the analysis.

It was found that the pre-flood grading curve envelopes are narrower and have a more uniform grading. This is due to the washing out of the fines and the more constant flows that passed at the sites during pre-flood surveys. The post-flood sediment samples are more a mixture of sediment from the catchment and the river channel and thus fall within broader envelope curves with non-uniform grading. However, these post-flood sediment samples can be regarded as the most representative of the bed sediments.

KOMATI RIVER

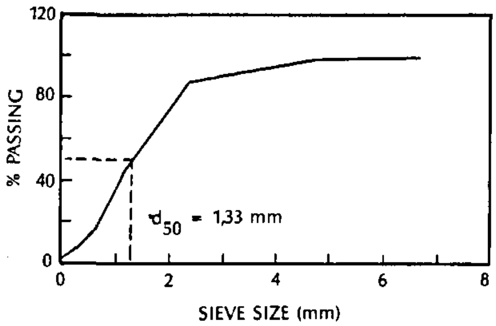

MKUZE RIVER

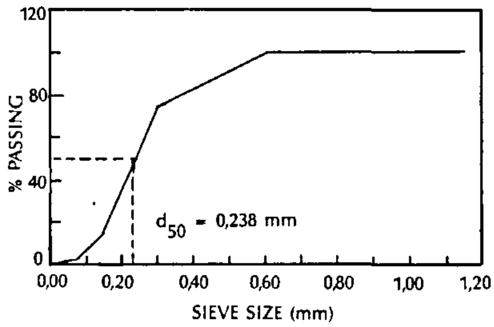

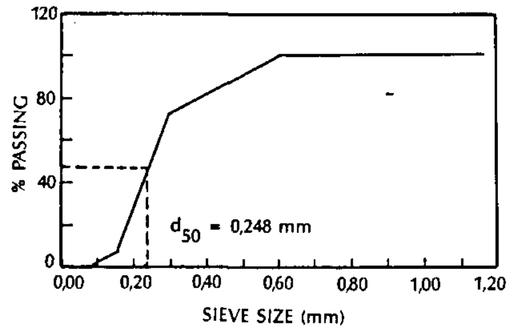

MHLATUZE RIVER

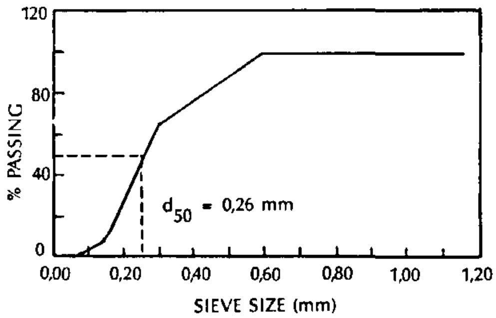

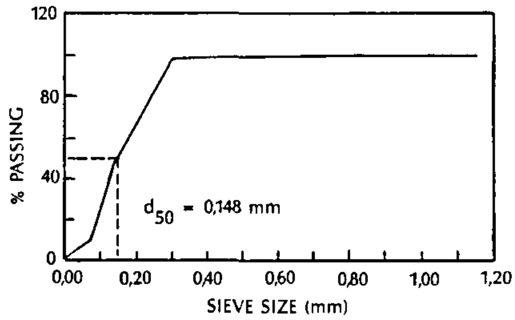

BLACK MFOLOZI RIVER

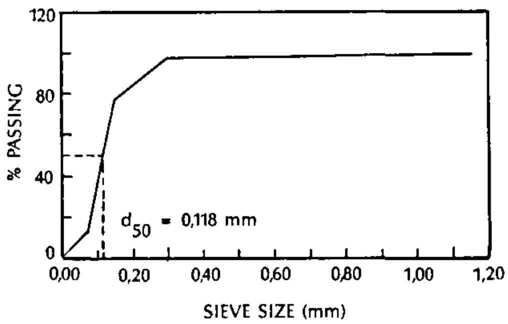

WHITE MFOLOZI RIVER

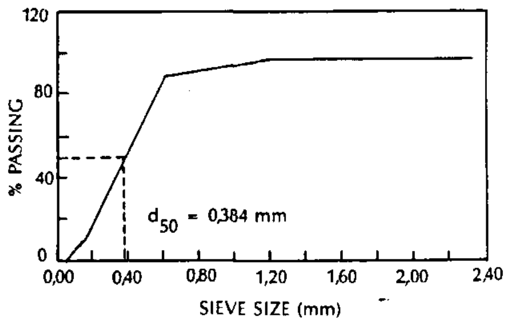

MKUZE RIVER

SECTION 1

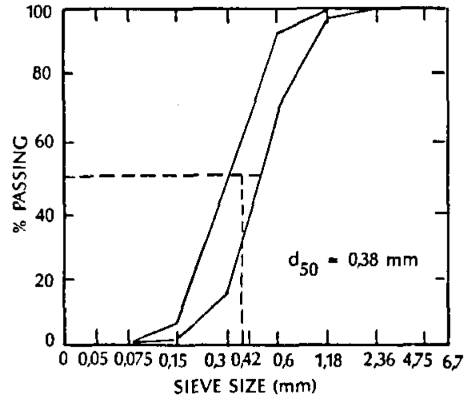

SECTION 4

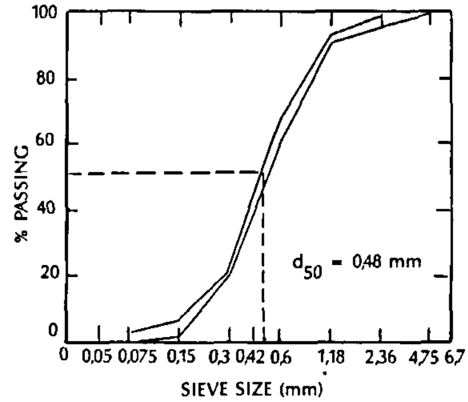

BLACK MFOLOZI RIVER

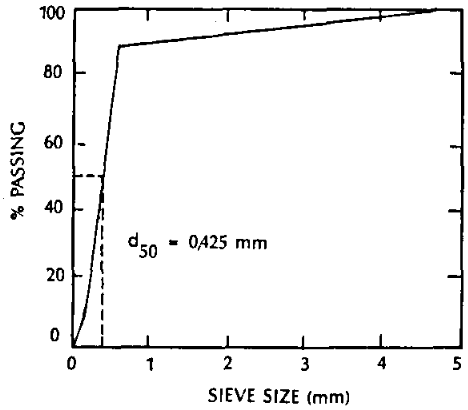

WHITE MFOLOZI RIVER

SECTION 1

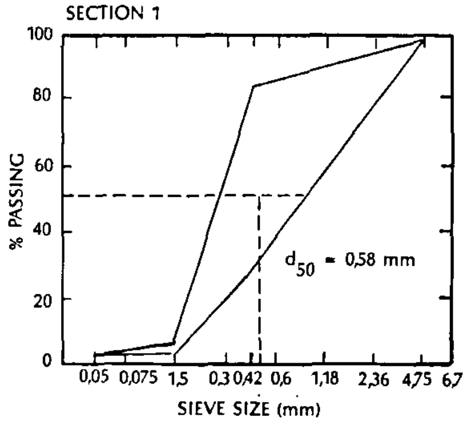

SECTION 4

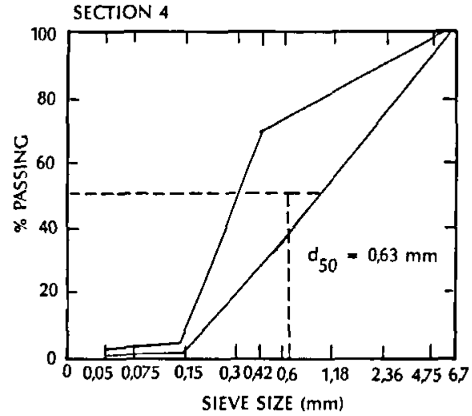

MHLATUZE RIVER

SECTION 1

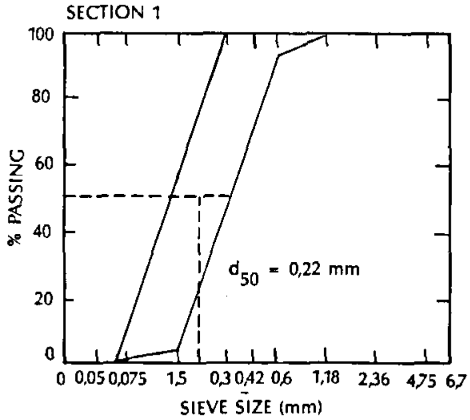

SECTION 4

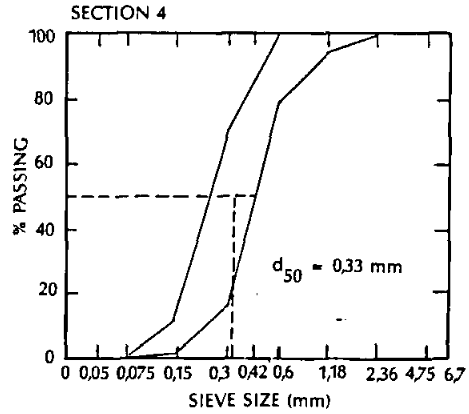

Table 5.2: Mean sediment diameter d_{50}

Site	River	Year				
		1984	1987			
		Mean sediment diameter d_{50} (mm)	Sample date	Mean sediment diameter d_{50} (mm)		
				Range	Mean	Analysis
A	Komati	1,33	-	-	-	-
B	Mkuze	0,243				0,43
	Section 1		8/1987	0,31-0,47	0,39	
			10/1987	0,29-0,46	0,38	
	Section 4		8/1987	0,27-0,39	0,33	
			10/1987	0,46-0,49	0,48	
C	Black Mfolozi	0,12				0,425
D	White Mfolozi	0,38				0,61
	Section 1		8/1987	0,4-0,46	0,43	
			10/1987	0,26-0,89	0,58	
	Section 4		8/1987	0,34-0,42	0,38	
			10/1987	0,31-0,94	0,63	
E	Mhlatuze	0,2				0,27
	Section 1		8/1987	0,37-0,41	0,39	
			10/1987	0,13-0,31	0,22	
	Section 4		8/1987	0,31-0,42	0,37	
			10/1987	0,24-0,42	0,33	

5.5.2 Fall velocity v_{ss}

The importance of size, shape and density in sediment transport emphasise the need for a representative measure of the range of sediment grain sizes.

Although the method of sieve analysis is one of the most appropriate methods to determine an appropriate representative sediment grain diameter, various disadvantages are associated with this method.

The sedimentation particle size as determined by the fall velocity or settling velocity, is a more representative parameter. The major advantage of this measure is that it combines the effects of several variables into a single parameter, i.e. size, shape, density and viscosity. In addition it depends on the extent of the fluid in which it falls, or the number of particles falling and on the level of turbulence intensity.

Although the fall velocity concept is straightforward, its precise evaluation or calculation is not. Various methods for the determination of fall velocity exist. Fall velocities used in this study were determined as the average of the results using the following methods:

i) *Graf and Acaroglu [1966]* design curve (**Figure 5.9**)
ii) American Society of Civil Engineers design curve *[ASCE, 1971]*(**Figure 5.10**)
iii) *Fromme [1977]*
iv) *Rubey [1933]*
v) *Rubey-Watson [Watson, 1969].*

Values of the fall velocities are summarized in **Table 5.3** and an average design curve is presented in **Figure 5.11**, while the average fall velocity v_{ss} can be given by

$$v_{ss} = 0{,}1441 \ (0{,}8603^{(1/d)} \ d^{0{,}5619}) \tag{5.1}$$

with v_{ss} in m/s and d in mm.

Table 5.3 : Sediment fall velocity v_{ss}

Site	River	Sediment diameter d_{50} (mm)	Fall velocity v_{ss} (m/s)					
			ASCE [1971]	Graf [1966]	Fromme [1977]	Rubey [1933]	Rubey-Watson [1969]	Average
C84	Black Mfolozi	0,12	0,0105	0,0105	0,0156	0,0104	0,0161	0,013
E84	Mhlatuze	0,2	0,0232	0,0223	0,0297	0,0235	0,0352	0,027
B84	Mkuze	0,243	0,032	0,029	0,0372	0,0303	0,0446	0,035
E87	Mhlatuze	0,27	0,037	0,0317	0,0418	0,0343	0,0501	0,039
D84	White Mfolozi	0,38	0,0547	0,0504	0,0596	0,0485	0,0693	0,057
C87	Black Mfolozi	0,425	0,063	0,0543	0,0664	0,0535	0,076	0,063
B87	Mkuze	0,43	0,0633	0,0565	0,0671	0,054	0,0767	0,064
D87	White Mfolozi	0,61	0,093	0,0838	0,0917	0,0707	0,099	0,088
A84	Komati	1,33	0,135	0,17	0,16	0,115	0,159	0,148

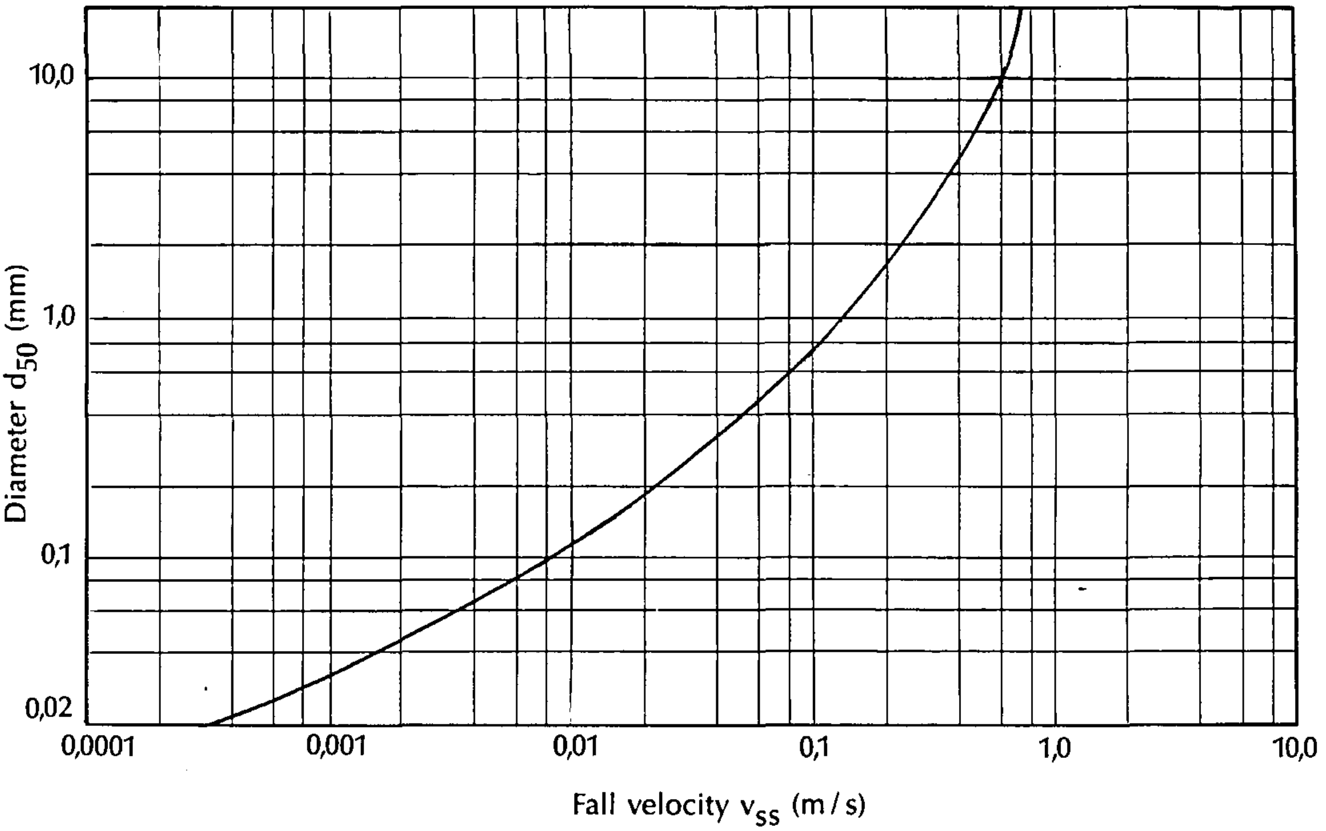

ALLUVIAL RIVER STUDY — Fall velocity determination (Graf, 1971) — **5.9**

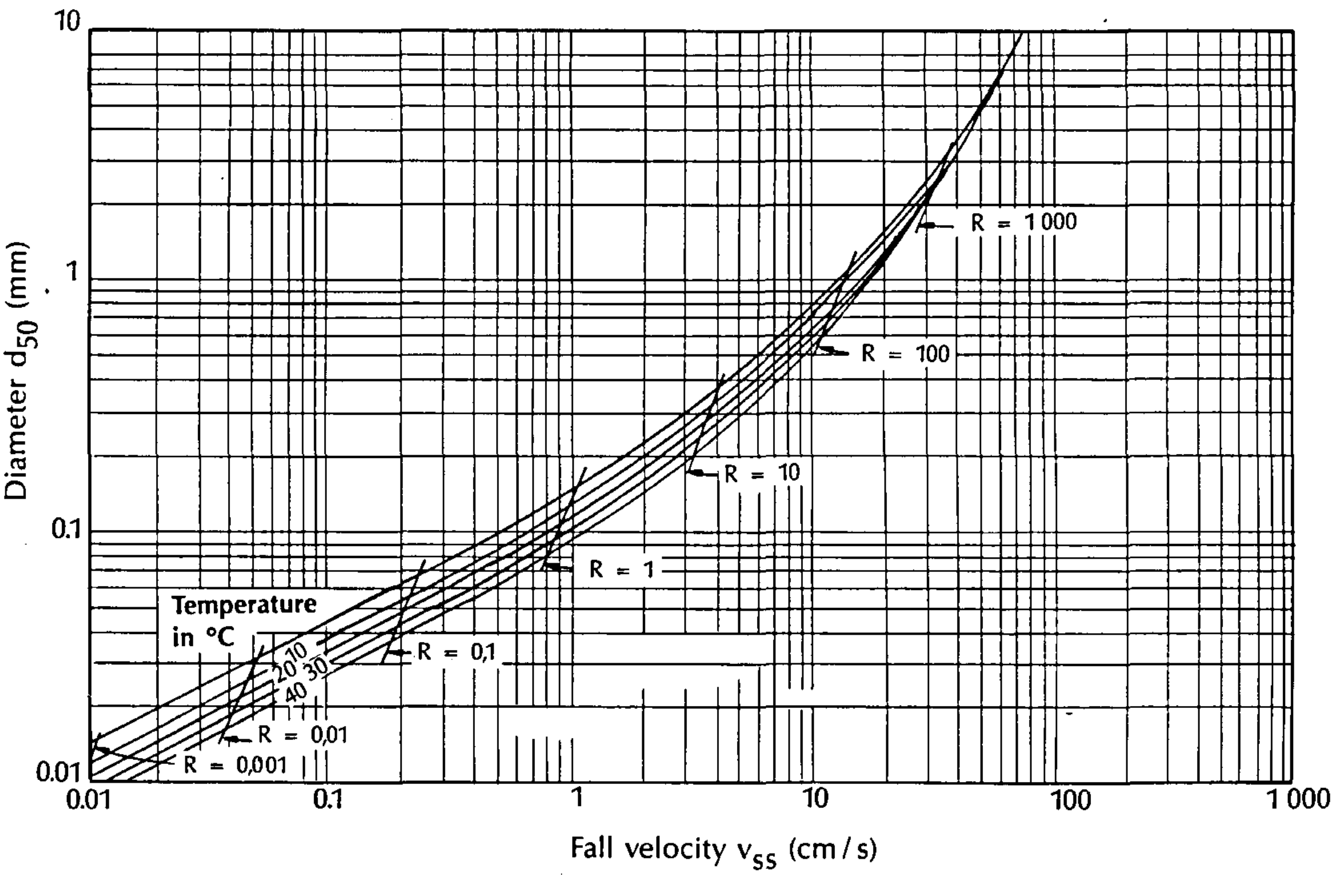

ALLUVIAL RIVER STUDY — Fall velocity determination (ASCE, 1971) — **5.10**

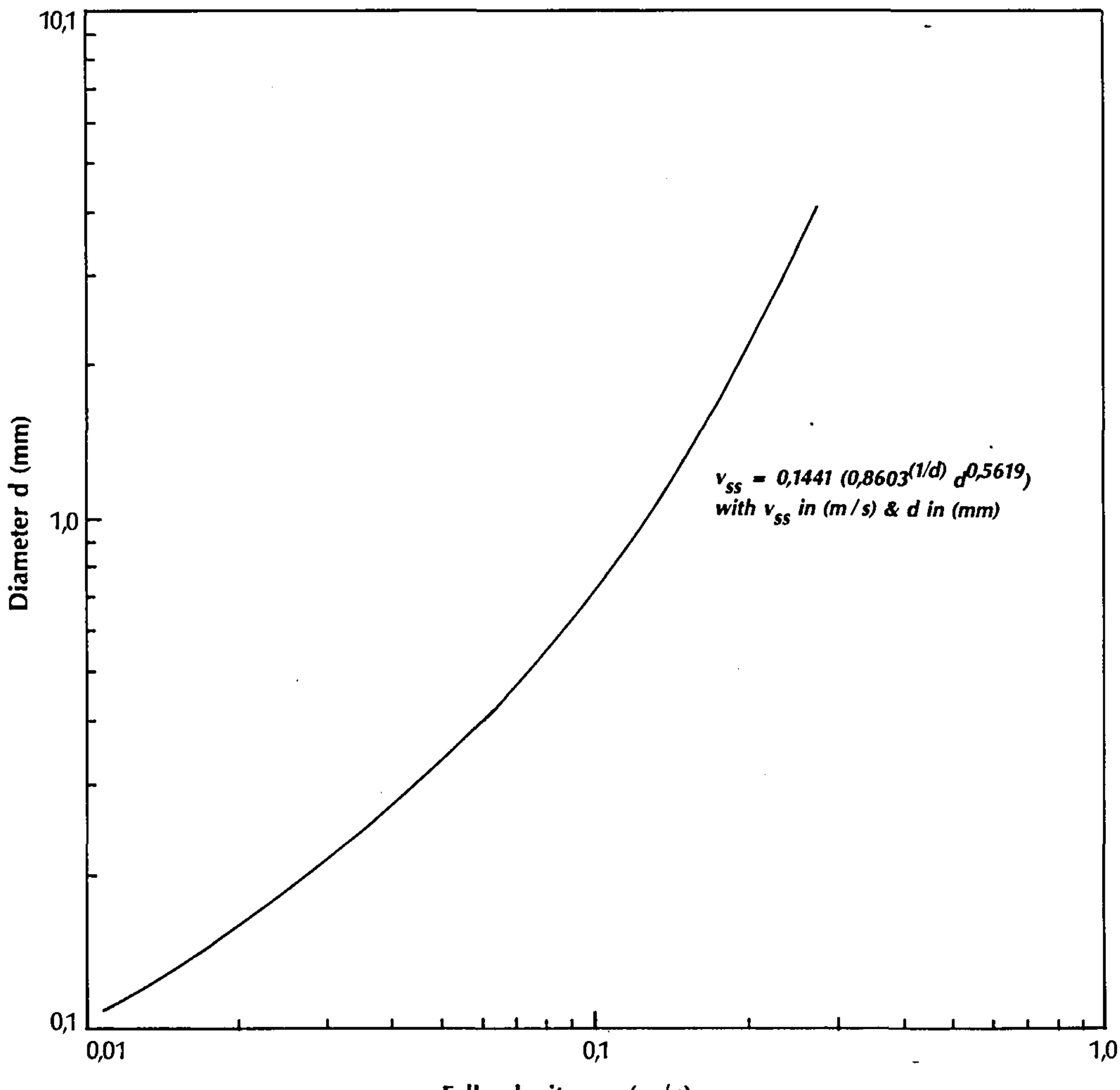

10,1
1,0
0,1
Diameter d (mm)
0,01
0,1
1,0
Fall velocity v_{ss} (m / s)
$v_{ss} = 0{,}1441\ (0{,}8603^{(1/d)}\ d^{0{,}5619})$
with v_{ss} in (m / s) & d in (mm)

6. EMPIRICAL VERIFICATION OF HYDRAULIC GEOMETRY FOR ALLUVIAL RIVER CHANNELS

6.1 INTRODUCTION

Alluvial rivers show certain consistencies in terms of flow and morphology. *Leopold and Maddock [1953]* have provided an empirical framework for the expression of this consistency. Plotting channel top-bank width B_T, cross-sectionally averaged (hydraulic) depth D, and mean velocity v at mean annual water discharge Q versus that discharge as it varies downstream for various streams, they established power-law relationships of the form

$$B_T = aQ^b \tag{6.1}$$

$$D = cQ^f \tag{6.2}$$

$$v = kQ^m \tag{6.3}$$

in which b = 0,5, f = 0,4 and m = 0,1. Subsequent investigations have shown that while the coefficients a, c and k vary from locality to locality, the exponents b, f and m display a surprising degree of constancy. They appear to be independent of location and only weakly dependent on channel type *[Parker, 1979]*.

The systematic behaviour of self-formed, straight and laterally symmetrical reaches of the alluvial research rivers, as discussed in **Section 5**, are analysed according to two methods, i.e. the well known regime theory of *[Blench, 1957]* and Parker's dimensional analysis *[Parker, 1979]* in this section. These two methods were chosen in order to establish whether Blench's widely-used relationships are applicable to southern African alluvial rivers and because Parker's theory was the only empirical regime theory found in the literature with a theoretical basis.

6.2 BLENCH'S REGIME THEORY

6.2.1 Methodology

Blench's regime theory *[Blench, 1957]* is the most well-known and widely-used regime concept. Blench argued that although width and depth unlike, mean meander size and river regime slope, vary enormously throughout a year and even from day to day there is no doubt about the existence of a regime of width and a regime of depth. The following equations have been deduced from the work of *Blench [1969]* for use in sand bed channels:

$$\bar{B} = 14 Q^{0,5}\, d_{50}^{0,25}\, F_s^{-0,5} \tag{6.4}$$

$$\bar{D} = 0,38\, q^{0,67}\, d_{50}^{-0,17} \tag{6.5}$$

where $\bar{B}$ is the mean channel width, $\bar{D}$ is the mean depth of flow, Q the equivalent steady discharge which would generate the same channel geometry, often assumed to be bankfull flow in alluvial channels (to estimate channel geometry under flood conditions the design flood flow may be used), q is the discharge per unit width $(=Q/\bar{B})$, d_{50} is the median size of bed material, and F_s is a side factor to describe bank material composition with the following values:

sandy loam:	$F_s = 0,1$
silty clay loam:	$F_s = 0,2$
cohesive:	$F_s = 0,3$

The equations quoted above should only serve as a guide for computing hydraulic geometry, since variations in channel slope and sediment load may have a significant affect on the width and depth of flow as calculated using these equations.

6.2.2 Verification of Blench's theory

The recorded field data was used to verify the applicability of Blench's theory. The comparison between the average recorded top width B_T and flow depth D with values predicted by the Blench theory, i.e. **Equations 6.4** and **6.5** respectively, is given in **Table 6.1.** According to field observations most of the bank material of the research rivers are of a cohesive type. Therefore, the side factor F_s was chosen as 0,3 for verification purposes.

Table 6.1 : Verification of Blench's regime theory

Site	River	Year	Observed values				Blench regime theory	
			Discharge Q (m^3/s)	Sediment diameter $d_{50}^{1)}$ (mm)	Width $B_T^{1)}$ (m)	Depth $D^{1)}$ (m)	Width $\bar{B}$ (m)	Depth $\bar{D}^{2)}$ (m)
A84	Komati	1984	2 640	1,33	168,6	11,0	250,8	5,67
B84	Mkuze	1984	5 600	0,243	275,2	11,5	238,82	12,95
B87	Mkuze	1987	1 060	0,43	132,2	4	119,8	6,11
C84	Black Mfolozi	1984	10 000	0,12	566,1	15,2	267,52	19,95
C87	Black Mfolozi	1987	1 740	0,425	153,7	5,2	153,09	7,25
D84	White Mfolozi	1984	6 500	0,38	304,9	12,4	287,72	11,70
D87	White Mfolozi	1987	2 150	0,61	177,7	5	186,26	6,89
E84	Mhlatuze	1984	2 400	0,2	131,5	6,7	148,9	10,41
E87	Mhlatuze	1987	3 600	0,27	154,8	7,4	196,6	10,78

1) Average values for site reach
2) $q = Q/\bar{B}_{Reach}$

From **Table 6.1** it can be seen, that although Blench's theory in some case predicts the rivers' behaviour in top width and depth, there is no general trend or relationship between observed values of top width and average flow depth and those predicted by Blench's theory.

Graphical comparisons as presented in **Figures 6.1** and **6.2** shows, taking an error margin of plus or minus 20 % as being acceptable for prediction purposes, a fair degree of general agreement between the calculated values of mean channel width $\bar{B}$, as calculated by means of the Blench theory, with average measured values of the top width B_T . However, the level of scatter for the comparison between calculated and measured values of mean flow depth is much higher.

6.3 PARKER'S DIMENSIONAL ANALYSIS

6.3.1 Methodology

Parker [1979] suggested that the relations for hydraulic geometry in the case of a threshold channel can be given by:

$$D^* = \phi_1(\tilde{Q}) \tag{6.6}$$

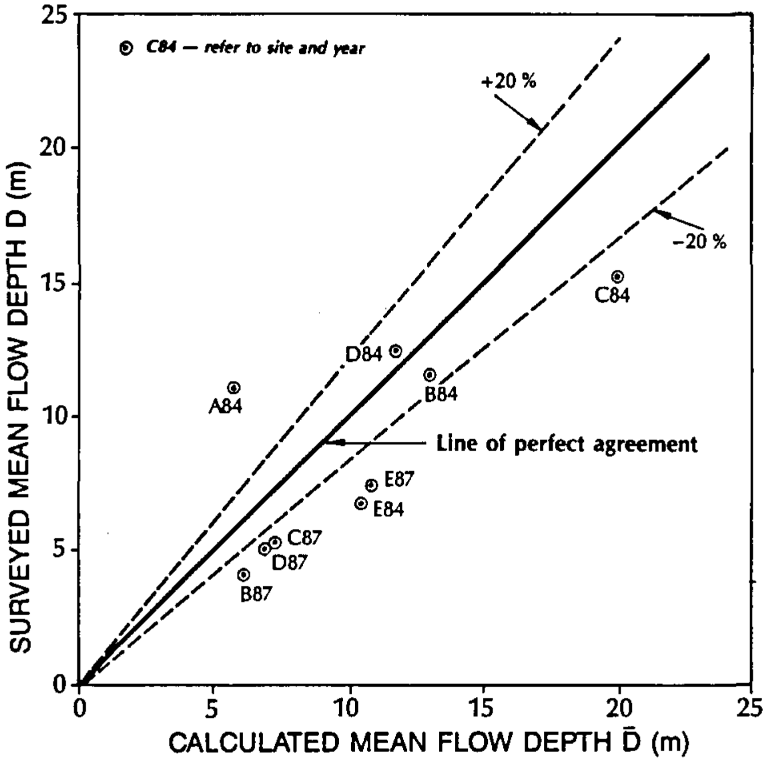

ALLUVIAL RIVER STUDY — Calculated (Blench) versus surveyed values of mean flow depth — 6.1

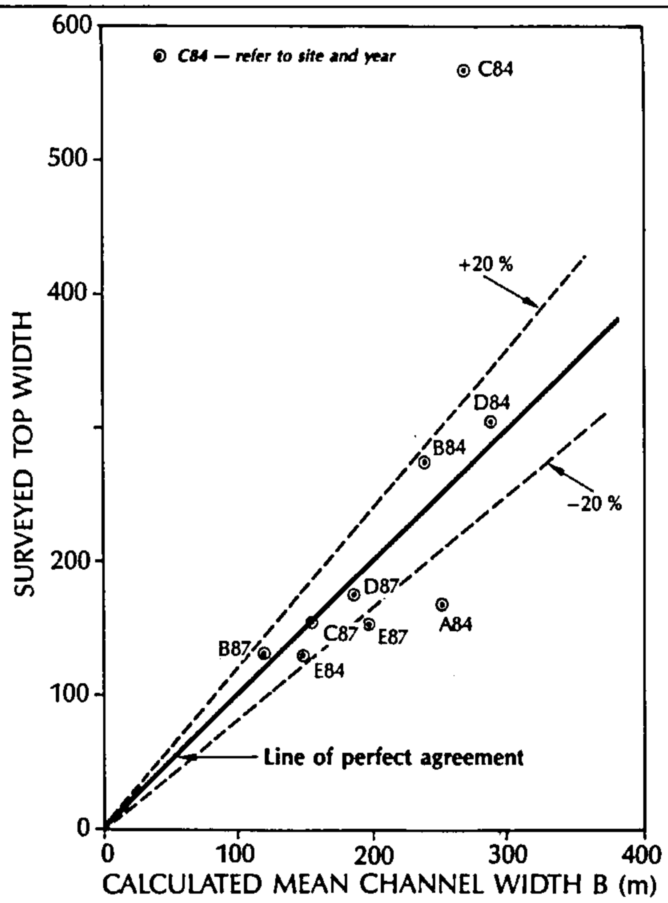

ALLUVIAL RIVER STUDY — Calculated (Blench) values of mean channel width versus surveyed values of top width — 6.2

$$B_T^* = \phi_2(\tilde{Q}) \tag{6.7}$$

$$v^* = \phi_3(\tilde{Q}) \tag{6.8}$$

where ϕ_1, ϕ_2, ϕ_3 are functions and D^*, B_T^*, v^* and $\tilde{Q}$ are dimensionless parameters defined as

$$D^* = D/d_{50} \tag{6.9}$$

$$B_T^* = B_T/d_{50} \tag{6.10}$$

$$v^* = v/\sqrt{(\rho_s/\rho - 1)gd_{50}}\ d_{50}^2 \tag{6.11}$$

$$\tilde{Q} = Q/\sqrt{(\rho_s/\rho - 1)gd_{50}}\ d_{50}^2 \tag{6.12}$$

with ρ and ρ_s the water and sediment densities respectively, d_{50} the median grain diameter, g the gravity acceleration and D, B_T, v and Q as defined earlier.

6.3.2 Verification of Parker's dimensional analysis

In this study an entirely empirical approach, based on Parker's dimensional analysis *[Parker, 1979]* was undertaken by plotting B_T^* versus $\tilde{Q}$ and D^* versus $\tilde{Q}$ for the data of the applicable alluvial research rivers, as shown in **Figures 6.3** and **6.4**. The data for these figures is presented in **Table 6.2**.

Table 6.2 : Dimensionless parameters for empirical study

Site	River	Year	Observed values				Dimensionless parameters		
			Discharge Q (m^3/s)	Sediment diameter $d_{50}^{1)}$ (mm)	Width $B_T^{1)}$ (m)	Depth $D^{1)}$ (m)	$\tilde{Q}$ (10^{10})	B_T^*	D^*
A84	Komati	1984	2 640	1,33	168,6	11,0	1,02	126 767	8 270
B84	Mkuze	1984	5 600	0,243	275,2	11,5	150	1132 510	47 325
B87	Mkuze	1987	1 060	0,43	132,2	4	6,87	307 442	9 302
C84	Black Mfolozi	1984	10 000	0,12	566,1	15,2	1 575	4717 500	126 667
C87	Black Mfolozi	1987	1 740	0,425	153,7	5,2	11,6	361 647	12 235
D84	White Mfolozi	1984	6 500	0,38	304,9	12,4	57,4	802 368	32 632
D87	White Mfolozi	1987	2 150	0,61	177,7	5	5,81	291 311	8 197
E84	Mhlatuze	1984	2 400	0,2	131,5	6,7	105	657 500	33 500
E87	Mhlatuze	1987	3 600	0,27	154,8	7,4	74,7	573 333	27 407

1) Reach averaged values

The observed field data was found to plot coherently with little scatter. The relationships

$$B_T^* = 3{,}228\ \tilde{Q}^{0{,}456} \tag{6.13}$$

$$D^* = 0{,}361\tilde{Q}^{0{,}416} \tag{6.14}$$

were determined by means of the method of least squares. In both cases a correlation coefficient of $r = 0{,}97$ was obtained.

Although the coeffients in **Equations 6.13** and **6.14** differ from those suggested by *Parker [1979]*, the exponents of the equations are very close. This is also consistent with what was established by *[Leopold and Maddock, 1953]*.

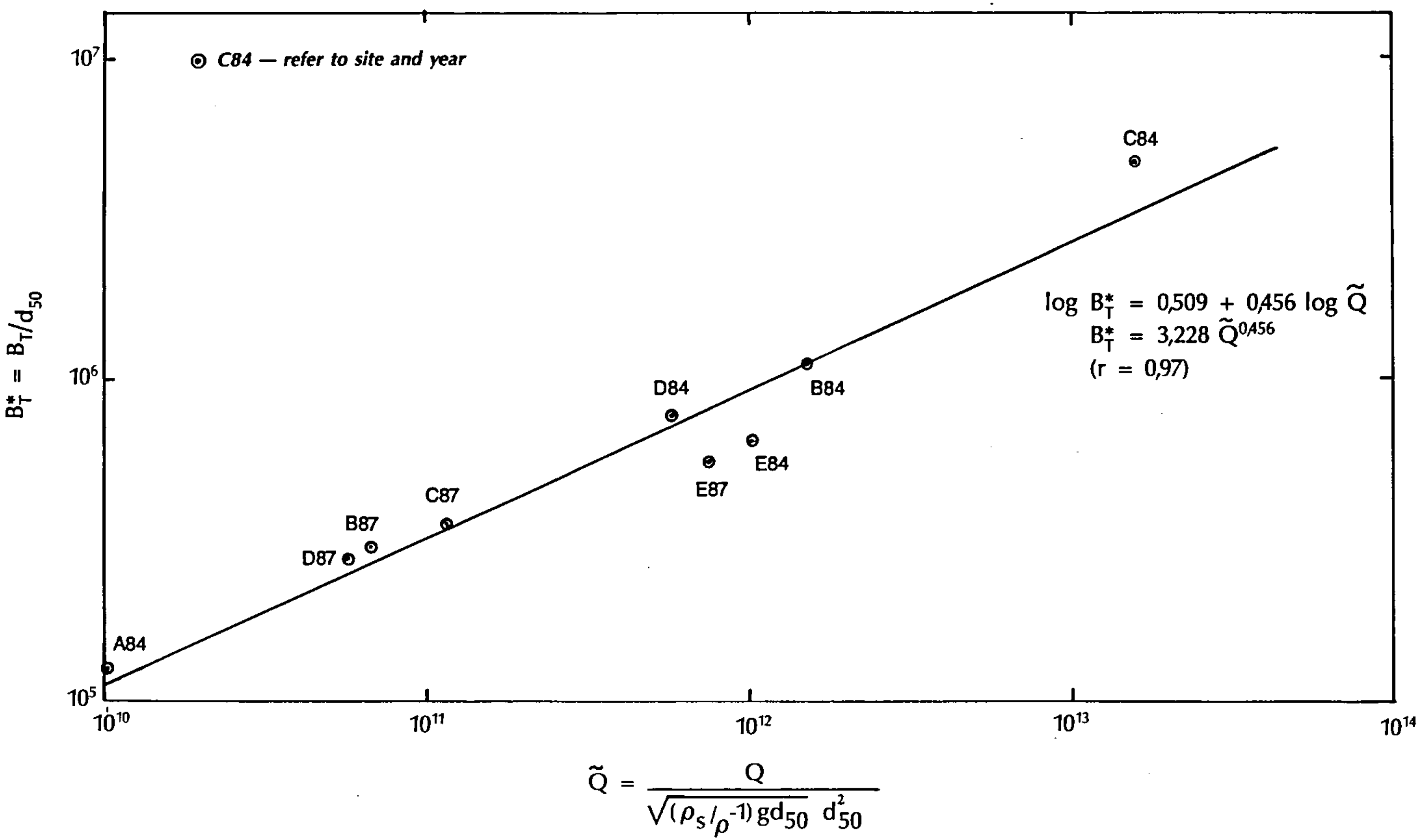

C84 — refer to site and year
10^7
10^6
10^5
$B_T^* = B_T/d_{50}$
C84
D84
B84
E84
E87
C87
B87
D87
A84
$\log B_T^* = 0{,}509 + 0{,}456 \log \tilde{Q}$
$B_T^* = 3{,}228\, \tilde{Q}^{0{,}456}$
$(r = 0{,}97)$
10^{10}
10^{11}
10^{12}
10^{13}
10^{14}
$\tilde{Q} = \dfrac{Q}{\sqrt{(\rho_s/\rho - 1)\, g d_{50}}\; d_{50}^2}$

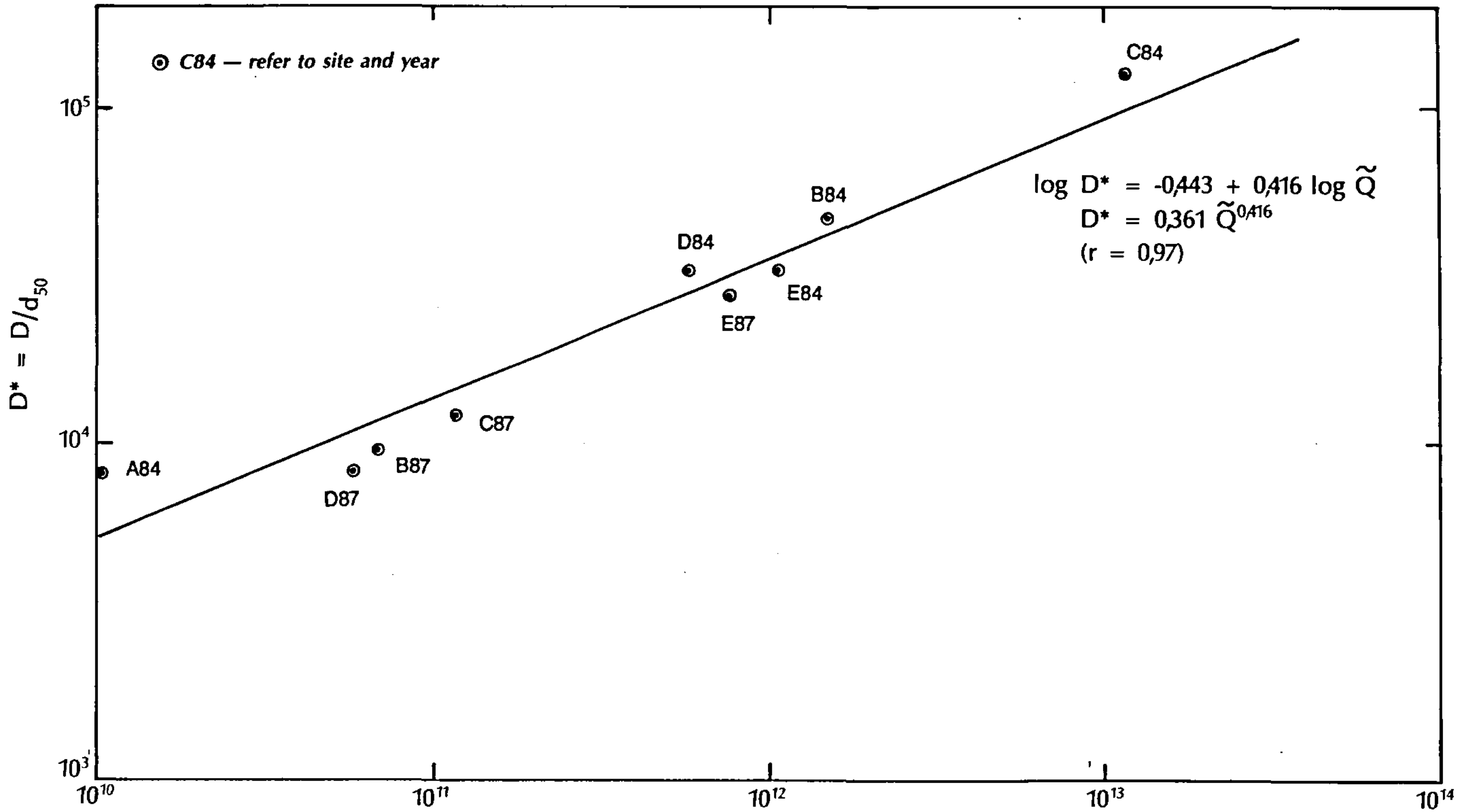

$$\tilde{Q} = \frac{Q}{\sqrt{(\rho_s/\rho - 1)\, g d_{50}}\; d_{50}^2}$$

6.4 CONCLUSIONS

It was found that the Parker-type empirical equations proved to be more reliable in the case of the rivers being considered than the theory of Blench. Thus, the empirical relationships, **Equations 6.13** and **6.14**, can be used to describe the regime behaviour of the alluvial research rivers and rivers similar to them. It must be kept in mind, however, that these relationships are empirical and give no explanation of how and why a channel adjusts its hydraulic geometry to a set of external constraints. Great care should always be taken not to apply them out of context.

7. THEORY REGARDING A FUNDAMENTAL APPROACH TO RIVER CROSS-SECTIONAL STABILITY

7.1 INTRODUCTION

Deposition and erosion of sediment and lateral migration of the river channel results in geometrical cross-sectional changes of an alluvial river channel. The behaviour of a river's cross-section not only depends on what is happening at the cross-section itself, but on the characteristics of the whole reach being studied. Thus, the problem of determining the geometry of a river's cross-section can be formulated as:

> *Given a discharge and an accompanying known sediment size, what width, depth and bed slope will the river channel adopt in order to convey both the water and sediment from one point to another if the discharge is to flow between banks and over a bed, all consisting of the river's own sediment?*

The equilibrium condition or stable condition can also be referred to as the critical condition associated with incipient motion in an alluvial channel. The perception is that nature will develop a stable cross-sectional shape, i.e. a conditon of zero net sediment transport over the wetted perimeter.

In summary it can be stated that because channel stability involves primarily the interaction of water with the bed and banks of a channel, it seems that a logical approach for analysing alluvial channel stability would be to study the nature of this interaction. Such a method has been devised based on the fundamental concept of applied stream power.

7.2 EQUILIBRIUM CONDITION

Where flow takes place over movable material and the relatively large amount of unit power required to maintain motion along the bed becomes greater than that which would be required in the process of deformation of the bed, the stream will begin to transport the bed material rather than persist in its existing mode of flow *[Rooseboom, 1974].*

Sediment being transported will lead to a change in the resistance to flow by changing the bed roughness and the suspended sediment concentration. As both of these increase, the applied stream power will decrease. A situation develops in which the sediment transport capacity of a stream will be in equilibrium with the supply. Such a situation is characterized by no further sediment transport, i.e. no degradation or aggradation, and can be referred to as the *equilibrium* condition.

A constant stream with a average flow velocity of v_i that flows for a long enough period will create a certain *stable* condition in an erodible conduit. In nature flow velocities are rarely constant for a significant period. If the flow velocity increases to v_{i+1} and the incipient erosion condition is crossed, it can be expected that the channel shape will change. This will result in changes in the flow depth, hydraulic radius, hydraulic roughness and possibly the channel slope. The tendency is thus towards a new stable or equilibrium condition. However, it might take a long time to change from one equilibrium condition to another.

Reference to an equilibrium condition tends to be confusing. It is better to refer to this condition as a *stable non-equilibrium* condition. All the processes within a non-equilibrium system are steady. Stability and order in non-equilibrium systems can only be maintained by continuous exchange of energy with the surrounding environment, resulting in such systems being called dissipative systems to distinguish them from equilibrium systems *[Annandale, 1987].*

For analysis of an equilibrium condition it must therefore be assumed that steady state flow conditions exist, i.e. $\frac{dv}{dt} = 0$. As flows in rivers are irregular, such a condition can only exist if the flow conditions are such that they are homogeneous in the long term, i.e. if a constant moving average is approached.

The critical condition of incipient motion in an alluvial channel can be referred to as an equilibrium condition. The critical condition is not constant for different flows, i.e. for different magnitudes of flows different critical conditions exist.

This condition can be regarded as the beginning of sediment transport for a certain magnitude of flow whilst it can also be the condition for the end of sediment transport for another (smaller) magnitude of flow, i.e. the latter flow's sediment transport capacity is satisfied at that stage. The incipient motion or critical condition thus represents a margin between sediment transport and non-sediment transport conditions.

7.3 SEDIMENT TRANSPORT IN ALLUVIAL OPEN CHANNEL FLOW

A stream in a loose boundary channel through which the material is being transported can change the geometry and the hydraulic roughness of the channel. Although the characteristics of channels with rigid boundaries can be determined with reasonable accuracy, it is not the case for erodible conduits like alluvial channels.

The cross-section of the channel may become displaced laterally and a complexity of bed forms can be developed thereby introducing form drag caused by the bed features, as well as energy losses due to secondary currents. The problem is further complicated by the movement of sediment both along the bed and in suspension, since the mixture of water and sediment does tends to develop velocity profiles which differ from those in clear water.

As soon as the stream begins to transport bed material (or material from other sources) the flow structure changes. When sediment is transported, the amount of unit stream power applied along the bed can be reduced in three ways *[Rooseboom, 1974]*:

i) through the formation of a pseodo-viscous zone of high concentration suspension along the bed - represented by an increase in the size of the eddies
ii) through the formation of ripples, dunes, etc., whereby eddies with larger radii are formed along the bed
iii) through the creation of a meandering course whereby the value of the slope S is reduced.

Computations of channel shape variations have to allow for

i) the hydraulic roughness that could vary with time
ii) the grain size distribution which might also vary.

The hydraulic roughness is likely to be time-dependent. Moreover, it can be assumed that the roughness at any moment will not be uniquely determined by the actual values of the various hydraulic parameters as foregoing events might affect the roughness (hysteresis effect).

The deformation of the stream-bed during changing flow conditions from a flat bed to a waved one at mild discharges and back to a flat bed with an undeterminable roughness factor at large discharges and velocities can cause that the absolute roughness factor for a given stream or river reach can vary by a factor of ten or more. Different discharges are thus possible for any combination of depth and slope.

The repetitive formation and decay of the bed forms and their shapes, sizes and patterns depend on the kinematic and dynamic characteristics of the flow and the material forming the channel geometry. The resistance of an alluvial river bed is thus influenced by these bed irregularities, and more specific by their dimensions at a specific stage. The flow resistance due to these bed surface irregularities are additional over and above those caused by the grain roughness alone *[Einstein and Barbarossa, 1951].*

It also has been established that the resistance to flow in alluvial channels varies with the flow regime and that the influence of these bed forms is far more important than that of the grain roughness in determining the total resistance at certain flow regimes *[Ilo, 1975].*

The influence of the grain-size distribution on the processes of aggradation and degradation is apparent. Degradation specifically is a function of the grain-size distribution. The grain-size distribution is of great importance in determining the final bed level. Segregation influences degradation as armouring may take place which can reduce the degradation rate considerably. An armoured sediment bed develops when degradation effectively removes finer bed material leaving a covering layer coarser particles which cannot be transported by the flow.

7.4 FUNDAMENTAL PRINCIPLES OF HYDRAULIC CALCULATIONS

7.4.1 General

In order to employ stage-discharge relationships in flows carrying heavy sediment loads, like alluvial streams, it is necessary to understand the mechanics of open channel flow, and also to understand the mechanics of sediment transport. An overview regarding the application of conservation laws, resistance, velocity distribution and power balance in open channel flow is given below.

7.4.2 Application of the conservation laws to fluid flows

Normally three fundamental principles are generally applied in hydraulic calculations. These principles relate to *[Rooseboom, 1974]*:

i) *conservation of mass (continuity principle)*
ii) *conservation of momentum*
iii) *conservation of energy (Bernoulli equation).*

Depending on what information is available and what is needed, every hydraulic calculation basically involves the application of one or more of these principles. Virtually all calculations involve the continuity principle, while the energy principle is often used together with the continuity principle. Forces which are exerted by flowing streams can only be calculated by means of the momentum equation. The momentum equation often provides more accurate answers where energy losses and gains cannot be determined accurately. An additional principle, the principle of *conservation of power*, is often very useful in the analysis of some aspects of fluid flow such as sediment transport. Because this principle is mathematically related to the laws of conservation of energy and momentum, it is not regarded as an independent law.

Unlike the momentum equations, power relationships are not functions of direction, i.e. they are scalar and unlike the energy equations they are directly time related. These special qualities make power relationships particularly useful in the analysis of flow phenomena.

The attempt to apply these laws to a fluid presents a problem. A flowing fluid is a continuum - that is to say, it is not possible to subdivide the flow into separate small masses. The answer to this problem of applying the basic laws to a fluid lies in the use of a *control volume* which is a purely imaginary region of any shape within a body of flowing fluid. Inside the region, all of the dynamic forces cancel out.

7.5 OPEN CHANNEL FLOW RESISTANCE AND VELOCITY VARIATION

7.5.1 General

Sediment transport in open channel flow is inseverably linked to flow resistance. The approach followed to investigate the basic mechanism of flow resistance is based on the theory of applied stream power *[Rooseboom, 1974]*.

The state of behaviour of open channel flow is governed basically by the effects of viscosity and gravity relative to the inertial forces of the flow. Open channel flow can be laminar, turbulent or transitional depending on the slope, the roughness of the wetted perimeter and the effect of viscosity relative to inertia. Mathematical description of velocity distribution is only possible if the relationship between the shear stress τ and velocity gradient $\frac{dv}{dy}$ is known.

The flow is *laminar* if the viscous forces are so strong relative to the inertial forces that viscosity plays a dominant part in determining flow behaviour. In laminar flow, the water particles appear to move in definite smooth parallel paths, or streamlines, and infinitesimally thin layers of fluid seem to slide over adjacent layers with no transverse component of velocity. The flow is *turbulent* if the viscous forces are weak relative the inertial forces. In turbulent flow, the water particles move in irregular paths which are neither smooth nor fixed but which in the aggregate still represent the forward motion of the entire stream. Individual particles are subject to fluctuating transverse velocities so that the motion is eddying and sinuous rather than rectilinear. This type of motion causes an exchange of momentum from one portion of the fluid to another. The origin of turbulence and the accompanying transition from laminar to turbulent flow is of fundamental importance to the whole science of fluid mechanics.

Wherever alternate modes of flow exist, that mode which requires the least applied power will prevail. The reason for this is that the mode which requires the least applied power represents the condition under which yield takes place most readily. Contrary to what may intuitively be assumed this often results in a lower average velocity than in the alternative case.

In what follows the theory is primarily based on uniform stationary flow. Uniform flow may be turbulent or laminar, depending upon such factors as discharge, slope, viscosity and degree of surface roughness.

7.5.2 Shear stress variation in open channel flow

Consider uniform stationary flow of a homogeneous liquid in a channel with infinite width, small longitudinal slope S, and depth of flow D *[Rooseboom, 1974]*. The average point velocity in the x-direction at a distance y from the bed is v, with the y-axis taken perpendicular to the bed and the x-axis along the bed as shown in **Figure 7.1**.

As there is no acceleration, the forces acting on an element with height $(D - y)$, length Δx, and unit width have to be in equilibrium. It is convenient to represent the resistance to movement being encountered by the element by a shearforce $(\tau \Delta x)$, acting along the lower plane of the element.

For equilibrium conditions this opposing force must be equal to the driving force which consists of the weight component of the element in the direction of flow. This weight component in the direction of flow can be given by

$$W = \gamma V \sin S \qquad (7.1)$$

Substituting for the volume V and putting $\sin S \simeq S$ it can be obtained that

$$W = \rho g (D-y) \Delta x \, S \qquad (7.2)$$

with ρ the mass density of the liquid and g the acceleration of gravity.

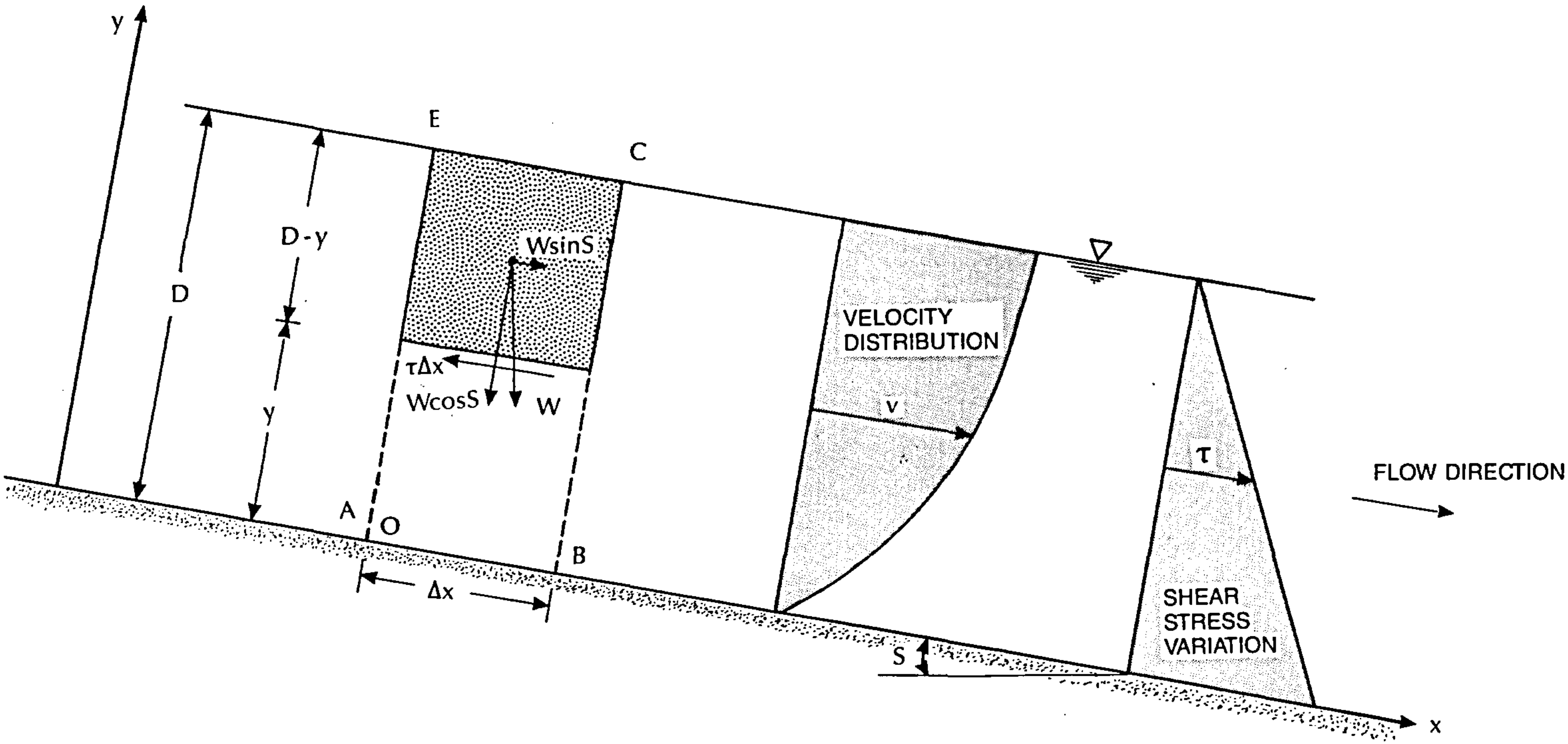

Force, velocity and shear stress diagram for open channel flow

7.1

Thus, opposing forces

$$\tau \Delta x = \rho g(D-y)\Delta x S$$

or (7.3)

$$\tau = \rho g(D-y)S$$

The shear stress τ therefore must increase linearly from a value of zero at the surface to the maximum value of ρgSD at the bed, irrespective of the mechanisms by which it is generated.

7.5.3 **Velocity variation in laminar flow**

In laminar flow the viscous forces predominate and no eddying or transverse current exists. Shear stresses are generated by liquid interaction and fluid behaviour may be depicted as a series of elemental layers sliding one over the other, with the relative motion being governed by Newton's law of viscosity. This law expresses the relation between the dynamic viscosity μ, the velocity gradient $\frac{dv}{dy}$ and the shear stress τ at a distance y from the boundary surface, as follows:

$$\tau = \mu \frac{dv}{dy} \tag{7.4}$$

Equations 7.3 and **7.4** can be equated to obtain

$$dv = \frac{gS}{\upsilon}(D-y)dy \tag{7.5}$$

where υ is the kinematic viscosity (μ/ρ) .

Integrating, and taking into account that $v = 0$ when $y = 0$,

$$v = \frac{gSy}{\upsilon}(D-\frac{y}{2}) \tag{7.6}$$

This is a quadratic equation indicating that the velocity of uniform laminar flow in a wide open channel has a parabolic distribution.

Integration of **Equation 7.6** from $y = 0$ to $y = D$ and division of the result by D, results in the average velocity $\bar{v}$:

$$\bar{v} = \frac{1}{D}\int_o^D v dy = \frac{1}{D}\int_o^D \frac{gSy}{\nu}(D - \frac{y}{2})\, dy$$

or (7.7)

$$\bar{v} = \frac{gSD^2}{3\upsilon}$$

It should be noted that the velocity is independent of the surface roughness and this is, of course, characteristic of laminar flow. The nature of the surface, however, is important since excessive roughness, being conductive to eddying and turbulence, tends to disrupt the rectilinear nature of flow. Laminar flow is not stable in situations involving combinations of low viscosity, high velocity, or large flow passages and breaks down into turbulent flow.

7.5.4 Velocity variation in turbulent flow

Turbulent flow differs from laminar flow in such a way that the flow particles move not according definite streamlines. A particle in the flow can thus be transported in various other directions different from the general flow direction. *Rooseboom [1974]* argued that in the case of turbulent flow, the apparent shear stresses are generated by eddying motion on a molar scale as opposed to movement on a molecular scale in laminar flow. Portions of the fluid temporarily move as units in the form of eddies, or parts of such eddies which instantaneously follow circular paths. From continuity considerations, the angular velocity of an eddy must equal the velocity gradient $\frac{dv}{dy}$ which exists at the centre of the eddy.

In the case of an eddy, a flow particle will rotate momentarily around the centre of the eddy. Consider a cylindrical element of an eddy with outer radius R which momentarily exists with its centre O in a plane $O' - O'$ where the apparent stress has to be τ (**Figure 7.2**).

According to Newton's second law, the resisting force in the x-direction can be given by

$$\begin{aligned}\delta F &= \rho Q \Delta v \\ &= \rho u \delta A v\end{aligned} \qquad (7.8)$$

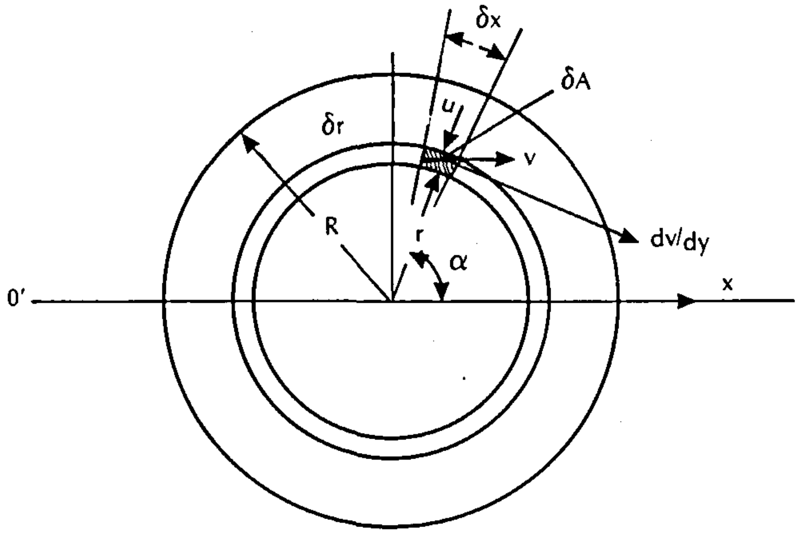

a. Momentarily eddy in turbulent flow

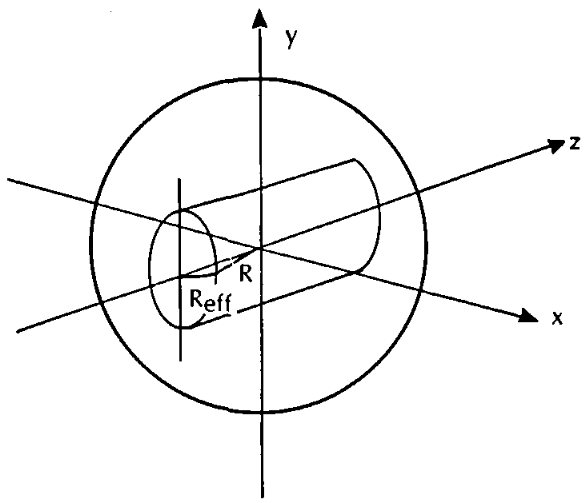

b. Boundary eddy

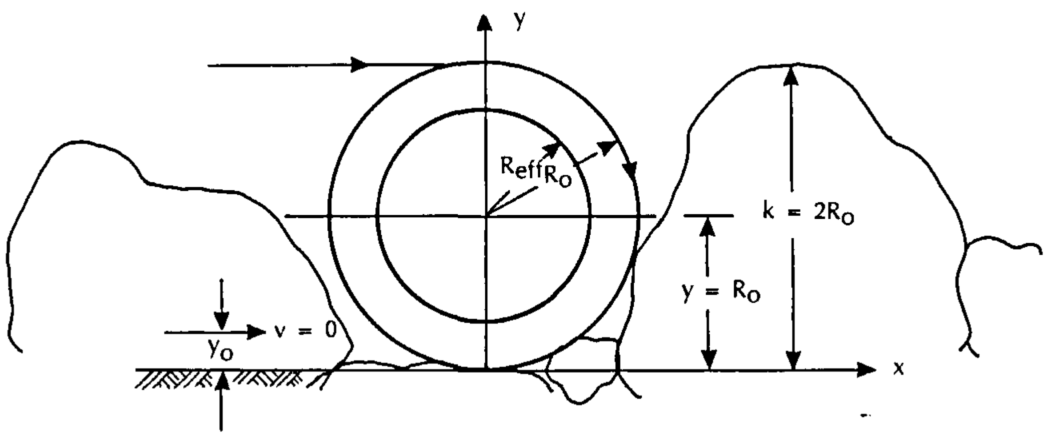

c. Eddy formed between irregularities on boundary

Thus,

$$\tau \delta A = \rho (r\frac{dv}{dy}\cos\alpha)\delta A(r\frac{dv}{dy}\sin\alpha)$$

$$\tau = \rho r^2 (\frac{dv}{dy})^2 \sin\alpha \cos\alpha \tag{7.9}$$

The average value of the shear stress across the cylindrical element therefore equals

$$\bar{\tau} = \frac{4\int_o^R \int_o^{\pi/2} \rho \, (\frac{dv}{dy})^2 r^3 \cos\alpha \sin\alpha \, dr \, d\alpha}{\pi R^2}$$

$$= \frac{\rho}{2\pi} R^2 (\frac{dv}{dy})^2$$

$$= (0{,}3989)^2 \rho R^2 (\frac{dv}{dy})^2$$

$$\approx (0{,}4)^2 \rho R^2 (\frac{dv}{dy})^2 \tag{7.10}$$

This formula is equivalent to the well-known Prandtl equation for turbulent shear stress:

$$\bar{\tau} = \rho \ell^2 (\frac{dv}{dy})^2 \tag{7.11}$$

in which ℓ = mixing length.

Thus

$$\ell = \frac{1}{\sqrt{2\pi}} R \approx 0{,}4R = \kappa y \tag{7.12}$$

where κ is the so-called von Karman constant, the value of which is found to be equal to 0,4 for homogeneous fluids. This factor compensates for the fact that the momentum exchange varies across the cylindrical element and y represents the distance from the boundary. This relationship is based on the contention that if the turbulent exchange increases, the greater the distance from the boundary and that at the boundary it is zero.

To be able to derive the velocity distribution equation, it is necessary to determine how R varies as a function of y.

Consider a thin element ABCE (**Figure 7.1.**) of a stream which momentarily has to move as a unit. The velocity at O next to the boundary, has to be equal to zero, and the only possible way in which ABCE can momentarily move as a unit, is by relative rotation around O. As the fluid flow in the channel is translatory, such rotational movement is not possible unless it is accompanied by translation of the centre of rotation O. A small fluid element at a distance y from the bed rotates with angular velocity $\frac{dv}{dy}$ and the translatory velocity relative to the centre of rotation is $y\frac{dv}{dy}$. Translatory flow in the channel will only be possible if the centre of rotation translates with a speed $y\frac{dv}{dy}$ and because the centre of rotation is common to all elements in the vertical *[Rooseboom, 1974]*.

It follows from **Equations 7.3** and **7.10** that

$$\tau = \rho g S(D-y) = \frac{\rho}{2\pi} R^2 \left(\frac{dv}{dy}\right)^2 \tag{7.13}$$

$$\therefore \quad \frac{dv}{dy} = \frac{\sqrt{2\pi g S(D-y)}}{R}$$

$$\therefore v_o = y\frac{dv}{dy} = y\frac{\sqrt{2\pi g S(D-y)}}{R} \tag{7.14}$$

where v_o represents the velocity of the centre of rotation.

At the bottom $y \to 0$, $(D-y) \to D$ and y can be equated to R_o, where R_o is the radius of eddies next to the bed:

$$v_o = y\frac{dv}{dy} = \sqrt{2\pi g D S} \tag{7.15}$$

where $\sqrt{gDS}$ is often called the shear velocity though no physical meaning is attached to it.

From **Equation 7.15** it follows that

$$\frac{dv}{dy} = \frac{\sqrt{2\pi g D S}}{y} \tag{7.16}$$

Combining **Equations 7.16** and **7.14**, it follows that

$$R = y\sqrt{\frac{(D-y)}{D}} \qquad (7.17)$$

Integration of **Equation 7.16** leads to

$$v = \sqrt{2\pi gDS}\ \ell n\ \frac{y}{y_o} \qquad (7.18)$$

where y_o is the ordinate of the level at which the velocity mathematically equals zero. For the simple case where the irregularities on the bed consist of identical half spheres, stacked closely together, with radii R_o, it is possible to determine the value of y_o theoretically.

To fit in with the geometry of the boundary, it is evident that the eddies which are formed right next to the boundary, will have practically the same diameter as the irregularities and that these eddies with radii R_o will be approximately spherical in shape.

Rooseboom [1974] argued that if the boundary eddies with spherical radius of R moves in a transverse x-direction on the boundary, an effective radius R_{eff} can be determined with regard to **Figure 7.2** as

$$R_{eff} = 0{,}8165\,R_o \qquad (7.19)$$

The effective flow boundary is therefore situated at a distance $0{,}1835\ R_o$ from the mathematical flow boundary. The translatory velocity of the eddies equals v_o at a distance $0{,}1835R_o$. Thus with $v_o = v$ it follows that *[Rooseboom, 1974]*

$$y_o = \frac{R_o}{14{,}8} \approx \frac{k_s}{29{,}6} \qquad (7.20)$$

where y_o is the depth in terms of the eddy radius where $v = 0$ and k_s representing the diameter of the irregularities on the bed.

Substitution of **Equation 7.20** in **Equation 7.18** leads to

$$v = \sqrt{2\pi g D S}\ \ell n\ \frac{14{,}8y}{R_o} \tag{7.21}$$

Integration of **Equation 7.21** leads to the average velocity at a flow depth $y = 0{,}37D$ *[Rooseboom, 1974]*

$$\begin{aligned} \bar{v} &= \sqrt{2\pi g D S}\ \ell n\ \frac{5{,}45D}{R_o} \\ &= \sqrt{2\pi g D S}\ \ell n\ \frac{11{,}84D}{k_s} \\ &= 5{,}75\ \sqrt{gDS}\ \log\ \frac{11{,}84D}{k_s} \end{aligned} \tag{7.22}$$

comparing to the Chezy equation

$$\bar{v} = 5{,}75\ \sqrt{gRS}\ \log\ \frac{12{,}2R}{k_s} \tag{7.23}$$

as found in literature *[Webber, 1971]*.

7.6 POWER BALANCE IN ONE-DIMENSIONAL OPEN CHANNEL FLOW

In the case of free surface flows the loss of energy can be given by

$$\gamma QS = \Delta p Q = -dp/dxQ \tag{7.24}$$

where Q is the discharge through a section of unit length and Δp is the pressure drop. In other words, $Q\Delta p$ is the rate at which potential energy is released to maintain flow. This is the process of dissipation or expenditure of energy of the flow, representing the rate of external entropy supply and referred to as input stream power. This input stream power is consumed in overcoming the resistance and is finally dissipated in the form of molecular heat. The rate of work required to overcome fluid friction is referred to as applied stream power and represents the rate of internal entropy production.

Thus, for total flow in a given section during a unit time the principle of conservation of power can be given by

$$\sum \textbf{ input stream power } = \sum \textbf{ applied stream power} \tag{7.25}$$

However, local values of input stream power and applied stream power are not equal and not mutual counterbalanced. Therefore, they must be mutually related by an intermediate process whose role consists in transferring energy from one point of the transverse section to another point where the mechanism of energy exchange cause loss thereof.

Consider the movement of a small fluid element with dimensions Δx, Δy and unit width as shown in **Figure 7.3a:**

The equation of motion applied to the fluid element relates the shear stress and pressure drop. For uniform flow $\frac{dv}{dy} = 0$ and there is no acceleration for the element under consideration. Hence, $\sum (forces)_x = 0$:

$$p\delta y - \left(p + \frac{dp}{dx}\delta x\right)\delta y - \tau\delta x + \left(\tau + \frac{d\tau}{dy}\delta y\right)\delta x = 0 \tag{7.26}$$

Thus, for a unit volume

$$\frac{dp}{dx} = \frac{d\tau}{dy} \tag{7.27}$$

which implies that the rate of change of pressure in the x-direction must equal the rate of change of shear in the y - direction. Clearly, $\frac{d\tau}{dy}$ is independent of y and $\frac{dp}{dy}$ is independent of x .

Also the unit rate of energy dissipation, i.e. work in unit time for unit volume of the fluid

$$-v\frac{dp}{dx} = -v\frac{d\tau}{dy} \tag{7.28}$$

where v equals the translatory velocity of the unit element in the x-direction.

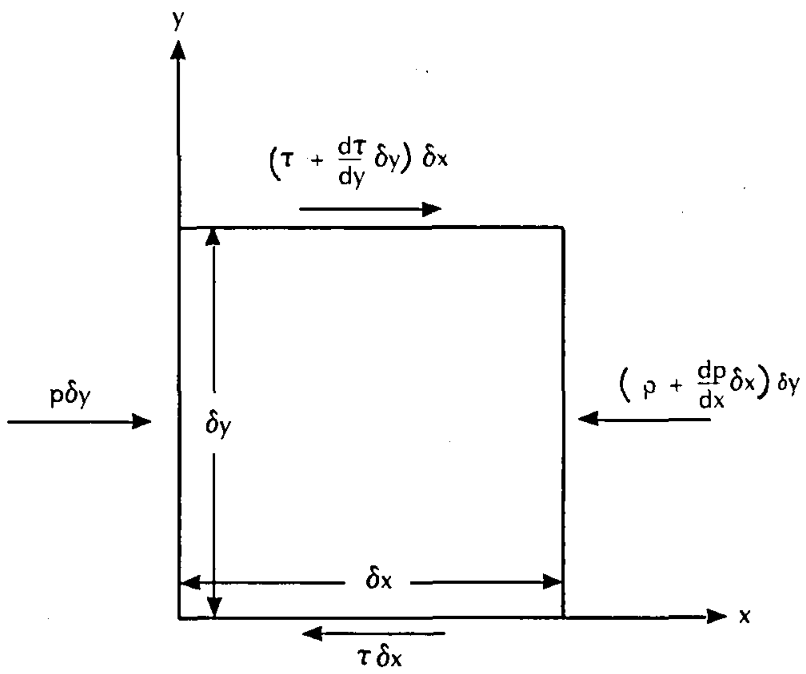

a. Forces on a fluid element

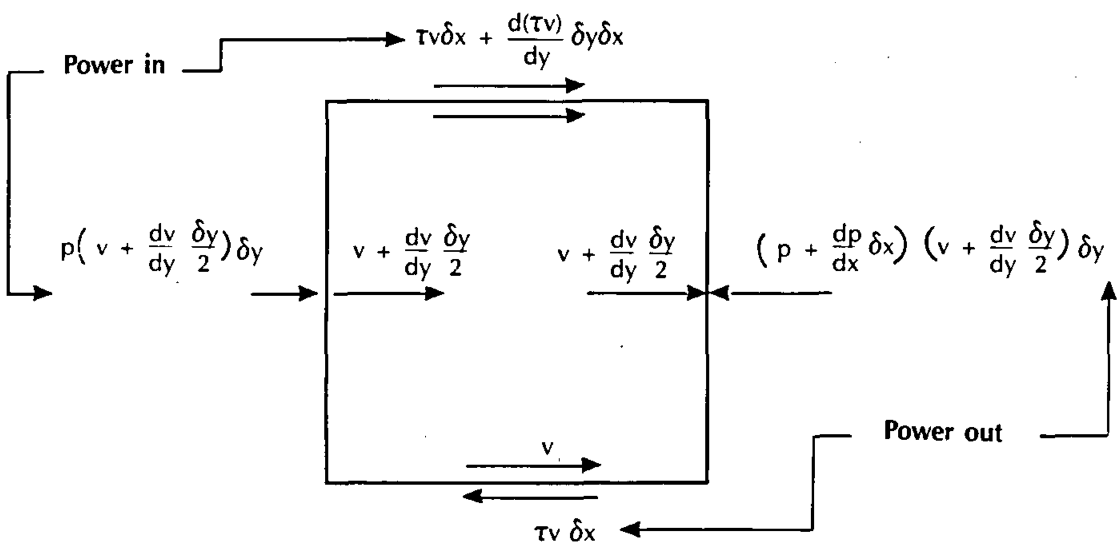

b. Work done on a fluid element

According to **Equation 7.3**

$$\tau = \rho g(D-y)S \tag{7.29}$$

$$\therefore \quad \frac{d\tau}{dy} = -\rho gS \tag{7.30}$$

Unit input stream power can thus be given by (from **Equation 7.28**) ρgvS.

To determine the applied stream power, i.e. the rate required to overcome fluid friction, it is necessary to consider the net applied power on a small fluid element as shown in **Figure 7.3b:**

$$\text{net applied power} = p\left(v + \frac{dv}{dy}\frac{\delta y}{2}\right)\delta y - \left(p + \frac{dp}{dx}\delta x\right)\left(v + \frac{dv}{dy}\frac{\delta y}{2}\right)\delta y$$
$$+ \tau v\delta x + \frac{d}{dy}(\tau v)\delta y\delta x - \tau v\delta x \tag{7.31}$$

and

$$\text{net applied power/unit volume} = \frac{d(\tau v)}{dy} - v\frac{dp}{dx}$$
$$= \tau\frac{dv}{dy} + v\frac{d\tau}{dy} - v\frac{dp}{dy} \tag{7.32}$$

From **Equation 7.28** it follows

$$\text{unit applied stream power} = \frac{\tau dv}{dy} + \frac{vd\tau}{dy} - \frac{vd\tau}{dy}$$
$$= \tau\frac{dv}{dy} \tag{7.33}$$

Although the total input stream power equals the total applied power over a unit length, there is a difference in the vertical distribution of these variables:

If shear stress is written as a function of vertical flow depth for free surface flow **(Equation 7.3)**

$$\tau = \rho g(D-y)S \tag{7.3}$$

and velocity as a logarithmic function of flow depth

$$v = \frac{\sqrt{gDS}}{\kappa} \ell n \frac{y}{y_o} \tag{7.18}$$

with y_o = flow depth where velocity equals zero, it follows that

$$\frac{dv}{dy} = \frac{\sqrt{gDS}}{y\kappa} \tag{7.34}$$

According to **Equations 7.3, 7.33** and **7.34** applied stream power can be rewritten as

$$\tau \frac{dv}{dy} = \rho g(D-y)S \frac{\sqrt{gDS}}{y\kappa} \quad , \; y_o \leq y \leq D \tag{7.35}$$

or

$$(\tau \frac{dv}{dy})_o = \rho g D S \frac{\sqrt{gDS}}{y_o \kappa} \tag{7.36}$$

with $D-y \approx D$ and $y \approx y_o$ at the bottom.

Input stream power per unit volume can be rewritten as

$$\rho g v S = \rho g S \frac{\sqrt{gDS}}{\kappa} \ell n \frac{y}{y_o} \quad , \; y_o \leq y \leq D \tag{7.37}$$

Thus, whereas the input stream power will have a logarithmic vertical distribution in an open channel, the vertical distribution of the applied stream power is such that most of it is applied along the boundary to overcome friction.

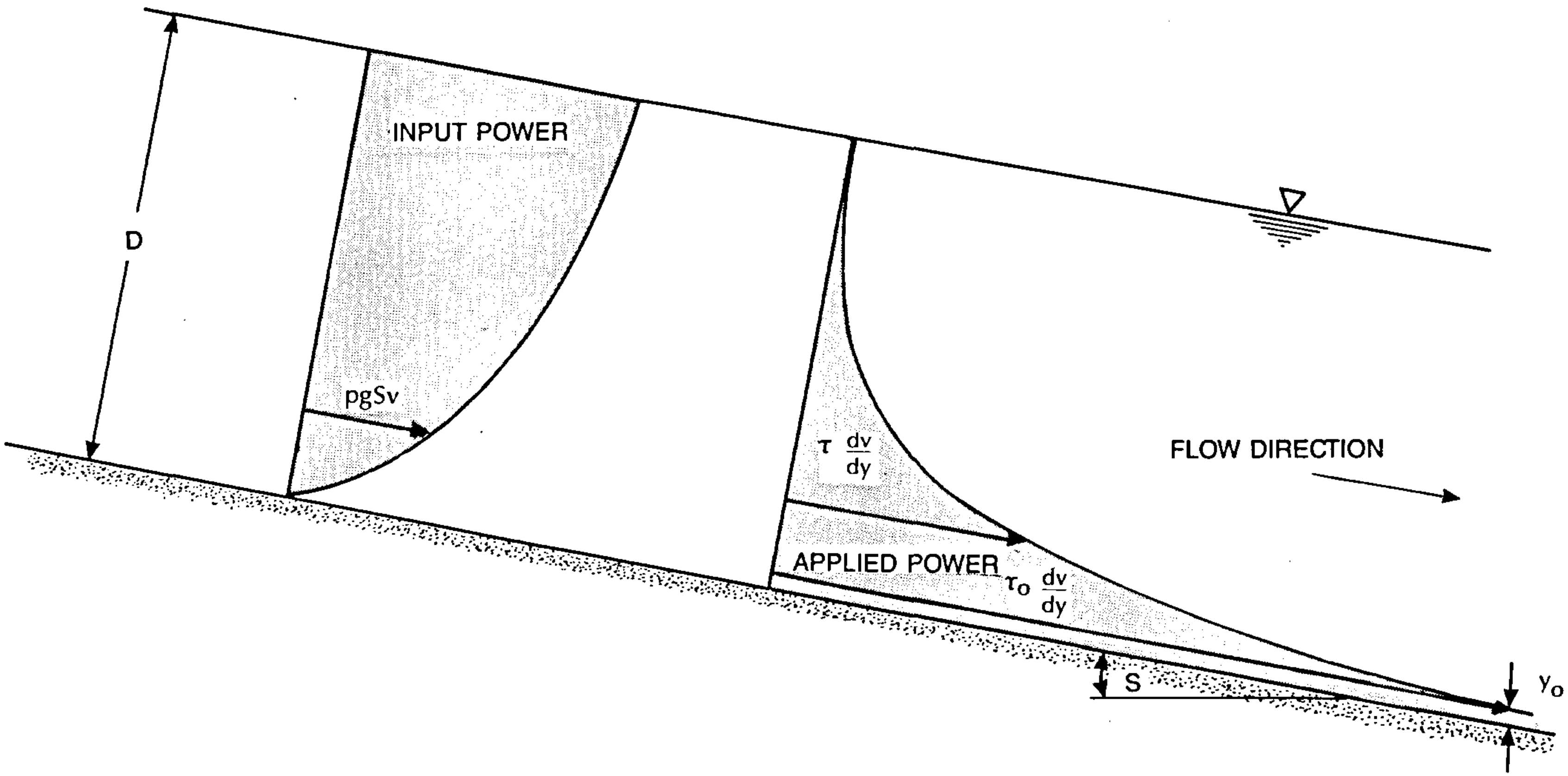

Distribution of available and applied stream power in open channel flow

The variation of the terms $\tau\frac{dv}{dy}$ and $\rho g S v$ is shown diagrammatically in **Figure 7.4.** It is evident that for the majority of flowing elements there is a considerable difference between the values of these forms. In accordance with the principle of the conservation of power (**Equation 7.25**), the areas enclosed by the graphs should be equal, i.e.

$$\sum \textbf{input stream power} = \sum \textbf{applied stream power} \tag{7.25}$$

$$\int_{y_o}^{D} \rho g S v \, dy = \int_{y_o}^{D} \tau \frac{dv}{dy} \, dy \tag{7.38}$$

This equation proves to be valid for both laminar and turbulent flow.

8. DETERMINATION OF A STABLE CROSS-SECTION

8.1 INTRODUCTION

In the theorectical stable hydraulic cross-section critical conditions will prevail at every point along the perimeter of the cross-section.

Not only the shear stress, but also the resistance to displacement of a particle depends upon its location on the perimeter of the cross-section. When a particle on the perimeter is in a state of impending motion, the forces acting to cause motion are in equilibrium with the forces resisting motion.

8.2 SHEAR STRESS VARIATION ON FLOW BOUNDARY

8.2.1 Shear stress variation along a flat bed

According to **Equation 7.3,** the shear stress on a flat bed for one-dimensional flow is given by

$$\tau = \rho g S(D-y) \tag{7.3}$$

Thus, on the bed where $y = 0$

$$\tau_o = \rho g S D \tag{8.1}$$

with D representing the flow depth above the bed. According to velocity variation for turbulent flow, it follows from **Equation 7.13** *[Rooseboom, 1974]* that

$$\tau_o = \rho \kappa^2 R_o^2 (\frac{dv}{dy})_o^2 \tag{8.2}$$

with $(\frac{dv}{dy})_o$ representing the velocity gradient and R_o the radius of the irregularities on a flat bed.

8.2.2 <u>Shear stress variation across side slope</u>

Consider an element of flowing fluid on a side slope with uniform curvature along the wetted perimeter. The perimeter shear stress τ_s can be derived in two ways:

A. Assume that the shear stress on the side is generated only by the weight of water above the bottom element (see **Figure 8.1a**). Lateral transfer of shear stress is thus ignored.

Consider the balance of forces acting on the element:

$$\text{opposing force} = \text{driving force}$$

$$\tau_s ds = \rho g \sin S dA \approx \rho g S y dz \tag{8.3}$$

$$\therefore \quad \tau_s = \rho g S y \frac{dz}{ds} = \rho g S y \cos\theta \tag{8.4}$$

Analogous to the velocity variation for turbulent flow on a flat bed, it follows that on the side

$$\tau_s = \rho \kappa^2 R_s^2 \left(\frac{dv}{dy}\right)_s^2 \tag{8.5}$$

with $\left(\frac{dv}{dy}\right)_s$ representing the velocity gradient and R_s the radius of the irregularities on the slope.

B. Assume the shear stress to be proportional to the distance between the water surface and perimeter and perpendicular to the perimeter (see **Figure 8.1b**) and ignore lateral transfer of shear stress.

Consider the balance of forces acting on the element:

$$\text{opposing force} = \text{driving force}$$

$$\tau_s ds = \rho g \sin S dA \approx \rho g\, S y' ds$$

$$= \rho g S \frac{y}{\cos\theta} \tag{8.6}$$

$$\therefore \quad \tau_s = \frac{\rho g S y}{\cos\theta} \tag{8.7}$$

$$\frac{dz}{ds} = \cos\theta$$

$$ds = \sqrt{(dy)^2 + (dz)^2}$$

$$\therefore \frac{dz}{\sqrt{(dy)^2 + (dz)^2}} = \cos\theta$$

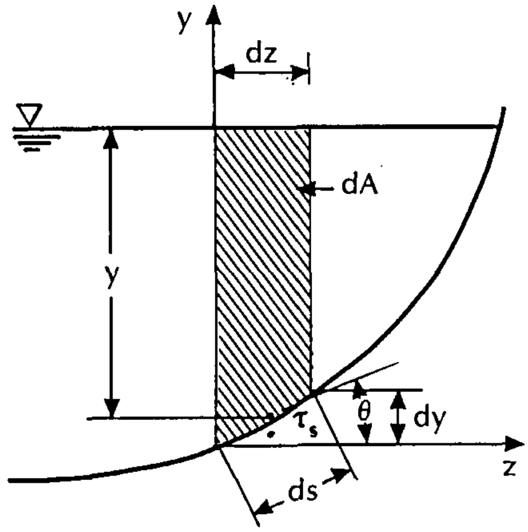

a. Shear stress due to vertical weight of water

$$\frac{dz}{ds} = \cos\theta$$

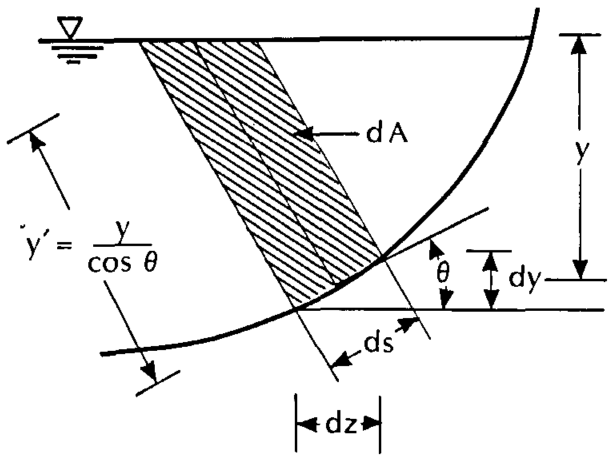

b. Shear stress due to perpendicular distance on bottom

As before

$$\tau_s = \rho\kappa^2 R_s^2 (\frac{dv}{dy})_s^2 \tag{8.5}$$

where $\left(\frac{dv}{dy}\right)_s$ represents the velocity gradient and R_s the radius of the irregularities on the perimeter.

8.3 MINIMIZATION OF APPLIED STREAM POWER ALONG PERIMETER

Flow in loose boundary channels is associated with yielding of the fluid as well as of the surface of the channel boundary. The unit power being applied reaches a high peak value at the bed (see **Figure 7.4**). If a criterion is to be derived to identify a stable cross-section, it is reasonable to ignore the power consumption in the upper regions and to concentrate on the power being applied along the perimeter. The error introduced in this way should be small.

According to *Rooseboom [1974]* applied stream power on a flat bed is given by **(Equation 7.36)**

$$(\tau\frac{dv}{dy})_o = \frac{\rho g D S \sqrt{gDS}}{\kappa\, y_o} \tag{7.36}$$

for turbulent flow conditions with $y = 0$.

From **Equation 8.2** it follows for a flat bed that

$$(\frac{dv}{dy})_o = \frac{\sqrt{\tau_o}}{\sqrt{\rho}\ \kappa R_o} \tag{8.8}$$

The product of **Equation 8.1** and **Equation 8.8** defines applied unit stream power and equating it to **Equation 7.36** results in

$$(\tau\frac{dv}{dy})_o = \frac{\tau_o^{3/2}}{\sqrt{\rho}\ \kappa R_o} = \frac{\rho(gDS)^{3/2}}{\kappa y_o} = \frac{14{,}8\rho(gDS)^{3/2}}{\kappa R_o} \tag{8.9}$$

Therefore,

$$\tau_o^{3/2} = 14{,}8(\rho g S D)^{3/2} = 14{,}8(\gamma S D)^{3/2} \tag{8.10}$$

With the assumption that the bottom irregularities are constant along the perimeter, i.e. $R_s = R_o$, it can be proved in the same way that for the two approaches being followed the side shear stresses are given by:

A:
$$\tau_s^{3/2} = 14{,}8(\gamma S y \cos\theta)^{3/2} \tag{8.11}$$

and B:
$$\tau_s^{3/2} = 14{,}8\left(\frac{\gamma S y}{\cos\theta}\right)^{3/2} \tag{8.12}$$

8.4 RELATIONSHIP BETWEEN BED AND SIDE VARIABLES

8.4.1 Shear stress relationship

According to the velocity variation under turbulent flow conditions:

$$\frac{\tau_s}{\tau_o} = \frac{\rho \kappa^2 R_s^2 (\frac{dv}{dy})_s^2}{\rho \kappa^2 R_o^2 (\frac{dv}{dy})_o^2}$$

The assumption that the eddy size R prevails everywhere along the flow boundary, i.e. $R_s = R_o = R$, results in

$$\sqrt{\frac{\tau_s}{\tau_o}} = \frac{(\frac{dv}{dy})_s}{(\frac{dv}{dy})_o} \tag{8.13}$$

From **Equations 8.1, 8.4** and **8.7** it follows from equating forces that for cases A and B:

A:
$$\frac{\tau_s}{\tau_o} = \frac{y\cos\theta}{D} \tag{8.14}$$

and B:
$$\frac{\tau_s}{\tau_o} = \frac{y}{D\cos\theta} \tag{8.15}$$

8.4.2 Applied stream power relationship

From **Equations 8.9** to **8.12** it follows that for the two cases:

A:
$$\frac{(\tau \frac{dv}{dy})_s}{(\tau \frac{dv}{dy})_o} = \left(\frac{y\cos\theta}{D}\right)^{3/2} \tag{8.16}$$

and B:
$$\frac{(\tau \frac{dv}{dy})_s}{(\tau \frac{dv}{dy})_o} = \left(\frac{y}{D\cos\theta}\right)^{3/2} \tag{8.17}$$

8.5 PROFILE DETERMINATION

A cross-section will be in a stable condition when the critical condition, i.e. state of incipient motion, exists along the full flow boundary. Therefore, for a stable condition, the applied stream power will be the same everywhere *[Rooseboom, 1991]*

$$\therefore \quad \frac{(\tau \frac{dv}{dy})_s}{(\tau \frac{dv}{dy})_o} = 1 \tag{8.18}$$

Accordingly, **Equations 8.16** and **8.17** can be simplified to

A:
$$\frac{y\cos\theta}{D} = 1$$

$$\therefore \frac{y}{D} = \frac{1}{\cos\theta} = \sqrt{1+\left(\frac{dy}{dz}\right)^2} \tag{8.19}$$

and B:
$$\frac{y}{D\cos\theta} = 1$$

$$\therefore \quad \frac{y}{D} = \cos\theta = \frac{1}{\sqrt{1+\left(\frac{dy}{dz}\right)^2}} \tag{8.20}$$

which represent two possible profiles of a stable cross-section. The mathematical derivation for both profiles is presented in **Appendix B**.

If the geometry of a cross-section is considered, only a part of the section, i.e. the bottom or centre channel section will contain a maximum flow depth D. The rest of the cross-section, i.e. the side channel or bank sections will contain flow depths smaller than D. The profile shape described by **Equations 8.19** and **8.20** is a symmetrical "*curve*" with a depth D at the centre. Therefore, **Equations 8.19** and **8.20** can be regarded as describing only the bank profile of a cross-section and not the nearly horizontal parts of wide river beds.

According to **Appendix B**, case A, with a hyperbolic cosine function describing the profile, is believed to provide the best solution. The relevant geometrical characteristics of a hydraulicly stable section with impending motion (critical condition) along its perimeter are as follows, all being functions of the centre flow depth D:

Top width	:	$B_T = 2{,}634D$	(8.21)
Cross-sectional area	:	$A = 1{,}804D^2$	(8.22)
Wetted Perimeter	:	$P = 3{,}464D$	(8.23)
Hydraulic Radius	:	$R = 0{,}5208D$	(8.24)

8.6 EQUILIBRIUM CROSS-SECTIONAL GEOMETRY

A river cross-section is considered as a centre channel with an average flow depth D and two side channels with hyperbolic cosine profiles (see case A, **Appendix B**) as indicated in **Figure 8.2**. The side channels are described in terms of top width B_s, hydraulic radius R_s and flow area A_s in terms of **Equations 8.21 - 8.24** (total of two side channels):

$$B_s = B_{T(\text{side channel})} = 2{,}634D \tag{8.25}$$

$$R_s = R_{(\text{side channel})} = 0{,}5208D \tag{8.26}$$

$$A_s = A_{(\text{side channel})} = 1{,}804D^2 \tag{8.27}$$

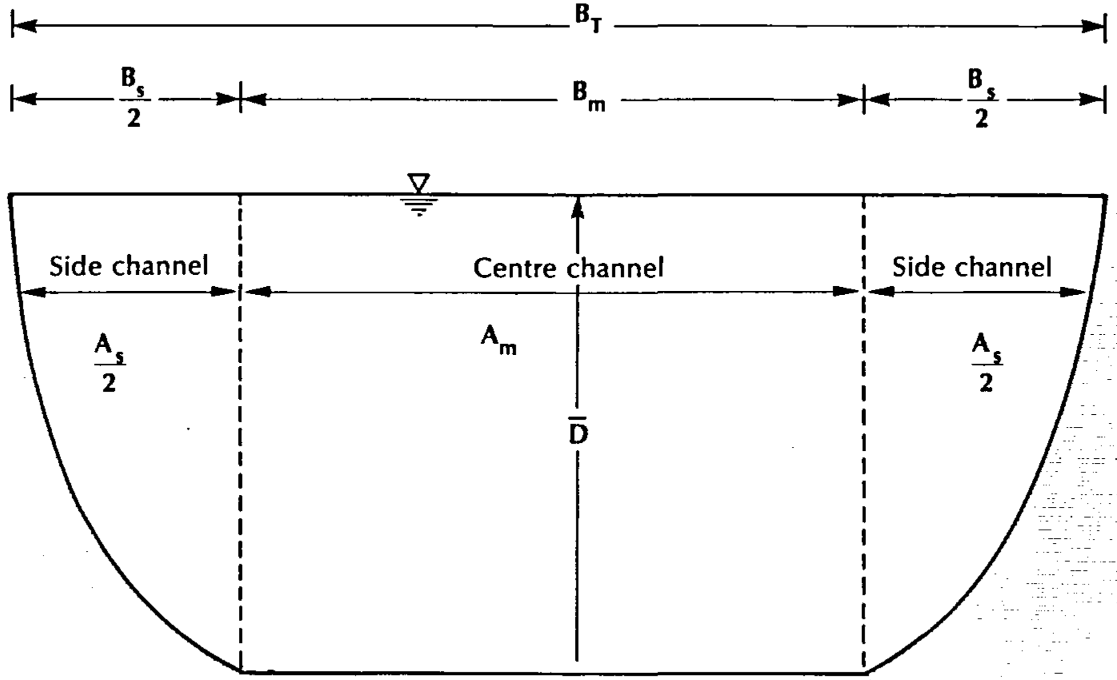

ALLUVIAL RIVER STUDY

Schematic representation of assumed cross-sectional geometry

8.2

With these values known, the average *side channel* velocity v_s can be calculated from

$$v_s = 5{,}75\sqrt{gRS}\,\log\frac{12{,}2R_s}{k_s} \tag{8.23}$$

with the *side channel* discharge Q_s equal to

$$Q_s = v_s\, A_s \tag{8.28}$$

The discharge Q_m through the *centre channel* section of the cross-section can then be assumed to be

$$Q_m = Q_t - Q_s \tag{8.29}$$

where Q_t equals the total design discharge.

Based on the principle of the conservation of power, i.e. **(Equation 7.25)**

$$\sum \textbf{input stream power} = \sum \textbf{applied stream power} \tag{7.25}$$

and the fact that most of the applied stream power is applied to the perimeter to overcome friction, **Equation 7.38** can be used to determine the bottom width B_m of the *centre channel* section. Application of **Equation 7.38** to a *centre channel* section with a discharge of Q_m leads to

$$\int_{y_o}^{D}\rho gSv\,dA = \int_{y_o}^{D}\tau\frac{dv}{dy}dA$$

$$\rho gSQ_m = \int_{y_o}^{D}\frac{\rho gSB_m(D-y)\sqrt{2\pi gDS}\,dy}{y}$$

$$= \rho gSB\sqrt{2\pi gDS}\int_{y_o}^{D}\left(\frac{D-y}{y}\right)dy$$

$$\therefore\ Q_m = B_m\sqrt{2\pi gS}\left(D^{1,5}\ell nD - D^{1,5}\ell ny_o - D^{1,5} + D^{0,5}y_o\right) \tag{8.30}$$

with
$$y_o \approx \frac{R_o}{14{,}8} \approx \frac{k_s}{29{,}6} \tag{7.20}$$

The predicted total top width of the cross-section can then be approximated by

$$B_T = B_m + B_s \tag{8.31}$$

8.7 CONCLUSIONS

Although all the geometric parameters can be expressed as functions of the flow depth at the channel centre, the remaining problem is to determine this flow depth, or equilibrium depth D and the accompanying absolute roughness k_s along on the flow perimeter.

The determination of the equilibrium or critical depth, i.e. the flow depth at which critical conditions will prevail, is thus very important in the analysis in the search for the equilibrium condition of a river cross-section.

It is widely accepted that an armour layer will develop as this depth is approached. Such a layer consists of elements large enough not to be transported by the prevailing flow, i.e. scour will take place until such a layer is established. However, an alluvial river tends to a condition of minimum energy, i.e. minimization of applied stream power. The presence, however, of fine sediments in an alluvial river provides an alternative mechanism whereby scour is limited, i.e. deformation of the river bed. As a river's bed is deformed and the value of k_s increases, the applied unit stream power along the bed is decreased. Deformation of the bed can thus lead to equilibrium being reached before an armour layer is developed.

As mentioned previously the critical condition or equilibrium condition can be regarded as the beginning of sediment transport for a certain magnitude of flow whilst it can be the condition for the end of sediment transport for a lower discharge. Incipient motion theory can thus be used to determine of estimated values of the equilibrium flow depth D and the corresponding absolute roughness k_s-value.

9. INTERACTION BETWEEN FLOWING FLUID AND TRANSPORTABLE MATERIAL

9.1 THEORETICAL BACKGROUND

It might be expected that when extremely large floods with high sediment carrying capacities occur in rivers with erodible bed and bank materials, scour will continue to take place until the erosive capacity of the stream approaches the minimum value required to transport the available material.

A stream will transport sediment only if the critical condition is exceeded. The critical stage is reached when the transporting capacity of a stream equals that which is required to dislodge material from the channel margin. Criteria which indicate whether sediment will be transported under given conditions are very important in sediment transport studies. A number of criteria have been developed which depict the critical stage where a stream's transporting capacity becomes sufficient to transport the available material. Classical examples of such criteria are presented in the *Hjulström [1935], Shields [1936]* and *Liu [1957]* diagrams.

Hjulström's diagram simply relates critical velocity to particle diameter and does not provide an accurate criterion. The Shields-diagram was developed on the basis of dimensional analysis of certain variables involved in sediment transport. Its main shortcoming is that particle grain size is neither a truly representative nor a unique measure of transportability. In certain practical situations e.g. where artificial armouring units are present, particle size becomes a meaningless concept. The settling velocity of particles is a more significant measure in the case of non-cohesive material *[Rooseboom, 1985]*.

Whilst the above-mentioned diagrams were developed primarily on an intuitive basis, rigorous theoretical analysis of flow transporting capacity and sediment transportability leads to the type of relationships represented in the Liu-diagram *[Rooseboom, 1974; 1991]*. The success of this applied power approach is attributed to the fact that both flow transporting capacity and sediment transportability can be expressed in directly comparable scalar terms.

It is a general characteristic of flowing media that whatever alternative modes of flow exist, that mode which requires the least amount of unit power will be followed. Accordingly fluid flowing over movable material will not transport such material unless this will result in a decrease in the amount of unit power which is required to maintain motion. Alternatively if two modes of yielding exists, yielding will take place according to that mode which offers the least resistance.

Where flow takes place over movable material and the relatively large amount of unit power required to maintain motion along the bed becomes greater than that which would be required in the process of deformation of the bed, the stream will begin to transport the bed material rather than persist in its existing mode of flow.

Rooseboom [1974] suggested that incipient motion can be analysed more comprehensively in terms of power considerations:

The unit potential energy per unit volume required to suspend a discrete particle with mass density ρ_s and settling velocity v_{ss} in a fluid with mass density ρ equals

$$(\rho_s - \rho)gy \tag{9.1}$$

where y corresponds to vertical distance. The applied unit stream power required can then be given by the reduction in unit potential energy per unit time

$$(\rho_s - \rho)g\,\frac{dy}{dt} = (\rho_s - \rho)gv_{ss} \tag{9.2}$$

where v_{ss} represents the fall velocity of the particle.

It follows from **Equation 7.36** that in rough turbulent flow, the unit stream power applied in maintaining motion along a bed, consisting of particles with diameter $d\ (=2R_o)$,
is proportional to

$$\frac{\rho g DS\sqrt{gDS}}{d} \tag{9.3}$$

in which S represents energy slope and D depth of flow.

In terms of the concept of minimum applied power or principle of least resistance, the stream will begin to entrain particles when the power required to suspend the particles becomes less than the power required to maintain the status quo *[Rooseboom, 1974]*.

At that stage

$$(\rho_s - \rho) g v_{ss} \propto \rho g D S \frac{\sqrt{gDS}}{d} \tag{9.4}$$

According to the general equation for settling velocity *[Graf, 1971]*,

$$v_{ss} \propto \sqrt{\left(\frac{\rho_s - \rho}{\rho}\right) \frac{gd}{C_d}} \tag{9.5}$$

and assuming that C_d, the drag coefficient, is a constant, which is true for larger diameters, it follows that

$$\left(\frac{\rho_s - \rho}{\rho}\right) \frac{gd}{v_{ss}^2} \propto constant \tag{9.6}$$

Then, from **Equations 9.4** and **9.6**, the condition of incipient sediment motion under rough turbulent flow conditions is depicted by

$$\frac{\sqrt{gDS}}{v_{ss}} = constant \tag{9.7}$$

In smooth turbulent flow as well as in completely laminar flow the unit stream power required to maintain motion can be given by

$$\left(\tau \frac{dv}{dy}\right)_{laminar} = \frac{(\rho g D S)^2}{\rho \upsilon} \tag{9.8}$$

The corresponding equation for settling velocity under viscous conditions, i.e. Stoke's Law *[Graf, 1971]* states that

$$v_{ss} \propto g d^2 \left(\frac{\rho_s - \rho}{\rho \upsilon}\right) \tag{9.9}$$

For critical conditions in laminar flow it follows that

$$\rho \frac{(gDS)^2}{\upsilon} \propto (\rho_s - \rho) g v_{ss} \tag{9.10}$$

and it can be proved that

$$\frac{\sqrt{gDS}}{v_{ss}} \propto \frac{1}{\frac{\sqrt{gDS}d}{\upsilon}} \tag{9.11}$$

Rooseboom [1974] used data of *Grass [1970]* and *Yang [1972]* to compare this stream power theory regarding critical conditions to the Liu-diagram. The results are presented in **Figure 9.1**. It can be seen that the relationship

$$\frac{\sqrt{gDS}}{v_{ss}} = constant \tag{9.12}$$

for rough turbulent flow fits measured data as compiled by *Yang [1973]* very well, with the value of the $constant = 0{,}12$ for values of $\frac{\sqrt{gDS}}{\upsilon} > 13$. Accordingly, the relationship for values of $\frac{\sqrt{gDS}}{\upsilon} < 13$, i.e. for smooth turbulent and completely laminar flow, calibrated with data by *Grass [1970]* and *Yang [1973]* is found to be

$$\frac{\sqrt{gDS}}{v_{ss}} = \frac{1{,}6}{\frac{\sqrt{gDS}}{\upsilon}d} \tag{9.13}$$

It is noteworthy that the above analysis logically leads to a Liu-type diagram and provides complete and logical mathematical relationships which describe the shape of this diagram.

The parameter $\frac{\sqrt{gDS}}{v_{ss}}$ can thus be used in cases of turbulent and smooth turbulent or laminar flow to represent the relationship between unit stream power required to maintain motion along the bed and unit power required to suspend a particle.

Two distinct relationships are thus identified, i.e. **Equations 9.7** and **9.13**, which are valid for describing incipient transport conditions along smooth beds consisting of particles with diameter ***d***. As long as the value of $\frac{\sqrt{gDSd}}{\upsilon} > 13$, boundary flow conditions are completely turbulent whilst laminar boundary conditions prevail where $\frac{\sqrt{gDSd}}{\upsilon} < 13$.

If a river's bed is flat and no bed form roughness is present the absolute roughness value k_s is represented by the grain diameter ***d***. However, with increasing flow, the applied stream power will increase. An alluvial river tends to a condition of minimum energy, i.e. minimization of applied stream power.

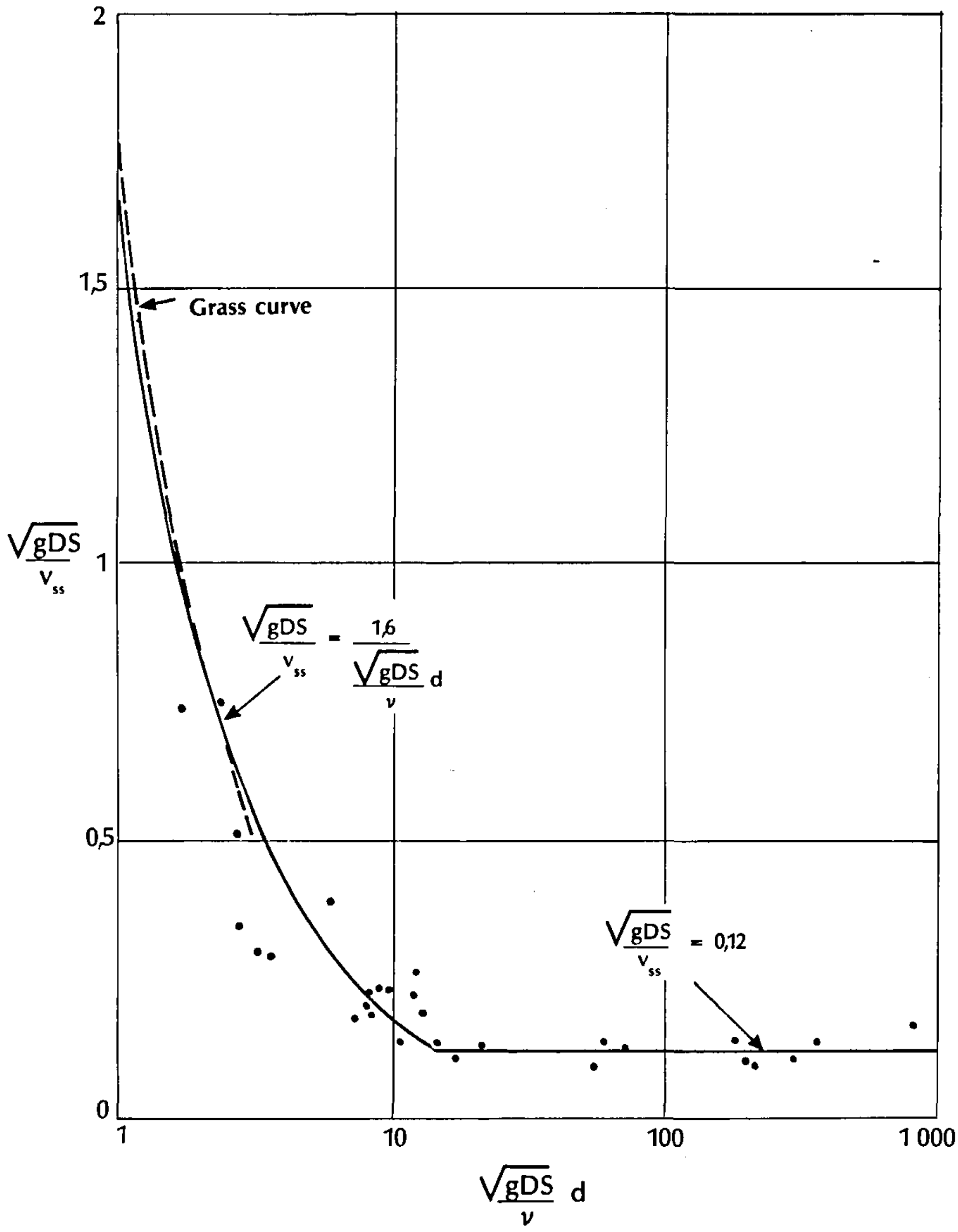

2
1,5
Grass curve
$\frac{\sqrt{gDS}}{v_{ss}}$
1
$\frac{\sqrt{gDS}}{v_{ss}} = \frac{1,6}{\frac{\sqrt{gDS}}{\nu} d}$
0,5
$\frac{\sqrt{gDS}}{v_{ss}} = 0,12$
0
1
10
100
1 000
$\frac{\sqrt{gDS}}{\nu} d$

As mentioned previously when sediment is being transported, the amount of stream power applied along the bed can be reduced by *[Rooseboom, 1974]*:

i) the formation of a pseudo-viscous zone of high concentration suspension along the bed which acts similarly to a true laminar sub-layer
ii) deformation of the bed through the formation of ripples, dunes, etc. whereby eddies with larger radii are formed along the bed.

An increase in the value of k_s represents a decrease in the high amount of power applied along the bed in maintaining motion. This is in agreement with the principle of least resistance. With the smaller amount of power being applied along the bed while sediment is being transported, power is saved and more power is available for propelling the upper layers of fluid, leading to higher velocity gradients and accordingly to higher average velocities.

With low discharges and depths of flow, resistance to flow is in accordance with the relationships that describe non-sediment carrying flows. At higher discharges and depths of flow, however, the friction factors are determined by the interaction between transported sediment and flowing fluid, i.e. the absolute roughness value k_s.

Thus, the relationship for unit stream power applied in maintaining turbulent motion along a bed, consisting of particles with diameter d but with bed irregularities represented by the absolute roughness value k_s **(Equation 9.3)** can be rewritten as

$$\text{applied power} \propto \frac{\rho g D S \sqrt{gDS}}{k_s} \tag{9.14}$$

As the value of the absolute roughness k_s increases, the transporting capacity, represented by the applied power function, decreases, whilst the unit power required to suspend particles with a given settling velocity remains the same, i.e. $(\rho_s - \rho) g v_{ss}$.

Following the same arguments as before, critical conditions are now represented by:

$$\rho g D S \frac{\sqrt{gDS}}{k_s} \propto (\rho_s - \rho) g v_{ss} \tag{9.15}$$

with v_{ss} the setting velocity under turbulent conditions as depicted by

$$v_{ss} \propto \sqrt{\frac{(\rho_s - \rho)gd}{\rho C_d}} \tag{9.5}$$

Substitution leads to the result

$$\frac{\sqrt{gDS}}{v_{ss}} \propto \left(\frac{k_s}{d}\right)^{\frac{1}{3}}$$

or (9.16)

$$\frac{\sqrt{gDS}}{v_{ss}} = constant \left(\frac{k_s}{d}\right)^{\frac{1}{3}}$$

which indicates that $\frac{\sqrt{gDS}}{v_{ss}} \neq constant$ for alluvial river flows with bed irregularities represented by the absolute roughness value k_s. **Equation 9.16** can be rewritten as

$$\frac{\sqrt{gDS}}{v_{ss}} \left(\frac{d}{k_s}\right)^{\frac{1}{3}} = constant \tag{9.17}$$

with $constant = 0{,}12$ if $d \approx k_s$

To allow for armouring that might have developed at critical conditions, d_{50} may not be representative of the grain size at critical conditions *[Henderson, 1961]*. Therefore

$$d \neq d_{50}$$

but

$$d = d_{representative\ armoured\ size}$$

From the literature and as proved in **Appendix C** it can be assumed that such a representative armoured or critical particle size can be given by d_{85} *[Henderson, 1961; Cruickshank and Maza, 1973; Simons and Richardson, 1966; Whiting and Dietrich, 1990]*.

9.2 APPLICATION OF THEORY TO FIELD DATA

Available alluvial river field data was analysed in order to establish whether the practically measured values fitted the theoretical relationships.

9.2.1 Hydraulic calculations

The computer program **Channel Flow Profiles (CFP)** *[Engineering Computing Company, 1987]* was used in the hydraulic analyses of the peak flows at the various sites as determined by the Departement of Water Affairs and Forestry (see **Section 5.4**). **CFP** is a fully interactive program based on the fundamental principles of hydraulic calculations. This program is highly suitable for the analysis of steady state profiles in open channels and rivers. A description of **CFP** is presented in **Appendix D.**

The results of hydraulic backwater calculations using the Manning resistance equation for steady, uniform flow conditions are presented in **Appendix E. CFP** was used to obtain the same slope S_w for the high flood line (HFL) as surveyed and as indicated in **Tables 9.1** and **9.2**. The flow depths and top widths for each cross-section in a specific reach were also compared with the surveyed values. The roughness coefficient used in the program, i.e. the Manning coefficient *n*'s value was adjusted accordingly to obtain corresponding values.

Values for the hydraulic parameters shear velocity v_* and absolute roughness k_s were derived from the hydraulic data produced by **CFP**. Shear velocities expressed in terms of both hydraulic radius and flow depth were determined for future use. In determining the absolute roughness value of the river sections the Manning resistance equation was equated to the Chézy equation:

$$\frac{1}{n}R^{2/3}S^{1/2} = 5{,}75\sqrt{gRS}\log(\frac{12{,}2R}{k_s}) \tag{9.18}$$

with n the Manning roughness coefficient.

It follows from **Equation 9.18** that the value of absolute roughness k_s is given by

$$k_s = \frac{12{,}2R}{10^{(\frac{R^{1/6}}{18n})}} \tag{9.19}$$

Computed values of the absolute roughness k_s compared well with independent estimates of k_s-values as used by the Department of Water Affairs and Forestry to calculate peak discharge values.

Basic results for the different sites are summarized in **Tables 9.1** and **9.2**.

9.2.2 Comparative behaviour of research rivers

In a first attempt to establish whether peak scour conditions in the rivers under investigation approached critical conditions, field results were plotted on the Liu-diagram (see **Figure 9.1**). The appropriate values of $\frac{\sqrt{gDS}}{V_{ss}}$ and $\frac{\sqrt{gDS}}{\upsilon} d_{85}$ are included in **Table 9.3**.

It is generally accepted that rough turbulent flow occurs when alluvial rivers are in flood and in terms of the Liu-diagram that the value of the function $\frac{\sqrt{gDS}}{V_{ss}}$ should be constant for cases where turbulent boundary conditions prevail $\left(\frac{\sqrt{gDS}}{\upsilon} d > 13\right)$ *[Rooseboom, 1974]*. The recorded values of this function displayed in **Table 9.3**, however, vary significantly.

By plotting the appropriate values of $\frac{\sqrt{gDS}}{V_{ss}}$ and $\frac{\sqrt{gDS}}{\upsilon} d_{85}$ on the modified Liu-diagram (which includes the transition from fully laminar to fully turbulent boundary conditions), i.e. **Figure 9.2**, the variation in $\frac{\sqrt{gDS}}{V_{ss}}$ follows the same pattern as for laminar boundary conditions and the question arises as to whether viscosity does come into the picture.

Table 9.1 : Summary of computed values - 1984

Site	River & cross-section (d_{50} (mm))		Computed hydraulic values according to CFP: Manning n (s/m$^{1/3}$)	Average velocity v (m/s)	Hydraulic radius R (m)	Average flow depth D (m)	Slope: HFL[2] S_w	Slope: Energy S_f	Shear velocity (m/s): $v_* = \sqrt{gRS_f}$	Shear velocity (m/s): $v_* = \sqrt{gDS_f}$	Absolute roughness k_s [3](m)
A84	Komati	1	0,041	2,67	6,13	11,07	0,00065	0,001	0,245	0,33	1,1
	(1,33)	2	0,041	2,29	7,21	10,63	0,00059	0,00069	0,221	0,268	1,15
		3	0,041	2,38	7,18	11,18	0,00068	0,00068	0,219	0,273	1,15
		4	0,041	2,20	6,13	11,07	0,00056	0,0007	0,205	0,276	1,1
		A[4]	0,041	2,39	6,8	11,0	0,00062 (0,00061)[5]	0,00076	0,223	0,286	1,13
B84	Mkuze	1	-	-	-	-	-	-	-	-	-
	(0,243)	2	0,044	3,03	6,97	11,51	0,00137	0,00131	0,3	0,385	1,53
		3	0,044	3,02	6,6	11,54	0,00162	0,00145	0,306	0,405	1,5
		4	0,044	3,28	6,33	11,33	0,00209	0,00169	0,324	0,433	1,48
		A[4]	0,044	3,08	6,66	11,49	0,00163 (0,0016)[5]	0,00145	0,308	0,404	1,5
C84	Black	1	0,044	2,94	6,04	15,38	0,00158	0,00148	0,296	0,473	1,45
	Mfolozi	2	0,044	2,98	6,23	15,26	0,00137	0,00142	0,295	0,461	1,47
	(0,12)	3	0,044	2,80	6,35	15,14	0,0011	0,0013	0,285	0,439	1,48
		4	0,044	2,64	6,59	15,08	0,00096	0,0011	0,267	0,403	1,5
		A[4]	0,044	2,84	6,32	15,2	0,0012 (0,0012)[5]	0,0013	0,285	0,442	1,48
D84	White	1	0,041	3,14	8,26	12,24	0,00096	0,0011	0,298	0,363	1,19
	Mfolozi	2	0,041	3,02	6,83	12,07	0,00099	0,0011	0,272	0,361	1,13
	(0,38)	3	0,041	2,82	7,84	12,86	0,00084	0,0009	0,263	0,337	1,17
		4	0,041	2,84	7,58	12,1	0,0009	0,0009	0,259	0,327	1,16
		A[4]	0,041	2,93	7,54	12,38	0,00092 (0,001)[5]	0,001	0,272	0,334	1,16
E84	Mhlatuze	1	0,042	3,96	4,62	7,25	0,0035	0,0035	0,4	0,5	1,10
	(0,2)	2	0,042	3,97	4,64	7,0	0,0034	0,0036	0,405	0,5	1,10
		3	0,042	3,83	4,76	6,56	0,0028	0,0032	0,387	0,454	1,12
		4	0,042	3,66	4,81	6,26	0,0026	0,00305	0,38	0,433	1,12
		A[4]	0,042	3,85	4,72	6,72	0,003 (0,003)[5]	0,0033	0,39	0,47	1,11

[1] According to channel flow profile (CFP) program
[2] Slope according to computed high flood levels (HFL)
[3] Computed with regards to Equation 9.19
[4] Weighted average value for reach
[5] Slope of surveyed high flood levels (DWA&F)

Table 9.2 : Summary of computed values - 1987

Site	River & cross-section (d_{50} (mm))		Computer hydraulic values according to CFP: Manning n (s/m$^{1/3}$)	Average velocity v (m/s)	Hydraulic radius R (m)	Average flow depth D (m)	Slope: HFL[2] S_w	Slope: Energy S_f	Shear velocity (m/s): $v_* = \sqrt{gRS_f}$	Shear velocity (m/s): $v_* = \sqrt{gDS_f}$	Absolute roughness k_s[3] (m)
A87	Komati		-	-	-	-	-	-	-	-	-
B87	Mkuze	1	0,045	2,73	3,36	4,1	0,0018	0,003	0,314	0,347	1,26
	(0,243)	2	0,045	2,22	3,56	4,26	0,0015	0,00183	0,253	0,277	1,3
		3	0,045	2,12	3,58	4,04	0,0025	0,00166	0,241	0,256	1,3
		4	0,045	2,46	3,35	3,88	0,0027	0,0024	0,281	0,302	1,26
		A[4]	0,045	2,3	3,5	4,07	0,0021	0,002	0,263	0,284	1,28
							(0,00188)[5]				
C87	Black	1	0,04	2,31	4,80	5,53	0,0014	0,001	0,217	0,233	0,92
	Mfolozi	2	0,04	2,60	4,23	5,47	0,0017	0,00156	0,254	0,289	0,88
	(0,12)	3	0,04	2,65	4,45	5,14	0,0018	0,00153	0,258	0,276	0,9
		4	0,04	2,98	3,95	4,75	0,0022	0,0022	0,292	0,320	0,86
		A[4]	0,04	2,68	4,31	5,17	0,00183	0,00164	0,260	0,285	0,89
							(0,00183)[5]				
D87	White	1	0,039	2,68	4,75	5,38	0,0015	0,00135	0,251	0,267	0,82
	Mfolozi	2	0,039	2,83	4,47	5,27	0,0017	0,00164	0,268	0,291	0,81
	(0,38)	3	0,039	2,92	4,29	5,05	0,0021	0,00188	0,281	0,305	0,8
		4	0,039	3,59	3,83	4,49	0,0033	0,0033	0,352	0,381	0,77
		A[4]	0,039	3,0	4,31	5,05	0,0021	0,002	0,288	0,312	0,8
							(0,0022)[5]				
E87	Mhlatuze	1	0,039	4,16	6,13	7,91	0,00346	0,00255	0,392	0,445	0,88
	(0,2)	2	0,039	4,52	5,42	7,38	0,00375	0,0031	0,406	0,474	0,85
		3	0,039	4,50	5,48	6,97	0,0015	0,0026	0,395	0,422	0,86
		4	0,039	3,46	6,3	8,0	-0,0002	0,00187	0,34	0,383	0,89
		A[4]	0,039	4,27	5,7	7,42	0,0022	0,0027	0,388	0,436	0,87
							(0,00223)[5]				

1) According to channel flow profile (CFP) program
2) Slope according to computed high flood levels (HFL)
3) Computed with regards to **Equation 9.19**
4) Weighted average value for reach
5) Slope of surveyed high levels (DWA&F)

Table 9.3: Comparative behaviour of research rivers

Site	River	Year	Representative particle diameter d_{85} (mm)	Absolute roughness k_s (m)	Settling velocity v_{ss} (m/s)	$\frac{\sqrt{gDS}d_{85}}{\upsilon}$	$\frac{\sqrt{gDS}}{v_{ss}}$	$\frac{k_s}{d_{85}}$	$\frac{\sqrt{gDS}}{v_{ss}}\left(\frac{d_{85}}{k_s}\right)^{\frac{1}{3}}$	$\sqrt{\frac{k_s}{d}\frac{1}{\frac{\sqrt{gDS}}{\upsilon}d}}$
A84	Komati	1984	2,33	1,13	0,217	672	1,33	485	0,167	0,850
B84	Mkuze	1984	0,429	1,5	0,063	176,21	6,52	3496,5	0,423	4,455
B87	Mkuze	1987	0,88	1,28	0,113	251,6	2,53	1454,5	0,222	2,404
C84	Black Mfolozi	1984	0,205	1,48	0,028	93,56	16,3	7219,5	0,803	8,784
C87	Black Mfolozi	1987	0,530	0,89	0,076	154,68	3,84	1679,5	0,32	3,295
D84	White Mfolozi	1984	0,605	1,16	0,085	212,9	4,14	1917,4	0,331	3,001
D87	White Mfolozi	1987	1,7	0,8	0,178	547,7	1,81	470,6	0,228	0,927
E84	Mhlatuze	1984	0,368	1,11	0,055	174,67	8,63	3016,3	0,592	4,155
E87	Mhlatuze	1987	0,471	0,87	0,069	214,82	6,31	1847,1	0,528	2,932

The function $\frac{\sqrt{gDS}}{v_{ss}}$ represents the ratio between applied power and power required to suspend particles and its value is affected by changes in the value of k_s (refer to arguments leading to **Equation 9.16**). The k_s-value should have a significant entrainment capacity. For an alluvial river with an undulated bed the criterion for incipient motion should thus be rewritten as in **Equations 9.16** and **9.17** as

$$\frac{\sqrt{gDS}}{v_{ss}} = constant \left(\frac{k_s}{d}\right)^{\frac{1}{3}} \tag{9.16}$$

or

$$\frac{\sqrt{gDS}}{v_{ss}}\left(\frac{d}{k_s}\right)^{\frac{1}{3}} = constant \ (= 0{,}12 \ for \ d = k_s) \tag{9.17}$$

where $d = d_{85}$.

Recorded values of the function $\frac{\sqrt{gDS}}{v_{ss}}\left(\frac{d_{85}}{k_s}\right)^{\frac{1}{3}}$ presented in **Table 9.3**, however, vary considerably and differ greatly from the expected constant value of 0,12.

Mere adjustment of the $\frac{\sqrt{gDS}}{v_{ss}}$ parameter to allow for variations in absolute roughness and consequential variation in applied power therefore does not clarify matters.

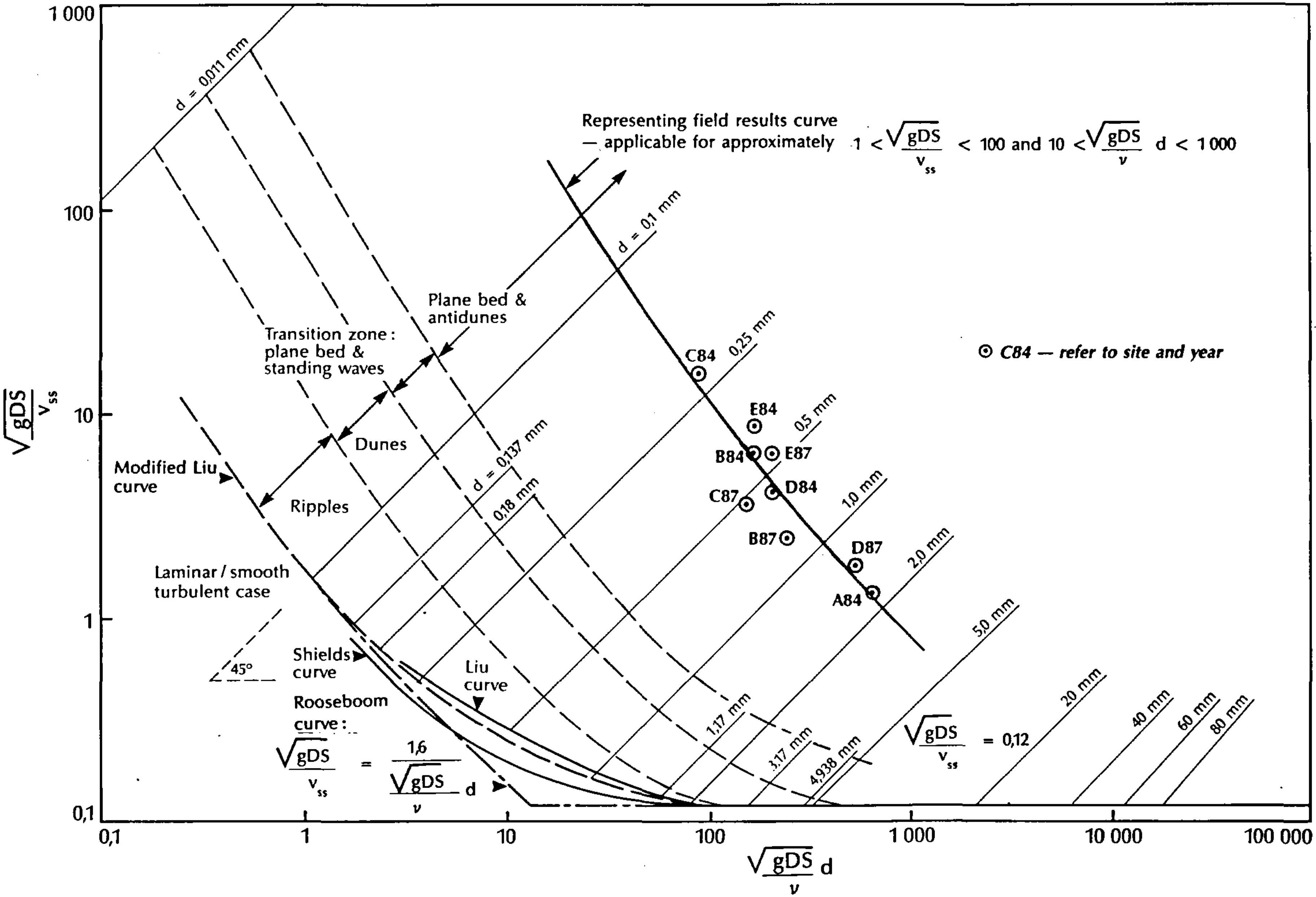

Representing field results curve
— applicable for approximately 1 < √gDS/v_ss < 100 and 10 < √gDS/ν d < 1 000
d = 0,011 mm
d = 0,1 mm
0,25 mm
0,5 mm
1,0 mm
2,0 mm
5,0 mm
20 mm
40 mm
60 mm
80 mm
d = 0,137 mm
0,18 mm
1,17 mm
3,17 mm
4,938 mm
Plane bed & antidunes
Transition zone : plane bed & standing waves
Dunes
Ripples
Modified Liu curve
Laminar / smooth turbulent case
45°
Shields curve
Liu curve
Rooseboom curve :
√gDS/v_ss = 1,6 / (√gDS/ν d)
√gDS/v_ss = 0,12
C84
E84
B84
E87
D84
C87
B87
D87
A84
⊙ C84 — refer to site and year
1 000
100
10
1
0,1
√gDS/v_ss
0,1
1
10
100
1 000
10 000
100 000
√gDS/ν d

9.3 BOUNDARY LAYER CONDITIONS

9.3.1 General

In order to understand which mode of flow will prevail at a certain discharge in an alluvial river, it is necessary to consider the instability of the boundary layer.

One of the important questions concerning the boundary layer is its transition from laminar to turbulent flow. This transition is described by *Schubauer and Skramstad [1947]*:

> *"It is not difficult to imagine a process here like that often assumed for the formation of eddies from a free vortex sheet. The sheet is imagined to take first a wave-like character, then as the wave grows, to curl up into discrete eddies. The disturbed laminar boundary layer may be regarded as a wavy vortex layer with the wave progressively increasing in amplitude and distorting until discrete eddies are formed. The eddies themselves are unstable and soon break up into a diffusive type of motion which characterizes turbulent flow."*

According to **Figure 7.4,** $(\tau\frac{dv}{dy})_o$, i.e. the stream power which is applied per unit volume to maintain motion along the bed, represents the maximum value of applied stream power $\tau\frac{dv}{dy}$, through the vertical section.

In the case of turbulent flow past a *smooth* boundary, that is a boundary where the formation of eddies with extremely small radii would fit in with the dimensions of the excrescences on the bed, the value of

$$\frac{dv}{dy} = \frac{\sqrt{2\pi gDS}}{y_o} \tag{9.21}$$

would become extremely high, because y_o is proportional to the radius of these eddies *[Rooseboom, 1974]*.

High values of the velocity gradient $\frac{dv}{dy}$ associated with small values of y_o will lead to high values of the applied stream power $\tau\frac{dv}{dy}$. In accordance with the concept of least applied power, flow near a boundary will be either turbulent or laminar, dependent upon which type of flow requires the smaller amount of power per unit volume, to maintain it.

For a given value of the shear stress against the bed τ_o , flow will start to change from laminar to turbulent at a depth y_1 (see **Figure 9.3**) where *[Rooseboom, 1974]*

$$(\frac{dv}{dy})_{o_{turbulent}} = (\frac{dv}{dy})_{o_{laminar}} \qquad (9.22)$$

$$\therefore \quad \frac{dv}{dy} = \frac{\sqrt{2\pi gDS}}{y_1} = \frac{\rho gS(D-y)}{\mu} \approx \frac{\rho gSD}{\mu}$$

$$\therefore \quad y_1 = \frac{\sqrt{2\pi}\upsilon}{\sqrt{gDS}} \qquad (9.23)$$

The laminar flow velocity at this level according to **Equation 7.7** equals

$$v = \rho\frac{gS}{\mu}Dy_1 = \sqrt{2\pi gDS} \qquad (9.24)$$

and in turn equals the required translatory velocity of the centre of rotation for turbulent flow (see **Section 7.5**).

It therefore follows that a thin layer of laminar flow exists in the transition zone. The existence of such a layer is of great importance as it creates the necessary moving platform relative to which the necessary condition for turbulent flow can be satisfied.

Two main cases of turbulent flow can be identified, i.e. *smooth turbulent* and *rough turbulent* flows. Smooth turbulent flow is encountered where the conduit roughness is relatively small and in such cases the magnitude of friction losses is determined by the laminar sublayer thickness or distance from the boundary where flow changes from laminar to turbulent.

In most cases of channel and river flows, flow is of the *rough turbulent* type in which case the magnitude of friction losses is determined by the size of physical irregularities along the flow boundaries.

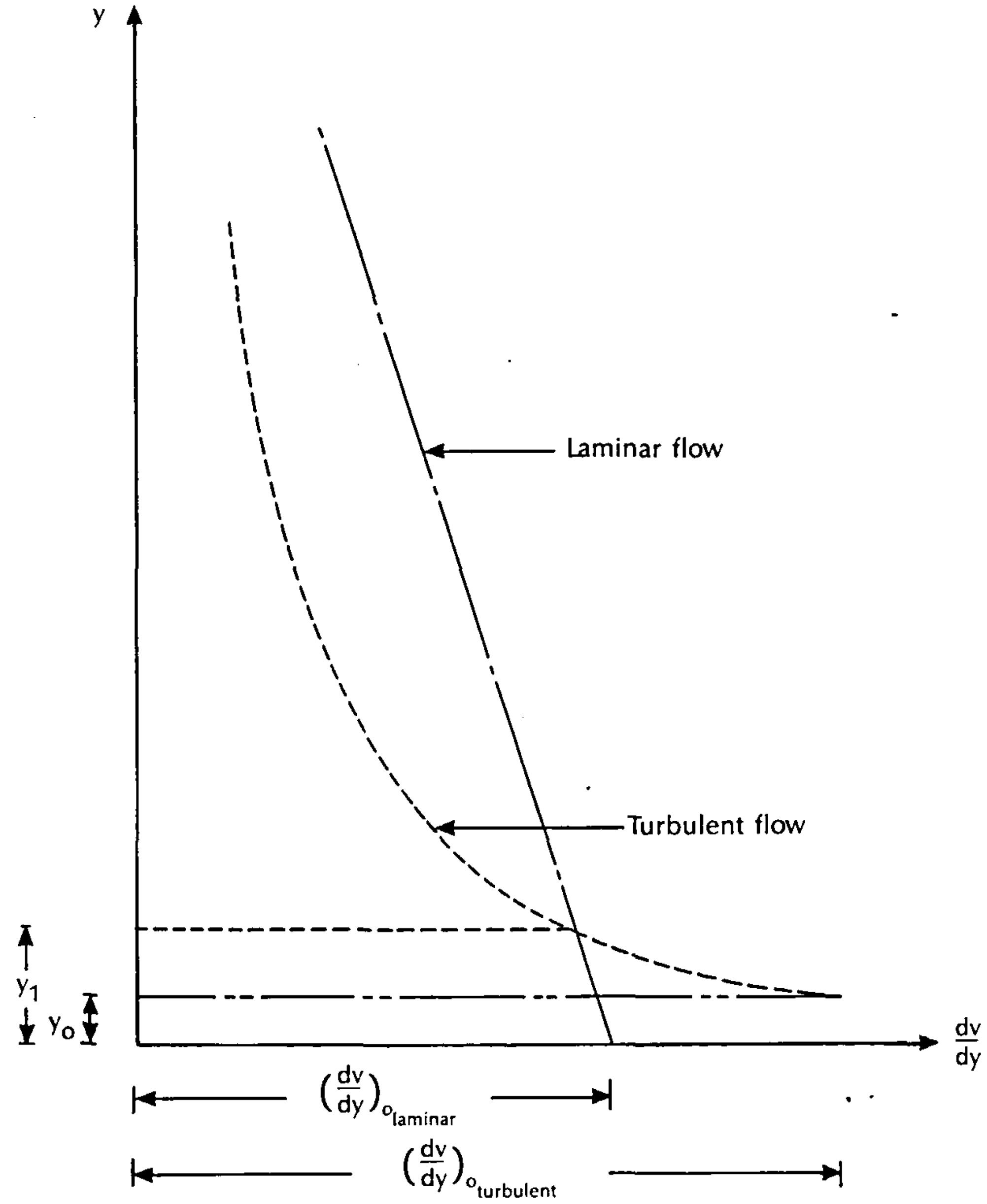

Transition between laminar and turbulent flow (Rooseboom, 1974)

9.3

It follows from **Section 7.5.4** that the velocity distribution for fully developed turbulent flow is given by

$$v = \sqrt{2\pi g D S}\ \ell n\ \frac{y}{y_o} = \sqrt{2\pi g D S}\ \ell n\ \frac{14{,}8y}{R_o} \tag{7.21}$$

where R_o represents the radius of eddies formed against the bed.

From the foregoing it is evident that in the case of flow for which the value of $\sqrt{2\pi g D S}$ is large, transition from laminar to turbulent flow will take place very near to the physical boundary. The onset of turbulence is a function of fluid velocity, viscosity and a typical dimension *[Chadwick and Morfett, 1986]*. This led to the formation of the dimensionless Reynolds number R_e which can be used as a measure of whether a stream as a whole will be turbulent or laminar and is defined for open channel flow as

$$R_e = \frac{\textit{inertia force}}{\textit{viscous force}} = \frac{\bar{v}R}{\upsilon} \tag{9.25}$$

with R the hydraulic radius, $\bar{v}$ the average flow velocity and υ the kinematic viscosity.

With $R_e < 500$ in open channels, viscous effects dominate and the flow is laminar. In this range, any eddy disturbances generated by boundary irregularities or other means tend to be damped out by the effect of viscosity. When $R_e > 500$ the turbulent motion become significant, and the flow is not strictly laminar. Between Reynolds numbers of 500 and 2 000, open channel flow is considered to be in the transitional state, i.e. some eddy disturbances are damped and some being propagated, i.e. turbulence may be present but not fully developed. When $R_e > 2000$, such disturbances are unstable and tend to propagate throughout the flow, resulting in fully developed turbulence.

However, regarding boundary layer instability, it follows from Nikuradse's pipe experiments that the transition region is defined by the limits

$$3{,}5 < R_* < 100 \tag{9.26}$$

where R_* is the particle Reynolds number based on the absolute roughness value k_s and the shear velocity v_* , i.e.

$$R_* = \frac{v_* k_s}{\upsilon} = \frac{\sqrt{gRS}}{\upsilon} k_s \qquad (9.27)$$

with υ the kinematic viscosity, R the hydraulic radius, and S the energy slope *[French, 1986]*.

9.3.2 Effect of roughness on boundary layer with critical conditions

With the river behaviour being described by using the absolute roughness k_s in stead of the particle diameter d in describing the relationship between the applied unit stream power maintaining motion along the bed and unit power required to suspend a particle (**Equation 9.14**), it is evident that in the case of flow over a flat alluvial bed, there may exist a laminar boundary layer or laminar sub-layer against the boundary even if the main flow is turbulent. Viscosity is dominant in such a laminar zone. If the laminar zone, which is usually very thin, is considered as an interface between the superposed fluid and the alluvial bed, the problem of alluvial river behaviour at equilibrium or critical conditions will become a problem of interface instability.

As discussed previously, the amount of unit stream power applied along the bed can be reduced through the formation of ripples, dunes, etc. whereby eddies with larger radii are formed along the beds. The absolute roughness k_s is determined by the size of these eddies.

With reference to **Figure 9.4** the turbulent boundary eddies depicted in size by k_s represent the turbulent boundary conditions. As their size is increased through deformation of the bed, the applied (turbulent) power along the bed given by (refer to **Equation 9.14**)

$$\textit{applied power} \propto \frac{\rho g D S \sqrt{gDS}}{k_s} \qquad (9.14)$$

decreases.

It must be expected that the value of this function will drop to the point where it approaches the critical value when equilibrium scour is approached. If it is assumed that a laminar boundary layer develops below the eddy, the applied (turbulent) power will be $\propto$ (laminar) power required to pick up the particles. There is good reason for believing that laminar boundary conditions will develop. It is evident from **Figure 9.2** that for sand particles less than say 2 mm in diameter incipient motion is always associated with laminar boundary conditions.

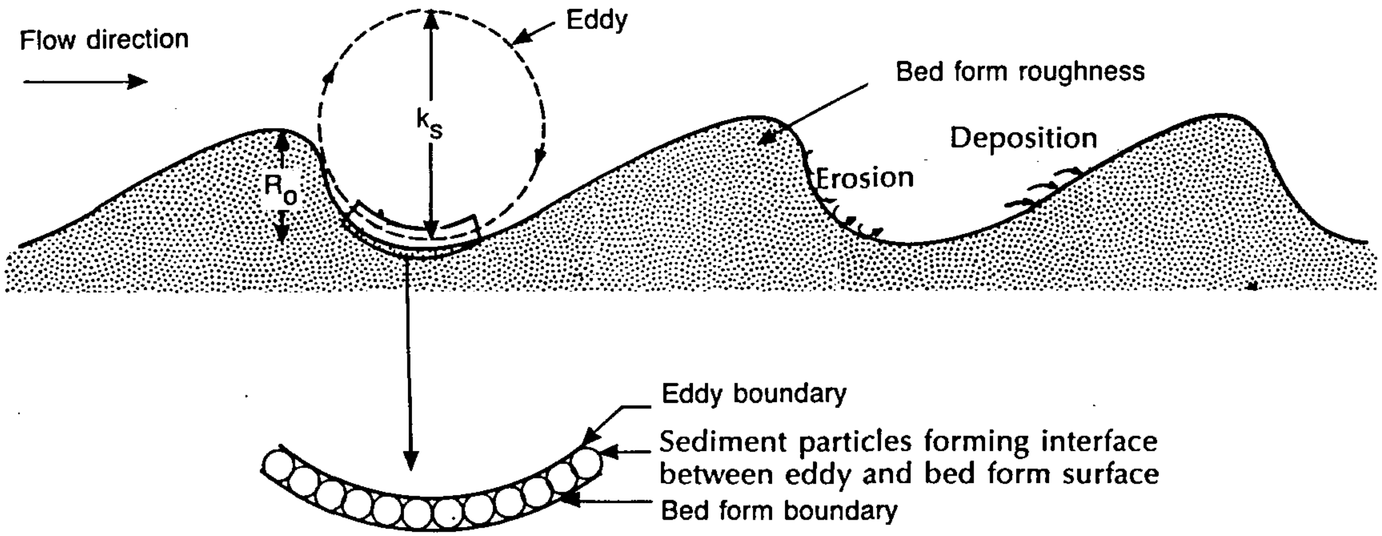
Flow direction
Eddy
k_s
R_o
Bed form roughness
Deposition
Erosion
Eddy boundary
Sediment particles forming interface
between eddy and bed form surface
Bed form boundary

Accordingly

$$\rho g D S \frac{\sqrt{gDS}}{k_s} \propto (\rho_s - \rho) g v_{ss} \qquad \text{(compare } \textbf{Equations 9.4} \text{ and } \textbf{9.15}\text{)}$$

with v_{ss} the settling velocity under viscous conditions as given by **Equation 9.9** as

$$v_{ss} \propto g d^2 \left(\frac{\rho_s - \rho}{\rho \upsilon} \right) \tag{9.9}$$

Substitution leads to

$$\frac{\sqrt{gDS}}{v_{ss}} \propto \sqrt{\frac{k_s}{d} \frac{1}{\frac{\sqrt{gDS}}{\upsilon} d}} \tag{9.28}$$

Using the data in **Table 9.3**, the validity of this relationship appears to be fully indicated in **Figure 9.5**. The linear relationship as given by **Equation 9.28** is the best approximated for all the data points in **Figure 9.5** by means of the method of least squares by

$$\frac{\sqrt{gDS}}{v_{ss}} = -0{,}7702 + 1{,}894 \sqrt{\frac{k_s}{d} \frac{1}{\frac{\sqrt{gDS}}{\upsilon} d}} \tag{9.29}$$

with a correlation coefficient of $r = 0{,}88$. This relationship is indicated as curve A in **Figure 9.5**. If, however, it is assumed that data point C84, although not an outlier, can be regarded as not within the range of the other data points, the linear relationship for the data excluding data point C84 can be given by

$$\frac{\sqrt{gDS}}{v_{ss}} = -0{,}2413 + 1{,}682 \sqrt{\frac{k_s}{d} \frac{1}{\frac{\sqrt{gDS}}{\upsilon} d}} \tag{9.30}$$

with a correlation coefficient of $r = 0{,}72$. This relationship is indicated as curve B in **Figure 9.5**.

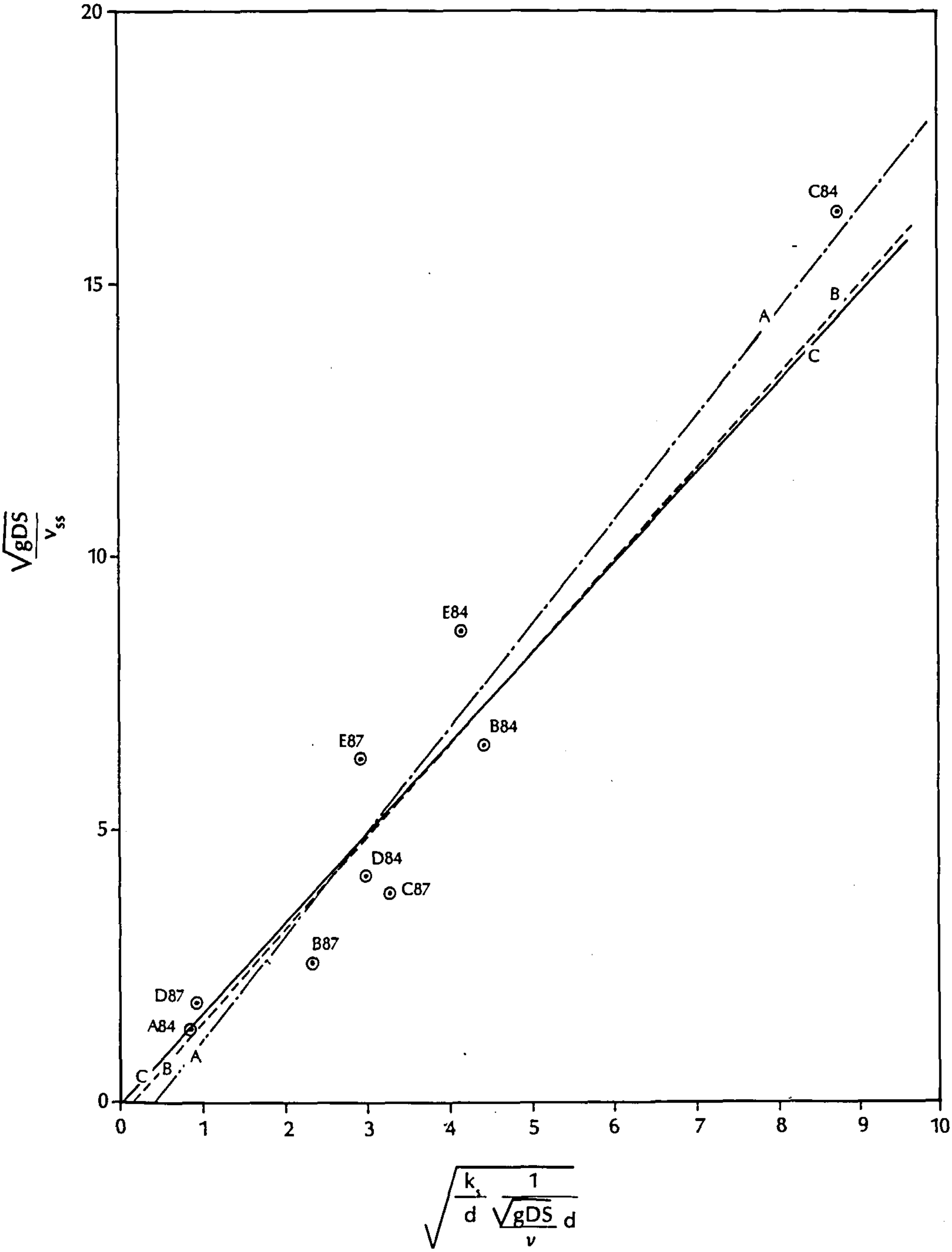

ALLUVIAL RIVER STUDY Relationship between applied (turbulent) power on the bed and (laminar) power required to pick up particles **9.5**

If, however, the arithmetic mean of all the data points in **Figure 9.5** is used, the relationship given by **Equation 9.28** can be approximated by

$$\frac{\sqrt{gDS}}{v_{ss}} = 1{,}63 \sqrt{\frac{k_s}{d} \frac{1}{\frac{\sqrt{gDS}}{\upsilon} d}} \tag{9.31}$$

which is indicated as curve C in **Figure 9.5**.

It follows from **Figure 9.5** that these two relationships given by **Equations 9.30** and **9.31** are very close in describing the data points for the range covered. Both the coefficients in these relationships are close to the coefficient of 1,6 given in **Equation 9.13** *[Rooseboom, 1974]*. More data is obviously required for a more accurate calibration of the relationship. However, **Equation 9.31** can be given in a simplified manner as

$$\frac{\sqrt{gDS}}{v_{ss}} = 1{,}6 \sqrt{\frac{k_s}{d} \frac{1}{\frac{\sqrt{gDS}}{\upsilon} d}} \tag{9.32}$$

The fact that the linear relationship given by **Equations 9.29** and **9.30** does not describe the zero point, resulted in the assumption to use **Equation 9.31** and the resulting **Figure 9.6** for prediction purposes in this report.

By equating the applied unit turbulent power along the bed with the unit power required to suspend the particles, it is thus possible to determine at what stage a sand bed river will reach equilibrium in terms of scouring of its bed.

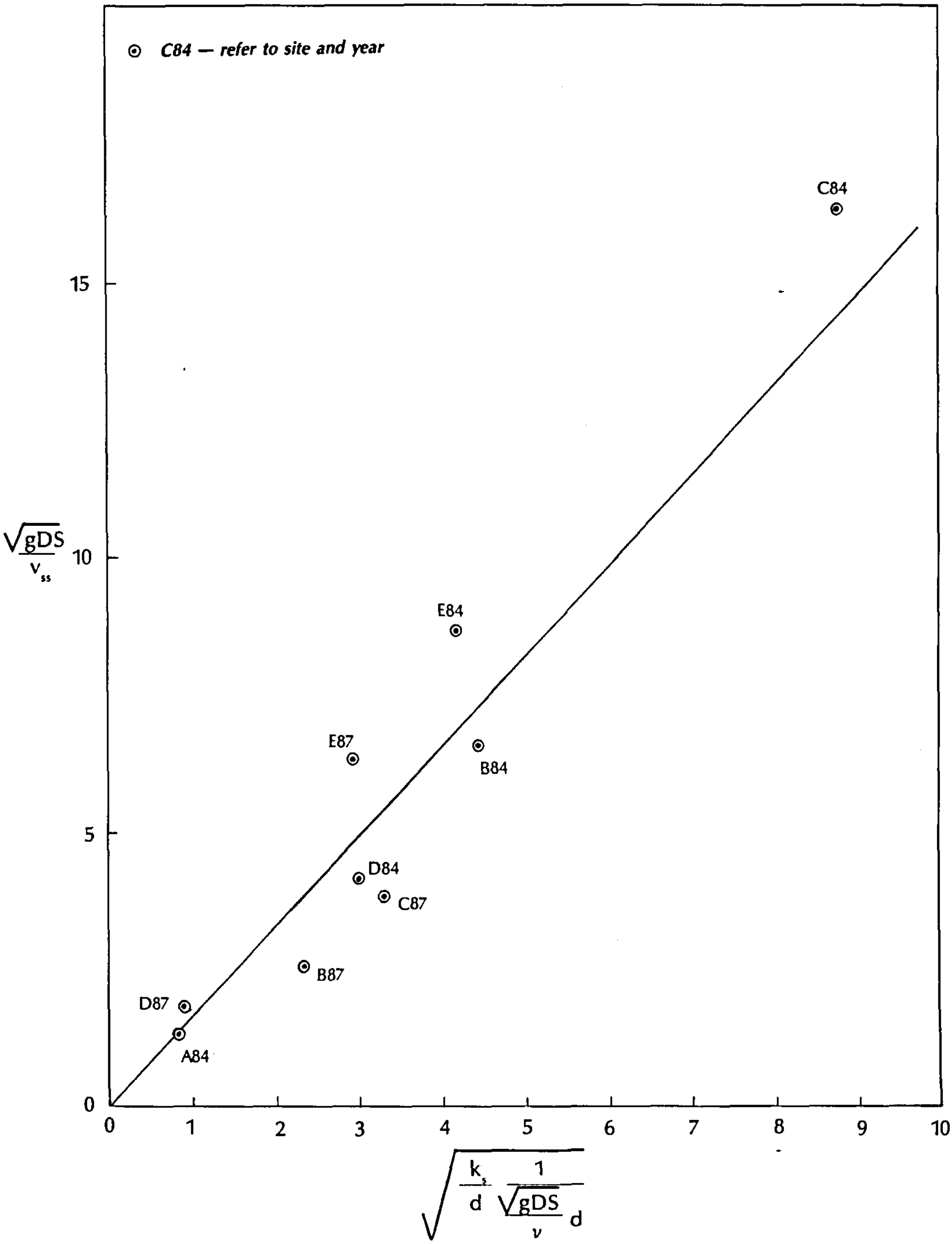

C84 — refer to site and year
C84
E84
E87
B84
D84
C87
B87
D87
A84
0
5
10
15
0
1
2
3
4
5
6
7
8
9
10
$\frac{\sqrt{gDS}}{v_{ss}}$
$\sqrt{\frac{k_s}{d}\frac{1}{\frac{\sqrt{gDS}}{\nu}d}}$

10. VERIFICATION OF THE FUNDAMENTAL APPROACH FOR THE PREDICTION OF THE CROSS-SECTIONAL GEOMETRY OF RIVERS

10.1 INTRODUCTION

It follows from **Section 9.2** that the relationship between applied and input stream power for critical conditions in **Figure 9.2** can be used to represent maximum scour conditions in the researched rivers during the floods of 1984 and 1987. The surveyed geometry of these rivers can be regarded as near equilibrium geometries with the surveyed depths equal to or near to the critical or equilibrium depths. It is thus believed that **Figures 9.2, 9.5** and **9.6** can be used for the determination of estimated values of equilibrium flow depth D and accompanying absolute roughness value k_s.

The fundamental approach is necessarily based on the energy slope, but the cross-sectional geometry was predicted by means of both the energy slope S_f and the bed slope S_o. The energy slope was determined by means of the **CFP** program while the bed slope was either known before the floods (*Van Bladeren, 1989*) or obtained from 1:50 000 maps.

The equilibrium flow depth D was derived for the new curve in **Figure 9.2**, which is assumed to be valid for $1 < \frac{\sqrt{gDS}}{v_{ss}} < 100$ and $10 < \frac{\sqrt{gDS}}{\upsilon} d_{85} < 1000$ in terms of the available data.

Values for the absolute roughness value k_s were derived from **Equation 9.31** which represents **Figure 9.6**. These values were used to predict cross-sectional dimensions.

10.2 METHODOLOGY

Prediction of the cross-sectional geometry of the researched rivers was based on the assumption that only a representative sediment particle size and the energy and/or bed slope is known. The following methodology has been applied in the determination of these two parameters:

i) determine representative particle size d_{85} and accompanying fall velocity v_{ss}

ii) use energy slope S_f and/or bed slope S_o as known before a flood or obtained from 1:50 000 maps

iii) use new curve in **Figure 9.2** to determine flow depth D according to particle size: determine values of $\frac{\sqrt{gDS}}{v_{ss}}$ and $\frac{\sqrt{gDS}}{\nu} d_{85}$ for which the value of $\sqrt{gDS}$ is equal and use this $\sqrt{gDS}$ - value to determine average flow depth D_o and D_f according to bed slope S_o and energy slope S_f , respectively

iv) use **Figure 9.6** by means of **Equation 9.31** to estimate the absolute roughness k_s

v) use the different values of the flow depth and absolute roughness to determine top width, hydraulic radius, flow area, flow velocity and discharge of the combined side channels as discussed in **Section 8.6**

vi) determine flow Q_m in centre channel by means of **Equation 8.29**

vii) determine bed width B_m of centre channel according to **Equation 8.30**

viii) determine top width of the total channel by means of **Equation 8.31**

10.3 PREDICTED CROSS-SECTIONAL GEOMETRY

Predicted cross-sectional geometry dimensions for the various cases, based on the methodology discussed in **Section 10.2**, are presented in **Tables 10.1** to **10.4**:

Representative particle diameter size d_{85}, energy slope S_f as obtained by means of the water profile program **CFP** and bed slope S_o as measured before the floods (*Van Bladeren, 1989*) or obtained from 1:50 000 maps are presented in **Table 10.1**. The average surveyed flow depth D_s as well as the predicted average flow depth D_o and D_f according to bed slope S_o and energy slope S_f, respectively, are also presented in **Table 10.1**.

Table 10.1: Predicted average flow depth D

Site	River	Year	Representative particle diameter d_{85} (mm)	Slope: Bed S_o	Slope: Energy S_f [3]	Average flow depth (m): D_s [4]	D_o [5]	D_f [6]
A84	Komati	1984	2,33	0,00062[1]	0,00076	11	13,2	10,75
B84	Mkuze	1984	0,429	0,0013[1]	0,00145	11,5	12,3	11
B87	Mkuze	1987	0,88	0,00245[2]	0,002	4	4,8	5,9
C84	Black Mfolozi	1984	0,205	0,0012[1]	0,0013	15,2	15	13,85
C87	Black Mfolozi	1987	0,53	0,0012[1]	0,00164	5,2	11,7	8,6
D84	White Mfolozi	1984	0,605	0,001[2]	0,001	12,4	13,2	13,3
D87	White Mfolozi	1987	1,7	0,00152[1]	0,002	5	6,88	5,2
E84	Mhlatuze	1984	0,368	0,0013[1]	0,0033	6,7	13,3	5,3
E87	Mhlatuze	1987	0,471	0,00128[1]	0,0027	7,4	13,0	6,2

1) according to 1:50 000 maps
2) according to known bed slope before flood (*Van Bladeren, 1989*)
3) according to CFP
4) surveyed depth according to **Tables 9.1 and 9.2**
5) according to S_o
6) according to S_f

Predicted values of the absolute roughness k_s determined according to **Figure 9.6** are presented in **Table 10.2**. These predicted k_s-values are the same for both the energy and bed slope conditions.

Table 10.2: Predicted absolute roughness k_s

Site	River	Year	Absolute roughness k_s (m): Estimated field values	Bed slope conditions	Energy slope conditions
A84	Komati	1984	1,13	0,98	0,98
B84	Mkuze	1984	1,5	1,08	1,08
B87	Mkuze	1987	1,28	0,9	0,9
C84	Black Mfolozi	1984	1,48	1,46	1,46
C87	Black Mfolozi	1987	0,89	0,94	0,94
D84	White Mfolozi	1984	1,16	0,9	0,9
D87	White Mfolozi	1987	0,8	1,13	1,13
E84	Mhlatuze	1984	1,11	1,2	1,2
E87	Mhlatuze	1987	0,87	1,17	1,17

The two side channels as shown in **Figure 8.2** were assumed as acting as a combined side channel. Representative flow characteristics, i.e. top width, hydraulic radius, flow area, flow velocity and discharge of such a channel are presented together with the flow and bottom width of the centre channel and the combined top width and average flow velocity of the total channel in **Tables 10.3** and **10.4**.

The results of the application of the fundamental approach to the field data and the measured cross-sectional geometries are compared in **Figures 10.1** to **10.9**. These figures represent verification of the predicted cross-sectional geometry estimated by means of the energy (case A) and bed slopes (case B).

Table 10.3: Prediction of cross-sectional channel characteristics by means of bed slope S_o

Site	River	Discharge	Average bed slope	Average predicted flow depth	Predicted absolute roughness	Predicted channel characteristics								
						Side channel characteristics[1]					Centre channel characteristics		Total channel characteristics	
		Q_t (m^3/s)	S_o	D (m)	k_s (m)	Top width B_s (m)	Hydraulic radius R_s (m)	Flow area A_s (m^2)	Flow velocity v_s (m/s)	Discharge Q_s (m^3/s)	Discharge[2] Q_m (m^3/s)	Bottom width[3] B_m (m)	Total top width[4] B_T (m)	Average velocity[5] v (m/s)
A84	Komati	2 640	0,00062	13,2	0,98	34,8	6,9	314,3	2,27	713,5	1926,5	41,2	76	3,41
B84	Mkuze	5 500	0,0013	12,3	1,08	32,4	6,4	272,9	3,06	835,2	4664,8	79,2	111,6	4,68
B87	Mkuze	1 060	0,00245	4,8	0,9	12,6	2,5	41,6	2,15	89,36	970,64	58,4	71	3,41
C84	Black Mfolozi	10 000	0,0012	15,0	1,46	39,5	7,8	405,9	3,16	1282,6	8717,4	116,9	156,4	4,87
C87	Black Mfolozi	1 740	0,0012	11,7	0,94	30,8	6,1	246,9	2,92	721,1	1018,9	19,1	49,9	4,31
D84	White Mfolozi	6 500	0,001	13,2	0,9	34,8	6,9	314,3	2,94	924,1	5578,9	92,3	127,1	4,49
D87	White Mfolozi	2 150	0,00152	6,88	1,13	18,1	3,6	85,4	2,1	179,3	1970,7	85	103,1	3,32
E84	Mhlatuze	2 400	0,0013	13,3	1,2	35	6,9	319,1	3,15	1005,2	1394,8	21,2	56,2	4,66
E87	Mhlatuze	3 600	0,00128	13	1,17	34,2	6,8	304,9	3,1	945,1	2654,9	42,0	76,2	4,69

[1] total of two side channels

[2] $Q_m = Q_t - Q_s$

[3] determined according to Equation 8.30

[4] $B_t = B_m + B_s$

[5] determined as $v = \dfrac{2Q_t}{D(B_T + B_m)}$

Table 10.4: Prediction of cross-sectional channel characteristics by means of energy slope S_f

Site	River	Discharge	Average energy slope	Average predicted flow depth	Predicted absolute roughness	Predicted channel characteristics								
						Side channel characteristics[1]					Centre channel characteristics		Total channel characteristics	
		Q_t (m^3/s)	S_f	D (m)	k_s (m)	Top width B_s (m)	Hydraulic radius R_s (m)	Flow area A_s (m^2)	Flow velocity v_s (m/s)	Discharge Q_s (m^3/s)	Discharge[2] Q_m (m^3/s)	Bottom width[3] B_m (m)	Total top width[4] B_T (m)	Average velocity[5] v (m/s)
A84	Komati	2 640	0,00076	10,75	0,98	28,3	5,6	208,5	2,16	450,3	2189,7	60	88,3	3,31
B84	Mkuze	5 500	0,00145	11	1,08	29	5,7	218,3	2,97	648,3	4851,7	94,4	123,4	4,59
B87	Mkuze	1 060	0,002	5,9	0,9	15,5	3,1	62,8	2,29	143,8	916,2	42,6	88,1	3,56
C84	Black Mfolozi	10 000	0,0013	13,85	1,46	36,5	7,2	346,1	3,1	1072,7	8927,3	131,8	168,3	4,8
C87	Black Mfolozi	1 740	0,00164	8,6	0,94	22,7	4,5	133,4	2,7	360,2	1379,8	37,35	60,05	4,15
D84	White Mfolozi	6 500	0,001	13,3	0,9	35	6,9	319,1	2,96	944,6	5555,4	90,8	125,8	4,3
D87	White Mfolozi	2 150	0,002	5,2	1,13	13,7	2,7	48,8	1,94	94,6	2055,4	125,9	139,6	3,1
E84	Mhlatuze	2 400	0,0033	5,3	1,2	14	2,8	50,7	2,5	126,7	2273,3	106,5	120,5	3,99
E87	Mhlatuze	3 600	0,0027	6,2	1,17	16,3	3,2	69,3	2,6	180,3	3419,7	133,7	150	4,1

[1] total of two side channels

[2] $Q_m = Q_t - Q_s$

[3] determined according to Equation 8.30

[4] $B_t = B_m + B_s$

[5] determined as $v = \dfrac{2Q_t}{D(B_T + B_m)}$

8275GA/ew

1993-05-24

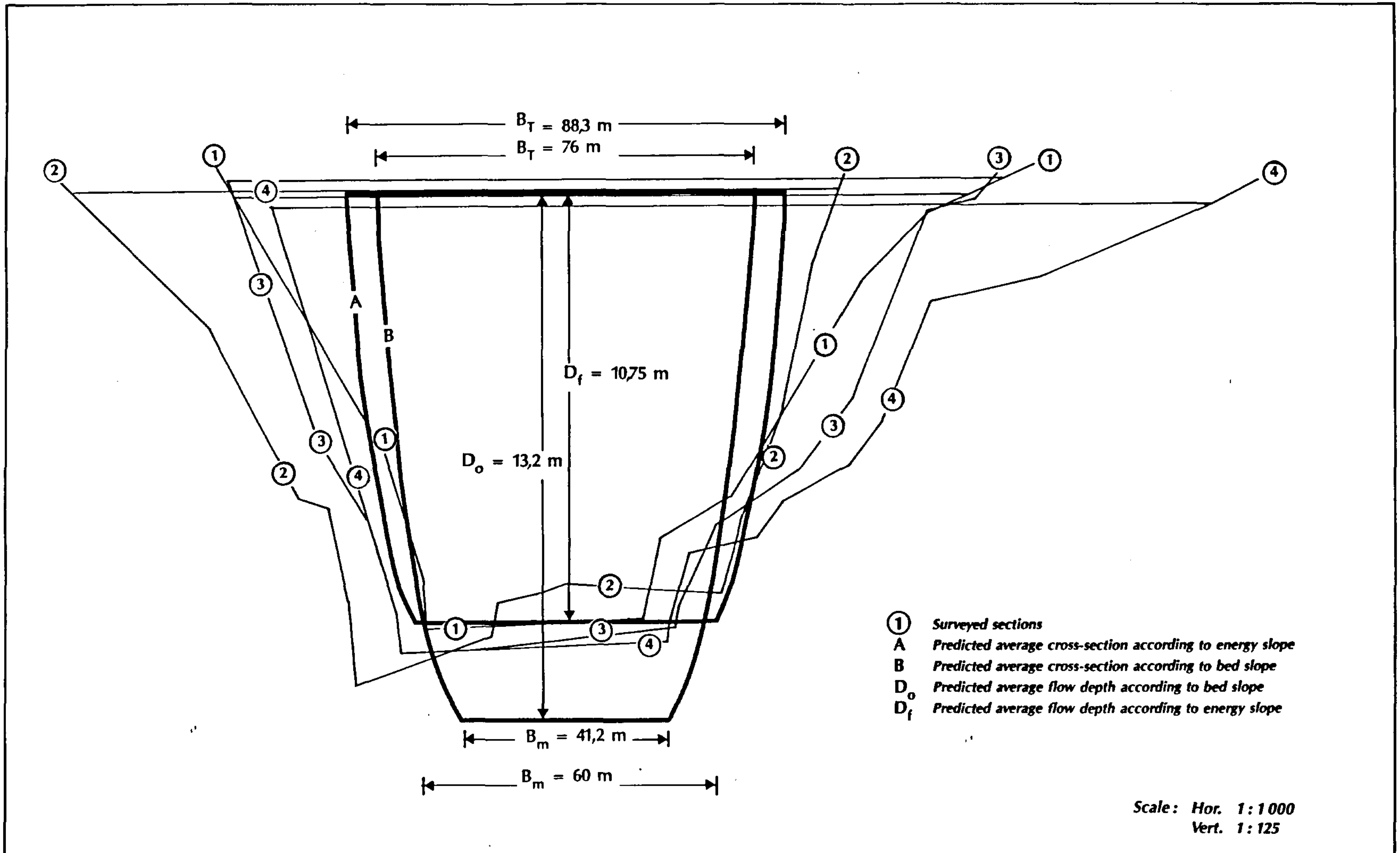

Comparative cross-sections: Site A84 — Komati River 1984

10.1

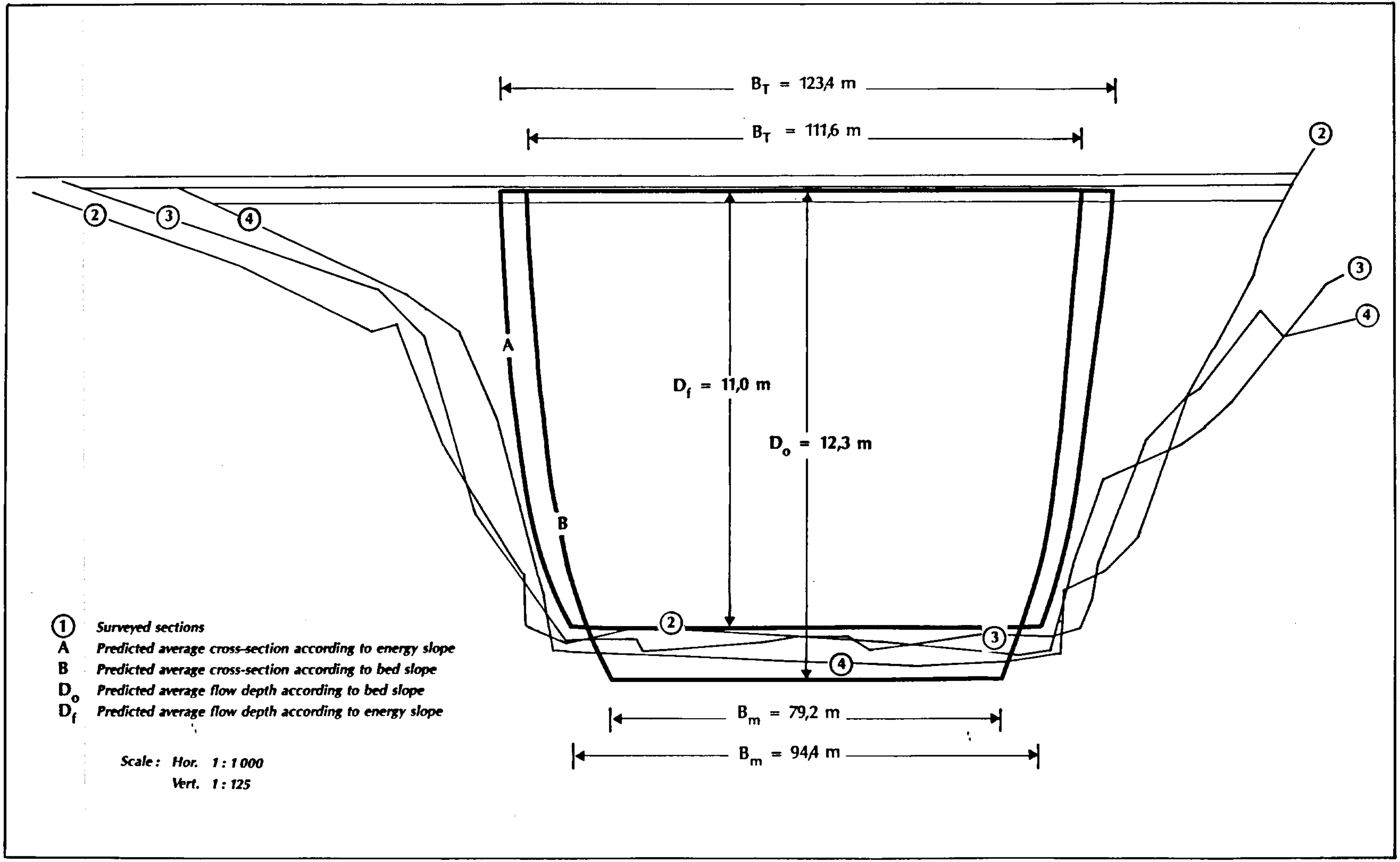

Comparative cross-sections: Site B84 — Mkuze River 1984 **10.2**

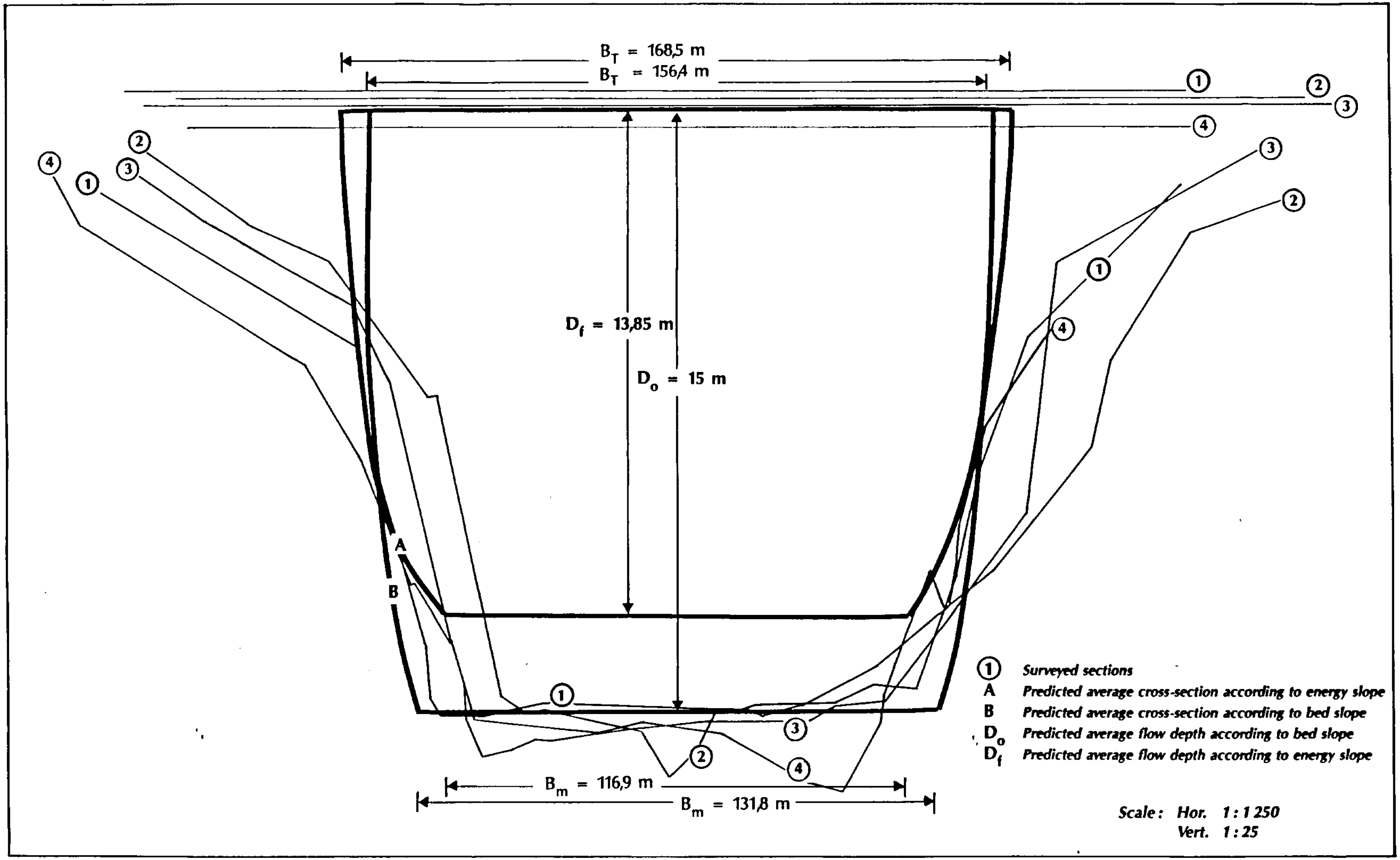

ALLUVIAL RIVER STUDY

Comparative cross-sections: Site C84 — Black Mfolozi River 1984

10.3

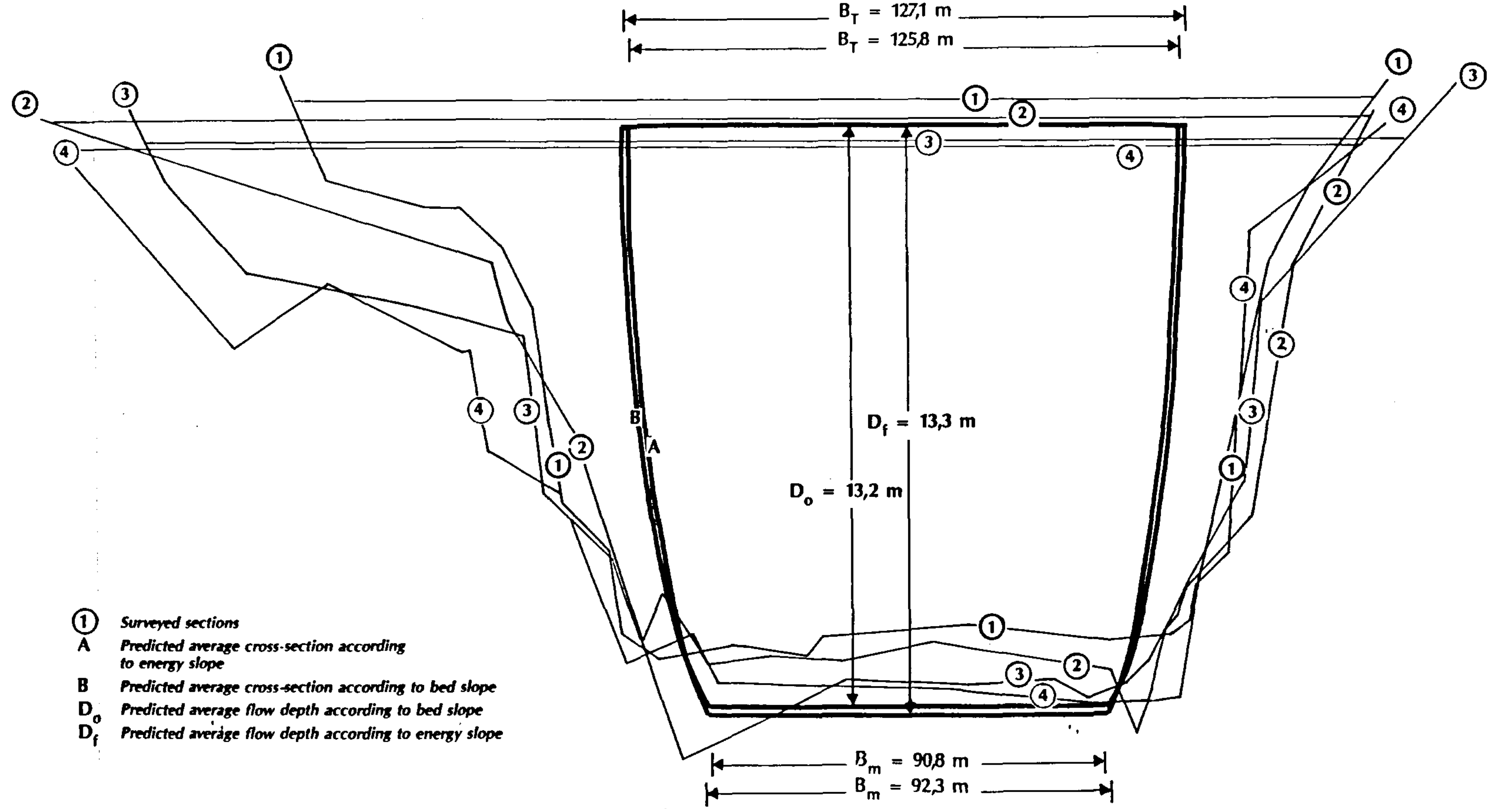

1 *Surveyed sections*
A *Predicted average cross-section according to energy slope*
B *Predicted average cross-section according to bed slope*
D_o *Predicted average flow depth according to bed slope*
D_f *Predicted average flow depth according to energy slope*

Scale: Hor. 1 : 1 250
Vert. 1 : 25

Comparative cross-sections: Site D84 — White Mfolozi River 1984 **10.4**

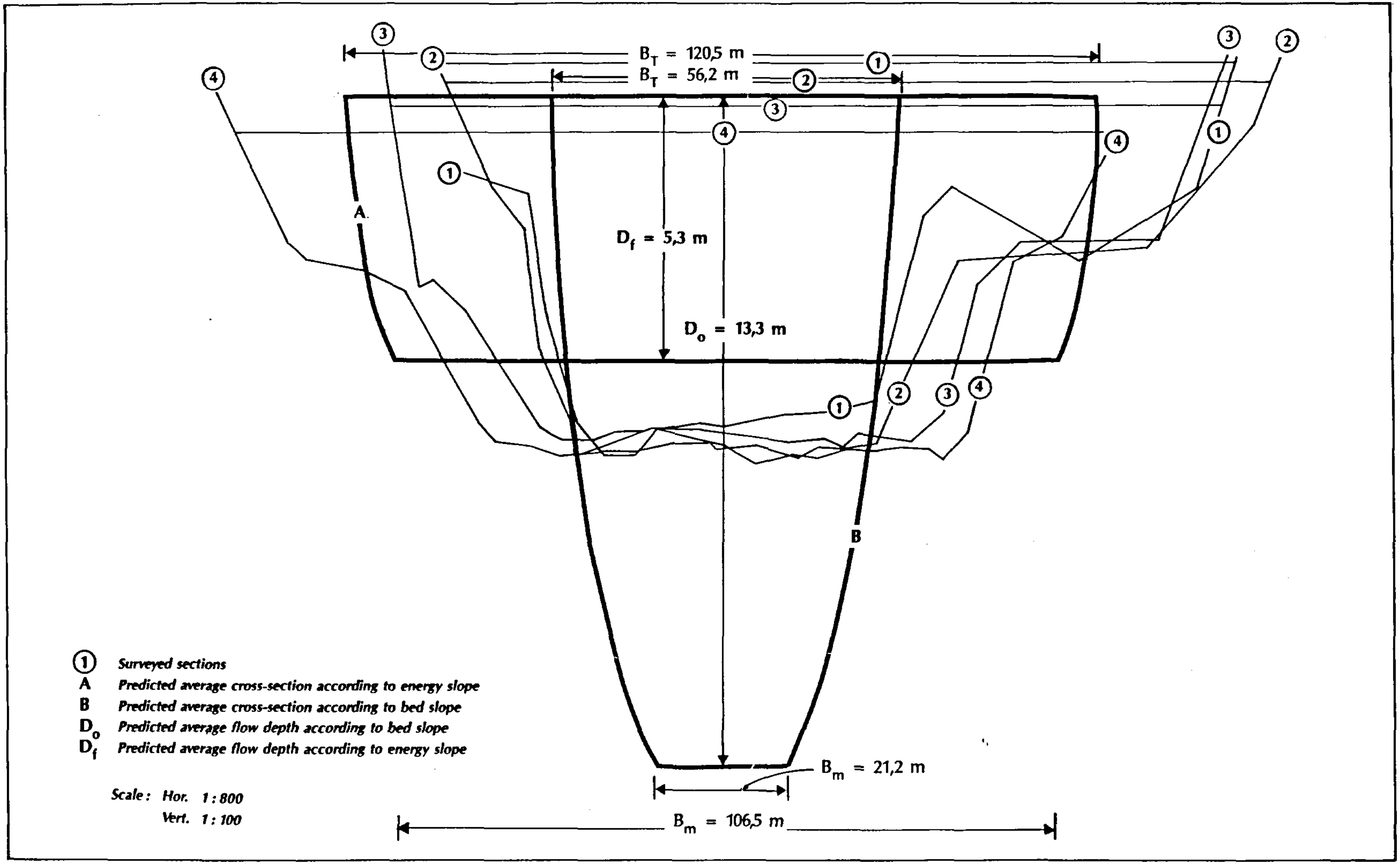

Comparative cross-sections: Site E84 — Mhlatuze River 1984

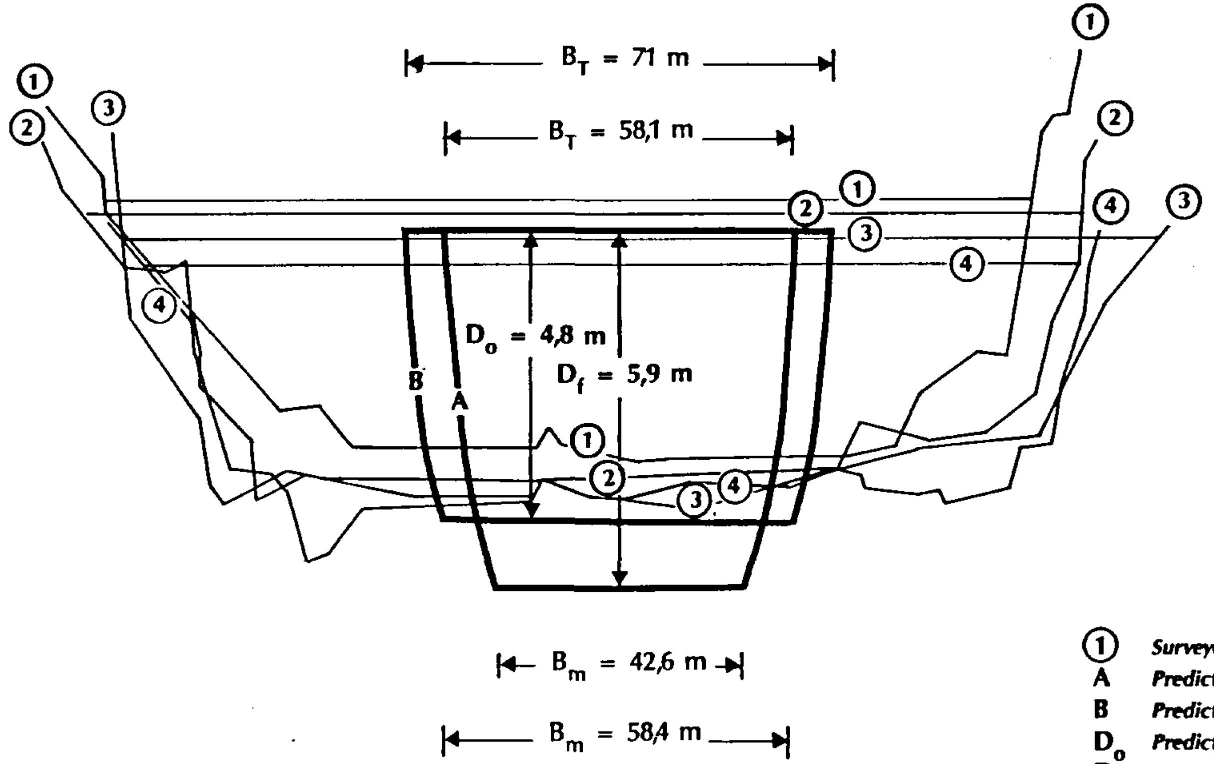

1 *Surveyed sections*
A *Predicted average cross-section according to energy slope*
B *Predicted average cross-section according to bed slope*
D_o *Predicted average flow depth according to bed slope*
D_f *Predicted average flow depth according to energy slope*

Scale: Hor. 1 : 1 250
Vert. 1 : 25

Comparative cross-sections: Site B87 — Mkuze River 1987

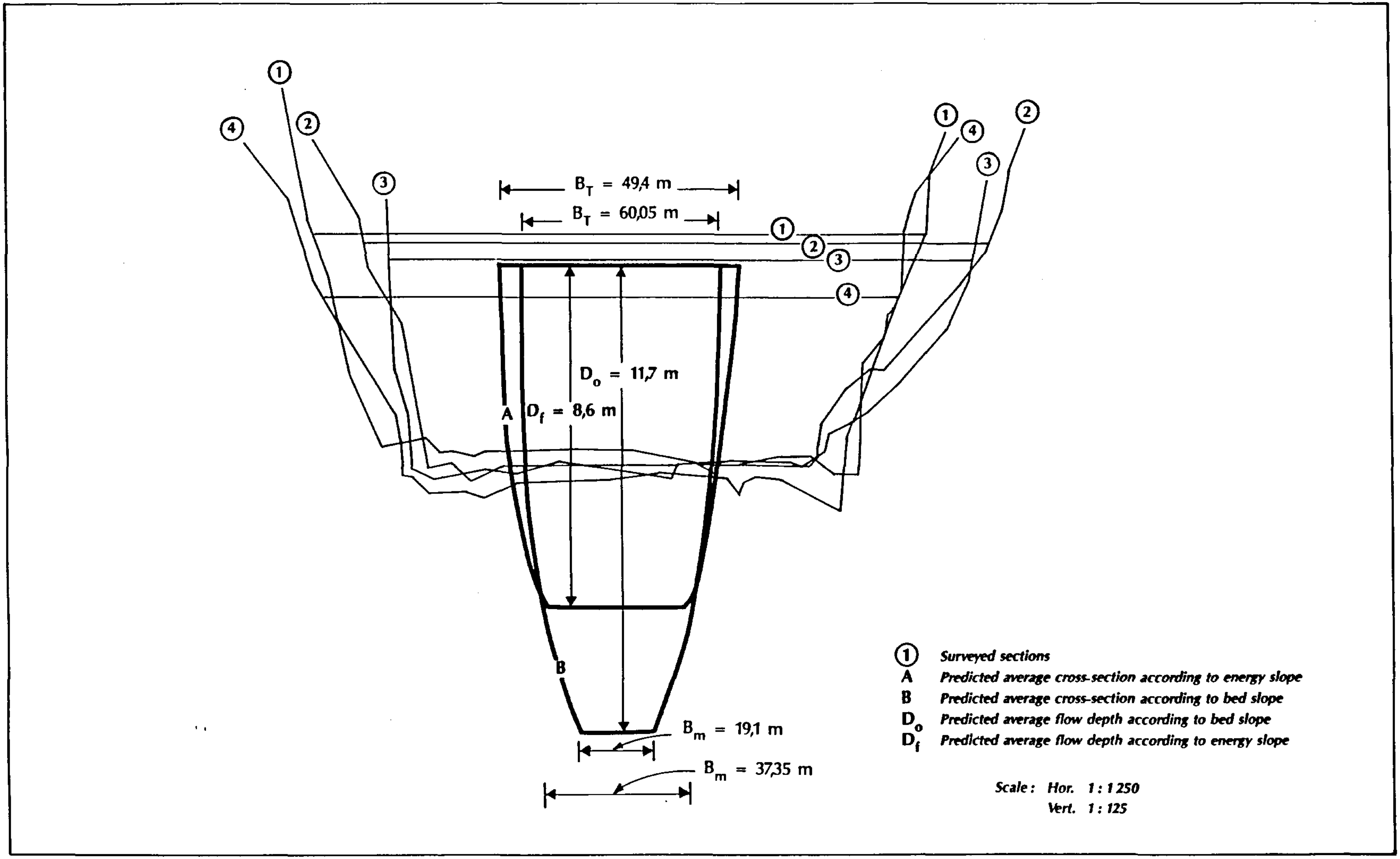

Comparative cross-sections: Site C87 — Black Mfolozi River 1987

10.7

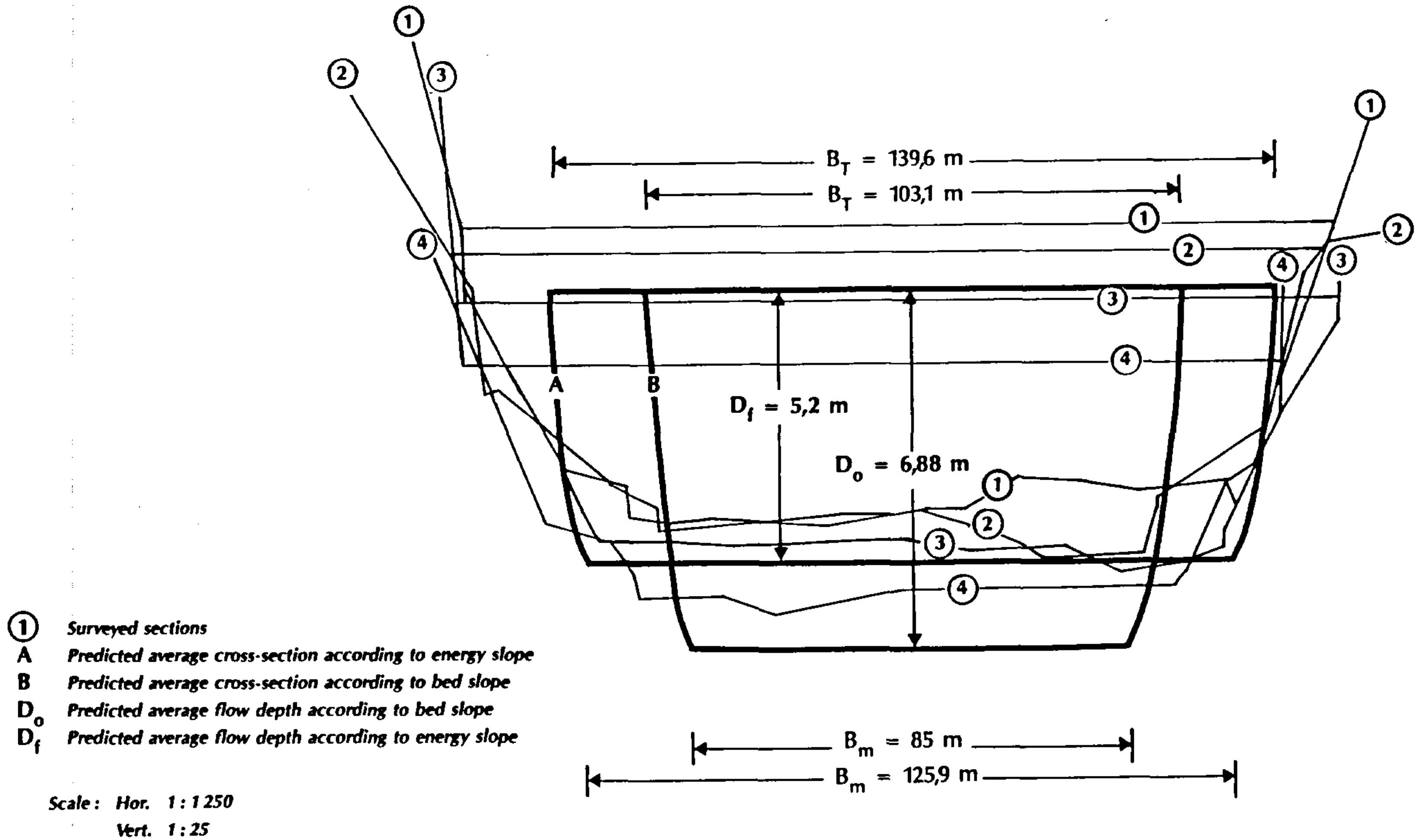

Comparative cross-sections: Site D87 — White Mfolozi River 1987

10.8

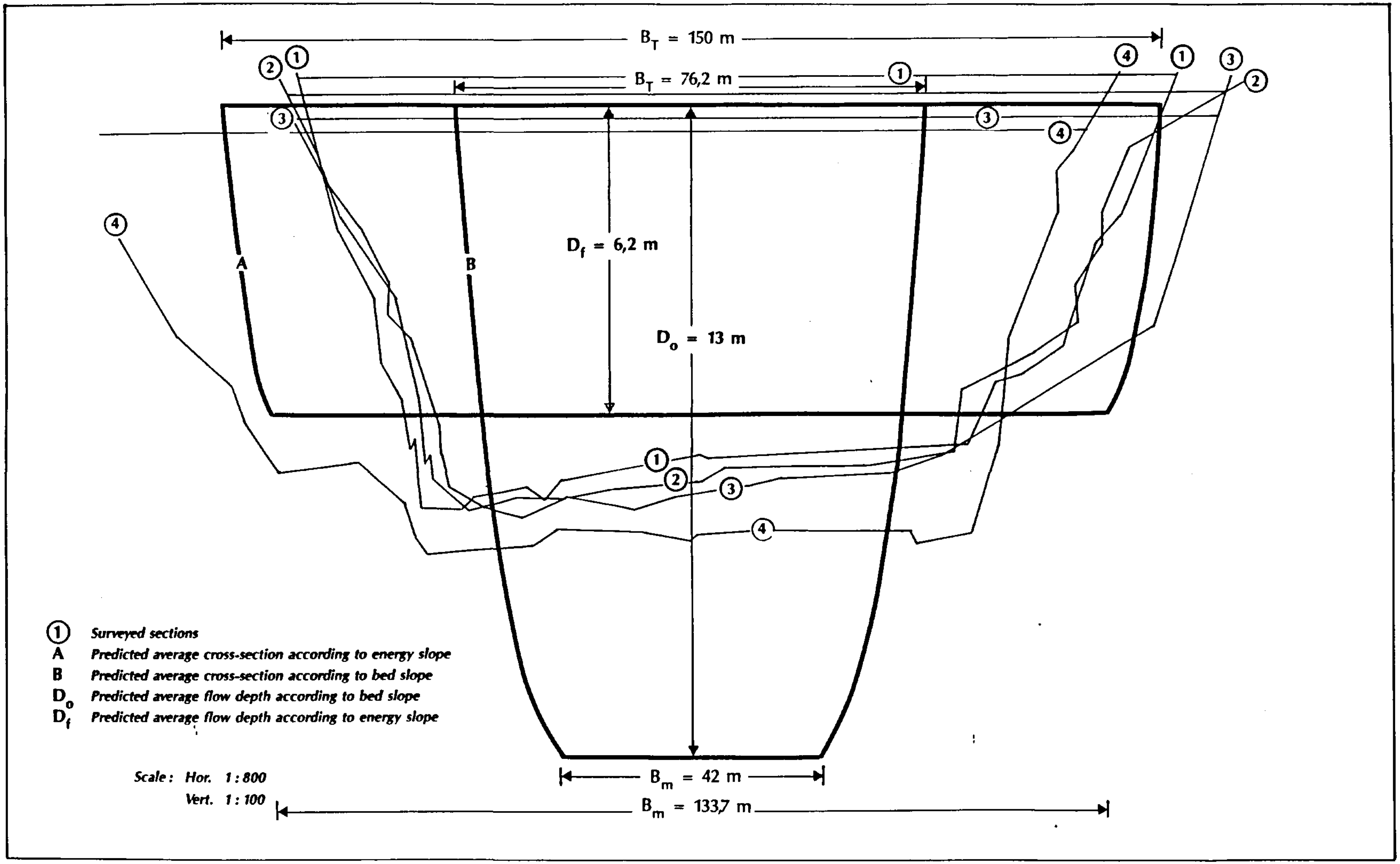

ALLUVIAL RIVER STUDY

Comparative cross-sections: Site E87 — Mhlatuze River 1987

10.9

10.4 DISCUSSION OF RESULTS

The applicability of the fundamental approach with regard to the observed "*field equilibrium*" conditions of the research rivers is discussed below. By using **Figures 10.1** to **10.9** the predicted cross-sectional deformation of the various field sites is discussed as follows:

Figure 10.1: Komati River 1984

Cross-sectional geometry is best predicted by means of the energy slope. Prediction of the average flow depth and the bottom width is good. The predicted top width, however, is considerably less than in the real case. Prediction by means of the bed slope leads to a realistic bottom width, whereas the average flow depth is slightly over-estimated and the top width under-estimated. In general, prediction of the cross-sectional geometry is satisfactory.

Figure 10.2: Mkuze River 1984

Average flow depth and bottom width are predicted well by means of both the energy and bed slope approaches. Both cases, however, under-estimated the top width. Both approaches can thus be used for prediction purposes.

Figure 10.3: Black Mfolozi River 1984

The average flow depth is well predicted by means of the bed slope approach while it under-estimated the bottom width. The energy slope approach, however, predicted the bottom width well while it under-estimated the flow depth. The top width is under-estimated in both cases. This can be attributed to overbank flows and associated erosion of top soil from the banks.

Figure 10.4: White Mfolozi River 1984

Both the bottom width and average flow depth are well approximated by means of both the energy and bed slopes. The top width, however, is under-estimated in both cases. This can be attributed to overbank flows and associated erosion of top soil from the banks.

Figure 10.5: Mhlatuze River 1984

Although the average flow depth is predicted reasonably well in terms of the energy slope, the fundamental approach produces unsatisfactory results regarding the other parameters. The behaviour of the Mhlatuze River might be influenced by the rock layer about 1 m below the river bed.

Figure 10.6: Mkuze River 1987

With a lower discharge in 1987 than in 1984 the predicted average cross-section is smaller than in reality. Although the average flow depth is predicted well in terms of the bed slope, the top width and bottom width are under-estimated. The energy slope approach leads to an over-estimatation of the flow depth and under-estimation of the width. It seems that the average field cross-section had not yet been built up since the 1984-flood.

Figure 10.7: Black Mfolozi River 1987

Prediction of the cross-sectional geometry by means of the fundamental approach is unsatisfactory.

Figure 10.8: White Mfolozi River 1987

Average flow depth is well predicted by means of the energy slope. An average of the two slope approaches, provides a good all-over approximation of the cross-sectional geometry.

Figure 10.9: Mhlatuze River 1987

Although the average flow depth is predicted reasonably well by means of the energy slope, the fundamental approach provides unsatisfactory results.

A summarized comparison between observed and predicted averaged values of flow depth and width is presented in **Table 10.5**.

Table 10.5: Comparison between observed and predicted reach averaged values of flow depth and width

Site	River	Year	Observed river behaviour: Flow depth D_o (m)	Bottom width B_m (m)	Top width[1] B_T (m)	Predicted river behaviour: Bed slope[2] Flow depth D_o (m)	Bed slope[2] Bottom width B_m (m)	Bed slope[2] Top width B_T (m)	Energy slope[3] Flow depth D_f (m)	Energy slope[3] Bottom width B_m (m)	Energy slope[3] Top width B_T (m)	Comments
A84	Komati	1984	11,0	57,8	168,6	13,2	41,2	76	10,75	60	88,3	satisfactory prediction except for under-estimation of top width
B84	Mkuze	1984	11,5	103,2	275,2	12,3	79,2	111,6	11	94,4	123,4	satisfactory prediction except for under-estimation of top width
B87	Mkuze	1987	4	95,9	132,2	4,8	58,4	71	5,9	42,6	58,1	unsatisfactory prediction
C84	Black Mfolozi	1984	15,2	105,3	566,1	15	116,9	156,4	13,85	131,8	168,5	satisfactory prediction except for under-estimation of top width
C87	Black Mfolozi	1987	5,2	107,8	153,7	11,7	19,1	49,9	8,6	37,35	60,05	unsatisfactory prediction
D84	White Mfolozi	1984	12,4	119,8	304,9	13,2	92,3	127,1	13,3	90,8	125,8	satisfactory prediction except for under-estimation of top width
D87	White Mfolozi	1987	5	112,8	177,7	6,88	85	103,1	5,2	125,9	139,6	prediction satisfactory
E84	Mhlatuze	1984	6,7	57,3	131,5	13,3	21,2	56,2	5,3	106,5	120,5	unsatisfactory prediction
E87	Mhlatuze	1987	7,4	85,7	154,8	13,0	42,0	76,2	6,2	133,7	150	unsatisfactory prediction

1) according to CFP (included overbank flow)
2) according to bed slope S_o
3) according to energy slope S_f

If the calculated values of top and bottom width and flow depth as presented in **Tables 10.3** to **10.5** and in **Figures 10.1** to **10.9**, as well as calculated values of the average flow velocity and absolute roughness (see **Tables 10.3** and **10.4**), are compared on a basis of perfect agreement with measured values of these parameters as presented in **Figures 10.10** to **10.18**, it follows that:

The results show a fair degree of general agreement between calculated (based on the energy slope) and measured values of the flow depth (see **Figure 10.11**). Taking an error margin of plus or minus 20 % as being acceptable for prediction purposes, about 70 % of the data points fall within this range. For depth prediction by means of the bottom slope only 55 % of the field data points fall into this range.

Independent estimates of the absolute roughness values were used by the DWA&F to calculate the peak discharge and energy slope values. According to these discharges absolute roughness values were determined by means of **Equation 9.19** for the purposes of this study. Although the predicted values of the absolute roughness k_s according to **Figure 9.6** differ from these assumed values, they are of the same order and the variation is mild according to **Figure 10.12**.

The comparison of the calculated and predicted values of flow velocity as shown in **Figures 10.13** and **10.14**, shows that velocity is in general over-estimated by means of both the energy and bed slope approaches.

It follows from **Figure 10.15** that the bottom width is in general under-estimated by the bed slope approach, while the level of scatter of predictions by means of the energy slope approach as shown in **Figure 10.16** is high. It follows from **Figures 10.17** and **10.18** that no general agreement between calculated and measured values of the top width exist and that the top-width is in general under-estimated. This is in agreement with the general case of under-estimation of the top width as shown in **Figures 10.1** to **10.9**.

In summary, it can be said that the proposed fundamental approach based on the energy slope and/or bed slope can be used in most of the field cases to give a fair approximation of recorded profiles.

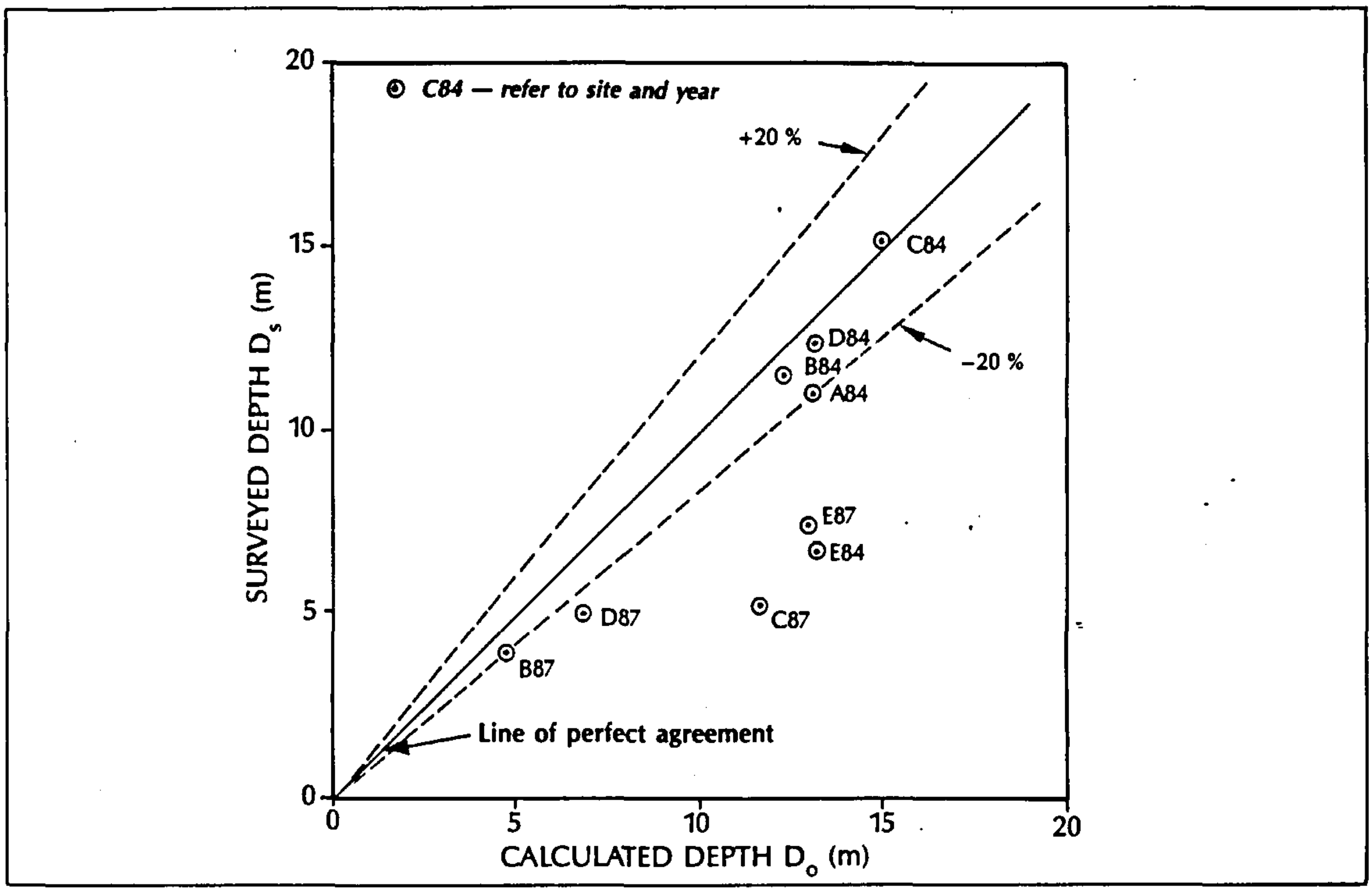

ALLUVIAL RIVER STUDY | Calculated (with regard to bed slope) versus surveyed values of flow depth | **10.10**

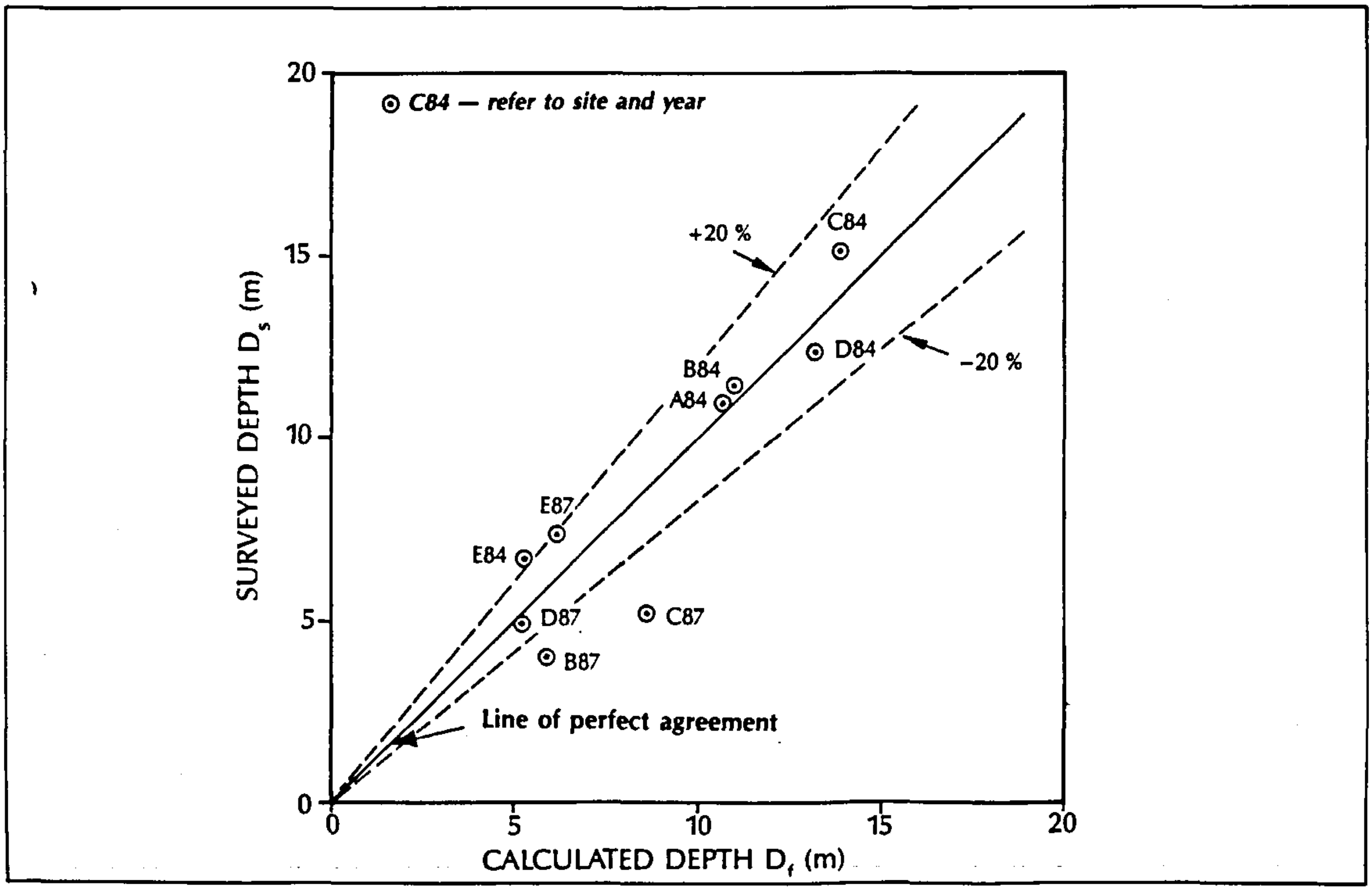

ALLUVIAL RIVER STUDY | Calculated (with regard to energy slope) versus surveyed values of flow depth | **10.11**

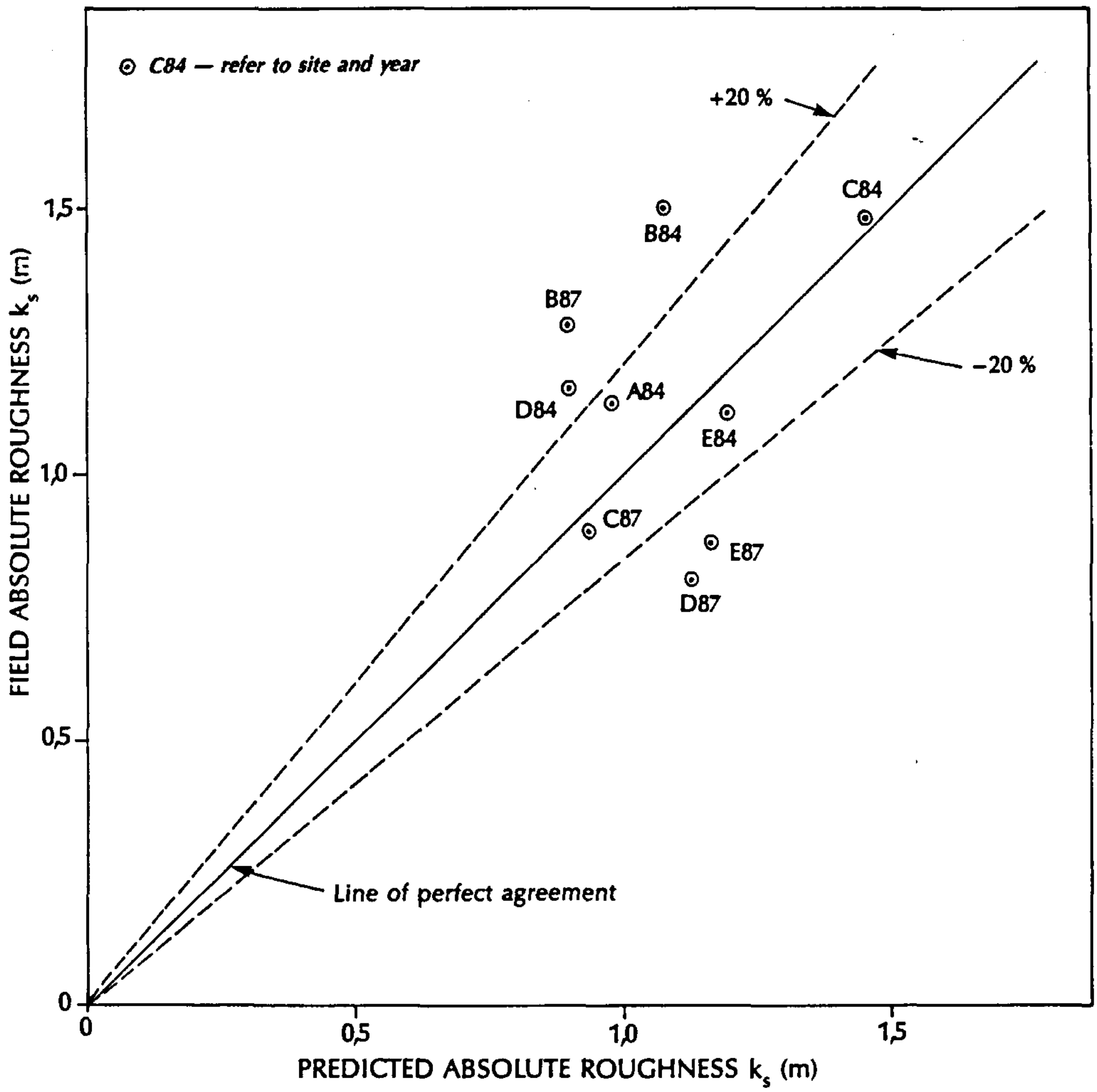
⊙ C84 — refer to site and year
+20 %
−20 %
C84
B84
B87
D84
A84
E84
C87
E87
D87
Line of perfect agreement
FIELD ABSOLUTE ROUGHNESS k_s (m)
PREDICTED ABSOLUTE ROUGHNESS k_s (m)
0
0,5
1,0
1,5

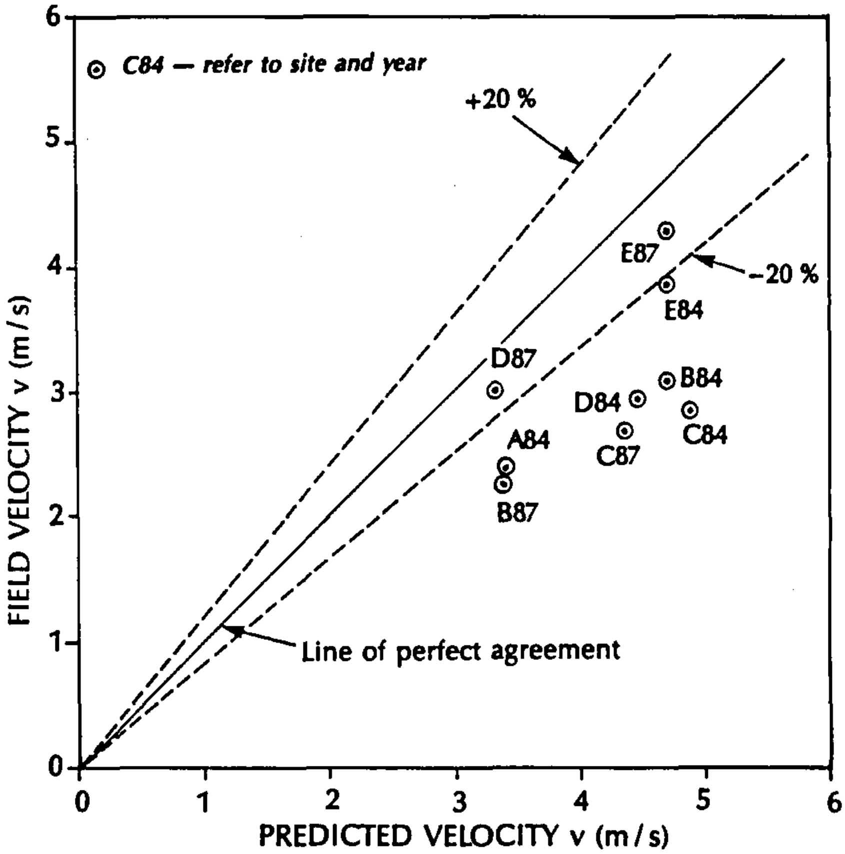

ALLUVIAL RIVER STUDY | Calculated (with regard to bed slope) versus field values of flow velocity | **10.13**

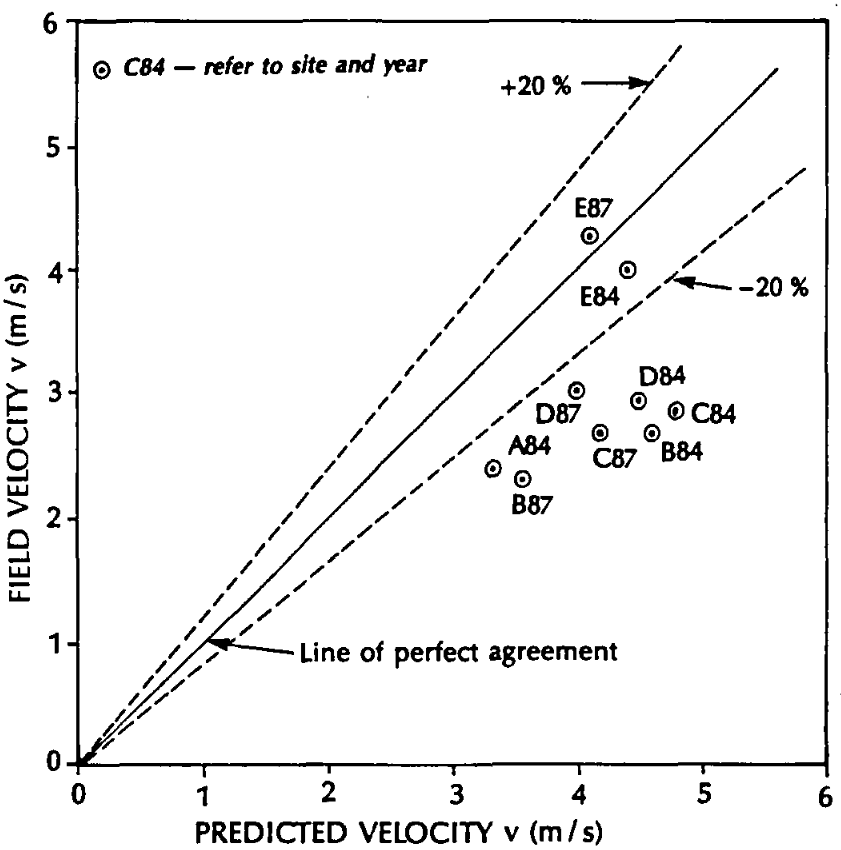

ALLUVIAL RIVER STUDY | Calculated (with regard to energy slope) versus field values of flow velocity | **10.14**

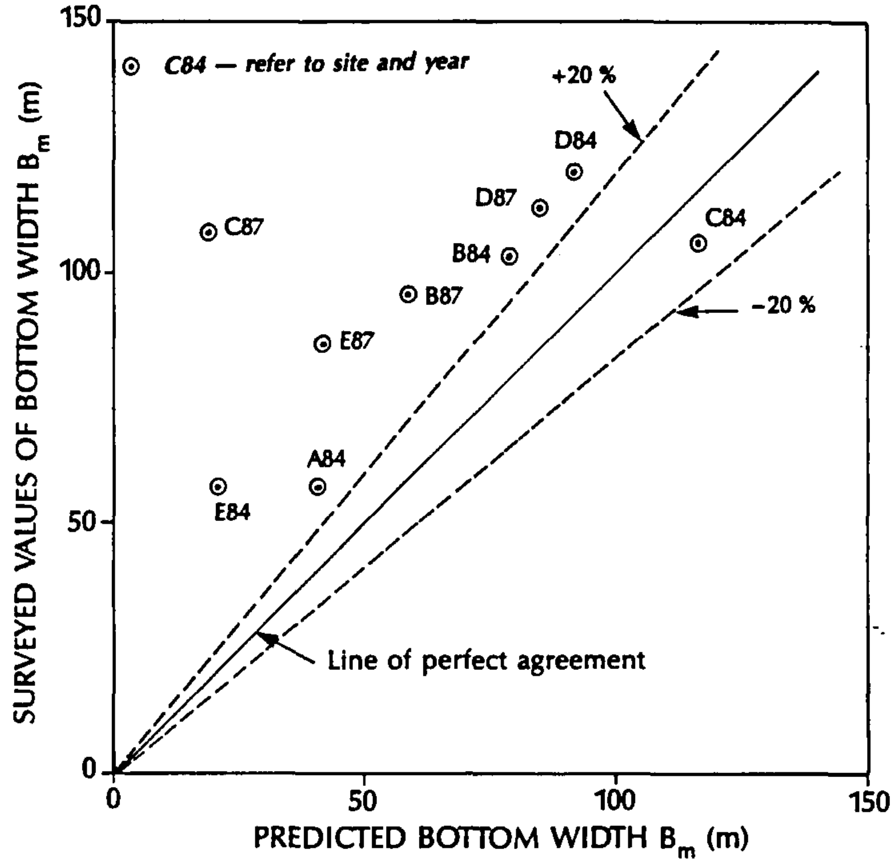

ALLUVIAL RIVER STUDY | Predicted (with regard to bed slope) versus surveyed values of bottom width | **10.15**

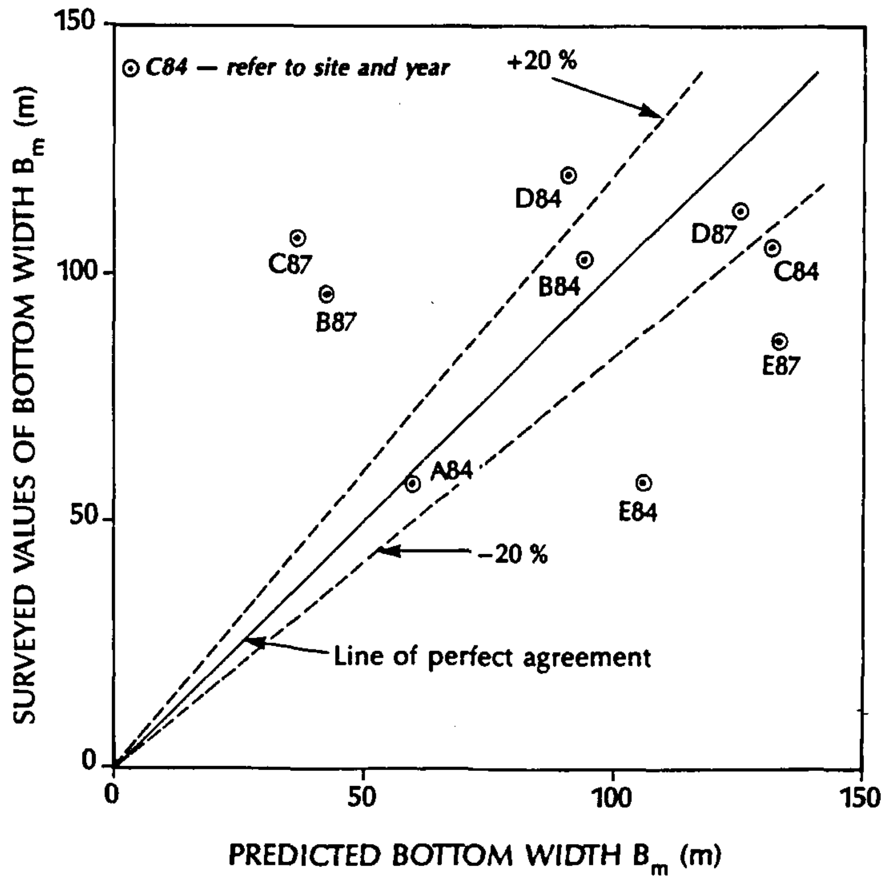

ALLUVIAL RIVER STUDY | Predicted (with regard to energy slope) versus surveyed values of bottom width | **10.16**

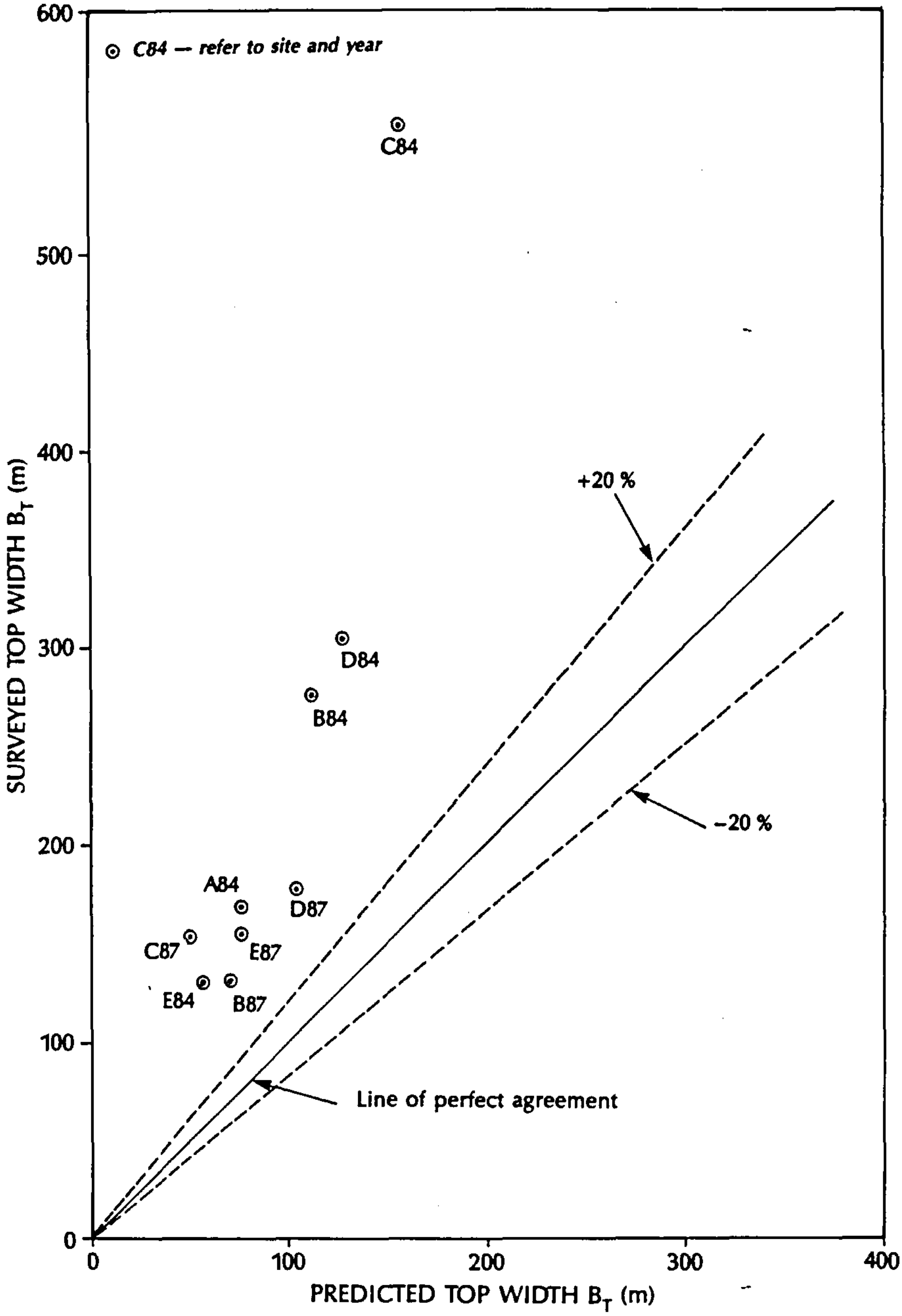

ALLUVIAL RIVER STUDY	**Predicted (with regard to bed slope) versus surveyed values of top width**	**10.17**

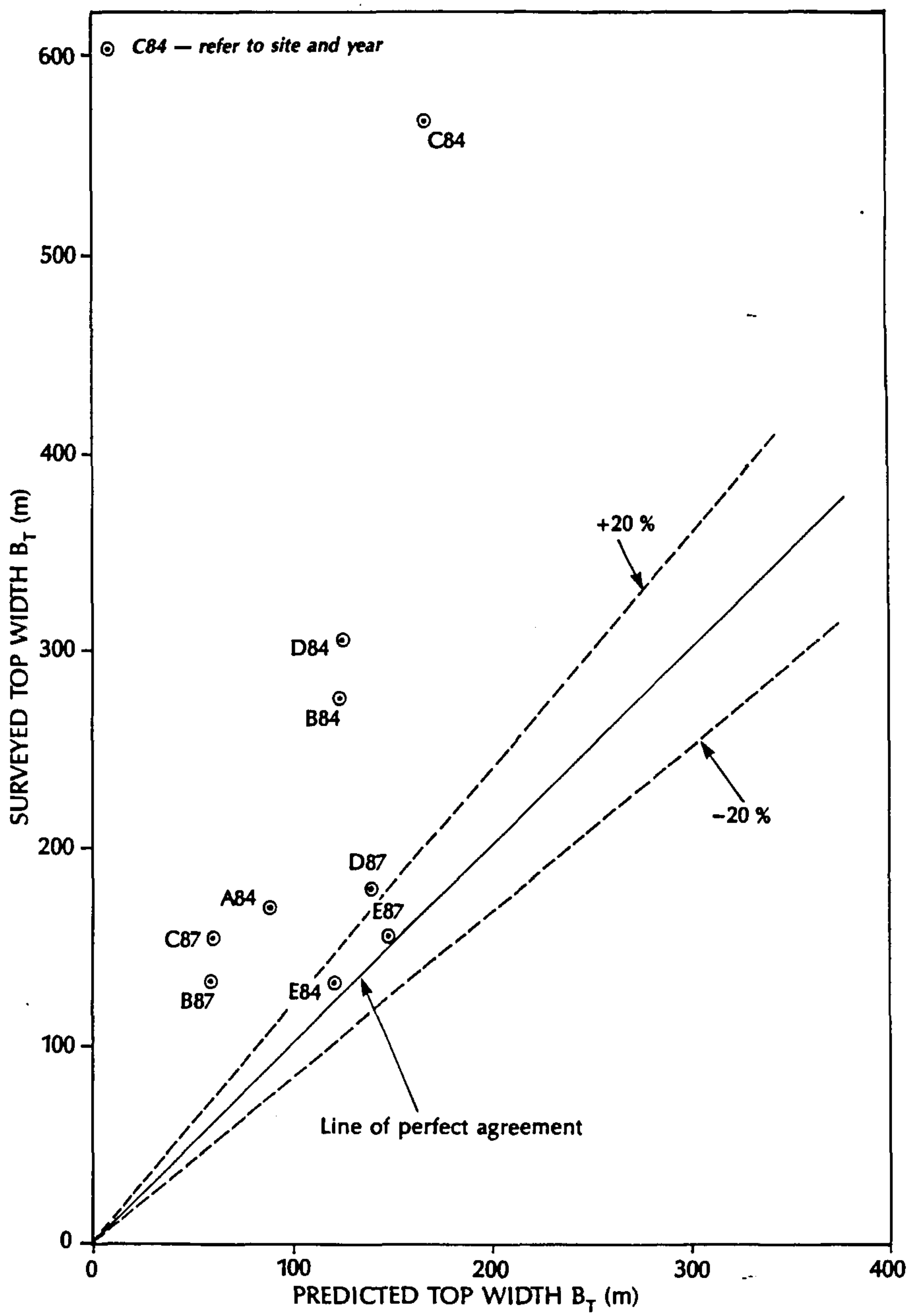

C84 — refer to site and year
C84
D84
B84
D87
A84
E87
C87
B87
E84
+20 %
−20 %
Line of perfect agreement
SURVEYED TOP WIDTH B_T (m)
PREDICTED TOP WIDTH B_T (m)
0
100
200
300
400
500
600

11. CONCLUSIONS

11.1 EMPIRICAL ANALYSIS REGARDING ALLUVIAL RIVER BEHAVIOUR

Results of the empirical relationships of Blench show a fair degree of general agreement between calculated values of mean channel width and average measured values of the top width. However, the level of scatter between calculated and measured values of mean flow depth is too high to be acceptable.

The analysis according to Parker shows good correlation between dimensionless parameters of flow depth, top width and discharge respectively (97 % correlation). The developed empirical relationships based on Parker's theory can be used as a simple but reliable method for predicting the width and depth of a river cross-section for a given discharge and sediment size. It is concluded that the Parker-type empirical equations are more reliable than those of Blench with regard to the researched rivers analysed. However, it must be kept in mind that such empirical relationships only describe averaged observed values and provide no explanation of how and why a channel adjusts its hydraulic geometry to a set of external constraints. Great care should always be taken not to apply such empirical relationships out of context.

11.2 FUNDAMENTAL APPROACH REGARDING ALLUVIAL RIVER BEHAVIOUR

The fundamental approach was used to develop tools, based on basic principles, to predict the regime or equilibrium behaviour of alluvial rivers. All the evidence with regard to sand bed rivers seem to indicate that equilibrium scour depths are approached only when the applied stream power drops below the critical value for laminar boundary conditions.

Given the uncertainties surrounding the measured variables, especially the absolute roughness, discharge and energy slope, it can be concluded that the results confirm the fundamental theory. The field curve presented in **Figure 9.2** fit well with regard to particle size into the structure of the Liu-diagram. Therefore, these curves represent the researched rivers' behaviour during the floods of 1984 and 1987. Whether a laminar boundary actually exists and whether the limiting turbulent applied power merely reaches a corresponding value is still debatable.

The repetitive formation and decay of bed forms together with their shapes, sizes and patterns depend on the flow pattern and the materials lining the channels. Flow resistance due to these bed surface irregularities are additional over and above those caused by the grain roughness alone. By creating large sand waves along its bed a river virtually armours itself and prevents the much deeper scour that would have taken place if the bed had remained smooth.

The application of the fundamental approach to measured river cross-sections indicated that some of the field data do not exactly represent the assumed critical or equilibrium condition. This can be attributed to:

i) time lag between time of flood and time of survey, i.e. influence of other inbetween flows
ii) non-representative sample of sediment due to variation in sediment characteristics with depth
iii) assuming bank material to be alluvial
iv) approximation of bank roughness by using an overall roughness parameter for a cross section
v) ignoring the influence of vegetation, especially bank vegetation
vi) approximate discharge calculation by means of the slope-area method
vii) influence of sinuosity
viii) the fact that southern African rivers do not flow at bankfull stage for long periods, but only for short times.

The most important of these factors might be the simplified way in which the banks were represented in the analysis. This is reflected in the differences between predicted and actual observed channel widths, especially with top widths generally being under-estimated.

The fundamental approach regarding alluvial river behaviour shows much promise. The fact that it can be proved, that, whilst rivers experience bed form changes, limiting scour conditions can still be expressed in terms of the basic relationship which depict critical conditions, is a valuable contribution to river hydraulics. Although cross-sectional geometry can not be predicted accurately in all cases, the fundamental approach provides insight into the deformation of river channels during extreme floods.

It can be concluded that the scoured sections of the alluvial rivers as surveyed point to equilibrium being approached during the floods of 1984 and 1987. The surveyed depths can thus be regarded as being critical or very near to critical. However, with no allowance for different bank materials and vegetate covers in the analysis, it is understandable that it has not been possible to predict top widths accurately.

This analysis is also the first calibration of the *Rooseboom theory* regarding critical conditions by means of field data representing extreme flood conditions. A most important result is the ability to predict absolute roughness values.

11.3 APPLICATION OF RESEARCH RESULTS

The results of this study can be used to predict aggradation (deposition) and degradation (erosion) of sand bed stream channels in a simplified way. This can be done by means of the empirical approach based on Parker's theory or the fundamental approach as developed in this report.

The empirical approach can only predict an average top width and a flow depth without any indication of channel shape. Care should also be taken to apply the empirical relationships for circumstances comparable to those originally analysed and not out of context. The fundamental approach, on the other hand, can be used for predictions of top width, bottom width, average flow depth and channel shape. Although top width may be under-estimated, the methodology could be improved in future research by allowing for bank retreat, bank material characteristics and bank vegetation. Such a geomorphological model could easily be linked to the more sophisticated open channel hydraulic flow models to predict loose boundary channel flow behaviour.

12. RECOMMENDATIONS

Problems encountered in predicting top widths indicated that riverbank behaviour should be more thoroughly investigated and incorporated in alluvial channel stability analysis. Alluvial riverbank retreat is a complicated phenomenom resulting from fluvial and mass instability and can be a significant source of sediment load in many rivers.

Although several attemps have been made in the past to relate bank stability to channel characteristics, there still is a definite need for a better understanding of the parameters representing the process of bank erosion and of how bank processes are linked to sediment movement processes in the channel as a whole.

It is important to distinguish between bank erosion and the rate of bank migration. The former gives a local description of the removal of bank material by fluvial entrainment and mass failure as a function of near-bank flow conditions and bank properties, whereas the latter describes actual bank retreat, which is influenced by the interactions within the morphological system as well. The amount of bank sediment contributed to the total load of the river depends not only on the geometry of the cross-section and the boundary flow shear, but also on the distribution and types of material in the cross-section.

Vegetation may increase or decrease the stability of the riverbank. The roots of plants, small trees, and grasses act as reinforcement of the bank soil, but big trees are additional weights to the bank that may decrease the stability of steep slopes. Also, plants introduce new complications in the form of anisotropic bank material properties and random variations in soil properties that cannot easily be accounted for.

Although it is extremely difficult to incorporate the effects of vegetation into bank stability analyses because these effects vary with the seasons and the degree of development of the plants, the effects of bank vegetation should be incorporated into the analytical procedure. As there is no simple relationship between vegetation, bank stability and channel geometry, this will require a considerable research effort. At present, there is no explicit mechanism to take the effects of bank vegetation into account when analyzing the stability of banks. The best available approach is to incorporate vegetation effects into the parameters used to represent the bank material's unit weight, effective friction angle and effective cohesion, i.e. the bank material characteristics.

It is suggested that the accuracy of predictions of hydraulic geometry can be markedly improved by future research through empirical modification of the calculated widths and depths to account for bank material and vegetation effects. Adequate field research and additional information on the geomorphological characteristics, i.e. strength properties of bank material, are needed and should be recorded with particular attention to the type of bank material and the type and density of bank vegetation. This, together with information regarding the bed level variation at the banks could help in the explanation of channel width variations. Empirical factors with regard to bank material and type and density of vegetation can be incorporated in the fundamental model to improve the prediction of geometrical channel changes. With this aim fulfilled a total integrated alluvial river flow model could be developed which can also predict changes as a function of time.

8376G/sw
1993-04-20

13. REFERENCES

1. ANNANDALE, G W [1987], *Reservoir Sedimentation,* Developments in Water Science, 29, Elsevier.

2. ASCE [1971], *Sedimentation Engineering*, Manuals and Reports on Engineering Practice - No 54, New York.

3. BETTESS, R, WHITE, W R and REEVE, C E [1988], *On the Width of Regime Channels*, International Conference on River Regime, Wallingford.

4. BLENCH, T [1957], *Regime Behaviour of Canals and Rivers*, Butterworths Scientific Publications, London.

5. BLENCH, T [1961], *Hydraulics of Canals and Rivers of Mobile Boundary*, in Butterworth's Civil Engineering Reference Book, 2nd ed, Butterworth, London.

6. BLENCH, T [1969], *Mobile Bed Fluviology*, University of Alberta Press, Edmonton.

7. BRAUNE, E [1984], *Density of Sediment in South African Reservoirs*, Proc. First South African National Hydrological Symposium, TR 119D, Department of Water Affairs and Forestry, Pretoria, SA.

8. CHADWICK, A J and MORFETT, J C [1986], *Hydraulics in Civil Engineering*, Allen & Urwin (Publishers) Ltd, London.

9. CHANG, H H [1979a], *Minimum Stream Power and River Channel Patterns*, J. Hydrology, Vol. 41.

10. CHANG, H H [1979b], *Geometry of Rivers in Regime*, J. Hydr. Div., Proc. ASCE, Vol. 105, No. HY6.

11. CHANG, H H [1980a], *Stable Alluvial Canal Design*, J. Hydr. Div., Proc. ASCE, Vol. 106, No. HY5.

12. CHANG, H H [1980b], ***Geometry and Gravel Streams***, J. Hydr. Div., Proc. ASCE, Vol. 106, No. HY9.

13. CHANG, H H and HILL, J C [1977], ***Minimum Stream Power for Rivers and Deltas***, J. Hydr. Div., Proc. ASCE, Vol. 103, No. HY12.

14. CRUICKSHANK, C and MAZA, J A [1973], ***Flow Resistance in Sand Bed Channels***, International Symposium on River Mechanics, Bangkok, Thailand.

15. DAVEY, B W and DAVIES, T R H [1979], ***Entropy Concepts in Fluvial Morphology - A Re-evaluation***, Water Resources, Research, Vol. 15, No 1.

16. DAVIES, T R H and SUTHERLAND, A J [1980], ***Resistance to Flow Past Deformable Boundaries***, Earth Surface Processes, Vol. 5.

17. DAVIES, T R H and SUTHERLAND, A T [1983], ***Extremal Hypotheses for River Behaviour***, Water Resources Research, Vol. 19, No. 1.

18. DU PLESSIS, D B and DUNN, P [1984], ***General Field and Office Procedures for Indirect Discharge Measurements***, Department of Environment Affairs, Division of Hydrology, Flood Studies Section (internal publication), Pretoria, SA.

19. EINSTEIN, H A and BARBAROSSA, N [1951], ***River Channel Roughness***, Transactions, ASCE, Paper 2528.

20. ENGINEERING COMPUTING COMPANY [1987], ***Channel Flow Profiles***, Computer Program, Cape Town.

21. FRENCH, R H [1986], ***Open-Channel Hydraulics***, McGraw Hill Book Company.

22. FROMME, G A Q [1977], ***Establishment of a Standard Relationship between Settling Velocity and Grain Size of Coastal Sand***, CSIR Research Report 356, National Research Institute for Oceanology, SA.

23. GRAF, W H [1971], *Hydraulics of Sediment Transport, McGraw* - Hill, New York.

24. GRAF, W H and ACAROGLU, E R [1966], *Settling Velocities of Natural Grains*, Bull., Intern. Assoc. of Sci. Hydrology, Vol. XI, no. 4.

25. GRASS, A J [1970], *The Initial Instability of Fine Sand,* J. Hydr. Div., Proc. ASCE, Vol. 96, No HY3.

26. GRIFFITHS, G A [1983], *Stable - Channel Design in Alluvial Rivers,* J Hydrology, Vol. 65, No. 4. Griffiths, G A [1984].

27. GRIFFITHS, G A [1984], *Extremal Hypotheses for River Regime: An Illusion of Progress*, Water Resources Research, Vol. 20, No. 1.

28. HENDERSON, F M [1961], *Stability of Alluvial Channels*, J. Hydr. Div., Proc. ASCE, Vol. 87, No HY6.

29. HENDERSON, F M [1963], *Stability of Alluvial Channels,* Trans. ASCE, Vol. 128, Part 1, Paper No. 3440.

30. HENDERSON, F M [1966], *Open Channel Flow,* McMillan, New York.

31. HEY, R D [1978], *Determinate Hydraulic Geometry of River Channels*, J. Hydr. Div., Proc. ASCE, Vol. 104, No. HY6.

32. HJULSTRÖM, F [1935], *The Morphological Activity of Rivers as Illustrated by Rivers Fyris*, Bull. Geol. Inst. Uppsala, Vol. 25 (Chapter III).

33. ILO, C G [1975], *Resistance to Flow in Alluvial Channels*, J. Hydr. Div., Proc. ASCE, Vol. 101, No. HY6.

34. INGLIS, C C [1949], *The Effect of Variations in Charge and Grade on the Slopes and Shapes of Channels*, Intrn. Assoc. Hydr. Res. 3rd Meeting, Grenoble.

35. KARIM, M F, HOLLY, F M and KENNEDY, J F [1982], *IALLUVIAL: A Computer Based Flow and Sediment Routing Model for Alluvial Streams and its Application to the Missouri River*, National Science Foundation, Washington, DC.

36. KENNEDY, R G [1895], *The Prevention of Silting in Irrigation Canals*, Paper No III-3, Third Meeting IAHR, Grenoble, France.

37. KOVÁCS, Z P, DU PLESSIS, D B, BRACHER, P R, DUNN, P and MALLORY, G C L [1985], *Documentation of the 1984 Domoina Floods*, Technical Report No 122, Department Water Affairs, Pretoria, SA.

38. KRISHNAPPAN, B G [1981], *User's Manual: Unsteady, Non-uniform Mobile Boundary Flow Model - MOBED*, Hydraulics Divisions, National Water Research Institute, Burlington.

39. KRISHNAPPAN, B G [1985], *Modelling of Unsteady Flows in Alluvial Streams*, J. Hydr. Eng., Vol. 111, No. 2.

40. LACEY, G [1929 - 1930], *Stable Channels in Alluvium*, Min. Proc. Inst. Civil Engr., Vol. 229.

41. LACEY, G [1933], *Uniform Flow in Alluvial Rivers and Canals*, Proc. Institution of Civil Engineers, London, England, Vol. 237.

42. LACEY, G [1958], *Flow in Alluvial Channels with Sandy Mobile Beds*, Paper No. 6274, Proc. Institution of Civil Engineers, London.

43. LANE, E W [1952], *Progress Report on Results of Studies on Design of Stable Channels*, Report No. Hyd - 352.

44. LANE, E W [1955], *Design of Stable Channels*, Trans. ASCE, Vol. 120, Paper No. 2776.

45. LANE, E W [1957], *A Study of the Shape of Channels Formed by Natural Streams Flowing in Erodible Material*, U.S. Army Div. Missouri River, Corps of Engineers, Omaha, Neb., MRD Sediment Series, No. 9.

46. LEOPOLD, L B and MADDOCK, T [1953], *The Hydraulic Geometry of Stream Channels and Some Physiographic Implications*, U.S. Geol. Survey, Prof. Paper 252.

47. LEOPOLD, L B and WOLMAN, M G [1957], *River Channel Patterns: Braided, Meandering and Straight*, U.S. Geol. Survey, Prof. Paper 282-B.

48. LEWIS, G N and RANDALL, M [1961], *Thermodynamics*, McGraw-Hill, New York.

49. LIU, H K [1957], *Mechanics of Sediment-Ripple Formation*, Proc. Am. Soc. Civil Engrs., Vol 83, No. HY2.

50. MARTIN, C S [1964], *The Role of a Permeable Bed in Incipient Sediment Motion*, Ph.D Thesis, Georgia Inst. of Tech.

51. MÜLKE, F J [1981], *Stormwaterdreinering van Spoorbane*, Ph.D-Thesis, University of Pretoria, Pretoria, SA.

52. OSMAN, A M and THORNE, C R [1988], *River Bank Stability Analysis*, J. Hydr. Eng., Proc. ASCE, Vol. 114, No. HY2.

53. PARKER, G [1978a], *Self-Formed Rivers with Stable Banks and Mobile Bed, Part 1, The Sand-Silt River*, J. Fluid Mech, Vol. 89.

54. PARKER, G [1978b], *Self-Formed Straight Rivers with Equilibrium Banks and Mobile Bed, Part 2, The Gravel River*, J. Fluid Mech., Vol. 89.

55. PARKER, G [1979], *Hydraulic Geometry of Active Gravel Rivers*, J. Hydr. Div., Proc. ASCE, Vol. 105, No. HY9.

56. PRIGOGINE, I [1955], *Introduction to Thermodynamics of Irreversible Processes*, C C Thomas, Springfield, Illinois.

57. RAMETTE, M [1979], *Une Approache Rationalle de la Morpholigie Fluviale*, La Houille Blanche, No. 8.

58. ROOSEBOOM, A [1974], ***Open Channel Fluid Mechanics***, Technical Report No. 62, Department of Water Affairs, Pretoria, SA.

59. ROOSEBOOM, A [1985], ***Sediment Transport***, Hydro '85, Chapter 8, University of Pretoria, Pretoria, SA.

60. ROOSEBOOM, A [1991], ***Personal Communications***.

61. ROUSE, H and INCE, S [1957], ***History of Hydraulics***, Iowa Institute of Hydraulic Research, Iowa City, Iowa.

62. RUBEY, W W [1933], ***Equilibrium Conditions in Debris Laden Streams***, 14th Annual Meeting, Trans. AM. Geophys. Union.

63. SCHUBAUER, G W, and SKRAMSTAD, H K, [1947], ***Laminar Boundary Layer Oscillations and Transition on Flat Plate***, National Bureau of Standards, Research Paper No. 1772.

64. SHEN, H W [1971a], ***Introduction***, River Mechanics, ed. by H W Shen, Vol. 1, Chapter 1.

65. SHEN, H W [1971b], ***Stability of Alluvial Channels***, River Mechanics, ed. by H W Shen, Vol. 1, Chapter 16.

66. SHIELDS, A [1936], ***Anwendung der Ähnlichkeitsmechanik und Turbulengforschung auf die Geschiebebewegung***, Mitteil, Preuss. Verscuchsanst, Wasser, Erd. Schiffsbau, Berlin, No.26.

67. SIMONS, D B and RICHARDSON, E V [1966], ***Resistance to Flow in Alluvial Channels***, River Mechanics, ed. by H W Shen, Vol. 1, Chapter 9.

68. SONG, C C S and YANG, C T [1979], ***Velocity Profiles and Minimum Stream Power***, J. Hydr. Div., Proc. ASCE, Vol. 105, No. HY8.

69. SONG, C C S and YANG, C T [1980], *Minimum Stream Power: Theory*, J. Hydr. Div., Proc. ASCE, Vol 106, No. HY9.

70. THORNE, C R [1978], *Processes of Bank Erosion in River Channels*, unpubl. Ph.D-Thesis, Sch. Env. Sciences, Univ. East Anglia, Norwich, UK.

71. THORNE, C R and OSMAN, A M [1988], *The Influence of Bank Stability on Regime Geometry of Natural Channels*, International Conference on River Regime, Wallingford.

72. VAN BLADEREN, D [1989], *Post Flood Channel Geometry and Recovery in Alluvial Rivers*, Fourth South African National Hydrological Symposium, 20 - 22 Nov., Pretoria, SA.

73. VAN BLADEREN, D and BURGER, C E [1989], *Documentation of the September 1987 Natal Floods*, Technical Report No. 139, Department Water Affairs, Pretoria, SA.

74. WATSON, R A [1969], *Explanation and Prediction in Geology*, J. of Geology, Vol. 77.

75. WEBBER, N B [1971], *Fluid Mechanics for Civil Engineers*, Chapman and Hall, London.

76. WHITE, W R BETTESS, R and PARIS, E [1982], *Analytical Approach to River Regime*, J. Hydr. Div., Proc. ASCE, Vol. 108, No. HY10.

77. WHITING, P J and DIETRICH, W E [1990], *Boundary Shear Stress and Roughness over Mobile Alluvial Beds*, J. Hydr. Eng., Vol. 116, No. 12.

78. YALIN, M S [1965], *Similarity in Sediment Transport by Currents*, Hydraulics Research Paper No. 6, Hydraulics Research Station, London, England.

79. YANG, C T [1971a], *The Potential Energy and Stream Morphology*, Water Resources Research, Vol. 7, No. 2.

80. YANG, C T [1971b], *On River Meanders*, J. Hydrology, Vol. 13.

81. YANG, C T [1971c], ***Formation of Riffles and Pools***, Water Resources, Research Vol. 7, No. 6.

82. YANG, C T [1972], ***Unit Stream Power and Sediment Transport***, J. Hydr. Div., Proc ASCE, Vol. 98, No. HY10.

83. YANG, C T [1973], ***Incipient Motion and Sediment Transport***, J. Hydr. Div., Proc ASCE, Vol 99, No HY10.

84. YANG, C T [1976], ***Minimum Unit Stream Power and Fluvial Hydraulics***, J. Hydr. Div., ASCE, Vol. 102, No. HY7.

85. YANG, C T and SONG, C S [1979], ***Theory of Minimum Rate of Energy Dissipation***, J. Hydr. Div., Proc. ASCE, Vol. 105, No. HY7.

86. YANG, C T, SONG C C S, and WOLDENBERG, M J [1981], ***Hydraulic Geometry and Minimum Rate of Energy Dissipation***, Water Resources Research, Vol. 17, No. 4.

87. YANG, C T, MOLINAS A, and SONG C C S [1988], ***G Stars - Generalized Stream Tube Model for Alluvial River Simulation"***, U.S. Interagency Subcommittee on Sedimentation.

APPENDIX A

SURVEYED CROSS-SECTIONS

SECTION 1

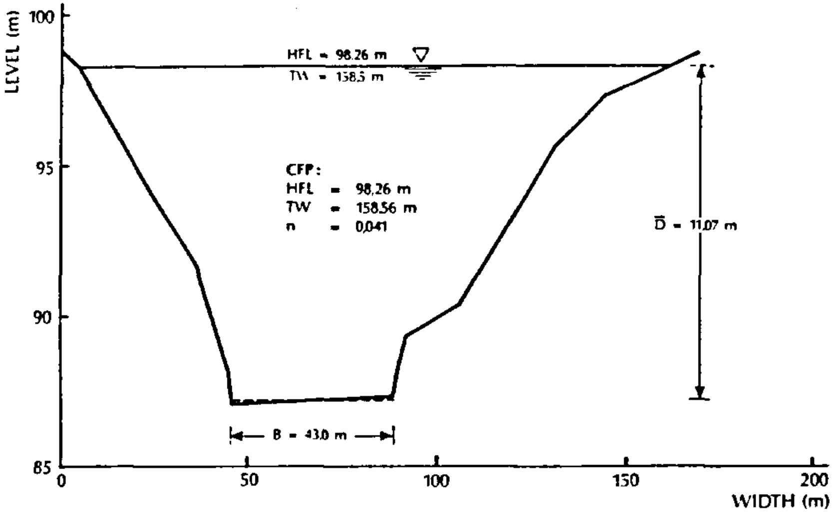

SECTION 2

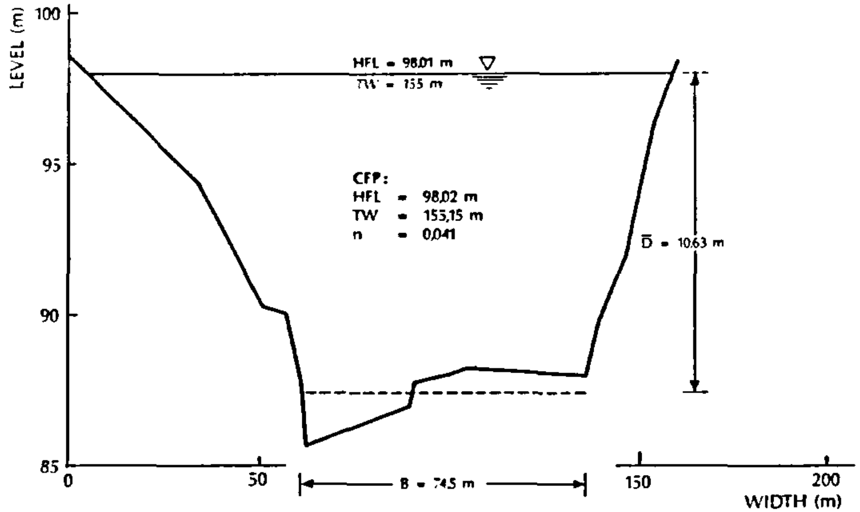

SECTION 3

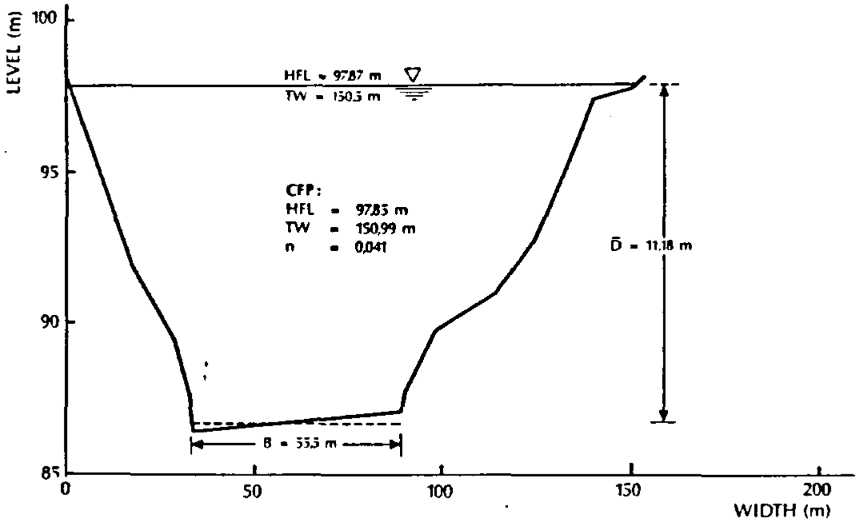

SECTION 4

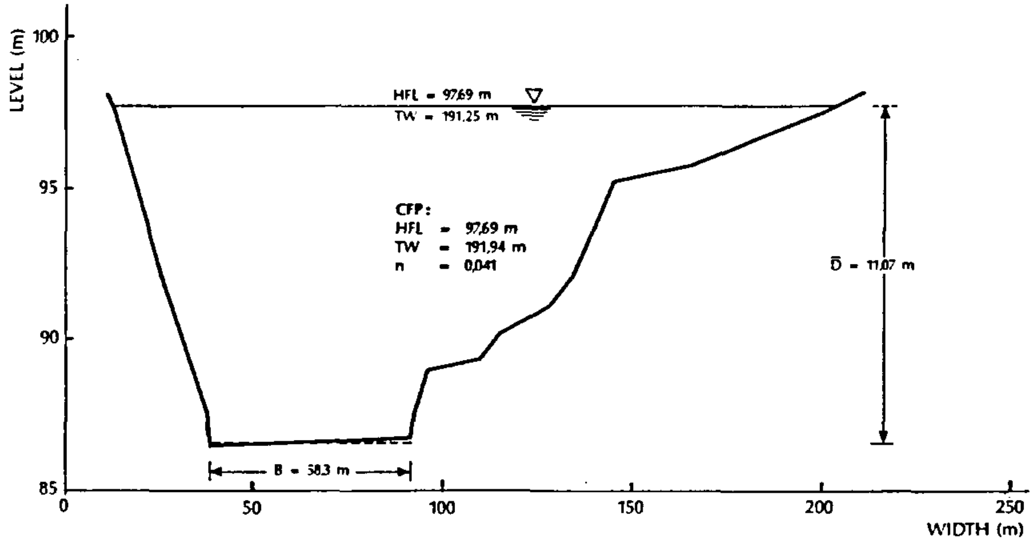

ALLUVIAL RIVER STUDY

Cross-sections : Site A – Komati River 1984 **A.1**

SECTION 2

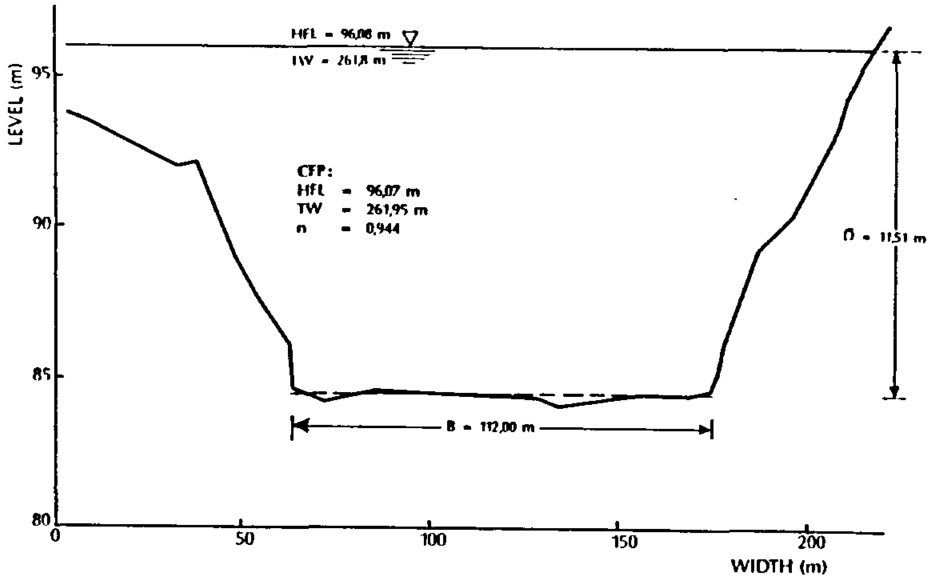

SECTION 3

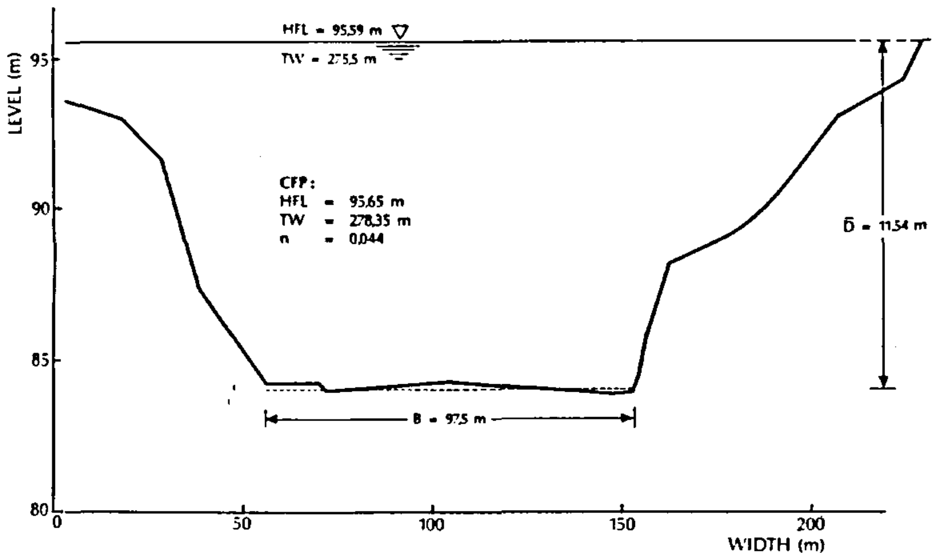

SECTION 4

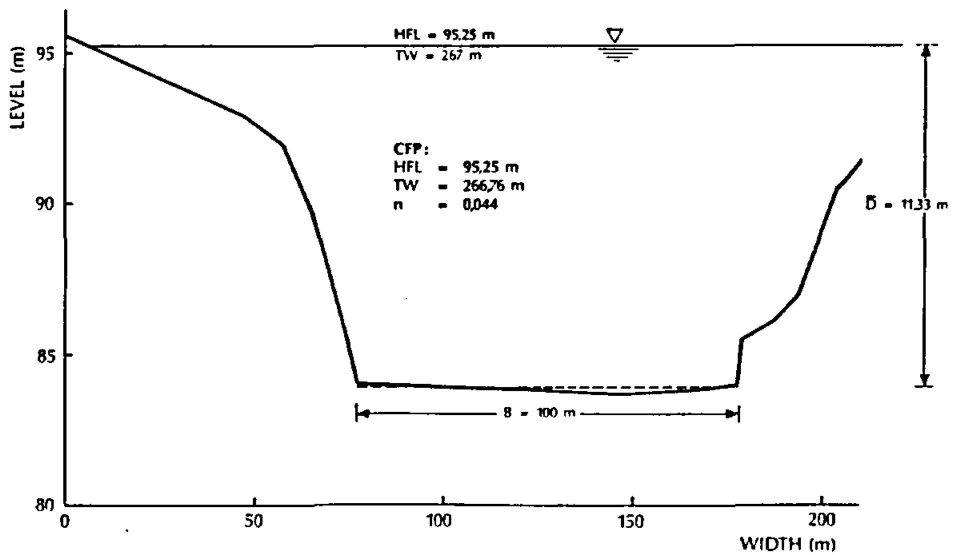

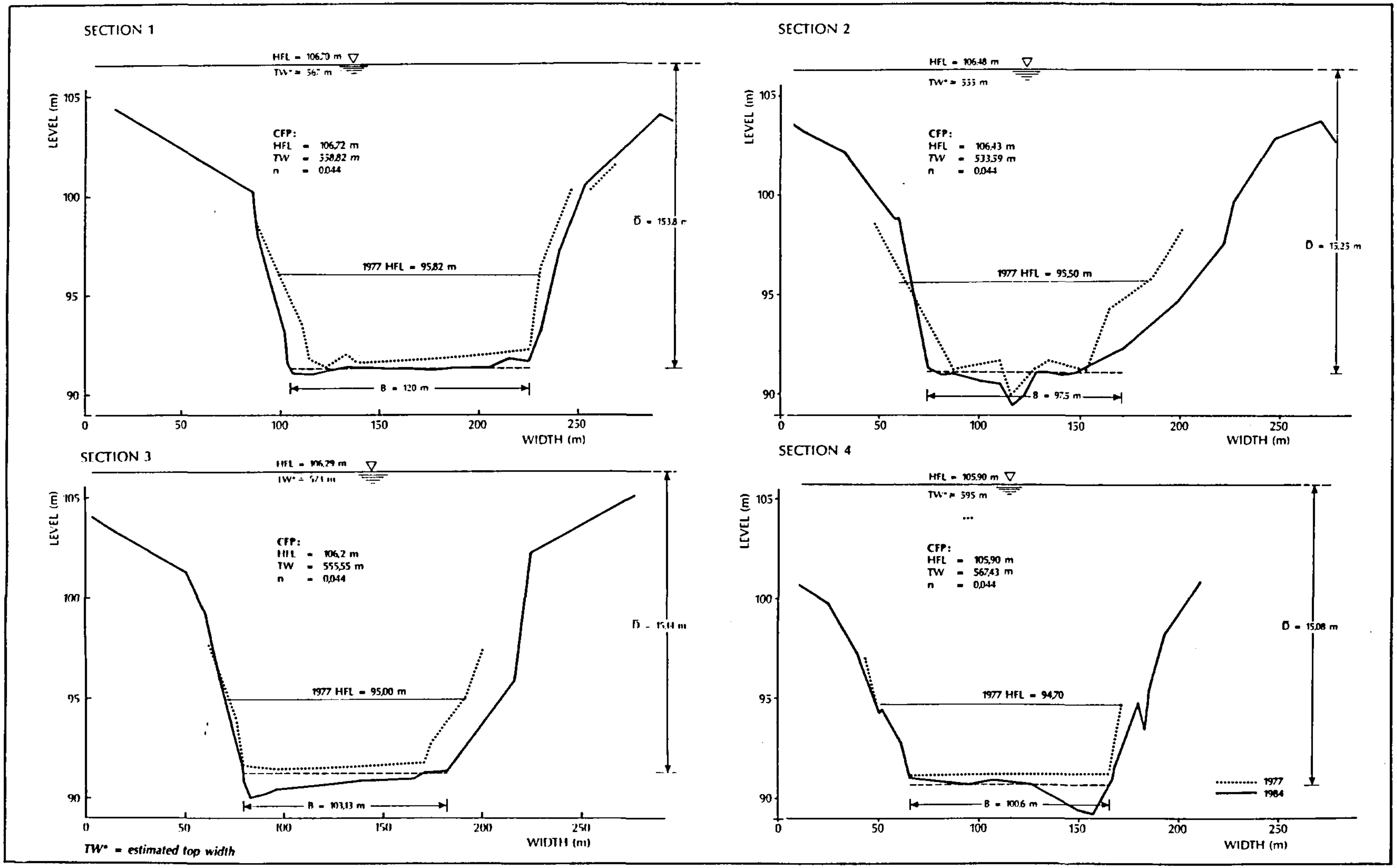

ALLUVIAL RIVER STUDY

Cross-sections : Site C – Black Mfolozi River 1984 **A.3**

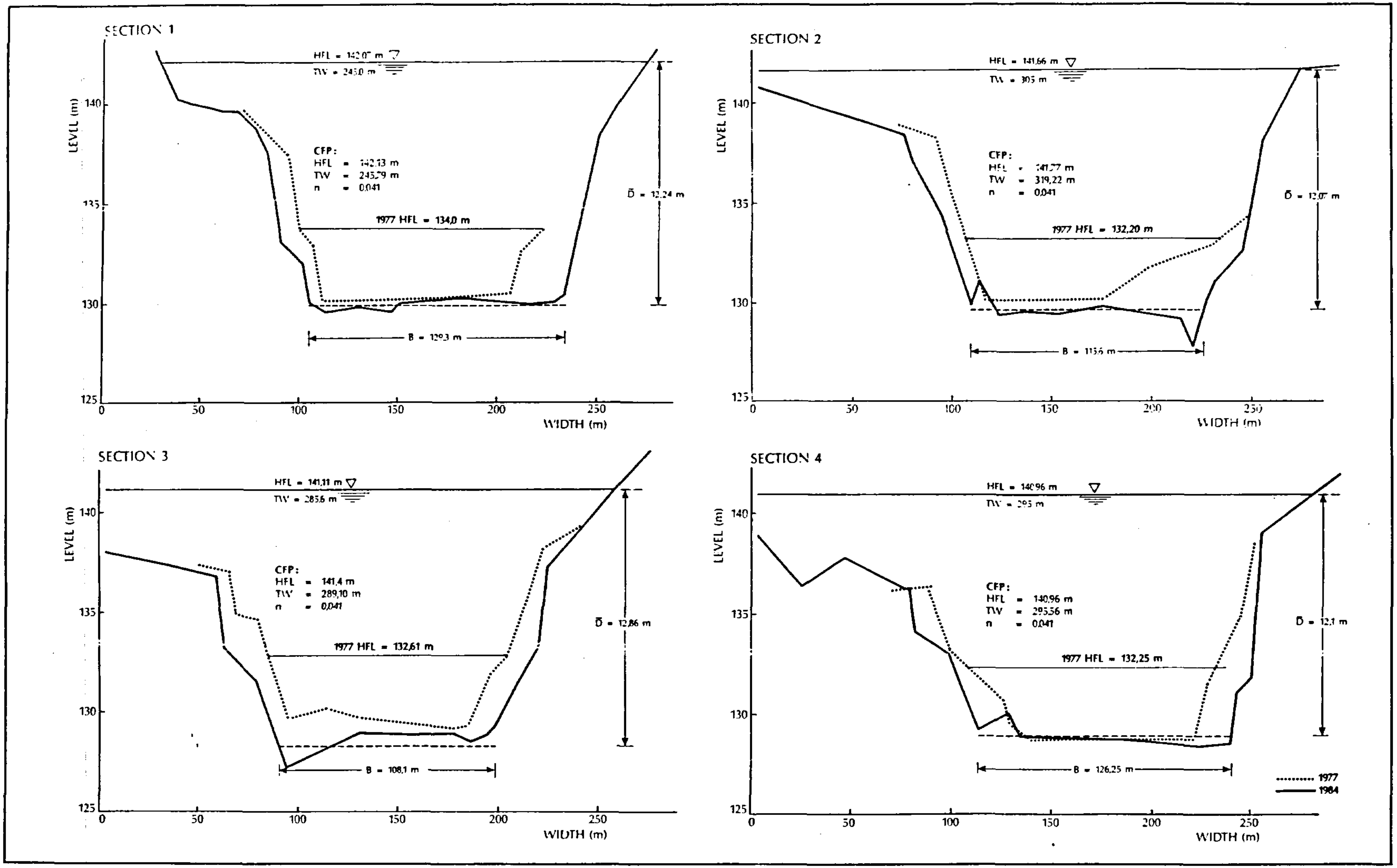

SECTION 1
HFL = 142,07 m
TW = 243,0 m
CFP:
HFL = 142,13 m
TW = 245,79 m
n = 0,041
1977 HFL = 134,0 m
D̄ = 12,24 m
B = 129,3 m
SECTION 2
HFL = 141,66 m
TW = 305 m
CFP:
HFL = 141,77 m
TW = 319,22 m
n = 0,041
1977 HFL = 132,20 m
D̄ = 12,07 m
B = 115,6 m
SECTION 3
HFL = 141,11 m
TW = 285,6 m
CFP:
HFL = 141,4 m
TW = 289,10 m
n = 0,041
1977 HFL = 132,61 m
D̄ = 12,86 m
B = 108,1 m
SECTION 4
HFL = 140,96 m
TW = 295 m
CFP:
HFL = 140,96 m
TW = 295,56 m
n = 0,041
1977 HFL = 132,25 m
D̄ = 12,1 m
B = 126,25 m
1977
1984
LEVEL (m)
WIDTH (m)

SECTION 1

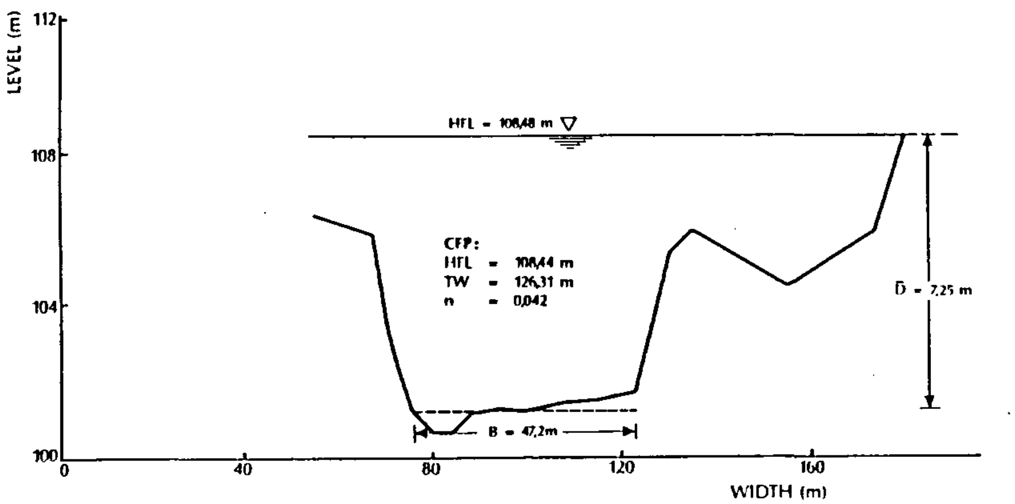

SECTION 2

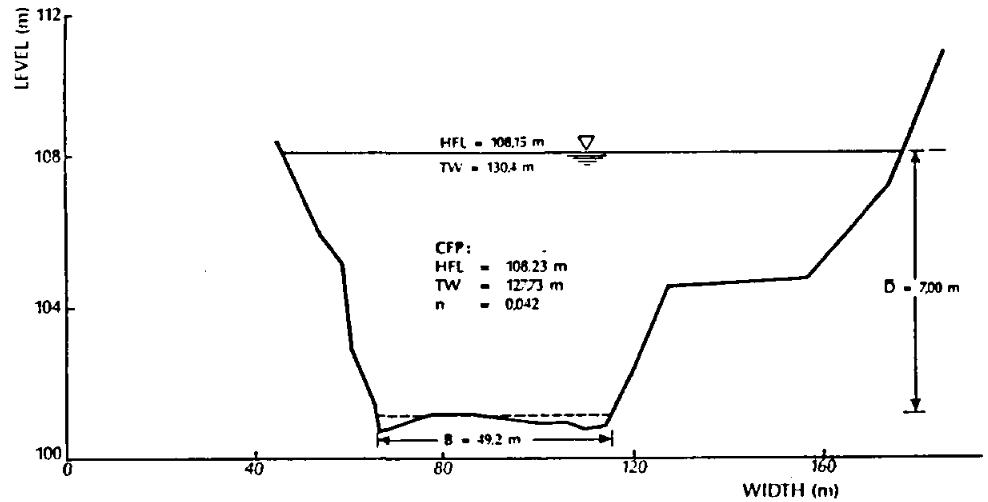

SECTION 3

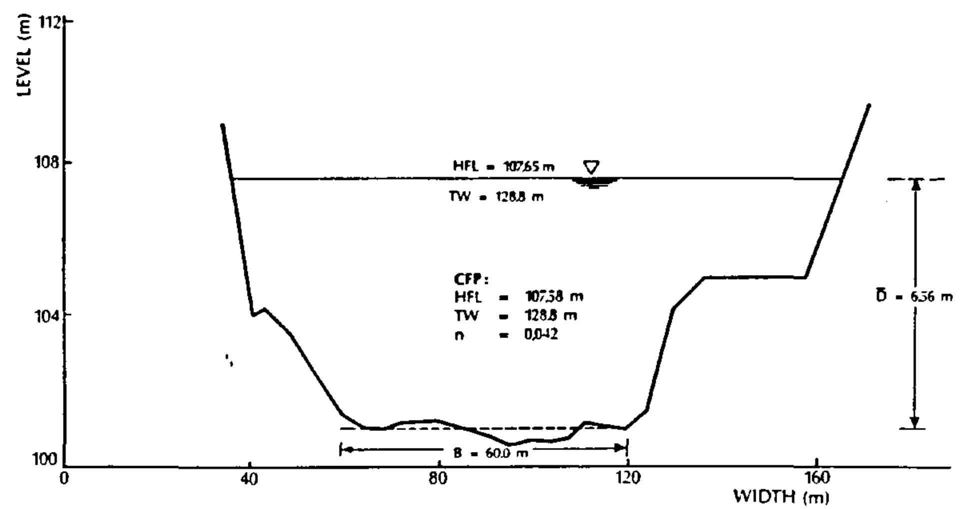

SECTION 4

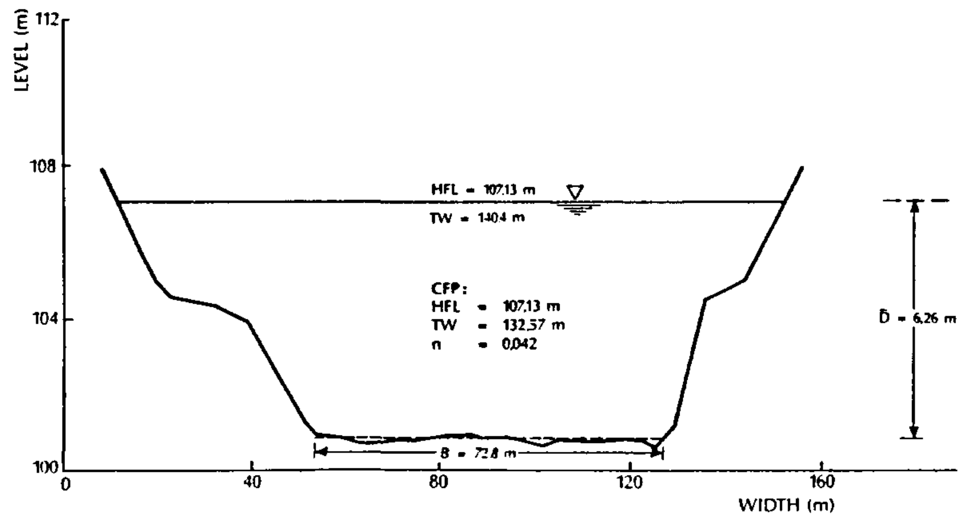

BKS

ALLUVIAL RIVER STUDY

Cross-sections : Site E – Mhlatuze River 1984

A.5

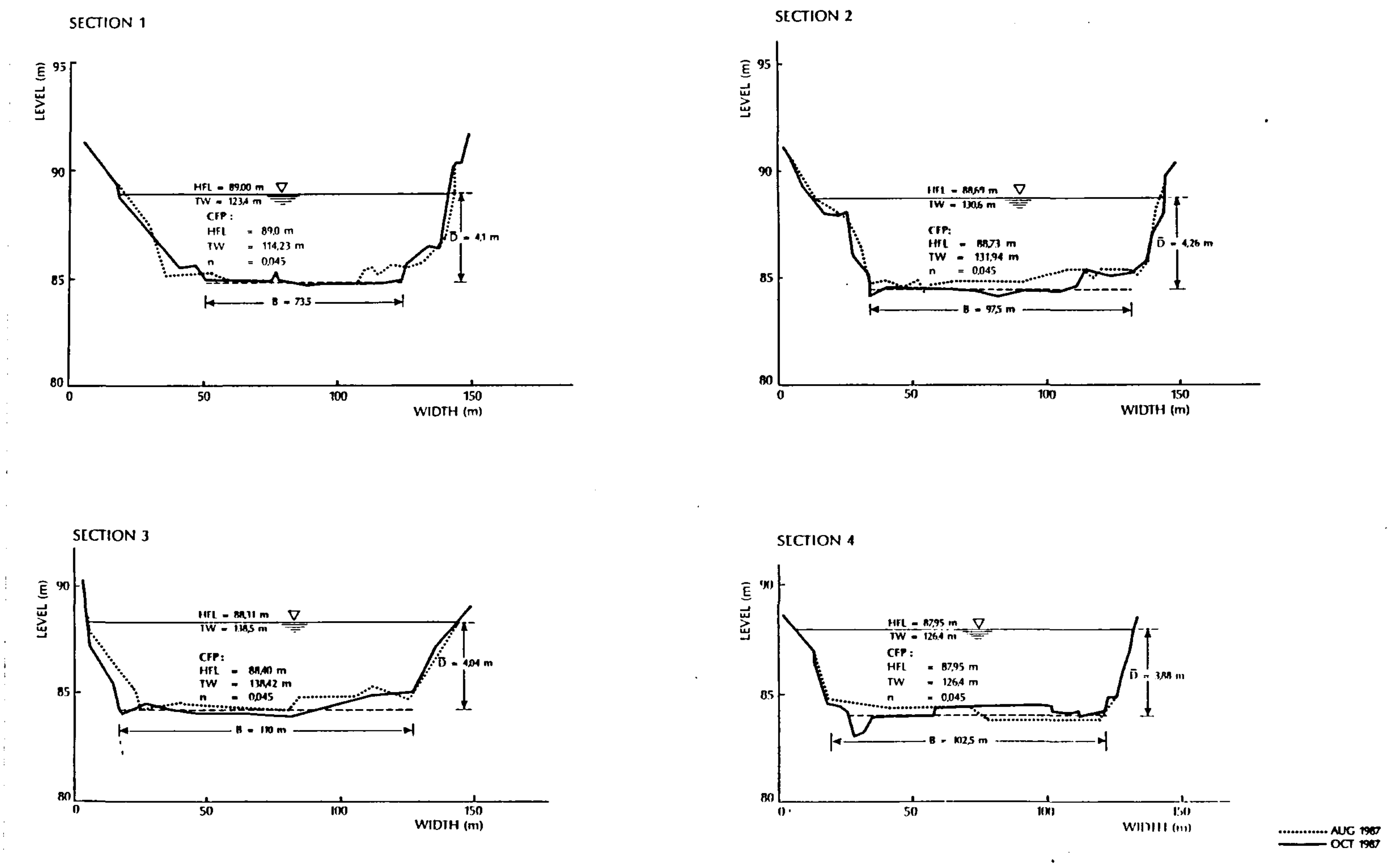

ALLUVIAL RIVER STUDY

Cross-sections : Site B – Mkuze River 1987 **A.6**

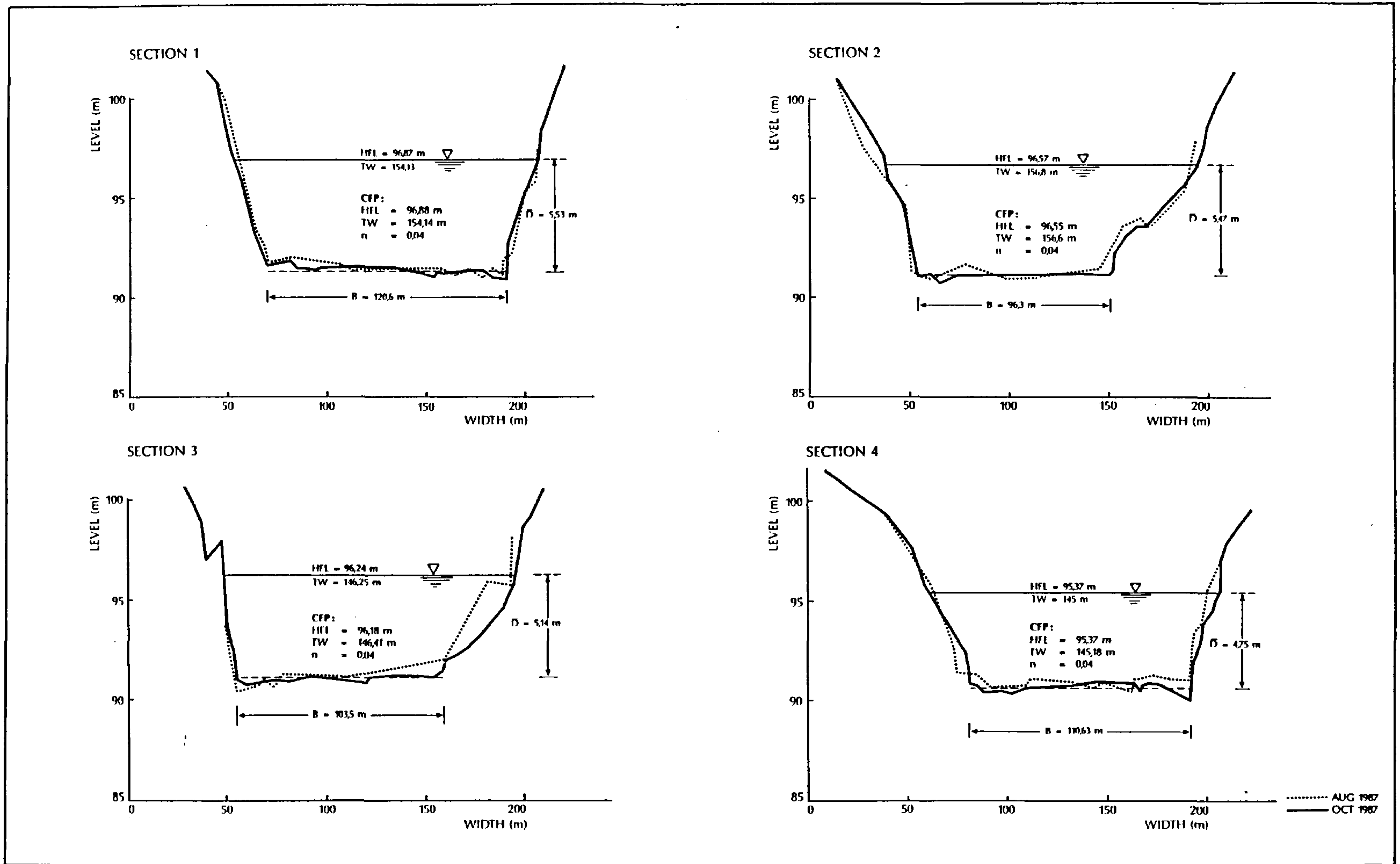

ALLUVIAL RIVER STUDY **Cross-sections : Site C – Black Mfolozi River 1987** **A.7**

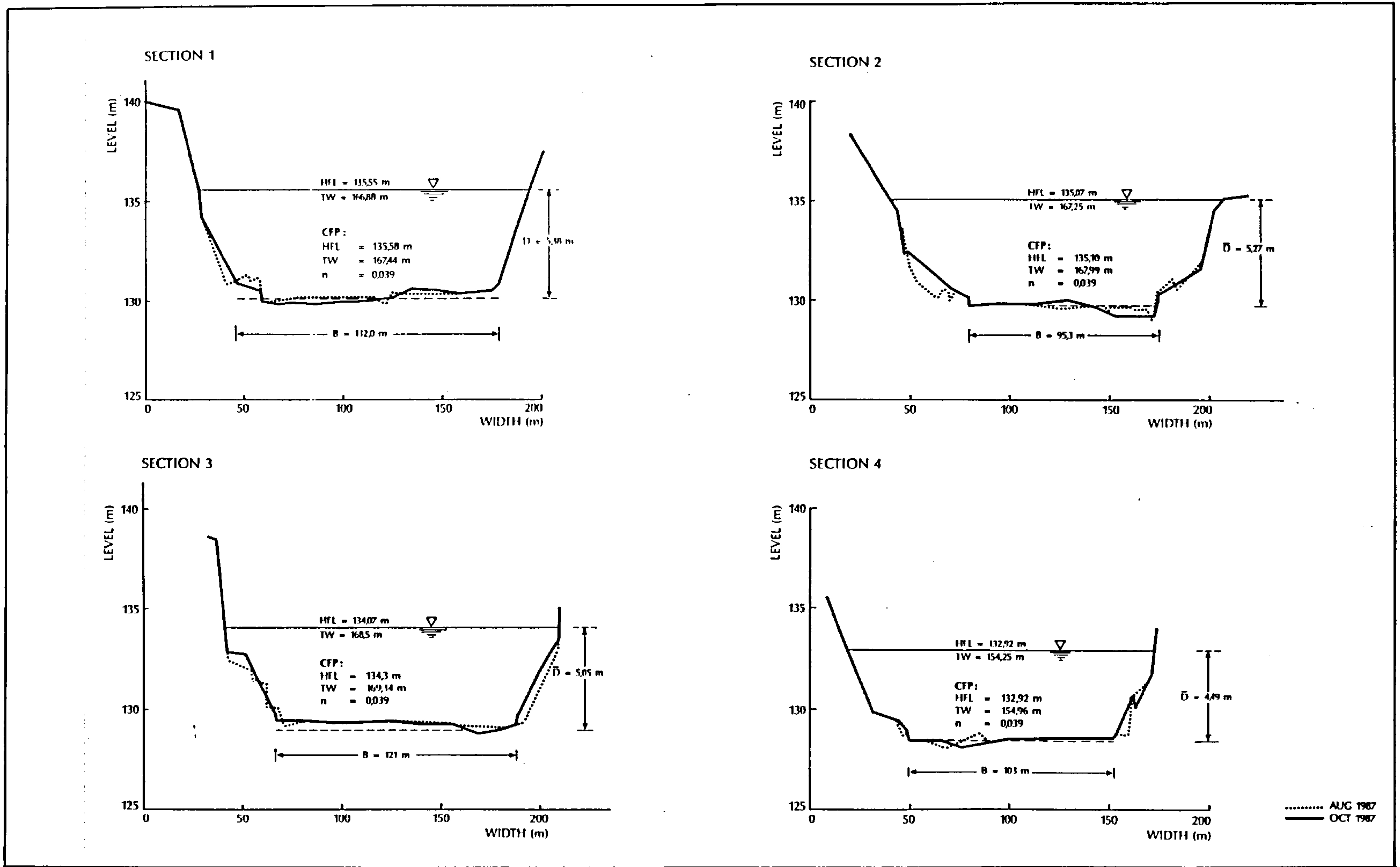

Cross-sections : Site D – White Mfolozi River 1987

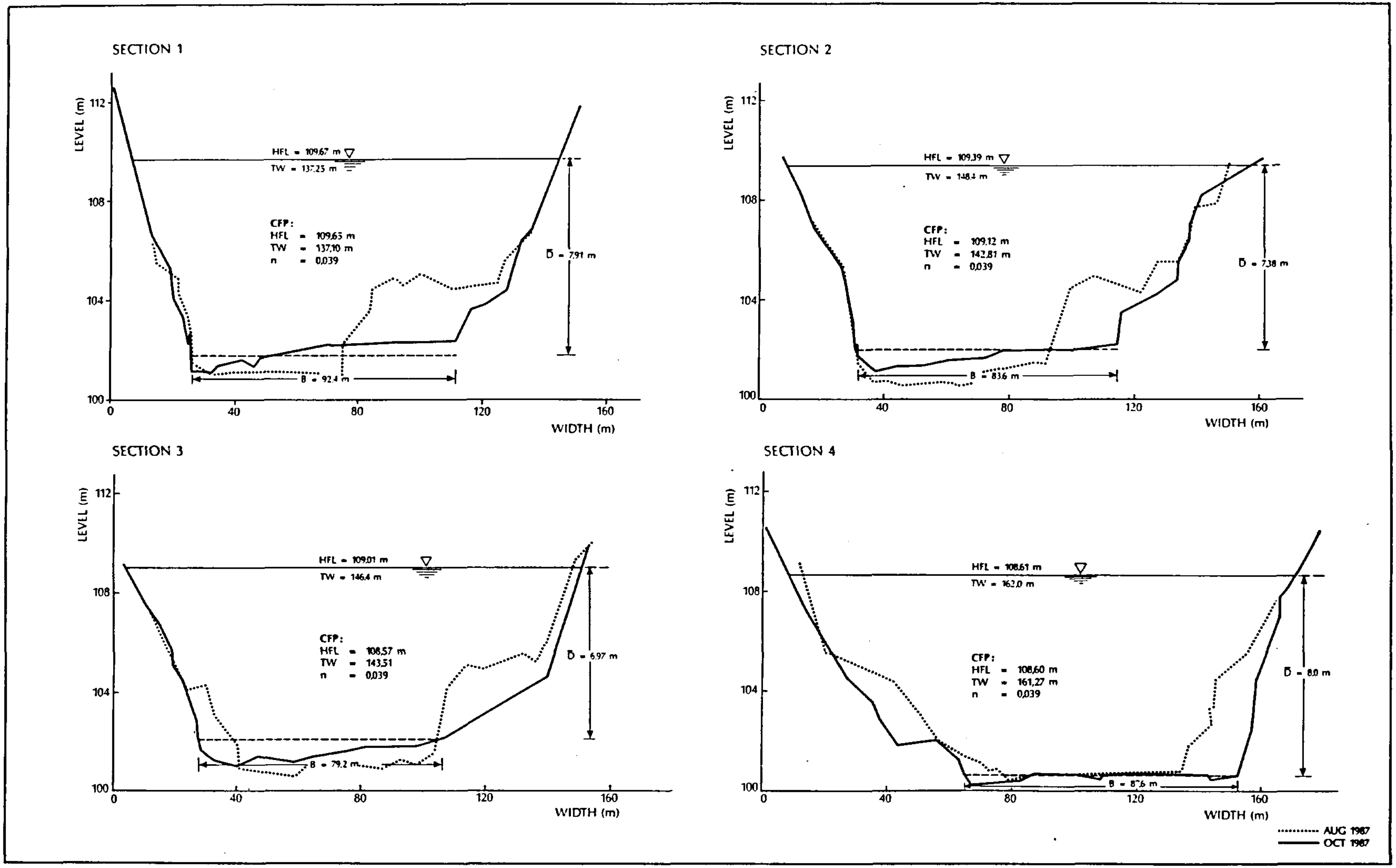

ALLUVIAL RIVER STUDY

Cross-sections : Site E – Mhlatuze River 1987 **A.9**

APPENDIX B

CROSS-SECTIONAL PROFILE DERIVATION

APPENDIX B

CROSS-SECTIONAL PROFILE DERIVATION

The mathematical derivation of the geometrical characteristics of both possible profile shapes as discussed in **Section 8.5** is presented below:

B.1 MATHEMATICAL DERIVATION

B.1.1 Case A: $\tau \propto y\cos\theta$

From **Equation 8.19** it follows

$$\frac{y}{D} = \sqrt{1+(\frac{dy}{dz})^2}$$

$$\therefore \frac{dy}{dz} = \sqrt{(\frac{y}{D})^2-1} \qquad \text{(B.1)}$$

or

$$D\int\frac{dy}{\sqrt{y^2-D^2}} = \int dz \qquad \text{(B.2)}$$

The solution of this differential equation is given by

$$D\cosh^{-1}\frac{y}{D} = D(\ell n(y+\sqrt{y^2-D^2})) = z+C_i \qquad \text{(B.3)}$$

With the boundary condition at $y = D$ and $z = 0$, the integration coefficient can be determined as

$$C_i = D\ \ell n\ D \qquad \text{(B.4)}$$

Substitution of **Equation B.4** in **Equation B.3** leads to

$$z = D\ell n\ (y+\sqrt{y^2-D^2})-D\ell nD$$

$$= D\ \cosh^{-1}\frac{y}{D}$$

Therefore, the solution of the differential equation can be given by (B.5)

$$z = D\cosh^{-1}\frac{y}{D} \tag{B.6}$$

and

$$y = D\cosh\frac{z}{D} \tag{B.7}$$

Equations B.6 and **B.7** represents a hyperbolic cosine curve of the type shown in **Figure B.1**. The cross-sectional characteristics of such a shape are:

<u>Maximum depth</u> $D : D$

<u>Top width</u> $B_s : B_s = 2z_{\max}$

with $z = z_{max}$ when $y = 2D$

$$\therefore \; z_{\max} = D\ell n(\frac{2D}{D} + \sqrt{(\frac{2D}{D})^2 - 1}) = 1{,}317D \tag{B.8}$$

$$\therefore \; B_s = 2{,}634 \; D \tag{B.9}$$

<u>Cross-sectional area</u> A_s:

Integration of the shaded part of **Figure B.1** leads to

$$A_s = 2(2Dz_{\max} - \int_o^{z_{\max}} y dz)$$

$$= 2(2{,}634D^2 - D\int_o^{z_{\max}} \cosh\frac{z}{D}\, dz)$$

$$= 2(2{,}634D^2 - D^2 \sinh\frac{z}{D}\Big|_0^{1{,}317D})$$

$$A_s = 1{,}804 \; D^2 \tag{B.10}$$

<u>Wetted Perimeter</u> P_s:

Integration of an element of the wetted perimeter according to **Figure B.1** leads to

$$P_s = 2\int_o^s ds = 2\int_o^{z_{\max}} \sqrt{(dz)^2 + (dy}$$

$$= 2\int_o^{z_{\max}} \sqrt{1 + (\frac{dy}{dz})^2}\, dz$$

From **Equation 8.19**

$$\frac{y}{D} = \sqrt{1+(\frac{dy}{dz})^2}$$

$$\therefore \quad P_s = 2\int_o^{z_{max}} \frac{y}{D} dz = \frac{2}{D}\int_0^{1,317D} y dz$$

$$= \frac{2}{D} D\int_0^{1,317D} \frac{z}{D}\ dz \qquad \text{(B.11)}$$

$$= 2D \sinh\frac{z}{D}\Big|_0^{1,317D}$$

$$\therefore \quad P = 3{,}464D$$

<u>**Hydraulic Radius**</u> R_s: $\quad R_s = \frac{A_s}{P_s} = 0{,}5208\ D$ (B.12)

B.1.2 <u>**Case B:** $\tau \propto \frac{y}{\cos\theta}$</u>

From **Equation 8.20** it follows

$$\frac{y}{D} = \frac{1}{\sqrt{1+(\frac{dy}{dz})^2}} \qquad \text{(B.13)}$$

$$\therefore \quad \frac{dy}{dz} = \sqrt{(\frac{y}{D})^2-1}$$

or (B.14)

$$D\int \frac{dy}{\sqrt{D^2 - y^2}} = \int dz$$

The solution of this differential equation is given by

$$z + C_i = -\sqrt{D^2 - y^2}$$

With the boundary condition at $y = D : z = 0$

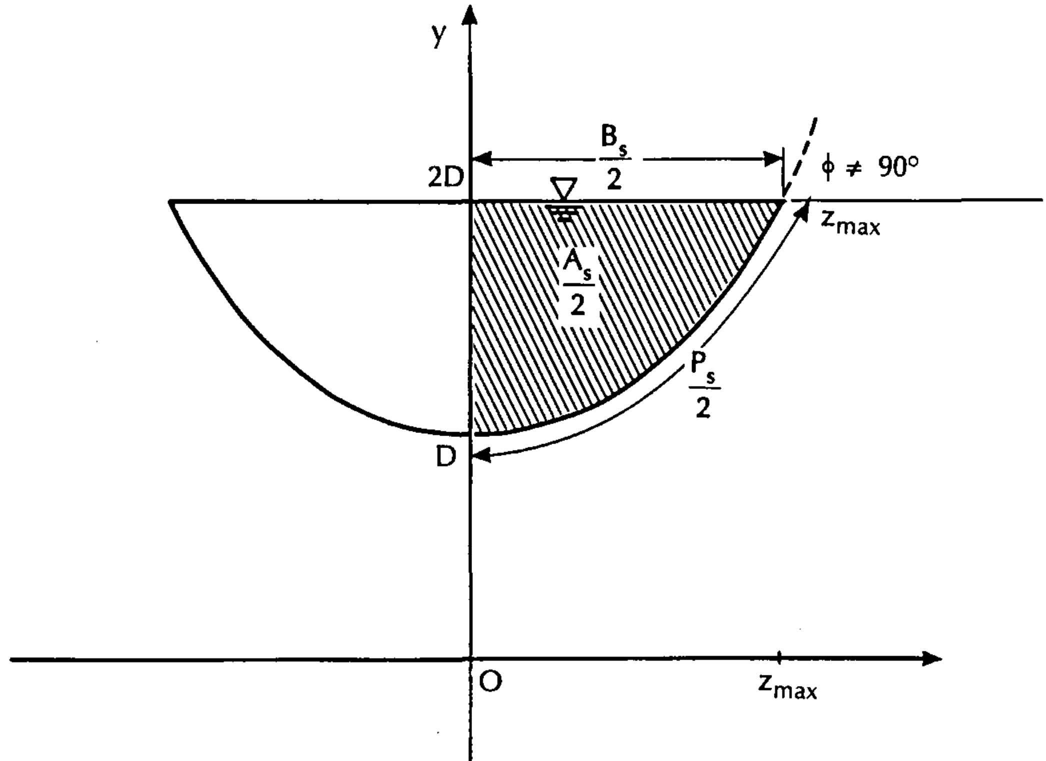

ϕ = *Angle between water surface and extension of profile*

ALLUVIAL RIVER STUDY — **Case A : Hyperbolic cosine profile** — **B.1**

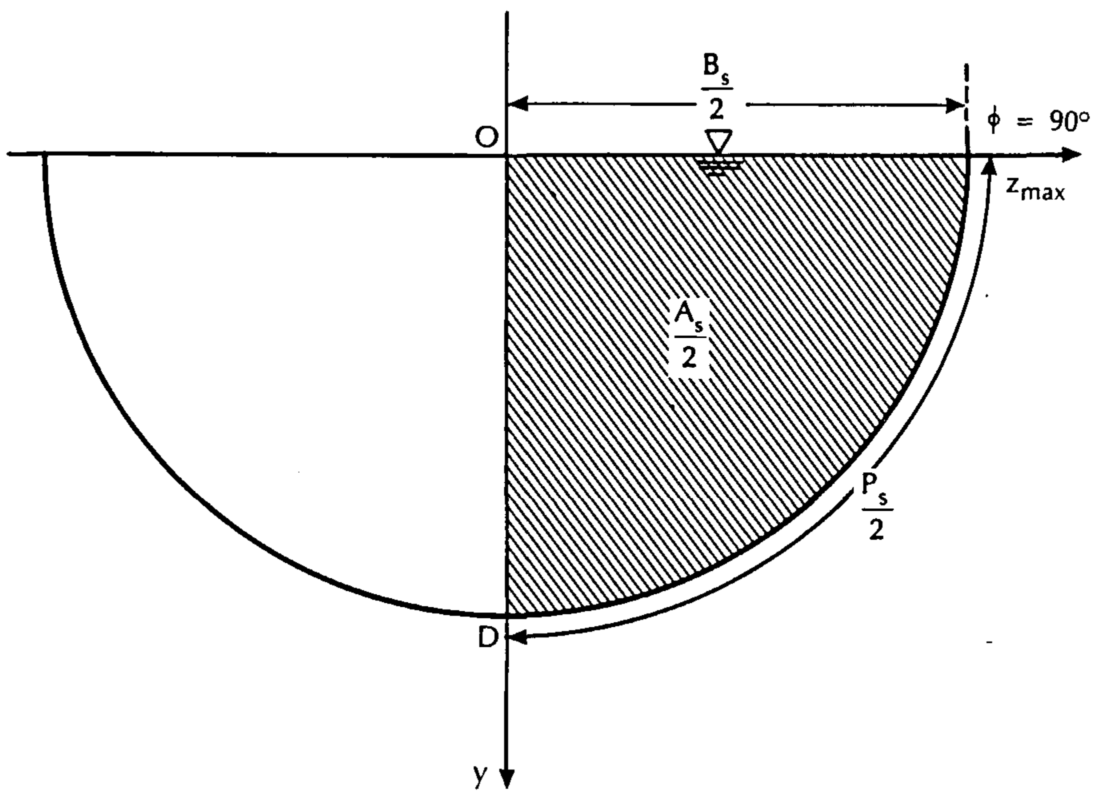

ϕ = *Angle between water surface and extension of profile*

ALLUVIAL RIVER STUDY — **Case B : Half circle profile** — **B.2**

Therefore, the integration coefficient

$$C_i = 0 \tag{B.15}$$

Thus, the solution of the differential equation can be given by

$$z = \pm\sqrt{D^2 - y^2} \tag{B.16}$$

and

$$y = (d^2 - z^2)^{1/2} \tag{B.17}$$

which defines a circle. In the case of a river cross-section, **Equation B.17** will describe a half circle with radius $r = D$ as shown in **Figure B.2**. The cross-sectional characteristics of such a shape are:

Maximum depth $D : D$

Top width $B_s : B_s = 2z_{\max}$

with $z = z_{\max}$ when $y = 0$. Thus

$$z_{\max} = D \tag{B.18}$$

and

$$B_s = 2D \tag{B.19}$$

Cross-section area A_s**:**

The cross-sectional area equals the area of a half circle:

$$A_s = \tfrac{1}{2}\pi r^2$$

with $r = D$. Therefore,

$$= \quad A_s = \tfrac{1}{2}\pi D^2 = 1{,}571\ D^2 \tag{B.20}$$

<u>Wetted Perimeter</u> P_s:

The wetted perimeter equals the circumference of a half circle:

$$P_s = \pi r = \pi D = 3{,}142\ D \qquad \text{(B.21)}$$

<u>Hydraulic Radius</u> R_s:

$$R_s = \frac{A}{p} = 0{,}5\ D \qquad \text{(B.22)}$$

B.2 CONCLUSION

The difference between the two solutions is obvious from **Figures B.1** and **B.2**, i.e. the angle ϕ between cross-sectional slope and water surface:

$$\phi_A \neq 90°$$
$$\phi_B = 90°$$

Although case B can be justified by factors like

i) water - and pore pressure during bank full flow conditions
ii) cohesion of bank material
iii) vegetation,

case A seems to be more applicable to the condition of flow in an alluvial channel.

APPENDIX C

REPRESENTATIVE ARMOURED PARTICLE SIZE

APPENDIX C
REPRESENTATIVE ARMOURED PARTICLE SIZE

Where flow takes place over movable material and the relatively large amount of unit power required to maintain motion along the bed becomes greater than that which would be required in the process of deformation of the bed, the stream should begin to transport the bed material rather than persist in its existing mode of flow. It can be argued that representative particle diameter of the bed material will change as the smaller particles will be removed first. It can be assumed that a stage will be reached, i.e. the critical condition, where the bed will be covered by particles of a size which can no longer be transported. This conditon can be described as the end of sediment motion for a certain flow and the beginning of sediment motion for a marginally larger flow. The particles on the bed are characterized as follows:

$$d \neq d_{50}$$

but

$$d = d_{\text{representative armoured size}}$$

Several suggestions for this representative armoured particle size exist in literature *[Henderson, 1961; Cruickshank and Maza, 1973; Simons and Richardson, 1966; Whiting and Dietrich, 1990]*. However, it was decided to test the behaviour of the research rivers accordingly.

It is assumed in terms of the arguments used in **Section 9.1** and the parameters of the modified Liu-diagram that the value of the $\frac{\sqrt{gDS}}{v_{ss}}$ function should be replaced by the corresponding value given by

$$\left(\frac{\sqrt{gDS}}{v_{ss}}\right)_{\textit{Liu-modified curve}} = \frac{\sqrt{gDS}}{v_{ss}} \left(\frac{d}{k_s}\right)^{\frac{1}{3}}_{\textit{turbulent}} \qquad \text{(C.1)}$$

with d the armoured or cirtical particle size as discussed in **Section 9.1**.

The following methodology has been applied in the determination of this representative (armoured) particle size:

i) determine the corresponding $\left(\frac{\sqrt{gDS}}{v_{ss}}\right)_c$ - value according to the modified Liu-diagram for the field conditions

ii) determine the parameter $\sqrt{gDS}$ and $\frac{\sqrt{gDS}}{k_s^{1/3}}$ according to observed field conditions

iii) with $\sqrt{gDS}$ and $\frac{\sqrt{gDS}}{k_s^{1/3}}$ known, determine the parameter $\frac{d^{1/3}}{v_{ss}}$ according to **Equation C.1**

iv) determine an equivalent particle size d_i which satisfy the $\frac{d^{1/3}}{v_{ss}}$ - value

v) compare d_i -values for different known particle sizes, i.e. d_{75}, d_{80}, d_{85} and d_{90} to the $\frac{d^{1/3}}{v_{ss}}$- value obtained from **Equation C.1**

vi) accept the nearest comparable $\frac{d^{1/3}}{v_{ss}}$ - value as the solution. These values are highlighted in **Table C.1**.

It follows from **Table C.1** that the particle size d_{85} is on the average the most suitable for the situation. Thus, it follows that

$$\left(\frac{\sqrt{gDS}}{v_{ss}}\right)_{Liu-critical} = \left(\frac{\sqrt{gDS}}{v_{ss_{85}}}\left(\frac{d_{85}}{k_s}\right)^{\frac{1}{3}}\right)_{river\ (turbulent)} \tag{C.2}$$

with the subscript 85 referring to the representative d_{85} particle size.

Table C.1: Determination of equivalent critical (armoured) particle diameter

Size	River	Year	Research rivers' properties (field conditions): Mean particle diameter d_{50} (mm)	Absolute roughness k_s (m)	Power relationship according to modified Liu-diagram $\left(\frac{\sqrt{gDS}}{v_{ss}}\right)_c^{1)}$	Parameters according to Equation C.1: $\sqrt{gDS}^{2)}$	$\frac{\sqrt{gDS}^{3)}}{k_s^{\frac{1}{3}}}$	$\frac{d^{1/3}\,{}^{4)}}{v_{ss}}$	Equivalent particle size: d_i (mm)	d_i (representative size)	Approximate Equivalent Solution[6]: d_{75} (mm)	$\frac{d_{75}^{\frac{1}{3}}}{v_{ss}}$	d_{80} (mm)	$\frac{d_{80}^{\frac{1}{3}}}{v_{ss}}$	d_{85} (mm)	$\frac{d_{85}^{\frac{1}{3}}}{v_{ss}}$	d_{90} (mm)	$\frac{d_{90}^{\frac{1}{3}}}{v_{ss}}$
A84	Komati	1984	1,33	1,13	0,153	0,286	0,275	0,556	3,25	d_{96}	2,02	0,638	2,14	0,627	2,33	0,611	2,8	0,58
B84	Mkuze	1984	0,243	1,5	0,47	0,404	0,353	1,331	0,361	d_{78}	0,3	1,513	0,372	1,311	0,429	1,191	0,483	1,108
B87	Mkuze	1987	0,43	1,28	0,28	0,283	0,26	1,076	0,52	d_{60}	0,714	0,923	0,81	0,873	0,88	0,85	0,97	0,82
C84	Black Mfolozi	1984	0,12	1,48	1,03	0,440	0,386	2,666	0,162	d_{78}	0,142	3,171	0,167	2,63	0,205	2,112	0,24	1,833
C87	Black Mfolozi	1987	0,425	0,89	0,285	0,288	0,3	0,951	0,67	d_{96}	0,483	1,108	0,5	1,075	0,53	1,054	0,555	1,03
D84	White Mfolozi	1984	0,38	1,16	0,31	0,348	0,332	0,935	0,7	d_{88}	0,454	1,15	0,562	1,021	0,605	0,98	0,735	0,914
D87	White Mfolozi	1987	0,61	0,8	0,22	0,315	0,339	0,649	1,91	d_{85}	1,05	0,796	1,415	0,717	1,91	0,649	2,72	0,624
E84	Mhlatuze	1984	0,2	1,11	0,57	0,466	0,450	1,265	0,392	d_{88}	0,31	1,488	0,337	1,396	0,368	1,306	0,4	1,248
E87	Mhlatuze	1987	0,27	0,87	0,43	0,443	0,464	0,924	0,72	d_{94}	0,36	1,333	0,41	1,221	0,471	1,127	0,574	1,0

1) corresponding $\frac{\sqrt{gDS}}{v_{ss}}$ - value according to modified Liu-diagram

2) determined according to observed field values of D and S

3) determined according to observed field values of D, S and k_s

4) determined according to Equation C-1 $\frac{d^{\frac{1}{3}}}{v_{ss}}$

5) corresponding d_i as determined from

6) evaluation of particle sizes on the basis of the value of the parameter $\frac{d^{\frac{1}{3}}}{v_{ss}}$

APPENDIX D

CHANNEL FLOW PROFILES PROGRAM (CFP)

APPENDIX D

CHANNEL FLOW PROFILES (CFP) *[ENGINEERING COMPUTING COMPANY]*

D.1 INTRODUCTION

CFP is a fully interactive program for the analysis of steady state flow profiles in open channels, rivers, spillways and flumes.

The program comprises a one-dimensional analysis for calculating the water surface profile taking into account the cross-sectional geometry as entered for sections along the channel, instead of only a unit width. Other main features include that the discharge along the channel may vary, hydraulic jump calculations can be specified to be based on momentum equations for a unit width of channel, or momentum equations for the true cross-sectional area, and the specification of transition losses for diverging or converging channel sections.

D.2 DEFINITIONS

The channel shape is approximated by a series of cross-sections with the assumption that property changes in between cross-sections are linear. The location of a cross-section is defined by a *stake value (SV)* which shall increase in value from upstream to downstream.

The geometry of each cross-section is approximated by a series of *points* connected by straight lines. Each point is defined by a *chainage* and a corresponding *level.* Points in cross-sections shall increase in chainage value from left to right when looking downstream.

The assumed straight line between two adjacent points is called the *bed-segment.* The roughness of a bed-segment is described by a *Manning's n* friction coefficient.

The *bed slope* between any two cross-sections is defined as the change in elevation between die lowest points in the two cross-sections.

The *calculation interval (dSV)* measured parallel to the channel defines at which stake values *subsections* and output should be generated. The number of subsections between two adjacent cross-sections depends on the integer quotient of the distance between the cross-sections and the calculation interval.

The *upstream depth* is defined to be the water surface depth at the cross-section with the lowest *SV*. Similarly the *downstream depth* is defined as the water surface depth at the cross- section with the highest *SV*.

D.3 THEORY

D.3.1 General

The dynamic equations of gradually varied flow in open channels are applicable. During the analysis the program performs the following tasks:

- (i) data checking
- (ii) processing the geometric data
- (iii) calculation of the critical depth profile
- (iv) determination of control points at and inbetween subsections
- (v) calculation of the subcritical profile starting from the downstream end and working upstream
- (vi) calculation of the supercritical profile starting from the upstream end and working downstream
- (vii) determination of the prevailing depth and hydraulic jumps
- (viii) confirmation of the existence of a control and correction of the prevailing depth and super critical depth where necessary.

Tasks (v) to (viii) are repeated until the number of controls remains constant.

D.3.2 **Geometric data processing**

The geometric data consisting of stake values, chainages, levels and *Manning's n* coefficients, is converted to a set of area, width, the product of (area* centroid) and conveyance values for 20 depths per cross-section. The conveyance is determined from the sum of the conveyances for each bed-segment or group of adjacent bed-segments for which the *Manning's n* is constant. The conveyance for a group of bed-segments is calculated from the area between the wetted perimeter of the bed segments, and the *Manning's n* coefficient applicable to all bed segments in the group.

D.3.3 **Critical depth profile**

The flow at each subsection equals critical depth when the function

$$F_2 = 1 - Q^2 \frac{B}{gA^3} = 0 \qquad \text{(D.1)}$$

After iterating to determine the critical depth the sub- and supercritical depths are set to 1,02 and 0,98 times the critical depth respectively.

D.3.4 **Control points**

Having calculated the critical depth profile, each subsection is checked to establish whether it serves as a potential control. The criterion applied is

$$F_1 = S_o - S_f + \left(\frac{Q^2}{gA^3}\right) \frac{dA}{dx} + \left(\frac{2Q}{gA^2}\right) \frac{dQ}{dx} = 0 \qquad \text{(D.2)}$$

(with S_o being the bed slope and S_f the friction slope)

is negative immediately upstream of the subsection and positive immediately downstream. For this case the sub- and supercritical depths are reset to 1,05 and 0,95 times the critical depth for the subsection.

Since the flow between two subsections may vary, a further check is made to test if a potential control exists between two successive subsections. Such a control occurs if F_1 is negatively immediately downstream of the upper subsection and positive immediately upstream of the lower subsection. For this case the subcritical depth is reset for the upper sub-section of 1,05 times the respective critical depth, whereas the supercritical depth is reset for the lower subsection to 0,95 of the respective critical depth. The exact location of the control is not calculated as it is assumed to be midway between the subsections.

Control at the upstream section is assumed to exist when the prevailing depth at that section is supercritical, i.e. either a flow depth equal to 0,95 times the respective critical depth as set by the program, or a depth as set by the user. Similarly, control at the downstream section is assumed to exist when the prevailing depth at that section is subcritical, i.e. either a depth of flow equal to 1,05 times the respective critical depth as set by the program, or a depth as set by the user.

D.3.5 Subcritical profile

Before calculating the subcritical profile the downstream depth is set to 1,05 times the critical depth or to the downstream depth entered, whichever is the greater.

Calculation of the subcritical depth at a subsection $(i - 1)$ immediately upstream of the current section section i is based on an iterative process. The iteration is terminated if one of the following conditions is encountered:

i) If the iterated depth is not within the range:

$$D_{c_{(i-1)}} < y_{(i-1)} < 1{,}2y_i \qquad \text{(D.3)}$$

with D_c being the critical depth and y the subcritical depth after repeatedly halving the calculation interval until it is equal to 1/64 th of its original value *(dSV)*.

ii) If for an adverse slope the iterated depth is not within the range:

$$D_{c_{(i-1)}} < y_{(i-1)} \tag{D.4}$$

after repeatedly halving the calculation interval until it is equal to 1/64 th of its original value *(dSV)*.

If the iteration is terminated for one of these conditions the subcritical depth is set to 1,02 times the respective critical depth.

If the above-mentioned conditions are passed, the iteration is ended once the present calculated depth is within 1 % of its previous value, or one the calculation interval has been repeatedly halved to 1/512 th of its original value *(dSV)*.

D.3.6 Supercritical profile

Before calculating the supercritical profile the upstream depth is set to 0,95 times the critical depth or to the upstream depth entered, whichever is the smaller.

Calculation of the supercritical depth at subsection $(i + 1)$ immediately downstream of the current section i is based on the same iterative process as for the subcritical depth. In this case the iteration is terminated when the following condition is not met:

$$0{,}20h < y_{(i+1)} < D_{c_{(i+1)}} \tag{D.5}$$

after repeatedly halving the calculation interval until it is equal to 1/64 th of its original value *(dSV)*.

If this condition is not met the supercritical depth is set to 0,98 times the respective critical depth.

D.3.7 Hydraulic jump and prevailing depth calculations

The prevailing depth is calculated for either the *AC* (area * centroid) option or the *UW* (unit width) option, as follows:

(i) *AC*-option: The momentum for the respective sub- or supercritical depth is calculated according to:

$$M = AC + \left(\frac{Q^2}{gA}\right) \tag{D.6}$$

(ii) *UW*-option: The momentum for the respective sub- or supercritical depth is calculated according to:

$$M = \frac{D^2}{2} + \frac{q^2}{(gD)} \tag{D.7}$$

with D being the depth

and

$$q = (g\ D_c^3)^{½} \tag{D.8}$$

with D_c being the critical depth

If the momentum for the subcritical depth is greater than that for the supercritical depth, the subcritical depth prevails. Similarly if the momentum for the supercritical depth is greater than that of the subcritical depth, the supercritical depth prevails. Where the sub- and supercritical depths are 1,02 and 0,98 times the critical depth respectively, the prevailing depth is taken as critical depth.

An hydraulic jump exists where the prevailing depth changes from supercritical to subcritical when working downstream. The exact location of the jump is not calculated but assumed to be midway between he two subsections at which these changes occur.

D.3.8 Comments

A velocity coefficient, to correct for a non-uniform velocity distribution due to friction or curvature, has not been incorporated in the algorithm of the program. The reasons for this are that the efforts caused in estimating suitable Mannings n coefficients as well as errors introduced by the nature of conveyance calculations outweigh the significance of such a factor.

APPENDIX E

COMPUTED HYDRAULIC DATA

CFP - DATA :

Run information :

No. of cross sections	:	4
Calculation interval dSV	:	20.000
Upstream depth	:	11.250
Downstream depth	:	11.250
Mult. factors - Discharge	:	1.000
- Manning's n	:	1.000
Run label	:	KOMATI 1984 (n = 0.041)
Hydraulic jump calcs	:	AC
Transition loss coef. applied	:	N
Conveyance Calculation type	:	2

Long Section Data :

Section No.	Stake Value [m]	Unit Flow [m^3/s]	Mann. n	Transition Loss Coef. Div. Conv. [-][-]	Section Title
1	110.000	2640.000	0.041	0.00 0.00	CROSS SECTION 1
2	513.000	2640.000	0.041	0.00 0.00	CROSS SECTION 2
3	740.000	2640.000	0.041	0.00 0.00	CROSS SECTION 3
4	1025.000	2640.000	0.041	0.00 0.00	CROSS SECTION 4

Cross Section Data :

Section No. : 1 S.V. = 110.000 Title : CROSS SECTION 1
No. of points : 17

Chainage : -2.000 0.000 5.000 22.500 36.300 45.000 46.000 89.000 90.000 92.500
106.300 117.500 131.300 145.000 162.500 170.500 176.000
Level : 99.000 98.740 98.210 94.390 91.670 88.070 87.010 87.280 88.080 89.330
90.340 92.620 95.580 97.280 98.270 98.670 99.000
Manning n: 0.041 0.041 0.041 0.041 0.041 0.041 0.041 0.041 0.041 0.041
0.041 0.041 0.041 0.041 0.041 0.041

Section No. : 2 S.V. = 513.000 Title : CROSS SECTION 2
No. of points : 17

Chainage : 0.000 7.500 32.500 51.250 57.500 61.300 62.500 90.000 91.300 98.800
105.000 136.300 140.000 146.300 155.000 160.000 162.000
Level : 98.600 97.670 94.500 90.330 90.040 87.730 85.680 86.910 87.710 87.930
88.220 87.960 89.860 91.760 96.440 98.100 98.600
Manning n: 0.041 0.041 0.041 0.041 0.041 0.041 0.041 0.041 0.041 0.041
0.041 0.041 0.041 0.041 0.041 0.041

Section No. : 3 S.V. = 740.000 Title : CROSS SECTION 3
No. of points : 16

Chainage : -2.000 0.000 17.500 28.800 32.500 33.500 89.000 90.000 97.500 103.800
113.800 123.800 140.000 150.000 153.000 157.000
Level : 98.400 98.000 92.030 89.400 87.660 86.360 87.050 87.650 89.580 90.130
90.930 92.510 97.370 97.720 98.000 98.400
Manning n: 0.041 0.041 0.041 0.041 0.041 0.041 0.041 0.041 0.041 0.041
0.041 0.041 0.041 0.041 0.041

Section No. : 4 S.V.= 1025.000 Title : CROSS SECTION 4
No. of points : 18

Chainage : 11.000 12.500 25.000 37.500 38.500 91.500 92.500 96.300 110.000 115.000
127.500 127.500 134.000 134.000 145.000 165.000 200.000 210.000
Level : 98.000 97.570 92.080 87.540 86.440 86.680 87.480 88.960 89.340 90.130
90.990 90.990 91.930 91.930 95.150 95.700 97.490 98.000
Manning n : 0.041 0.041 0.041 0.041 0.041 0.041 0.041 0.041 0.041 0.041
0.041 0.041 0.041 0.041 0.041 0.041 0.041

Final Profiles :

Point	Stake Value [m]	Bed Level [m]	Depth [m]	Surface level [m]	Surface Width [m]	Area [m^2]	Discharge [m^3/s]	Velo-city level [m/s]	Energy [m]	Froude No.
1	110.000	87.010	11.25	98.26	158.56	986.99	2640.00	2.67	98.63	0.34
						Section 1				
2	130.150	86.944	11.30	98.25	158.99	995.10	2640.00	2.65	98.61	0.34
3	150.300	86.877	11.36	98.23	159.37	1003.21	2640.00	2.63	98.59	0.33
4	170.450	86.811	11.41	98.22	159.73	1011.57	2640.00	2.61	98.56	0.33
5	190.600	86.744	11.46	98.20	160.09	1020.35	2640.00	2.59	98.54	0.33
6	210.750	86.678	11.51	98.19	160.38	1029.05	2640.00	2.57	98.53	0.32
7	230.900	86.611	11.57	98.18	160.59	1037.67	2640.00	2.54	98.51	0.32
8	251.050	86.545	11.62	98.16	160.72	1046.21	2640.00	2.52	98.49	0.32
9	271.200	86.478	11.67	98.15	160.78	1054.78	2640.00	2.50	98.47	0.31
10	291.350	86.411	11.73	98.14	160.76	1063.33	2640.00	2.48	98.45	0.31
11	311.500	86.345	11.78	98.13	160.66	1071.83	2640.00	2.46	98.43	0.30
12	331.650	86.279	11.84	98.11	160.48	1080.28	2640.00	2.44	98.42	0.30
13	351.800	86.212	11.89	98.10	160.22	1088.67	2640.00	2.42	98.40	0.30
14	371.950	86.146	11.95	98.09	159.87	1097.00	2640.00	2.41	98.39	0.29
15	392.100	86.079	12.00	98.08	159.45	1105.27	2640.00	2.39	98.37	0.29
16	412.250	86.013	12.06	98.07	158.94	1113.49	2640.00	2.37	98.36	0.29
17	432.400	85.946	12.11	98.06	158.34	1121.63	2640.00	2.35	98.34	0.28
18	452.550	85.880	12.17	98.05	157.66	1129.72	2640.00	2.34	98.33	0.28
19	472.700	85.813	12.23	98.04	156.89	1137.73	2640.00	2.32	98.31	0.28
20	492.850	85.746	12.28	98.03	156.05	1145.75	2640.00	2.30	98.30	0.27
21	513.000	85.680	12.34	98.02	155.15	1154.05	2640.00	2.29	98.29	0.27
						Section 2				
22	533.636	85.742	12.26	98.01	154.98	1149.88	2640.00	2.30	98.28	0.27
23	554.273	85.804	12.19	97.99	154.82	1146.15	2640.00	2.30	98.26	0.27
24	574.909	85.865	12.11	97.98	154.60	1142.33	2640.00	2.31	98.25	0.27
25	595.545	85.927	12.03	97.96	154.33	1138.45	2640.00	2.32	98.24	0.27
26	616.182	85.989	11.96	97.95	154.01	1134.49	2640.00	2.33	98.22	0.27
27	636.818	86.051	11.88	97.93	153.64	1130.46	2640.00	2.34	98.21	0.27
28	657.455	86.113	11.80	97.91	153.21	1126.35	2640.00	2.34	98.19	0.28
29	678.091	86.175	11.72	97.90	152.74	1122.18	2640.00	2.35	98.18	0.28
30	698.727	86.236	11.65	97.88	152.21	1117.93	2640.00	2.36	98.17	0.28
31	719.364	86.298	11.57	97.87	151.63	1113.64	2640.00	2.37	98.15	0.28
32	740.000	86.360	11.49	97.85	150.99	1109.20	2640.00	2.38	98.14	0.28
						Section 3				
33	760.357	86.366	11.47	97.84	154.07	1116.35	2640.00	2.36	98.12	0.28
34	780.714	86.371	11.46	97.83	157.12	1123.39	2640.00	2.35	98.11	0.28
35	801.071	86.377	11.44	97.82	160.15	1130.31	2640.00	2.34	98.10	0.28
36	821.429	86.383	11.42	97.81	163.09	1137.23	2640.00	2.32	98.08	0.28
37	841.786	86.389	11.41	97.80	166.00	1144.03	2640.00	2.31	98.07	0.28
38	862.143	86.394	11.39	97.79	168.90	1150.70	2640.00	2.29	98.05	0.28
39	882.500	86.400	11.37	97.77	171.80	1157.21	2640.00	2.28	98.04	0.28
40	902.857	86.406	11.36	97.76	174.70	1163.58	2640.00	2.27	98.02	0.28
41	923.214	86.411	11.34	97.75	177.59	1169.80	2640.00	2.26	98.01	0.28
42	943.571	86.417	11.32	97.74	180.47	1175.86	2640.00	2.25	98.00	0.28
43	963.929	86.423	11.30	97.73	183.35	1181.77	2640.00	2.23	97.98	0.28
44	984.286	86.429	11.29	97.71	186.22	1187.52	2640.00	2.22	97.97	0.28
45	1004.643	86.434	11.27	97.70	189.08	1193.11	2640.00	2.21	97.95	0.28
46	1025.000	86.440	11.25	97.69	191.94	1198.54	2640.00	2.20	97.94	0.28
						Section 4				

DESIGN INFO: Hydraulic Radii

Section: 1 S.V. = 110.000 Title: CROSS SECTION 1

Chainage		Points		Mann.	Perimeter	Hydraulic
From ...:	To .....:	From	To	n	[m]	Radius [m]
0.000	162.500	2	15	0.041	161.012	6.125

Section: 2 S.V. = 513.000 Title: CROSS SECTION 2

Chainage		Points		Mann.	Perimeter	Hydraulic
From ...:	To .....:	From	To	n	[m]	Radius [m]
0.000	160.000	1	16	0.041	160.049	7.209

Section: 3 S.V. = 740.000 Title: CROSS SECTION 3

Chainage		Points		Mann.	Perimeter	Hydraulic
From ...:	To .....:	From	To	n	[m]	Radius [m]
0.000	153.000	2	15	0.041	154.564	7.175

Section: 4 S.V. = 1025.000 Title: CROSS SECTION 4

Chainage		Points		Mann.	Perimeter	Hydraulic
From ...:	To .....:	From	To	n	[m]	Radius [m]
11.000	210.000	1	18	0.041	195.539	6.125

Project: ALLUVIAL RIVER STUDY
Subject: MKUZE RIVER : 1984

CFP - DATA :

Run information :

No. of cross sections	:	3
Calculation interval dSV	:	20.000
Upstream depth	:	11.820
Downstream depth	:	11.560
Mult. factors - Discharge	:	1.000
- Manning's n	:	1.000
Run label	:	MKUZE 1984 POST (n = 0.044)
Hydraulic jump calcs	:	AC
Transition loss coef. applied	:	N
Conveyance Calculation type	:	2

Long Section Data :

Section No.	Stake Value [m]	Unit Flow [m^3/s]	Deflt Mann. n	Transition Loss Coef. Div. Conv. [-][-]	Section Title
1	500.000	5600.000	0.044	0.00 0.00	CROSS SECTION 2
2	801.000	5600.000	0.044	0.00 0.00	CROSS SECTION 3
3	1002.000	5600.000	0.044	0.00 0.00	CROSS SECTION 4

Cross Section Data :

Section No. : 1 S.V.= 500.000 Title : CROSS SECTION 2
No. of points : 29

Chainage : -14.500 0.000 51.000 56.100 81.500 82.300 87.700 98.100 103.900 112.300
113.400 120.700 135.600 178.200 183.700 191.500 205.100 216.900 224.200 226.200
227.500 234.000 236.900 245.300 256.100 259.600 265.600 271.700 275.000
Level : 97.000 96.280 93.980 93.750 92.140 92.090 92.270 89.080 87.790 86.250
84.760 84.360 84.710 84.520 84.260 84.360 84.640 84.590 84.740 85.390
86.350 88.640 89.400 90.540 93.020 94.390 95.915 96.870 97.470
Manning n: 0.044 0.044 0.044 0.044 0.044 0.044 0.044 0.044 0.044 0.044
0.044 0.044 0.044 0.044 0.044 0.044 0.044 0.044 0.044 0.044
0.044 0.044 0.044 0.044 0.044 0.044 0.044 0.044

Section No. : 2 S.V.= 801.000 Title : CROSS SECTION 3
No. of points : 24

Chainage : -22.930 0.000 49.000 67.700 78.200 80.400 87.900 105.600 119.700 121.900
130.400 154.600 187.200 202.200 203.700 206.200 211.700 213.800 232.000 238.300
256.100 273.600 280.900 283.000
Level : 96.600 95.700 93.700 92.940 91.520 90.700 87.370 84.370 84.240 83.990
84.080 84.280 83.940 83.940 84.350 85.920 88.170 88.340 89.430 90.080
93.060 94.270 96.010 96.600
Manning n: 0.044 0.044 0.044 0.044 0.044 0.044 0.044 0.044 0.044 0.044
0.044 0.044 0.044 0.044 0.044 0.044 0.044 0.044 0.044 0.044
0.044 0.044 0.044

Section No. : 3 S.V.= 1002.000 Title : CROSS SECTION 4

Project: ALLUVIAL RIVER STUDY
Subject: MKUZE RIVER : 1984

CFP - DATA :

Run information :

No. of cross sections	:	3
Calculation interval dSV	:	20.000
Upstream depth	:	11.820
Downstream depth	:	11.560
Mult. factors - Discharge	:	1.000
- Manning's n	:	1.000
Run label	:	MKUZE 1984 POST (n = 0.044)
Hydraulic jump calcs	:	AC
Transition loss coef. applied	:	N
Conveyance Calculation type	:	2

Long Section Data :

Section No.	Stake Value [m]	Unit Flow [m³/s]	Deflt Mann. n	Transition Loss Coef. Div. Conv. [-][-]	Section Title
1	500.000	5600.000	0.044	0.00 0.00	CROSS SECTION 2
2	801.000	5600.000	0.044	0.00 0.00	CROSS SECTION 3
3	1002.000	5600.000	0.044	0.00 0.00	CROSS SECTION 4

Cross Section Data :

Section No. : 1 S.V. = 500.000 Title : CROSS SECTION 2
No. of points : 29

Chainage : -14.500 0.000 51.000 56.100 81.500 82.300 87.700 98.100 103.900 112.300
113.400 120.700 135.600 178.200 183.700 191.500 205.100 216.900 224.200 226.200
227.500 234.000 236.900 245.300 256.100 259.600 265.600 271.700 275.000
Level : 97.000 96.280 93.980 93.750 92.140 92.090 92.270 89.080 87.790 86.250
84.760 84.360 84.710 84.520 84.260 84.360 84.640 84.590 84.740 85.390
86.350 88.640 89.400 90.540 93.020 94.390 95.915 96.870 97.470
Manning n: 0.044 0.044 0.044 0.044 0.044 0.044 0.044 0.044 0.044 0.044
0.044 0.044 0.044 0.044 0.044 0.044 0.044 0.044 0.044 0.044
0.044 0.044 0.044 0.044 0.044 0.044 0.044 0.044

Section No. : 2 S.V. = 801.000 Title : CROSS SECTION 3
No. of points : 24

Chainage : -22.930 0.000 49.000 67.700 78.200 80.400 87.900 105.600 119.700 121.900
130.400 154.600 187.200 202.200 203.700 206.200 211.700 213.800 232.000 238.300
256.100 273.600 280.900 283.000
Level : 96.600 95.700 93.700 92.940 91.520 90.700 87.370 84.370 84.240 83.990
84.080 84.280 83.940 83.940 84.350 85.920 88.170 88.340 89.430 90.080
93.060 94.270 96.010 96.600
Manning n: 0.044 0.044 0.044 0.044 0.044 0.044 0.044 0.044 0.044 0.044
0.044 0.044 0.044 0.044 0.044 0.044 0.044 0.044 0.044 0.044
0.044 0.044 0.044

Section No. : 3 S.V. = 1002.000 Title : CROSS SECTION 4

No. of points : 24

Chainage : -9.230 0.000 27.000 46.800 57.500 65.000 70.400 74.800 77.600 82.900
121.300 145.800 167.700 177.400 178.800 187.200 193.700 204.200 205.900 217.800
221.800 251.900 273.600 280.770

Level : 96.000 95.500 94.010 92.920 91.950 89.660 87.330 85.480 83.980 83.910
83.790 83.690 83.820 84.010 85.500 87.300 88.120 90.500 90.700 92.520
91.830 93.910 95.410 96.000

Manning n: 0.044 0.044 0.044 0.044 0.044 0.044 0.044 0.044 0.044 0.044
0.044 0.044 0.044 0.044 0.044 0.044 0.044 0.044 0.044 0.044
0.044 0.044 0.044

Final Profiles :

Point	Stake Value [m]	Bed Level [m]	Depth [m]	Surface level [m]	Surface Width [m]	Area [m²]	Discharge [m³/s]	Velo-city level [m/s]	Energy [m]	Froude No.
1	500.000	84.260	11.81	96.07	261.95	1850.12	5600.00	3.03	96.53	0.36
						Section	1			
2	520.067	84.239	11.80	96.04	263.08	1850.65	5600.00	3.03	96.51	0.36
3	540.133	84.217	11.80	96.01	264.21	1851.13	5600.00	3.03	96.48	0.36
4	560.200	84.196	11.79	95.99	265.33	1851.57	5600.00	3.02	96.45	0.37
5	580.267	84.175	11.78	95.96	266.45	1851.95	5600.00	3.02	96.43	0.37
6	600.333	84.153	11.78	95.93	267.56	1852.27	5600.00	3.02	96.40	0.37
7	620.400	84.132	11.77	95.90	268.67	1852.55	5600.00	3.02	96.37	0.37
8	640.467	84.111	11.77	95.88	269.77	1852.76	5600.00	3.02	96.34	0.37
9	660.533	84.089	11.76	95.85	270.86	1852.92	5600.00	3.02	96.32	0.37
10	680.600	84.068	11.75	95.82	271.95	1853.02	5600.00	3.02	96.29	0.37
11	700.667	84.047	11.75	95.79	273.04	1853.06	5600.00	3.02	96.26	0.37
12	720.733	84.025	11.74	95.77	274.11	1853.04	5600.00	3.02	96.23	0.37
13	740.800	84.004	11.73	95.74	275.18	1852.96	5600.00	3.02	96.20	0.37
14	760.867	83.983	11.73	95.71	276.25	1852.81	5600.00	3.02	96.18	0.37
15	780.933	83.961	11.72	95.68	277.30	1852.59	5600.00	3.02	96.15	0.37
16	801.000	83.940	11.71	95.65	278.35	1852.30	5600.00	3.02	96.12	0.37
						Section	2			
17	821.100	83.915	11.70	95.62	277.37	1838.90	5600.00	3.05	96.09	0.38
18	841.200	83.890	11.69	95.58	276.35	1825.27	5600.00	3.07	96.06	0.38
19	861.300	83.865	11.68	95.54	275.30	1811.46	5600.00	3.09	96.03	0.38
20	881.400	83.840	11.66	95.50	274.21	1797.44	5600.00	3.12	96.00	0.39
21	901.500	83.815	11.65	95.46	273.08	1783.21	5600.00	3.14	95.97	0.39
22	921.600	83.790	11.63	95.42	271.91	1768.76	5600.00	3.17	95.93	0.40
23	941.700	83.765	11.62	95.38	270.69	1754.08	5600.00	3.19	95.90	0.40
24	961.800	83.740	11.60	95.34	269.43	1739.15	5600.00	3.22	95.87	0.40
25	981.900	83.715	11.58	95.30	268.12	1723.98	5600.00	3.25	95.83	0.41
26	1002.000	83.690	11.56	95.25	266.76	1708.55	5600.00	3.28	95.80	0.41
						Section	3			
							CONTROL			

DESIGN INFO : Hydraulic Radii

Section : 1 S.V.= 500.000 Title : CROSS SECTION 2

Chainage From ...:	To .....:	Points From	To	Mann. n	Perimeter [m]	Hydraulic Radius [m]
0.000	271.700	2	28	0.044	265.193	6.971

Section : 2 S.V. = 801.000 Title : CROSS SECTION 3

Chainage		Points		Mann.	Perimeter	Hydraulic
From ...:	To .....:	From	To	n	[m]	Radius [m]
0.000	280.900	2	23	0.044	280.972	6.587

Section : 3 S.V. = 1002.000 Title : CROSS SECTION 4

Chainage		Points		Mann.	Perimeter	Hydraulic
From ...:	To .....:	From	To	n	[m]	Radius [m]
0.000	273.600	2	23	0.044	269.919	6.326

MKUZE84

CFP - DATA :

Run information :

No. of cross sections	..... :	4
Calculation interval dSV	..... :	20.000
Upstream Depth	..... :	15.680
Downstream depth	..... :	16.760
Mult. factors - Discharge	..... :	1.000
- Manning's n	..... :	1.000
Run label	:	BLACK MFOLOZI 1984 (n = 0.044)
Hydraulic jump calcs	..... :	AC
Transition loss coef. applied	..... :	N
Conveyance Calculation type	..... :	2

Long Section Data :

Section No.	Stake Value [m]	Unit Flow [m³/s]	Deflt Mann. n	Transition Loss Coef. Div. Conv. [-][-]		Section Title
1	3483.000	10000.000	0.044	0.00	0.00	CROSS SECTION 1
2	3665.000	10000.000	0.044	0.00	0.00	CROSS SECTION 2
3	3869.000	10000.000	0.044	0.00	0.00	CROSS SECTION 3
4	4160.000	10000.000	0.044	0.00	0.00	CROSS SECTION 4

Cross Section Data :

Section No. : 1 S.V. = 3483.000 Title : CROSS SECTION 1
No. of points : 26

Chainage : 8.200 73.500 135.500 137.500 152.200 154.000 156.600 165.100 175.400 185.200
195.700 204.800 215.200 225.000 234.900 245.200 255.500 265.300 274.800 279.000
289.600 302.700 340.000 351.200 582.100 582.100
Level : 107.540 103.970 100.220 98.070 93.090 91.590 91.030 90.990 91.210 91.370
91.350 91.260 91.270 91.180 91.300 91.310 91.360 91.780 91.630 92.620
97.170 100.540 104.110 103.520 105.580 108.000
Manning n: 0.044 0.044 0.044 0.044 0.044 0.044 0.044 0.044 0.044 0.044
0.044 0.044 0.044 0.044 0.044 0.044 0.044 0.044 0.044 0.044
0.044 0.044 0.044 0.044 0.044

Section No. : 2 S.V. = 3665.000 Title : CROSS SECTION 2
No. of points : 30

Chainage : -10.000 7.200 58.200 79.300 104.700 107.000 121.200 122.300 128.100 134.000
140.200 145.700 152.100 158.200 164.100 170.100 175.900 182.000 187.900 194.200
200.200 219.100 245.500 268.100 273.800 293.500 316.100 323.800 548.300 548.300

Level : 108.000 106.960 103.360 102.320 98.950 98.970 92.040 91.430 91.080 91.130
90.930 90.820 90.730 90.550 89.530 90.030 91.220 91.200 91.040 91.140
91.430 92.410 94.730 97.620 99.760 103.040 103.910 102.800 104.880 107.500

Manning n: 0.044 0.044 0.044 0.044 0.044 0.044 0.044 0.044 0.044 0.044
0.044 0.044 0.044 0.044 0.044 0.044 0.044 0.044 0.044 0.044
0.044 0.044 0.044 0.044 0.044 0.044 0.044 0.044 0.044

Section No. : 3 S.V. = 3869.000 Title : CROSS SECTION 3
No. of points : 31

Chainage : -10.000 7.000 68.200 88.000 97.900 103.200 115.700 117.100 119.600 125.700
131.900 137.600 143.400 149.800 155.800 161.600 167.800 173.100 179.300 185.600
191.800 197.900 203.500 209.100 220.000 254.200 259.700 262.900 314.100 562.400
562.400
Level : 107.200 106.200 102.390 101.920 99.300 96.840 92.000 91.030 90.050 90.180
90.420 90.510 90.540 90.620 90.680 90.740 90.800 90.860 90.800 90.890
90.890 90.950 90.920 91.200 91.250 95.810 98.720 102.170 101.940 103.960
107.200
Manning n: 0.044 0.044 0.044 0.044 0.044 0.044 0.044 0.044 0.044 0.044
0.044 0.044 0.044 0.044 0.044 0.044 0.044 0.044 0.044 0.044
0.044 0.044 0.044 0.044 0.044 0.044 0.044 0.044 0.044 0.044

Section No. : 4 S.V. = 4160.000 Title : CROSS SECTION 4
No. of points : 24

Chainage : -5.000 8.100 16.200 74.000 88.400 100.000 101.700 111.600 116.100 144.800
158.200 176.800 198.500 207.800 217.800 219.000 225.000 230.200 233.900 235.400
243.000 261.000 569.870 569.870
Level : 107.200 104.910 103.410 99.770 97.340 94.260 94.440 92.730 90.990 90.660
90.870 90.650 89.470 89.140 90.850 91.590 90.950 94.660 93.380 95.380
98.190 100.840 103.830 107.200
Manning n: 0.044 0.044 0.044 0.044 0.044 0.044 0.044 0.044 0.044 0.044
0.044 0.044 0.044 0.044 0.044 0.044 0.044 0.044 0.044 0.044
0.044 0.044 0.044

Final Profiles :

Point	Stake Value [m]	Bed Level [m]	Depth [m]	Surface level [m]	Surface Width [m]	Area [m^2]	Discharge [m^3/s]	Velo-city level [m/s]	Energy [m]	Froude No.
1	3483.000	90.990	15.73	106.72	558.82	3406.75	10000.00	2.94	107.15	0.38
						Section 1				
2	3503.222	90.828	15.86	106.68	556.18	3406.13	10000.00	2.94	107.12	0.38
3	3523.444	90.666	15.99	106.65	553.70	3404.02	10000.00	2.94	107.09	0.38
4	3543.667	90.503	16.12	106.62	551.36	3400.37	10000.00	2.94	107.06	0.38
5	3563.889	90.341	16.25	106.59	548.84	3395.59	10000.00	2.94	107.03	0.38
6	3584.111	90.179	16.38	106.56	546.04	3389.85	10000.00	2.95	107.00	0.38
7	3604.333	90.017	16.51	106.53	543.11	3382.91	10000.00	2.96	106.97	0.38
8	3624.556	89.854	16.64	106.50	540.06	3374.74	10000.00	2.96	106.94	0.38
9	3644.778	89.692	16.77	106.46	536.89	3365.30	10000.00	2.97	106.91	0.38
10	3665.000	89.530	16.90	106.43	533.59	3354.57	10000.00	2.98	106.88	0.38
						Section 2				
11	3685.400	89.582	16.82	106.41	535.95	3378.17	10000.00	2.96	106.85	0.38
12	3705.800	89.634	16.75	106.38	538.27	3401.42	10000.00	2.94	106.82	0.37
13	3726.200	89.686	16.67	106.36	540.55	3424.32	10000.00	2.92	106.79	0.37
14	3746.600	89.738	16.60	106.34	542.79	3446.83	10000.00	2.90	106.76	0.37
15	3767.000	89.790	16.52	106.31	545.00	3468.97	10000.00	2.88	106.74	0.36
16	3787.400	89.842	16.45	106.29	547.16	3490.70	10000.00	2.86	106.71	0.36
17	3807.800	89.894	16.37	106.27	549.29	3512.02	10000.00	2.85	106.68	0.36
18	3828.200	89.946	16.30	106.25	551.38	3532.92	10000.00	2.83	106.65	0.36
19	3848.600	89.998	16.23	106.22	553.48	3554.25	10000.00	2.81	106.63	0.35
20	3869.000	90.050	16.15	106.20	555.55	3575.50	10000.00	2.80	106.60	0.35
						Section 3				
21	3889.786	89.985	16.19	106.18	556.79	3589.10	10000.00	2.79	106.57	0.35
22	3910.572	89.920	16.24	106.16	557.98	3602.74	10000.00	2.78	106.55	0.35
23	3931.357	89.855	16.28	106.13	559.10	3616.70	10000.00	2.76	106.52	0.35
24	3952.143	89.790	16.32	106.11	560.18	3631.23	10000.00	2.75	106.50	0.35
25	3972.928	89.725	16.36	106.09	561.21	3646.10	10000.00	2.74	106.47	0.34
26	3993.714	89.660	16.41	106.07	562.17	3661.17	10000.00	2.73	106.45	0.34
27	4014.500	89.595	16.45	106.04	563.07	3676.42	10000.00	2.72	106.42	0.34
28	4035.286	89.530	16.49	106.02	563.89	3691.86	10000.00	2.71	106.40	0.34

29	4056.072	89.465	16.54	106.00	564.66	3707.49	10000.00	2.70	106.37	0.34
30	4076.857	89.400	16.58	105.98	565.35	3723.31	10000.00	2.69	106.35	0.33
31	4097.643	89.335	16.62	105.96	565.98	3739.32	10000.00	2.67	106.32	0.33
32	4118.429	89.270	16.67	105.94	566.53	3755.52	10000.00	2.66	106.30	0.33
33	4139.214	89.205	16.71	105.92	567.02	3771.91	10000.00	2.65	106.28	0.33
34	4160.000	89.140	16.76	105.90	567.43	3788.48	10000.00	2.64	106.26	0.33
							Section 4			

DESIGN INFO : Hydraulic Radii

Section : 1 S.V. = 3483.000 Title : CROSS SECTION 1

Chainage From ...:	To .....:	Points From	To	Mann. n	Perimeter [m]	Hydraulic Radius [m]
8.200	582.100	1	26	0.044	564.186	6.038

Section : 2 S.V. = 3665.000 Title : CROSS SECTION 2

Chainage From ...:	To .....:	Points From	To	Mann. n	Perimeter [m]	Hydraulic Radius [m]
7.200	548.300	2	30	0.044	538.590	6.227

Section : 3 S.V. = 3869.000 Title : CROSS SECTION 3

Chainage From ...:	To .....:	Points From	To	Mann. n	Perimeter [m]	Hydraulic Radius [m]
-10.000	562.400	1	31	0.044	562.641	6.353

Section : 4 S.V. = 4160.000 Title : CROSS SECTION 4

Chainage From ...:	To .....:	Points From	To	Mann. n	Perimeter [m]	Hydraulic Radius [m]
-5.000	569.870	1	24	0.044	574.474	6.594

Project: ALLUVIAL RIVER STUDY
Subject: WHITE MFOLOZI RIVER : 1984

CFP - DATA :

Run information :

No. of cross sections	:	4
Calculation interval dSV	:	20.000
Upstream Depth	:	12.580
Downstream depth	:	12.590
Mult. factors - Discharge	:	1.000
- Manning's n	:	1.000
Run label	:	WHITE MFOLOZI (n = 0.041)
Hydraulic jump calcs	:	AC
Transition loss coef. applied	:	N
Conveyance Calculation type	:	2

Long Section Data :

Section No.	Stake Value [m]	Unit Flow [m^3/s]	Defit Mann. n	Transition Loss Coef. Div. Conv. [-][-]		Section Title
1	134.000	6500.000	0.041	0.00	0.00	CROSS SECTION 1
2	510.000	6500.000	0.041	0.00	0.00	CROSS SECTION 2
3	923.000	6500.000	0.041	0.00	0.00	CROSS SECTION 3
4	1413.000	6500.000	0.041	0.00	0.00	CROSS SECTION 4

Cross Section Data :

Section No. : 1 S.V. = 134.000 Title : CROSS SECTION 1
No. of points : 24

Chainage : 75.000 77.000 78.000 89.000 110.500 119.000 128.000 134.000 141.000 152.000
155.000 163.000 180.500 196.500 201.000 233.500 267.000 278.000 283.000 300.000
310.000 325.000 330.000 332.222
Level : 143.100 142.700 142.590 140.160 139.570 139.550 138.700 137.450 132.980 131.830
130.020 129.500 129.710 129.490 129.950 130.210 129.900 129.990 130.350 138.110
139.910 142.020 142.700 143.000
Manning n: 0.041 0.041 0.041 0.041 0.041 0.041 0.041 0.041 0.041 0.041
0.041 0.041 0.041 0.041 0.041 0.041 0.041 0.041 0.041 0.041
0.041 0.041 0.041

Section No. : 2 S.V. = 510.000 Title : CROSS SECTION 2
No. of points : 23

Chainage : 3.106 18.000 88.000 125.000 127.000 129.500 143.000 159.000 163.000 173.000
184.000 203.000 225.000 263.500 270.000 275.000 281.000 295.000 305.000 324.500
351.000 398.000 432.000
Level : 142.600 141.920 139.660 138.420 138.160 137.120 134.590 129.850 131.100 129.380
129.550 129.430 129.820 129.140 127.810 129.650 131.000 132.660 138.030 141.690
141.910 142.220 142.600
Manning n: 0.041 0.041 0.041 0.041 0.041 0.041 0.041 0.041 0.041 0.041
0.041 0.041 0.041 0.041 0.041 0.041 0.041 0.041 0.041 0.041
0.041 0.041

Section No. : 3 S.V. = 923.000 Title : CROSS SECTION 3
No. of points : 17

Chainage : 14.500 28.000 47.000 83.500 109.000 113.000 129.000 144.000 181.500 227.000
236.000 243.000 247.000 270.000 274.000 310.000 325.000
Level : 142.770 140.250 138.090 137.350 136.730 133.170 131.460 127.220 128.940 128.840
128.460 128.740 129.090 133.340 137.190 141.300 142.890
Manning n: 0.041 0.041 0.041 0.041 0.041 0.041 0.041 0.041 0.041 0.041
0.041 0.041 0.041 0.041 0.041 0.041

Section No. : 4 S.V. = 1413.000 Title : CROSS SECTION 4
No. of points : 18

Chainage : 25.000 75.000 97.000 126.500 128.500 132.000 149.000 163.500 179.000 184.000
237.000 274.000 289.500 293.000 300.000 305.000 329.000 349.000
Level : 142.140 136.300 137.730 136.180 136.170 134.040 132.870 129.150 130.400 128.820
128.680 128.370 128.470 131.040 131.950 139.000 140.840 142.310
Manning n: 0.041 0.041 0.041 0.041 0.041 0.041 0.041 0.041 0.041 0.041
0.041 0.041 0.041 0.041 0.041 0.041 0.041

Final Profiles :

Point	Stake Value [m]	Bed Level [m]	Depth [m]	Surface level [m]	Surface Width [m]	Area [m^2]	Discharge [m^3/s]	Velocity level [m/s]	Energy [m]	Froude No.
1	134.000	129.490	12.64	142.13	245.70	2066.57	6500.00	3.15	142.63	0.35
						Section 1				
2	154.889	129.397	12.71	142.11	247.14	2068.87	6500.00	3.14	142.61	0.35
3	175.778	129.303	12.78	142.09	248.78	2071.36	6500.00	3.14	142.59	0.35
4	196.667	129.210	12.86	142.07	250.64	2074.19	6500.00	3.13	142.57	0.35
5	217.556	129.117	12.93	142.05	252.75	2077.50	6500.00	3.13	142.55	0.35
6	238.444	129.023	13.00	142.03	255.04	2080.92	6500.00	3.12	142.52	0.35
7	259.333	128.930	13.08	142.01	257.54	2084.45	6500.00	3.12	142.50	0.35
8	280.222	128.837	13.15	141.99	260.22	2088.07	6500.00	3.11	142.48	0.35
9	301.111	128.743	13.23	141.97	263.09	2091.80	6500.00	3.11	142.46	0.35
10	322.000	128.650	13.30	141.95	266.16	2095.61	6500.00	3.10	142.44	0.35
11	342.889	128.557	13.37	141.93	270.33	2100.53	6500.00	3.09	142.42	0.35
12	363.778	128.463	13.45	141.91	275.06	2105.93	6500.00	3.09	142.40	0.36
13	384.667	128.370	13.52	141.89	280.19	2111.65	6500.00	3.08	142.37	0.36
14	405.556	128.277	13.59	141.87	285.71	2117.67	6500.00	3.07	142.35	0.36
15	426.444	128.183	13.67	141.85	291.64	2123.98	6500.00	3.06	142.33	0.36
16	447.333	128.090	13.74	141.83	297.96	2130.57	6500.00	3.05	142.30	0.36
17	468.222	127.997	13.81	141.81	304.66	2137.43	6500.00	3.04	142.28	0.37
18	489.111	127.903	13.88	141.79	311.75	2144.53	6500.00	3.03	142.26	0.37
19	510.000	127.810	13.96	141.77	319.22	2151.85	6500.00	3.02	142.23	0.37
						Section 2				
20	530.650	127.780	13.96	141.74	317.99	2158.34	6500.00	3.01	142.21	0.37
21	551.300	127.751	13.97	141.72	316.75	2164.95	6500.00	3.00	142.18	0.37
22	571.950	127.721	13.98	141.70	315.50	2171.67	6500.00	2.99	142.16	0.36
23	592.600	127.692	13.99	141.68	314.23	2178.50	6500.00	2.98	142.13	0.36
24	613.250	127.662	14.00	141.66	312.94	2185.45	6500.00	2.97	142.11	0.36
25	633.900	127.633	14.01	141.64	311.63	2192.53	6500.00	2.96	142.09	0.36
26	654.550	127.604	14.02	141.62	310.29	2199.73	6500.00	2.95	142.06	0.35
27	675.200	127.574	14.03	141.60	308.92	2207.04	6500.00	2.95	142.04	0.35
28	695.850	127.545	14.04	141.58	307.52	2214.47	6500.00	2.94	142.02	0.35
29	716.500	127.515	14.05	141.56	306.09	2222.00	6500.00	2.93	142.00	0.35
30	737.150	127.485	14.06	141.54	304.96	2230.04	6500.00	2.91	141.98	0.34
31	757.800	127.456	14.07	141.53	303.76	2238.15	6500.00	2.90	141.96	0.34
32	778.450	127.426	14.08	141.51	302.44	2246.26	6500.00	2.89	141.94	0.34
33	799.100	127.397	14.10	141.49	300.99	2254.38	6500.00	2.88	141.92	0.34
34	819.750	127.368	14.11	141.48	299.39	2262.49	6500.00	2.87	141.90	0.33
35	840.400	127.338	14.12	141.46	297.65	2270.60	6500.00	2.86	141.88	0.33
36	861.050	127.309	14.13	141.44	295.76	2278.69	6500.00	2.85	141.86	0.33
37	881.700	127.279	14.15	141.43	293.71	2286.76	6500.00	2.84	141.84	0.33
38	902.350	127.250	14.16	141.41	291.49	2294.80	6500.00	2.83	141.82	0.32
39	923.000	127.220	14.18	141.40	289.10	2302.82	6500.00	2.82	141.80	0.32

						Section 3				
40	943.417	127.268	14.11	141.38	289.86	2303.69	6500.00	2.82	141.79	0.32
41	963.833	127.316	14.05	141.36	290.57	2304.41	6500.00	2.82	141.77	0.32
42	984.250	127.364	13.98	141.35	291.25	2305.11	6500.00	2.82	141.75	0.32
43	1004.667	127.412	13.92	141.33	291.91	2306.14	6500.00	2.82	141.73	0.32
44	1025.083	127.460	13.85	141.31	292.53	2306.97	6500.00	2.82	141.71	0.32
45	1045.500	127.507	13.79	141.29	293.10	2307.59	6500.00	2.82	141.70	0.32
46	1065.917	127.555	13.72	141.27	293.63	2308.01	6500.00	2.82	141.68	0.32
47	1086.333	127.603	13.65	141.26	294.11	2308.22	6500.00	2.82	141.66	0.32
48	1106.750	127.651	13.59	141.24	294.54	2308.23	6500.00	2.82	141.64	0.32
49	1127.167	127.699	13.52	141.22	294.93	2308.03	6500.00	2.82	141.63	0.32
50	1147.583	127.747	13.46	141.20	295.28	2307.61	6500.00	2.82	141.61	0.32
51	1168.000	127.795	13.39	141.18	295.57	2306.99	6500.00	2.82	141.59	0.32
52	1188.417	127.843	13.32	141.17	295.83	2306.16	6500.00	2.82	141.57	0.32
53	1208.833	127.891	13.26	141.15	296.03	2305.11	6500.00	2.82	141.55	0.32
54	1229.250	127.939	13.19	141.13	296.16	2303.97	6500.00	2.82	141.54	0.32
55	1249.667	127.987	13.12	141.11	296.22	2302.74	6500.00	2.82	141.52	0.32
56	1270.083	128.035	13.06	141.09	296.25	2301.48	6500.00	2.82	141.50	0.32
57	1290.500	128.083	12.99	141.07	296.24	2300.48	6500.00	2.83	141.48	0.32
58	1310.917	128.130	12.92	141.06	296.21	2299.30	6500.00	2.83	141.46	0.32
59	1331.333	128.178	12.86	141.04	296.14	2297.93	6500.00	2.83	141.44	0.32
60	1351.750	128.226	12.79	141.02	296.05	2296.37	6500.00	2.83	141.43	0.32
61	1372.167	128.274	12.72	141.00	295.92	2294.63	6500.00	2.83	141.41	0.32
62	1392.583	128.322	12.66	140.98	295.75	2292.69	6500.00	2.84	141.39	0.33
63	1413.000	128.370	12.59	140.96	295.56	2290.56	6500.00	2.84	141.37	0.33

DESIGN INFO : Hydraulic Radii

Section : 1 S.V. = 134.000 Title : CROSS SECTION 1

Chainage From ...:	To .....:	Points From	To	Mann. n	Perimeter [m]	Hydraulic Radius [m]
78.000	330.000	3	23	0.041	249.994	8.264

Section : 2 S.V. = 510.000 Title : CROSS SECTION 2

Chainage From ...:	To .....:	Points From	To	Mann. n	Perimeter [m]	Hydraulic Radius [m]
18.000	351.000	2	21	0.041	314.914	6.826

Section : 3 S.V. = 923.000 Title : CROSS SECTION 3

Chainage From ...:	To .....:	Points From	To	Mann. n	Perimeter [m]	Hydraulic Radius [m]
14.500	325.000	1	17	0.041	293.585	7.841

Section : 4 S.V. = 1413.000 Title : CROSS SECTION 4

Chainage From ...:	To .....:	Points From	To	Mann. n	Perimeter [m]	Hydraulic Radius [m]
25.000	349.000	1	18	0.041	301.910	7.583

CFP - DATA :

Run information :

No. of cross sections	:	4
Calculation interval dSV	:	20.000
Upstream depth	:	7.830
Downstream depth	:	6.460
Mult. factors - Discharge ...	:	1.000
- Manning's n ...	:	1.000
Run label	:	MHLATUZE 1984 (n = 0.042)
Hydraulic jump calcs	:	AC
Transition loss coef. applied	:	N
Conveyance Calculation type	:	2

Long Section Data :

Section No.	Stake Value [m]	Unit Flow [m³/s]	Deflt Mann. n	Transition Loss Coef. Div. Conv. [-][-]	Section Title
1	37.500	2400.000	0.042	0.00 0.00	CROSS SECTION 1
2	137.500	2400.000	0.042	0.00 0.00	CROSS SECTION 2
3	299.500	2400.000	0.042	0.00 0.00	CROSS SECTION 3
4	469.500	2400.000	0.042	0.00 0.00	CROSS SECTION 4

Cross Section Data :

Section No. : 1 S.V. = 37.500 Title : CROSS SECTION 1
No. of points : 24

Chainage : 0.000 0.000 11.000 14.300 17.500 20.400 23.500 28.000 31.700 36.000
40.000 44.000 48.000 52.000 55.700 60.000 63.900 68.000 75.600 82.100
100.000 119.700 126.500 130.000
Level : 110.000 106.320 105.850 103.350 101.780 101.210 100.710 100.650 101.140 101.260
101.290 101.210 101.230 101.430 101.440 101.520 101.650 101.720 105.300 105.950
104.490 105.890 108.510 110.000
Manning n: 0.042 0.042 0.042 0.042 0.042 0.042 0.042 0.042 0.042 0.042
0.042 0.042 0.042 0.042 0.042 0.042 0.042 0.042 0.042 0.042
0.042 0.042 0.042

Section No. : 2 S.V. = 137.500 Title : CROSS SECTION 2
No. of points : 25

Chainage : -1.666 0.000 8.000 13.500 15.300 19.500 21.000 24.500 28.700 31.400
36.400 40.500 44.500 48.700 53.000 56.000 60.700 64.500 68.000 72.000
75.000 82.300 111.500 126.000 135.500
Level : 109.000 108.290 105.980 105.100 102.910 101.520 100.710 100.910 101.060 101.220
101.240 101.220 101.150 101.060 101.020 100.960 101.010 100.820 100.870 101.520
102.400 104.600 104.800 107.140 110.790
Manning n: 0.042 0.042 0.042 0.042 0.042 0.042 0.042 0.042 0.042 0.042
0.042 0.042 0.042 0.042 0.042 0.042 0.042 0.042 0.042 0.042
0.042 0.042 0.042 0.042

Section No. : 3 S.V. = 299.500 Title : CROSS SECTION 3
No. of points : 27

Chainage : 0.000 6.300 9.500 14.300 25.500 29.500 33.700 37.300 41.500 45.500
49.500 53.500 57.500 61.500 65.500 69.500 73.500 77.500 81.500 85.000
89.500 92.500 95.000 101.500 123.700 131.400 134.000
Level : 109.160 104.030 104.170 103.620 101.410 101.050 101.000 101.210 101.230 101.250
101.120 100.940 100.620 100.610 100.750 100.690 100.810 101.170 101.130 100.980
101.440 102.920 104.200 105.010 105.030 107.810 109.000
Manning n: 0.042 0.042 0.042 0.042 0.042 0.042 0.042 0.042 0.042 0.042
0.042 0.042 0.042 0.042 0.042 0.042 0.042 0.042 0.042 0.042
0.042 0.042 0.042 0.042 0.042 0.042

Cross Section Data :

Section No. : 4 S.V. = 469.500 Title : CROSS SECTION 4
No. of points : 32

Chainage : 0.000 0.000 6.200 9.500 18.000 26.500 35.500 39.000 41.000 49.300
53.000 57.500 61.000 65.000 69.000 73.500 77.000 80.500 85.000 89.000
93.000 97.000 101.000 105.000 109.000 113.500 117.000 120.000 124.000 125.000
132.500 132.600
Level : 108.000 106.660 105.090 104.620 104.420 103.950 101.830 101.280 100.990 100.930
100.760 100.740 100.830 100.930 101.010 101.020 100.900 100.950 100.870 100.710
100.880 100.840 100.840 100.940 100.900 100.670 101.260 102.720 104.600 104.650
105.120 108.000
Manning n: 0.042 0.042 0.042 0.042 0.042 0.042 0.042 0.042 0.042 0.042
0.042 0.042 0.042 0.042 0.042 0.042 0.042 0.042 0.042 0.042
0.042 0.042 0.042 0.042 0.042 0.042 0.042 0.042 0.042 0.042
0.042

Final Profiles :

Point	Stake Value [m]	Bed Level [m]	Depth [m]	Surface level [m]	Surface Width [m]	Area [m^2]	Discharge [m^3/s]	Velo-city level [m/s]	Energy [m]	Froude No.
1	37.500	100.650	7.79	108.44	126.31	606.15	2400.00	3.96	109.24	0.58
								Section	1	
2	57.500	100.662	7.71	108.37	126.80	606.14	2400.00	3.96	109.17	0.58
3	77.500	100.674	7.63	108.30	127.19	605.98	2400.00	3.96	109.10	0.58
4	97.500	100.686	7.54	108.23	127.49	605.66	2400.00	3.96	109.03	0.58
5	117.500	100.698	7.46	108.15	127.69	605.18	2400.00	3.97	108.96	0.58
6	137.500	100.710	7.37	108.08	127.73	604.74	2400.00	3.97	108.88	0.58
								Section	2	
7	157.750	100.698	7.32	108.02	127.74	607.05	2400.00	3.95	108.81	0.58
8	178.000	100.685	7.27	107.95	127.80	609.48	2400.00	3.94	108.74	0.58
9	198.250	100.673	7.21	107.89	127.89	612.02	2400.00	3.92	108.67	0.57
10	218.500	100.660	7.16	107.82	128.03	614.67	2400.00	3.90	108.60	0.57
11	238.750	100.647	7.12	107.76	128.19	617.42	2400.00	3.89	108.53	0.57
12	259.000	100.635	7.07	107.70	128.38	620.32	2400.00	3.87	108.47	0.56
13	279.250	100.622	7.02	107.64	128.60	623.35	2400.00	3.85	108.40	0.56
14	299.500	100.610	6.97	107.58	128.84	626.48	2400.00	3.83	108.33	0.55
								Section	3	
15	320.750	100.618	6.91	107.52	129.07	629.95	2400.00	3.81	108.26	0.55
16	342.000	100.625	6.84	107.47	129.38	633.49	2400.00	3.79	108.20	0.55
17	363.250	100.632	6.78	107.41	129.75	637.09	2400.00	3.77	108.13	0.54
18	384.500	100.640	6.71	107.35	130.18	640.74	2400.00	3.75	108.07	0.54
19	405.750	100.647	6.65	107.29	130.68	644.46	2400.00	3.72	108.00	0.54
20	427.000	100.655	6.58	107.24	131.25	648.18	2400.00	3.70	107.94	0.53
21	448.250	100.662	6.52	107.18	131.88	651.90	2400.00	3.68	107.88	0.53
22	469.500	100.670	6.46	107.13	132.57	655.59	2400.00	3.66	107.81	0.53
								Section	4	
							CONTROL			

DESIGN INFO : Hydraulic Radii

Section : 1 S.V.= 37.500 Title : CROSS SECTION 1

Chainage From ...:	To .....:	Points From	To	Mann. n	Perimeter [m]	Hydraulic Radius [m]
0.000	126.500	1	23	0.042	131.225	4.619

Section : 2 S.V.= 137.500 Title : CROSS SECTION 2

Chainage From ...:	To .....:	Points From	To	Mann. n	Perimeter [m]	Hydraulic Radius [m]
0.000	135.500	2	25	0.042	130.448	4.635

Section : 3 S.V.= 299.500 Title : CROSS SECTION 3

Chainage From ...:	To .....:	Points From	To	Mann. n	Perimeter [m]	Hydraulic Radius [m]
0.000	131.400	1	26	0.042	131.596	4.760

Section : 4 S.V.= 469.500 Title : CROSS SECTION 4

Chainage From ...:	To .....:	Points From	To	Mann. n	Perimeter [m]	Hydraulic Radius [m]
0.000	132.600	1	32	0.042	136.382	4.807

MHLA94

Project: ALLUVIAL RIVER STUDY
Subject: MKUZE RIVER : 1987

CFP - DATA :

Run information :

No. of cross sections	:	4
Calculation interval dSV	:	20.000
Upstream depth	:	4.290
Downstream depth	:	4.993
Mult. factors - Discharge	:	1.000
- Manning's n	:	1.000
Run label	:	MKUZE 1987 (n = 0.045)
Hydraulic jump calcs	:	AC
Transition loss coef. applied	:	N
Conveyance Calculation type	:	2

Long Section Data :

Section No.	Stake Value [m]	Unit Flow [m³/s]	Deflt Mann. n	Transition Loss Coef. Div. Conv. [-][-]	Section Title
1	123.000	1060.000	0.045	0.00 0.00	CROSS SECTION 1
2	289.000	1060.000	0.045	0.00 0.00	CROSS SECTION 2
3	490.200	1060.000	0.045	0.00 0.00	CROSS SECTION 3
4	680.300	1060.000	0.045	0.00 0.00	CROSS SECTION 4

Cross Section Data :

Section No. : 1 S.V. = 123.000 Title : CROSS SECTION 1
No. of points : 21

Chainage : 5.700 26.400 27.600 49.800 55.800 59.400 59.900 71.600 75.200 77.000
77.500 88.300 95.300 115.000 123.700 125.600 132.800 133.300 137.800 142.800
144.000
Level : 92.170 89.330 88.760 85.510 85.660 85.020 84.990 84.910 84.930 85.340
85.000 84.710 84.770 84.740 84.940 85.650 86.390 86.450 86.390 90.100
90.350
Manning n: 0.045 0.045 0.045 0.045 0.045 0.045 0.045 0.045 0.045 0.045
0.045 0.045 0.045 0.045 0.045 0.045 0.045 0.045 0.045 0.045

Section No. : 2 S.V. = 289.000 Title : CROSS SECTION 2
No. of points : 29

Chainage : 1.300 2.000 2.400 4.600 9.700 17.400 22.500 26.500 28.700 33.700
34.400 34.800 41.300 51.300 62.300 74.200 83.000 93.000 104.800 111.700
112.200 115.200 123.800 132.400 138.200 140.300 144.300 145.200 148.700
Level : 91.340 91.330 91.020 90.570 89.270 87.920 87.820 87.940 85.900 85.100
84.600 84.080 84.050 84.490 84.460 84.340 84.100 84.360 84.290 84.510
84.700 85.330 85.040 85.180 85.790 87.030 87.970 89.720 90.300
Manning n: 0.045 0.045 0.045 0.045 0.045 0.045 0.045 0.045 0.045 0.045
0.045 0.045 0.045 0.045 0.045 0.045 0.045 0.045 0.045 0.045
0.045 0.045 0.045 0.045 0.045 0.045 0.045 0.045

Section No. : 3 S.V. = 490.200 Title : CROSS SECTION 3
No. of points : 18

Chainage : 0.000 5.300 6.000 14.700 16.700 17.800 26.700 32.700 45.800 62.900
80.500 94.000 95.100 111.200 126.200 134.800 139.300 148.700
Level : 94.530 88.020 87.160 85.460 84.290 83.980 84.460 84.270 84.050 84.050
83.890 84.330 84.340 84.890 85.050 87.150 87.850 89.120
Manning n: 0.045 0.045 0.045 0.045 0.045 0.045 0.045 0.045 0.045 0.045
0.045 0.045 0.045 0.045 0.045 0.045 0.045

Section No. : 4 S.V. = 680.300 Title : CROSS SECTION 4
No. of points : 36

Chainage : 0.000 5.700 10.800 13.300 13.800 15.900 18.000 22.400 25.700 26.100
28.000 31.800 35.000 36.100 42.800 57.200 58.300 69.100 70.200 81.400
91.200 95.900 101.600 102.100 106.500 111.800 112.300 115.700 116.500 121.300
122.800 125.700 127.700 130.600 131.900 133.900
Level : 88.817 87.990 87.250 86.000 86.400 85.370 84.560 84.450 84.150 83.930
82.960 83.170 83.890 83.890 83.980 83.960 84.340 84.430 84.460 84.460
84.500 84.530 84.470 84.200 84.130 84.220 83.960 84.070 84.020 84.160
84.840 84.870 85.910 86.920 87.790 88.520
Manning n: 0.045 0.045 0.045 0.045 0.045 0.045 0.045 0.045 0.045 0.045
0.045 0.045 0.045 0.045 0.045 0.045 0.045 0.045 0.045 0.045
0.045 0.045 0.045 0.045 0.045 0.045 0.045 0.045 0.045 0.045
0.045 0.045 0.045 0.045 0.045

Final Profiles :

Point	Stake Value [m]	Bed Level [m]	Depth [m]	Surface level [m]	Surface Width [m]	Area [m^2]	Discharge [m^3/s]	Velocity level [m/s]	Energy [m]	Froude No.
1	123.000	84.710	4.29	89.00	114.23	388.62	1060.00	2.73	89.38	0.47
						Section	1			
2	143.750	84.628	4.33	88.96	116.29	398.03	1060.00	2.66	89.32	0.46
3	164.500	84.545	4.37	88.92	118.39	407.93	1060.00	2.60	89.26	0.45
4	185.250	84.463	4.42	88.88	120.53	418.35	1060.00	2.53	89.21	0.43
5	206.000	84.380	4.47	88.85	122.71	429.30	1060.00	2.47	89.16	0.42
6	226.750	84.298	4.52	88.82	124.95	440.76	1060.00	2.40	89.11	0.41
7	247.500	84.215	4.57	88.79	127.27	452.75	1060.00	2.34	89.07	0.40
8	268.250	84.132	4.63	88.76	129.60	465.23	1060.00	2.28	89.02	0.38
9	289.000	84.050	4.68	88.73	131.94	478.19	1060.00	2.22	88.98	0.37
						Section	2			
10	309.120	84.034	4.67	88.70	132.61	480.32	1060.00	2.21	88.95	0.37
11	329.240	84.018	4.65	88.67	133.27	482.46	1060.00	2.20	88.91	0.37
12	349.360	84.002	4.63	88.63	133.93	484.62	1060.00	2.19	88.88	0.37
13	369.480	83.986	4.61	88.60	134.58	486.80	1060.00	2.18	88.84	0.37
14	389.600	83.970	4.60	88.57	135.23	489.00	1060.00	2.17	88.80	0.36
15	409.720	83.954	4.58	88.53	135.88	491.21	1060.00	2.16	88.77	0.36
16	429.840	83.938	4.56	88.50	136.52	493.44	1060.00	2.15	88.74	0.36
17	449.960	83.922	4.55	88.47	137.15	495.69	1060.00	2.14	88.70	0.36
18	470.080	83.906	4.53	88.44	137.79	497.96	1060.00	2.13	88.67	0.36
19	490.200	83.890	4.51	88.40	138.42	500.25	1060.00	2.12	88.63	0.36
						Section	3			
20	511.322	83.787	4.58	88.36	137.13	494.52	1060.00	2.14	88.60	0.36
21	532.444	83.683	4.64	88.32	135.83	488.36	1060.00	2.17	88.56	0.37
22	553.567	83.580	4.70	88.28	134.51	481.74	1060.00	2.20	88.52	0.37
23	574.689	83.477	4.75	88.23	133.20	474.72	1060.00	2.23	88.48	0.38
24	595.811	83.373	4.81	88.18	131.88	467.23	1060.00	2.27	88.44	0.38
25	616.933	83.270	4.86	88.13	130.54	459.17	1060.00	2.31	88.40	0.39
26	638.056	83.167	4.91	88.08	129.19	450.49	1060.00	2.35	88.36	0.40
27	659.178	83.063	4.95	88.02	127.81	441.13	1060.00	2.40	88.31	0.41
28	680.300	82.960	4.99	87.95	126.40	430.99	1060.00	2.46	88.26	0.43
						Section	4			

DESIGN INFO : Hydraulic Radii

Section : 1 S.V. = 123.000 Title : CROSS SECTION 1

Chainage From ...:	To .....:	Points From	To	Mann. n	Perimeter [m]	Hydraulic Radius [m]
26.400	142.800	2	20	0.045	115.768	3.357

Section : 2 S.V. = 289.000 Title : CROSS SECTION 2

Chainage From ...:	To .....:	Points From	To	Mann. n	Perimeter [m]	Hydraulic Radius [m]
9.700	145.200	5	28	0.045	134.363	3.559

Section : 3 S.V. = 490.200 Title : CROSS SECTION 3

Chainage From ...:	To .....:	Points From	To	Mann. n	Perimeter [m]	Hydraulic Radius [m]
0.000	148.700	1	18	0.045	139.913	3.575

Section : 4 S.V. = 680.300 Title : CROSS SECTION 4

Chainage From ...:	To .....:	Points From	To	Mann. n	Perimeter [m]	Hydraulic Radius [m]
5.700	133.900	2	36	0.045	128.728	3.348

CFP - DATA :

Run information :

No. of cross sections	.....	:	4
Calculation interval dSV	.....	:	20.000
Upstream depth	.....	:	5.980
Downstream depth	.....	:	5.350
Mult. factors - Discharge	.....	:	1.000
- Manning's n	.....	:	1.000
Run label		:	BLACK MFOLOZI 1987 (n = 0.04)
Hydraulic jump calcs	.....	:	AC
Transition loss coef. applied	.....	:	N
Conveyance Calculation type	.....	:	2

Long Section Data :

Section No.	Stake Value [m]	Unit Flow [m³/s]	Deflt Mann. n	Transition Loss Coef. Div. Conv. [-][-]	Section Title
1	3493.000	1740.000	0.040	0.00 0.00	CROSS SECTION 1
2	3698.000	1740.000	0.040	0.00 0.00	CROSS SECTION 2
3	3923.000	1740.000	0.040	0.00 0.00	CROSS SECTION 3
4	4313.000	1740.000	0.040	0.00 0.00	CROSS SECTION 4

Cross Section Data :

Section No. : 1 S.V. = 3493.000 Title : CROSS SECTION 1
No. of points : 26

Chainage : 39.500 44.600 51.500 56.900 62.800 70.000 81.600 85.100 88.600 93.500
97.200 113.500 132.100 147.700 154.300 155.800 159.500 170.600 178.400 183.500
190.300 192.200 200.000 207.300 209.100 220.200
Level : 101.350 100.710 97.330 95.790 93.320 91.560 91.780 91.230 91.420 91.370
91.430 91.490 91.370 91.220 91.000 91.220 91.130 91.340 91.310 90.980
90.890 93.010 95.076 96.760 98.510 101.530
Manning n: 0.040 0.040 0.040 0.040 0.040 0.040 0.040 0.040 0.040 0.040
0.040 0.040 0.040 0.040 0.040 0.040 0.040 0.040 0.040 0.040
0.040 0.040 0.040 0.040 0.040

Section No. : 2 S.V. = 3698.000 Title : CROSS SECTION 2
No. of points : 34

Chainage : 0.000 11.200 19.600 26.900 37.300 39.100 47.200 49.100 50.600 53.000
54.300 60.900 65.300 69.700 86.000 102.800 115.000 128.600 136.000 142.300
150.800 152.000 153.000 159.000 164.300 169.800 177.600 188.400 194.900 197.800
200.000 205.200 214.000 226.600
Level : 102.380 101.300 100.110 98.960 97.170 95.950 94.680 93.560 92.890 91.780
91.050 91.170 90.740 90.940 91.120 91.080 91.150 91.120 91.180 91.130
91.160 91.370 92.130 93.040 93.580 93.560 94.530 95.670 96.560 97.480
98.581 99.700 101.430 102.580
Manning n: 0.040 0.040 0.040 0.040 0.040 0.040 0.040 0.040 0.040 0.040
0.040 0.040 0.040 0.040 0.040 0.040 0.040 0.040 0.040 0.040
0.040 0.040 0.040 0.040 0.040 0.040 0.040 0.040 0.040 0.040
0.040 0.040 0.040

Section No. : 3 S.V.= 3923.000 Title : CROSS SECTION 3
No. of points : 35

Chainage : 3.000 17.600 23.500 28.300 34.300 35.000 37.900 39.900 48.400 50.300
52.100 53.800 56.000 60.000 66.600 74.800 81.100 92.700 110.900 120.800
121.700 133.000 146.500 153.300 159.500 161.000 166.900 171.400 179.100 189.000
194.900 200.000 204.100 212.200 222.100
Level : 102.070 102.150 101.280 100.890 99.610 99.590 98.780 97.020 97.910 93.860
93.190 92.450 90.960 90.740 90.820 90.960 90.890 91.160 90.970 90.810
91.080 91.230 91.180 91.060 91.430 91.960 92.250 92.560 93.340 94.470
95.790 98.538 99.130 100.870 102.000
Manning n: 0.040 0.040 0.040 0.040 0.040 0.040 0.040 0.040 0.040 0.040
0.040 0.040 0.040 0.040 0.040 0.040 0.040 0.040 0.040 0.040
0.040 0.040 0.040 0.040 0.040 0.040 0.040 0.040 0.040 0.040
0.040 0.040 0.040 0.040

Section No. : 4 S.V.= 4313.000 Title : CROSS SECTION 4
No. of points : 35

Chainage : 8.800 19.700 39.500 52.600 58.800 73.600 79.600 80.700 81.700 85.600
87.800 90.800 97.500 102.700 109.700 122.000 122.900 132.800 144.000 164.100
166.400 167.900 171.200 176.400 192.400 194.000 196.600 198.400 203.000 204.800
206.900 207.400 210.000 215.600 222.600
Level : 101.510 100.640 99.350 97.640 95.740 93.350 92.340 91.750 90.780 90.730
90.400 90.390 90.430 90.350 90.630 90.660 90.730 90.710 90.920 90.830
90.460 90.750 90.860 90.780 90.020 91.950 92.810 93.800 94.480 94.930
95.470 96.980 97.743 98.620 99.510
Manning n: 0.040 0.040 0.040 0.040 0.040 0.040 0.040 0.040 0.040 0.040
0.040 0.040 0.040 0.040 0.040 0.040 0.040 0.040 0.040 0.040
0.040 0.040 0.040 0.040 0.040 0.040 0.040 0.040 0.040 0.040
0.040 0.040 0.040 0.040

Final Profiles :

Point	Stake Value [m]	Bed Level [m]	Depth [m]	Surface level [m]	Surface Width [m]	Area [m^2]	Discharge [m^3/s]	Velocity level [m/s]	Energy [m]	Froude No.
1	3493.000	90.890	5.99	96.88	154.14	752.85	1740.00	2.31	97.15	0.33
						Section	1			
2	3513.500	90.875	5.98	96.85	154.41	745.55	1740.00	2.33	97.13	0.34
3	3534.000	90.860	5.97	96.83	154.68	738.08	1740.00	2.36	97.11	0.34
4	3554.500	90.845	5.95	96.80	154.94	730.43	1740.00	2.38	97.09	0.35
5	3575.000	90.830	5.94	96.77	155.20	722.57	1740.00	2.41	97.06	0.36
6	3595.500	90.815	5.92	96.73	155.46	714.49	1740.00	2.44	97.04	0.36
7	3616.000	90.800	5.90	96.70	155.70	706.17	1740.00	2.46	97.01	0.37
8	3636.500	90.785	5.88	96.67	155.95	697.58	1740.00	2.49	96.98	0.38
9	3657.000	90.770	5.86	96.63	156.19	688.70	1740.00	2.53	96.95	0.38
10	3677.500	90.755	5.83	96.59	156.42	679.48	1740.00	2.56	96.92	0.39
11	3698.000	90.740	5.81	96.55	156.60	669.93	1740.00	2.60	96.89	0.40
						Section	2			
12	3718.455	90.740	5.77	96.51	155.47	668.33	1740.00	2.60	96.86	0.40
13	3738.909	90.740	5.74	96.48	154.38	666.78	1740.00	2.61	96.83	0.40
14	3759.364	90.740	5.71	96.45	153.34	665.30	1740.00	2.62	96.80	0.40
15	3779.818	90.740	5.67	96.41	152.34	663.87	1740.00	2.62	96.76	0.40
16	3800.273	90.740	5.64	96.38	151.37	662.49	1740.00	2.63	96.73	0.40
17	3820.727	90.740	5.61	96.35	150.45	661.19	1740.00	2.63	96.70	0.40
18	3841.182	90.740	5.57	96.31	149.56	659.95	1740.00	2.64	96.67	0.40
19	3861.636	90.740	5.54	96.28	148.72	658.77	1740.00	2.64	96.64	0.40
20	3882.091	90.740	5.51	96.25	147.91	657.65	1740.00	2.65	96.60	0.40
21	3902.545	90.740	5.47	96.21	147.14	656.59	1740.00	2.65	96.57	0.40
22	3923.000	90.740	5.44	96.18	146.41	655.59	1740.00	2.65	96.54	0.40
						Section	3			

23	3943.526	90.702	5.44	96.15	146.39	652.93	1740.00	2.66	96.51	0.40
24	3964.053	90.664	5.45	96.11	146.38	650.19	1740.00	2.68	96.47	0.41
25	3984.579	90.626	5.45	96.07	146.36	647.36	1740.00	2.69	96.44	0.41
26	4005.105	90.588	5.45	96.04	146.34	644.44	1740.00	2.70	96.41	0.41
27	4025.632	90.551	5.45	96.00	146.32	641.43	1740.00	2.71	96.37	0.41
28	4046.158	90.513	5.45	95.96	146.29	638.31	1740.00	2.73	96.34	0.42
29	4066.684	90.475	5.45	95.92	146.26	635.09	1740.00	2.74	96.30	0.42
30	4087.210	90.437	5.44	95.88	146.23	631.75	1740.00	2.75	96.27	0.42
31	4107.737	90.399	5.44	95.84	146.19	628.28	1740.00	2.77	96.23	0.43
32	4128.263	90.361	5.44	95.80	146.15	624.68	1740.00	2.79	96.19	0.43
33	4148.790	90.323	5.43	95.76	146.09	620.94	1740.00	2.80	96.16	0.43
34	4169.316	90.285	5.43	95.71	146.03	617.04	1740.00	2.82	96.12	0.44
35	4189.842	90.247	5.42	95.67	145.96	612.98	1740.00	2.84	96.08	0.44
36	4210.368	90.209	5.41	95.62	145.87	608.75	1740.00	2.86	96.04	0.45
37	4230.895	90.172	5.40	95.58	145.77	604.31	1740.00	2.88	96.00	0.45
38	4251.421	90.134	5.39	95.53	145.65	599.67	1740.00	2.90	95.96	0.46
39	4271.947	90.096	5.38	95.48	145.52	594.79	1740.00	2.93	95.91	0.46
40	4292.474	90.058	5.37	95.42	145.36	589.66	1740.00	2.95	95.87	0.47
41	4313.000	90.020	5.35	95.37	145.18	584.25	1740.00	2.98	95.82	0.47
								Section	4	
							CONTROL			

DESIGN INFO : Hydraulic Radii

Section : 1 S.V.= 3493.000 Title : CROSS SECTION 1

Chainage From ...:	To .....:	Points From	To	Mann. n	Perimeter [m]	Hydraulic Radius [m]
51.500	209.100	3	25	0.040	156.755	4.802

Section : 2 S.V.= 3698.000 Title : CROSS SECTION 2

Chainage From ...:	To .....:	Points From	To	Mann. n	Perimeter [m]	Hydraulic Radius [m]
37.300	194.900	5	29	0.040	158.340	4.231

Section : 3 S.V.= 3923.000 Title : CROSS SECTION 3

Chainage From ...:	To .....:	Points From	To	Mann. n	Perimeter [m]	Hydraulic Radius [m]
48.400	200.000	9	32	0.040	149.142	4.395

Section : 4 S.V.= 4313.000 Title : CROSS SECTION 4

Chainage From ...:	To .....:	Points From	To	Mann. n	Perimeter [m]	Hydraulic Radius [m]
58.800	206.900	5	31	0.040	147.783	3.952

CFP - DATA :

Run information :

No. of cross sections	.... :	4
Calculation interval dSV	... :	20.000
Upstream depth	..... :	5.830
Downstream depth	...... :	4.840
Mult. factors - Discharge	.. :	1.000
- Manning's n	... :	1.000
Run label	..... :	WHITE MFOLOZI 1987 (n = 0.039)
Hydraulic jump calcs	..... :	AC
Transition loss coef. applied	:	N
Conveyance Calculation type	:	2

Long Section Data :

Section No.	Stake Value [m]	Unit Flow [m³/s]	Deflt Mann. n	Transition Loss Coef. Div. Conv. [-][-]	Section Title
1	191.000	2150.000	0.039	0.00 0.00	CROSS SECTION 1
2	486.000	2150.000	0.039	0.00 0.00	CROSS SECTION 2
3	930.000	2150.000	0.039	0.00 0.00	CROSS SECTION 3
4	1426.000	2150.000	0.039	0.00 0.00	CROSS SECTION 4

Cross Section Data :

Section No. : 1 S.V. = 191.000 Title : CROSS SECTION 1
No. of points : 23

Chainage : 16.900 27.500 28.800 47.200 58.800 59.300 67.200 71.200 74.800 88.200
99.100 99.600 111.400 125.500 134.800 136.200 146.200 158.300 167.200 174.600
178.700 189.000 200.000
Level : 139.690 135.560 134.210 130.880 130.420 129.950 129.790 129.720 129.890 129.790
129.920 130.000 129.960 130.160 130.560 130.510 130.480 130.380 130.400 130.500
130.850 133.870 137.100
Manning n: 0.039 0.039 0.039 0.039 0.039 0.039 0.039 0.039 0.039 0.039
0.039 0.039 0.039 0.039 0.039 0.039 0.039 0.039 0.039 0.039
0.039 0.039

Section No. : 2 S.V. = 486.000 Title : CROSS SECTION 2
No. of points : 20

Chainage : 20.200 43.500 47.000 48.800 71.100 79.600 79.900 87.400 94.700 111.300
128.100 139.600 154.000 172.700 174.800 174.900 196.100 203.100 208.000 220.000

Level : 138.360 134.510 132.320 132.390 130.560 130.100 129.690 129.740 129.770 129.820
130.010 129.670 129.150 129.190 130.080 130.270 131.550 134.520 135.110 136.490

Manning n: 0.039 0.039 0.039 0.039 0.039 0.039 0.039 0.039 0.039 0.039
0.039 0.039 0.039 0.039 0.039 0.039 0.039 0.039 0.039

Section No. : 3 S.V. = 930.000 Title : CROSS SECTION 3
No. of points : 21

Chainage : 33.200 36.700 42.300 51.700 56.500 66.500 67.100 81.000 94.000 106.200
124.000 140.800 154.600 168.000 179.900 188.000 188.300 199.400 205.200 210.000
210.300
Level : 138.580 138.440 132.830 132.740 131.660 129.710 129.470 129.450 129.340 129.300
129.390 129.230 129.260 128.790 128.930 129.290 129.630 131.770 132.680 133.430
135.000
Manning n: 0.039 0.039 0.039 0.039 0.039 0.039 0.039 0.039 0.039 0.039
0.039 0.039 0.039 0.039 0.039 0.039 0.039 0.039 0.039 0.039

Section No. : 4 S.V.= 1426.000 Title : CROSS SECTION 4
No. of points : 18

Chainage : 8.100 19.200 30.500 44.100 47.900 49.800 65.100 77.200 88.900 100.500
118.100 134.700 152.600 154.500 162.200 163.200 172.000 174.400
Level : 135.600 132.680 129.870 129.440 128.970 128.430 128.450 128.080 128.400 128.500
128.530 128.530 128.550 128.860 130.550 130.080 131.760 134.000
Manning n: 0.039 0.039 0.039 0.039 0.039 0.039 0.039 0.039 0.039 0.039
0.039 0.039 0.039 0.039 0.039 0.039 0.039

Final Profiles :

Point	Stake Value [m]	Bed Level [m]	Depth [m]	Surface level [m]	Surface Width [m]	Area [m²]	Discharge [m³/s]	Velocity level [m/s]	Energy [m]	Froude No.
1	191.000	129.720	5.86	135.58	167.44	803.53	2150.00	2.68	135.95	0.39
						Section	1			
2	212.071	129.679	5.87	135.55	167.44	800.90	2150.00	2.68	135.92	0.39
3	233.143	129.639	5.88	135.52	167.45	798.22	2150.00	2.69	135.89	0.39
4	254.214	129.598	5.89	135.49	167.48	795.46	2150.00	2.70	135.86	0.40
5	275.286	129.557	5.90	135.46	167.50	792.63	2150.00	2.71	135.83	0.40
6	296.357	129.516	5.91	135.42	167.54	789.73	2150.00	2.72	135.80	0.40
7	317.429	129.476	5.91	135.39	167.59	786.75	2150.00	2.73	135.77	0.40
8	338.500	129.435	5.92	135.35	167.65	783.69	2150.00	2.74	135.74	0.41
9	359.571	129.394	5.93	135.32	167.70	780.53	2150.00	2.75	135.71	0.41
10	380.643	129.354	5.93	135.28	167.76	777.28	2150.00	2.77	135.67	0.41
11	401.714	129.313	5.94	135.25	167.81	773.92	2150.00	2.78	135.64	0.41
12	422.786	129.272	5.94	135.21	167.86	770.45	2150.00	2.79	135.61	0.42
13	443.857	129.231	5.94	135.18	167.91	766.86	2150.00	2.80	135.58	0.42
14	464.929	129.191	5.95	135.14	167.96	763.14	2150.00	2.82	135.54	0.42
15	486.000	129.150	5.95	135.10	167.99	759.29	2150.00	2.83	135.51	0.43
						Section	2			
16	506.182	129.134	5.93	135.06	167.82	758.53	2150.00	2.83	135.47	0.43
17	526.364	129.117	5.91	135.03	167.68	757.75	2150.00	2.84	135.44	0.43
18	546.545	129.101	5.89	135.00	167.55	756.96	2150.00	2.84	135.41	0.43
19	566.727	129.085	5.88	134.96	167.45	756.14	2150.00	2.84	135.37	0.43
20	586.909	129.068	5.86	134.93	167.37	755.35	2150.00	2.85	135.34	0.43
21	607.091	129.052	5.84	134.89	167.31	754.56	2150.00	2.85	135.31	0.43
22	627.273	129.035	5.82	134.86	167.27	753.74	2150.00	2.85	135.27	0.43
23	647.455	129.019	5.80	134.82	167.25	752.88	2150.00	2.86	135.24	0.43
24	667.636	129.003	5.78	134.79	167.26	751.98	2150.00	2.86	135.20	0.43
25	687.818	128.986	5.76	134.75	167.28	751.04	2150.00	2.86	135.17	0.43
26	708.000	128.970	5.74	134.71	167.33	750.05	2150.00	2.87	135.13	0.43
27	728.182	128.954	5.73	134.68	167.39	749.02	2150.00	2.87	135.10	0.43
28	748.364	128.937	5.71	134.64	167.48	747.94	2150.00	2.87	135.06	0.43
29	768.545	128.921	5.69	134.61	167.59	746.81	2150.00	2.88	135.03	0.44
30	788.727	128.905	5.66	134.57	167.73	745.61	2150.00	2.88	134.99	0.44
31	808.909	128.888	5.64	134.53	167.88	744.35	2150.00	2.89	134.96	0.44
32	829.091	128.872	5.62	134.49	168.06	743.03	2150.00	2.89	134.92	0.44
33	849.273	128.855	5.60	134.46	168.27	741.63	2150.00	2.90	134.89	0.44
34	869.455	128.839	5.58	134.42	168.50	740.15	2150.00	2.90	134.85	0.44
35	889.636	128.823	5.56	134.38	168.75	738.60	2150.00	2.91	134.81	0.44
36	909.818	128.806	5.53	134.34	169.03	736.96	2150.00	2.92	134.78	0.45

37	930.000	128.790	5.51	134.30	169.34	735.23	2150.00	2.92	134.74	0.45
						Section 3				
38	950.667	128.760	5.50	134.26	168.85	731.68	2150.00	2.94	134.70	0.45
39	971.333	128.731	5.48	134.22	168.37	728.02	2150.00	2.95	134.66	0.45
40	992.000	128.701	5.47	134.17	167.88	724.27	2150.00	2.97	134.62	0.46
41	1012.667	128.672	5.45	134.13	167.38	720.40	2150.00	2.98	134.58	0.46
42	1033.333	128.642	5.44	134.08	166.88	716.41	2150.00	3.00	134.54	0.46
43	1054.000	128.612	5.42	134.03	166.37	712.30	2150.00	3.02	134.50	0.47
44	1074.667	128.583	5.40	133.99	165.85	708.05	2150.00	3.04	134.45	0.47
45	1095.333	128.553	5.38	133.94	165.32	703.66	2150.00	3.06	134.41	0.47
46	1116.000	128.524	5.36	133.89	164.79	699.11	2150.00	3.08	134.37	0.48
47	1136.667	128.494	5.34	133.84	164.24	694.40	2150.00	3.10	134.32	0.48
48	1157.333	128.465	5.32	133.78	163.69	689.51	2150.00	3.12	134.28	0.49
49	1178.000	128.435	5.30	133.73	163.13	684.43	2150.00	3.14	134.23	0.49
50	1198.667	128.405	5.27	133.68	162.55	679.16	2150.00	3.17	134.19	0.49
51	1219.333	128.376	5.24	133.62	161.96	673.66	2150.00	3.19	134.14	0.50
52	1240.000	128.346	5.21	133.56	161.36	667.93	2150.00	3.22	134.09	0.51
53	1260.667	128.317	5.18	133.50	160.74	661.92	2150.00	3.25	134.04	0.51
54	1281.333	128.287	5.15	133.44	160.10	655.62	2150.00	3.28	133.99	0.52
55	1302.000	128.257	5.12	133.38	159.45	648.98	2150.00	3.31	133.93	0.52
56	1322.667	128.228	5.08	133.31	158.77	641.97	2150.00	3.35	133.88	0.53
57	1343.333	128.198	5.04	133.24	158.07	634.52	2150.00	3.39	133.82	0.54
58	1364.000	128.169	5.00	133.17	157.34	626.62	2150.00	3.43	133.77	0.55
59	1384.667	128.139	4.95	133.09	156.59	618.19	2150.00	3.48	133.70	0.56
60	1405.333	128.110	4.90	133.01	155.79	609.11	2150.00	3.53	133.64	0.57
61	1426.000	128.080	4.84	132.92	154.96	599.26	2150.00	3.59	133.58	0.58
						Section 4				

DESIGN INFO : Hydraulic Radii

Section : 1 S.V. = 191.000 Title : CROSS SECTION 1

Chainage From ...:	To .....:	Points From	To	Mann. n	Perimeter [m]	Hydraulic Radius [m]
16.900	200.000	1	23	0.039	169.184	4.749

Section : 2 S.V. = 486.000 Title : CROSS SECTION 2

Chainage From ...:	To .....:	Points From	To	Mann. n	Perimeter [m]	Hydraulic Radius [m]
20.200	208.000	1	19	0.039	169.929	4.467

Section : 3 S.V. = 930.000 Title : CROSS SECTION 3

Chainage From ...:	To .....:	Points From	To	Mann. n	Perimeter [m]	Hydraulic Radius [m]
36.700	210.300	2	21	0.039	171.528	4.286

Section : 4 S.V. = 1426.000 Title : CROSS SECTION 4

Chainage From ...:	To .....:	Points From	To	Mann. n	Perimeter [m]	Hydraulic Radius [m]
8.100	174.400	1	18	0.039	156.381	3.832

37	930.000	128.790	5.51	134.30	169.34	735.23	2150.00	2.92	134.74	0.45
						Section 3				
38	950.667	128.760	5.50	134.26	168.85	731.68	2150.00	2.94	134.70	0.45
39	971.333	128.731	5.48	134.22	168.37	728.02	2150.00	2.95	134.66	0.45
40	992.000	128.701	5.47	134.17	167.88	724.27	2150.00	2.97	134.62	0.46
41	1012.667	128.672	5.45	134.13	167.38	720.40	2150.00	2.98	134.58	0.46
42	1033.333	128.642	5.44	134.08	166.88	716.41	2150.00	3.00	134.54	0.46
43	1054.000	128.612	5.42	134.03	166.37	712.30	2150.00	3.02	134.50	0.47
44	1074.667	128.583	5.40	133.99	165.85	708.05	2150.00	3.04	134.45	0.47
45	1095.333	128.553	5.38	133.94	165.32	703.66	2150.00	3.06	134.41	0.47
46	1116.000	128.524	5.36	133.89	164.79	699.11	2150.00	3.08	134.37	0.48
47	1136.667	128.494	5.34	133.84	164.24	694.40	2150.00	3.10	134.32	0.48
48	1157.333	128.465	5.32	133.78	163.69	689.51	2150.00	3.12	134.28	0.49
49	1178.000	128.435	5.30	133.73	163.13	684.43	2150.00	3.14	134.23	0.49
50	1198.667	128.405	5.27	133.68	162.55	679.16	2150.00	3.17	134.19	0.49
51	1219.333	128.376	5.24	133.62	161.96	673.66	2150.00	3.19	134.14	0.50
52	1240.000	128.346	5.21	133.56	161.36	667.93	2150.00	3.22	134.09	0.51
53	1260.667	128.317	5.18	133.50	160.74	661.92	2150.00	3.25	134.04	0.51
54	1281.333	128.287	5.15	133.44	160.10	655.62	2150.00	3.28	133.99	0.52
55	1302.000	128.257	5.12	133.38	159.45	648.98	2150.00	3.31	133.93	0.52
56	1322.667	128.228	5.08	133.31	158.77	641.97	2150.00	3.35	133.88	0.53
57	1343.333	128.198	5.04	133.24	158.07	634.52	2150.00	3.39	133.82	0.54
58	1364.000	128.169	5.00	133.17	157.34	626.62	2150.00	3.43	133.77	0.55
59	1384.667	128.139	4.95	133.09	156.59	618.19	2150.00	3.48	133.70	0.56
60	1405.333	128.110	4.90	133.01	155.79	609.11	2150.00	3.53	133.64	0.57
61	1426.000	128.080	4.84	132.92	154.96	599.26	2150.00	3.59	133.58	0.58
						Section 4				

DESIGN INFO : Hydraulic Radii

Section : 1 S.V. = 191.000 Title : CROSS SECTION 1

Chainage From ...:	To .....:	Points From	To	Mann. n	Perimeter [m]	Hydraulic Radius [m]
16.900	200.000	1	23	0.039	169.184	4.749

Section : 2 S.V. = 486.000 Title : CROSS SECTION 2

Chainage From ...:	To .....:	Points From	To	Mann. n	Perimeter [m]	Hydraulic Radius [m]
20.200	208.000	1	19	0.039	169.929	4.467

Section : 3 S.V. = 930.000 Title : CROSS SECTION 3

Chainage From ...:	To .....:	Points From	To	Mann. n	Perimeter [m]	Hydraulic Radius [m]
36.700	210.300	2	21	0.039	171.528	4.286

Section : 4 S.V. = 1426.000 Title : CROSS SECTION 4

Chainage From ...:	To .....:	Points From	To	Mann. n	Perimeter [m]	Hydraulic Radius [m]
8.100	174.400	1	18	0.039	156.381	3.832

Project: ALLUVIAL RIVER STUDY
Subject: MHLATUZE RIVER 1987

CFP - DATA :

Run information :

No. of cross sections	:	4
Calculation interval dSV	:	20.000
Upstream depth	:	8.592
Downstream depth	:	8.410
Mult. factors - Discharge	:	1.000
- Manning's n .	:	1.000
Run label	:	MHLATUZE 1987 (n = 0.039)
Hydraulic jump calcs	:	AC
Transition loss coef. applied ..	:	N
Conveyance Calculation type ..	:	2

Long Section Data :

Section No.	Stake Value [m]	Unit Flow [m³/s]	Deflt Mann. n	Transition Loss Coef. Div. Conv. [-][-]		Section Title
1	150.000	3600.000	0.039	0.00	0.00	CROSS SECTION 1
2	283.000	3600.000	0.039	0.00	0.00	CROSS SECTION 2
3	459.000	3600.000	0.039	0.00	0.00	CROSS SECTION 3
4	630.000	3600.000	0.039	0.00	0.00	CROSS SECTION 4

Cross Section Data :

Section No. : 1 S.V. = 150.000 Title : CROSS SECTION 1
No. of points : 29

Chainage : 0.000 9.400 13.450 19.500 20.600 23.500 25.500 25.700 26.500 28.600
32.500 35.000 42.700 46.750 48.800 56.800 69.800 71.300 81.700 96.100
111.300 116.400 120.500 127.750 130.500 132.800 136.000 139.700 150.800
Level : 112.970 108.580 106.690 105.250 104.090 103.340 102.190 102.690 101.130 101.160
101.080 101.380 101.610 101.340 101.720 101.921 102.230 102.210 102.280 102.330
102.340 103.620 103.840 104.380 105.740 106.450 106.900 108.220 111.720
Manning n: 0.039 0.039 0.039 0.039 0.039 0.039 0.039 0.039 0.039 0.039
0.039 0.039 0.039 0.039 0.039 0.039 0.039 0.039 0.039 0.039
0.039 0.039 0.039 0.039 0.039 0.039 0.039 0.039

Section No. : 2 S.V. = 283.000 Title : CROSS SECTION 2
No. of points : 31

Chainage : 5.000 7.400 13.400 17.700 25.700 27.200 28.600 29.600 30.700 31.250
31.300 37.000 43.700 51.300 60.600 71.600 77.500 82.500 88.200 98.800
114.300 115.500 126.600 133.400 133.900 137.000 137.600 141.500 149.700 155.000
167.500
Level : 110.450 109.770 108.200 106.840 105.410 104.760 103.910 103.240 101.930 102.330
101.810 101.090 101.320 101.360 101.590 101.650 101.940 101.960 102.000 101.970
102.160 103.510 104.260 104.830 105.660 106.380 107.140 108.280 108.890 109.280
110.450
Manning n: 0.039 0.039 0.039 0.039 0.039 0.039 0.039 0.039 0.039 0.039
0.039 0.039 0.039 0.039 0.039 0.039 0.039 0.039 0.039 0.039
0.039 0.039 0.039 0.039 0.039 0.039 0.039 0.039 0.039 0.039

Section No. : 3 S.V. = 459.000 Title : CROSS SECTION 3
No. of points : 24

Chainage : 0.000 3.600 10.300 15.200 19.100 19.200 22.600 27.100 27.400 28.200
29.200 32.900 39.900 46.200 57.750 64.200 74.200 81.000 91.000 97.500
106.100 139.200 151.100 152.500
Level : 110.000 109.140 107.590 106.710 105.690 105.140 104.470 102.800 102.060 101.720
101.590 101.290 101.060 101.450 101.200 101.430 101.620 101.800 101.800 101.800
102.140 104.610 109.140 110.000
Manning n: 0.039 0.039 0.039 0.039 0.039 0.039 0.039 0.039 0.039 0.039
0.039 0.039 0.039 0.039 0.039 0.039 0.039 0.039 0.039 0.039
0.039 0.039 0.039

Section No. : 4 S.V. = 630.000 Title : CROSS SECTION 4
No. of points : 29

Chainage : 0.000 9.600 15.300 27.700 35.200 37.700 43.700 55.900 63.200 64.200
65.400 67.500 82.800 87.400 99.400 108.800 109.100 117.200 122.300 142.800
144.200 152.500 153.200 156.900 158.200 165.600 165.700 173.300 177.700
Level : 110.740 108.370 106.960 104.450 103.540 102.830 101.780 101.990 101.240 100.930
100.560 100.190 100.370 100.680 100.680 100.460 100.570 100.680 100.650 100.680
100.500 100.670 101.030 102.350 104.380 106.920 107.770 109.260 110.380
Manning n: 0.039 0.039 0.039 0.039 0.039 0.039 0.039 0.039 0.039 0.039
0.039 0.039 0.039 0.039 0.039 0.039 0.039 0.039 0.039 0.039
0.039 0.039 0.039 0.039 0.039 0.039 0.039 0.039

Final Profiles :

Point	Stake Value [m]	Bed Level [m]	Depth [m]	Surface level [m]	Surface Width [m]	Area [m^2]	Discharge [m^3/s]	Velocity level [m/s]	Energy [m]	Froude No.
1	150.000	101.080	8.57	109.65	137.10	865.86	3600.00	4.16	110.53	0.53
						Section 1				
2	172.167	101.082	8.49	109.57	138.95	857.32	3600.00	4.20	110.47	0.54
3	194.333	101.083	8.41	109.50	140.53	847.74	3600.00	4.25	110.42	0.55
4	216.500	101.085	8.33	109.42	141.74	837.08	3600.00	4.30	110.36	0.57
5	238.667	101.087	8.24	109.33	142.56	825.12	3600.00	4.36	110.30	0.58
6	260.833	101.088	8.14	109.23	142.94	811.64	3600.00	4.44	110.23	0.59
7	283.000	101.090	8.03	109.12	142.81	796.36	3600.00	4.52	110.16	0.61
						Section 2				
8	305.000	101.086	7.96	109.05	142.36	796.61	3600.00	4.52	110.09	0.61
9	327.000	101.082	7.90	108.98	142.02	797.34	3600.00	4.52	110.02	0.61
10	349.000	101.079	7.83	108.91	141.85	798.07	3600.00	4.51	109.95	0.61
11	371.000	101.075	7.77	108.84	141.85	798.72	3600.00	4.51	109.88	0.61
12	393.000	101.071	7.70	108.77	142.01	799.24	3600.00	4.50	109.81	0.61
13	415.000	101.067	7.64	108.70	142.35	799.60	3600.00	4.50	109.74	0.61
14	437.000	101.064	7.57	108.64	142.84	799.83	3600.00	4.50	109.67	0.61
15	459.000	101.060	7.51	108.57	143.51	799.97	3600.00	4.50	109.60	0.61
						Section 3				
16	480.375	100.951	7.62	108.57	145.53	828.49	3600.00	4.35	109.53	0.58
17	501.750	100.842	7.73	108.58	147.58	857.55	3600.00	4.20	109.47	0.56
18	523.125	100.734	7.85	108.58	149.71	886.91	3600.00	4.06	109.42	0.53
19	544.500	100.625	7.96	108.58	151.90	916.55	3600.00	3.93	109.37	0.51
20	565.875	100.516	8.07	108.59	154.14	946.48	3600.00	3.80	109.33	0.49
21	587.250	100.408	8.19	108.59	156.43	976.83	3600.00	3.69	109.28	0.47
22	608.625	100.299	8.30	108.60	158.80	1007.74	3600.00	3.57	109.25	0.45
23	630.000	100.190	8.41	108.60	161.27	1038.97	3600.00	3.46	109.21	0.44
						Section 4				
							CONTROL			

DESIGN INFO : Hydraulic Radii

Section : 1 S.V. = 150.000 Title : CROSS SECTION 1

Chainage		Points		Mann.	Perimeter	Hydraulic
From ...:	To .....:	From	To	n	[m]	Radius [m]
0.000	150.800	1	29	0.039	141.280	6.128

Section : 2 S.V. = 283.000 Title : CROSS SECTION 2

Chainage		Points		Mann.	Perimeter	Hydraulic
From ...:	To .....:	From	To	n	[m]	Radius [m]
7.400	155.000	2	30	0.039	146.990	5.416

Section : 3 S.V. = 459.000 Title : CROSS SECTION 3

Chainage		Points		Mann.	Perimeter	Hydraulic
From ...:	To .....:	From	To	n	[m]	Radius [m]
3.600	151.100	2	23	0.039	146.093	5.475

Section : 4 S.V. = 630.000 Title : CROSS SECTION 4

Chainage		Points		Mann.	Perimeter	Hydraulic
From ...:	To .....:	From	To	n	[m]	Radius [m]
0.000	173.300	1	28	0.039	164.871	6.300